Improvements to Meteorological Analysis over the Antarctic and Southern Ocean Region from the Inclusion of Additional Observing Systems

by

Kieran Jo Jacka, BSc GradDipMet

IASOS

Submitted in fulfilment of the requirements for the Degree of Master of Science

University of Tasmania (February, 2003)

This thesis contains no material which has been accepted for a degree or diploma by the University or any other institution, except by way of background information and duly acknowledged in the thesis, and to the best of my knowledge and belief no material previously published or written by another person except where due acknowledgement is made in the text of the thesis.

Signed: 

Kieran Jo Jacka

This thesis may be made available for loan and limited copying in accordance with the *Copyright Act 1968.*

Signed: 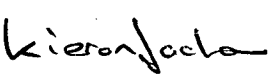

Kieran Jo Jacka

ABSTRACT

The *in situ* meteorological observing network in the Antarctic and Southern Ocean region is sparsely populated relative to other continents. Numerical weather prediction skill in Antarctica is poor, and as a scientific community our understanding of Antarctic atmospheric processes is underdeveloped. Yet the atmospheric dynamics occurring in the Antarctic region impact greatly on the weather of populated continents further north. Here several meteorological analysis and forecasting problems are investigated with close attention to the Antarctic continent and the surrounding Southern Ocean.

Scatterometer wind data, derived from satellite measurements of microwave backscatter by the ocean surface, are an important modern source of data for Southern Ocean Meteorology. Wind speed and direction estimates from the scatterometer instrument flown on-board the European Space Agency ERS-1 satellite are tested for accuracy against numerical model fields. Alternative algorithms have been developed by several meteorological agencies to deduce surface wind speed and direction from microwave backscatter measurements. Comparison is made between 10m wind estimates generated by two alternative algorithms and co-located data from the European Centre for Medium Range Weather Forecasts' numerical analyses. Some limitations in the derivation algorithms, unique to the Southern Ocean, are detected.

A data impact study, conducted within the framework of the Australian Bureau of Meteorology global data assimilation and prediction system (GASP), was conducted to assess the influence of ERS-1 scatterometer winds on numerical analyses and forecasts. The study identified several cases of substantial analysis impact, predominantly over the Southern Ocean. Mean impact statistics from 120 six-hourly assimilation cycles indicated a small positive impact on 24 and 48 hour forecast skill. The number of positive impact events exceeded the number of negative impact events and the inclusion of scatterometer data reduced the magnitude of forecast errors.

The majority of large impact events arose from simultaneous assimilation of two or more observing systems coincident in time and space. Large discrepancies between model air-pressure predictions and drifting buoy reports often resulted in the elimination of the latter on quality control grounds. On numerous occasions the superposition of scatterometer winds provided sufficient supporting evidence for the inclusion to proceed and subsequently generate improved analyses and forecasts.

Another valuable form of remotely sensed atmospheric data comes from the TIROS Operational Vertical Sounder (TOVS). Estimates of thickness between pressure surfaces, variously from the surface to 250hPa, were used heavily for meteorological analysis during the Antarctic First Regional Observing Study of the Troposphere (FROST). Here TOVS estimates are compared with co-incident radiosonde data from Antarctic and sub-Antarctic meteorological stations, supporting their validation.

The representation of the Antarctic surface temperature inversion in the GASP analyses is measured against results from observational studies. Improved boundary layer structure in later versions of the model is confirmed and surface wind forecasting skill has improved. Fluctuations in inversion depth and strength in successive model analyses and prognoses is identified as a wind strength forecasting aid for coastal locations.

The forecast skill of numerical weather prediction systems has increased steadily over the past two decades. The GASP system, on which the bulk of this work focuses, has also seen substantial skill increases. Improvements in forecast skill of the Australian global system have come from a combination of incremental changes over many years. While horizontal and vertical resolution has increased substantially, skill improvements in the Antarctic and Southern Ocean region have also come from the marked increase in data supply and usage. Particularly important are remotely sensed data, automatic weather stations and drifting buoys.

The potential for further dramatic skill improvement in the years ahead is real. Proposed future satellite missions will offer a great deal to Antarctic Atmospheric

Science. Significant new satellite systems will include NPOESS (USA; programme beginning 2005), COSMIC (USA/Taiwan; programme beginning 2005), ADEOS-II (Japan; launch planned for 2002), ENVISAT (European Space Agency; launched March 2002), Coriolis (USA; launch planned for August 2002) and MetOp-1 (European Space Agency; launch planned for 2005). Together they will provide the Meteorological Community with advanced atmospheric profiling technology, improved quality and resolution surface wind data, higher resolution multi-channel imagery and more. These remote sensing advances will come alongside an expanding network of automatic weather stations on the Antarctic continent and ongoing improvements to numerical modelling systems. Antarctic Meteorology is set to continue to benefit from the incorporation of existing observing systems as well as from new systems as they become available.

ACKNOWLEDGEMENTS

The Australian Bureau of Meteorology (ABOM) helped fund this work. The Australian Academy of Science and the Australian Meteorological and Oceanographic Society provided some travel funding.

The European Space Agency provided ERS-1 and ERS-2 data via experiment code AO2.AUS104. The Australian Antarctic Division provided logistics support in Antarctica.

Mr Neil Adams, Dr Phillip Reid, Professor Bill Budd, Dr Bill Bourke, Mr Bob Seaman, Mr Peter Steinle and Mr Hugh Hutchinson all provided valuable support and assistance.

ABOM Research Centre provided Figures 6.2.1 and 6.2.2.

Mr Matthew Lazzara (Space Science and Engineering Center, University of Wisconsin-Madison) provided Figure 1.2.1. Dr Phillip Reid (ABOM) provided the data for, and helped produce, Figure 1.3.3. Dr Roland Warner (Antarctic CRC and AAD) provided Figure 1.3.2. Mr Stephen Pendlebury (ABOM) provided the data for, and helped produce, Table 6.3.1 and Figure 6.3.3.

The Commonwealth of Australia granted permission to reproduce the paper in Appendix 4.

Mary, Olivia and Harry have been very patient, very helpful and enormously encouraging.

CONTENTS

LIST OF FIGURES

LIST OF TABLES

ACRONYMS

3D-Var	3-Dimensional Variational Analysis
4D-Var	4-Dimensional Variational Analysis
AAD	Australian Antarctic Division
ABOM	Australian Bureau of Meteorology
ADEOS	Advanced Earth Observing Satellite
AGO	Automatic Geophysical Observatory (USAP)
AMDAR	Automated Meteorological Data Relay
AMI	Active Microwave Instrument
ANARE	Australian National Antarctic Research Expeditions
ASCAT	Advanced Scatterometer (EUMETSAT)
AWS	Automatic Weather Station
Antarctic CRC	Co-operative Research Centre for Antarctica and the Southern Ocean (Australia)
Antarctic-LAPS	Antarctic Limited Area Prediction System (ABOM)
BAS	British Antarctic Survey
CERSAT	Centre ERS d'Archivage et de Traitement (France)
CMOD-n	C-band Scatterometer Model Functions
CNES	Centre National d'Etudes Spatiales (France)
COSMIC	Constellation Observing System for Meteorology, Ionosphere and Climate (USA/Taiwan)
DMSP	Defence Meteorological Satellite Program (USA)
ECMWF	European Centre for Medium-Range Weather Forecasts
ENVISAT	Environmental Satellite (ESA)
ERS	European Remote Sensing Satellite (ESA)
ESA	European Space Agency
EUMETSAT	European Organisation for the Exploration of Meteorological Satellites
FROST	First Regional Observing Study of the Antarctic Troposphere
GASP	Global Assimilation and Prediction System (ABOM)
GTS	Global Telecommunications System

HASP	Hemispheric Assimilation and Prediction System (ABOM)
HF	High Frequency
HIRS	High Resolution Infrared Radiation Sounder
IFREMER	Institut Français de Recherche pour l'Exploitation de la Mer
IGY	International Geophysical Year (July 1957 to December 1958)
JJA	June to August inclusive
JMA	Japan Meteorological Agency
LAPS	Limited Area Prediction System (ABOM)
Lat	Latitude
Lon	Longitude
Meso-LAPS	Mesoscale Limited Area Prediction System (ABOM)
MetOp	Meteorological Operational Polar Satellites (EUMETSAT)
MSLP	Mean Sea Level Pressure
MVSI	Multivariate Statistical Interpolation
NASA	National Aeronautics and Space Administration (USA)
NASDA	National Space Development Agency (Japan)
NCC	National Climate Centre (ABOM)
NCEP	National Centers for Environmental Prediction (USA)
NESDIS	National Environmental Satellite, Data and Information Service (NOAA)
NMC	National Meteorological Centre (ABOM)
NMOC	National Meteorological and Oceanographic Centre (ABOM)
NOAA	National Oceanic and Atmospheric Administration (USA)
NPOESS	National Polar Orbiting Environmental Satellite System (USA)
NSCAT	NASA Scatterometer
NWP	Numerical Weather Prediction
QuikSCAT	NASA Quick Scatterometer
RxLy	Rhomboidal truncation of x waves; y σ levels
RMSE	Root Mean Square Error
SAR	Synthetic Aperture Radar
SASS	Seasat-A Satellite Scatterometer
SCAR	Scientific Committee on Antarctic Research
SCM	Successive Correction Method
SI	International System of Units

SOP	Special Observing Period of First Regional Observing Study of the Antarctic Troposphere
SSI	Spectral Statistical Interpolation
SSM/I	Special Sensor Microwave/Imager
$T_L xLy$	Triangular truncation of x waves with linear reduced Gaussian grid; y σ levels
$TxLy$	Triangular truncation of x waves; y σ levels
TIROS	Television Infrared Operational Satellite
TLAPS	Tropical Limited Area Prediction System (ABOM)
TOVS	TIROS Operational Vertical Sounder
UKMO	United Kingdom Meteorological Office
USAP	United States Antarctic Program
UTC	Universal Time Co-ordinate
VHF	Very High Frequency
WindSat	Satellite Based Wind Speed and Direction System (USA)

SYMBOLS

b	Byte
°C	Degrees Celsius
E	East
Hz	Hertz
K	Kelvin
m	Metre
N	North
P; P_{surf}	Air pressure; Surface air pressure
Pa	Pascal
s	Second
S	South
S_1	Skill-score from Teweles and Wobus (1954)
t	Time
T; T_x	Air temperature; Air temperature at height $\sigma = x$
T_{surf}	Surface temperature
u; u_{10}	Zonal wind component; Ditto at 10m elevation
v; v_{10}	Meridional wind component; Ditto at 10m elevation
V; V_x	Wind speed; Wind speed at height x metres
W	West
ΔT_x	T_x - T_{surf}
λ	Wavelength
ϕ	Wind direction
θ	Incidence angle
σ	Height co-ordainate where $\sigma = P / P_{surf}$
σ°	Normalised radar cross section
σ°_{fore}; σ°_{mid}; σ°_{aft}	Normalised radar cross section at the fore; mid; aft antenna

The International System of Units (SI) is used throughout this thesis. The following SI prefixes are also used.

G	10^{9}
M	10^{6}
k	10^{3}
h	10^{2}
da	10^{1}
d	10^{-1}
c	10^{-2}
m	10^{-3}
μ	10^{-6}

SYNOPSIS

Chapter 1 provides the reader with a brief introduction to Antarctic geography and the role of the Antarctic continent in influencing the meteorological processes of the southern hemisphere. This chapter covers the availability of meteorological data from Antarctica – manual, automated and remotely sensed – and some of the challenges of meteorological analysis of the Antarctic and Southern Ocean region.

In Chapter 2 background is given on two of the tools of greatest focus throughout the thesis: The scatterometer instrument flown on-board the ERS-1 satellite; and the Australian Bureau of Meteorology (ABOM) Global Assimilation and Prediction System (GASP). The details of the development and evolution of GASP over the past decade is covered in this chapter and further in Appendix 2.

The quality of wind data from the ERS-1 scatterometer is discussed in Chapter 3. Two investigations were carried out to measure the reliability of these data for Southern Ocean Meteorology. The first study compares scatterometer winds with winds from co-incident GASP analyses. The second compares scatterometer winds calculated using two different wind derivation algorithms with co-incident data from the European Centre for Medium-Range Weather Forecasts (ECMWF) analyses.

A series of experiments to assess the impact of scatterometer winds on the GASP system is discussed in Chapter 4. The focus of the discussion is on the magnitude of the impact of scatterometer winds during a one-month experiment involving multiple assimilation, analysis and prognosis cycles. Mean forecast impact statistics show a small degree of improvement in average skill. The daily variation of analysis and prognosis skill shows that the addition of the extra data has a substantial influence on the system – usually positive.

The results of two companion studies are given in Chapter 5. The first is a study of vertical profile data from the TIROS Operational Vertical Sounder (TOVS)

instrument over Antarctica and the Southern Ocean. TOVS thickness data are compared with data from co-incident radiosonde flights from Antarctic and sub-Antarctic stations. Evidence is established to justify the use of low altitude TOVS derived thickness measurements for the First Regional Observational Study of the Antarctic Troposphere (FROST) and for the use of TOVS above 700hPa over the Antarctic continent.

The second companion study detailed in Chapter 5 concentrates on the accuracy of the representation of the Antarctic surface inversion in the GASP system. This representation is found to be reliable. Further, the distribution and strength of the surface inversion in GASP analyses are found to be useful tools for forecasting the onset of strong winds at coastal locations.

Chapter 6 provides the reader with an historical review of the stepwise improvements in the prognostic skill of the Australian GASP system. Comparisons are made between the skill and error statistics of several global numerical systems over the past decade, with particular emphasis on the Antarctic region.

Chapter 7 is a review and conclusion chapter. The results documented in this thesis are discussed in the context of international developments in numerical weather prediction, remote sensing technology and atmospheric science generally, with particular reference to the continuing improvements that are evident in the quality of synoptic analyses and prognoses over Antarctica.

CHAPTER 1

INTRODUCTION

1.1 Geography and climatology of Antarctica and the Southern Ocean

The Antarctic continent is vast. Its surface area of about 14 million km^2 is almost double that of Australia (about 7.7 million km^2). When considered together with the equally large area of sea ice that surrounds Antarctica annually, the high albedo region extends to over 30 million km^2.

Surrounded by the vast Southern Ocean, and located over the South Pole, Antarctica is a most influential landmass in the southern hemisphere in the operation of the atmospheric circulation.

The greater part of the Antarctic continent is approximately dome-shaped consisting of bedrock capped with solid ice. The surface altitude of the interior plateau reaches 4000m above sea level in a region offset from the South Pole by approximately 900km.

The lesser part of the continent, West Antarctica, is characterised by the Antarctic Peninsula: a mountainous peninsula forming an extension of the South American Andes; and the three large, flat ice shelves: Ross, Ronne and Filschner.

The mean annual ice-surface temperature on the high Antarctic Plateau is less than -50°C. By contrast the ocean surface temperature surrounding Antarctica beyond the sea ice is closer to 0°C. These features, together with some less dominant circulation processes at lower latitudes, provide the main driving force behind the notoriously strong Antarctic katabatic winds down the steep surface slopes towards the coast (Parish and Bromwich 1987).

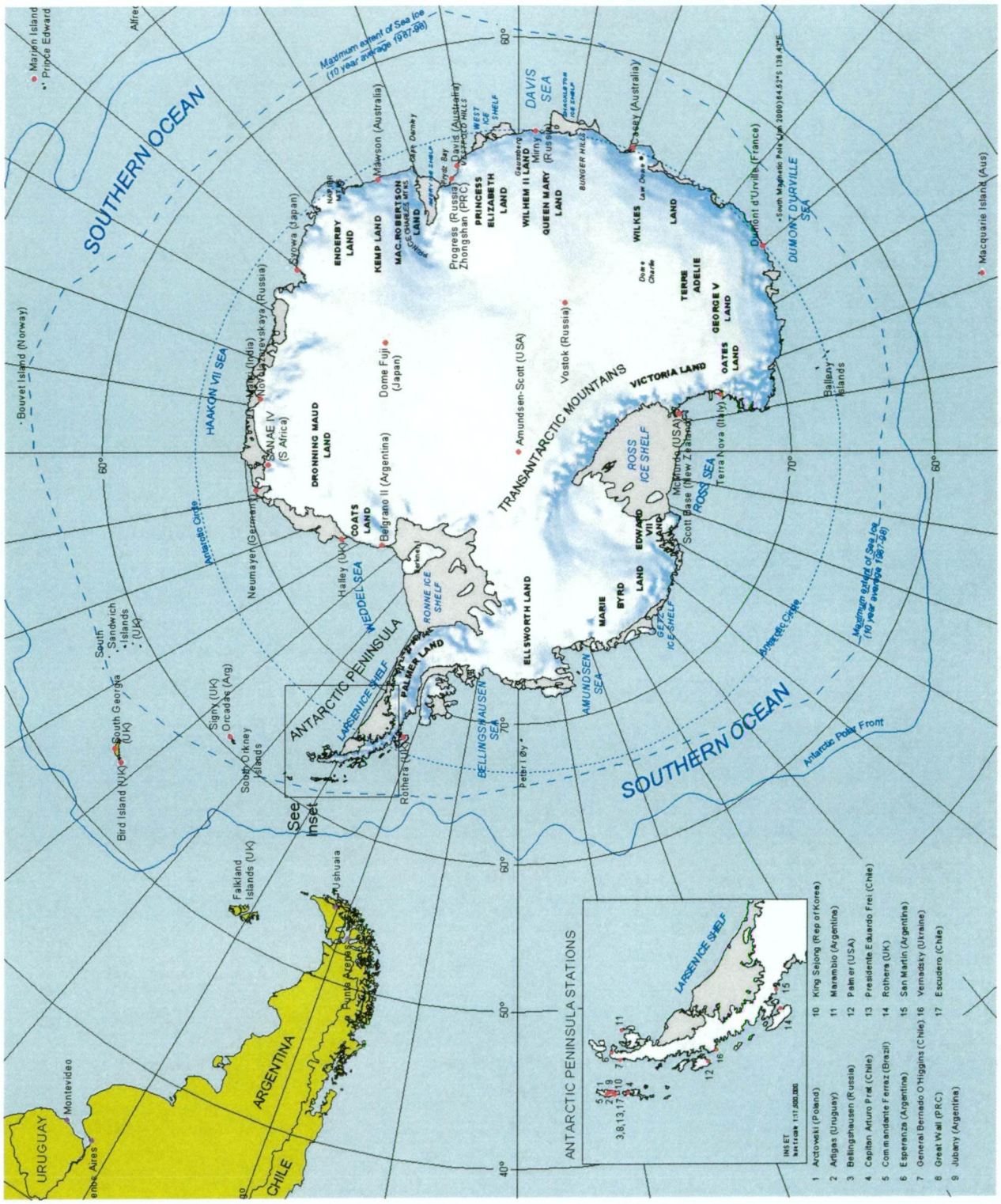

Figure 1.1.1 Map of Antarctica showing principal locations discussed in the text (reproduced from www.aad.gov.au). Polar-stereographic projection. Scale 1:48,000,000 at 71°S. Dashed lines show maximum extent of sea ice. See Appendix 1 for a comprehensive list of locations.

This surface temperature regime is also behind the mechanisms that cause deep atmospheric subsidence over the Antarctic Plateau. The low temperatures over Antarctica are also responsible for low atmospheric column moisture. Both features oppose cloud formation and contribute to markedly limiting the precipitation. These conditions are associated with Antarctica being the driest continent.

Furthermore, the Antarctic surface temperature regime causes a net near-surface outward air flow and northward mass flux. Subsequent convergence over the relatively warm ocean waters of the sea ice leads (or polynyas), and adjacent to the sea ice edge, leads to the formation of the polar trough. The low pressure systems of the polar trough, and the strong mean surface pressure gradient to the north, are predominant features associated with the gales and high seas of the Southern Ocean.

1.2 Limitations in Antarctic and Southern Ocean Meteorology

The sparseness of meteorological data from the Southern Ocean has long been regarded as one of the primary factors limiting our ability to predict southern hemisphere mid-latitude weather.

Prior to the use of satellite imagery in operational meteorology, daily weather forecasts for the southern regions of Australia hinged largely on reports from remote offshore islands (eg: Amsterdam Island in the mid-Indian Ocean, and Macquarie Island south-southeast of Hobart). The situation improved considerably with the regular availability of high quality satellite imagery, but even today reports from remote islands play a significant role in meteorological analysis and weather forecasting activities.

The difficulties of meteorological analysis and prediction in a sparse data region are further hampered in the unique Antarctic environment. The harshness of the weather makes observing the Antarctic atmosphere problematic. The continent is vast and particularly difficult to reach via air and sea. Furthermore, as a scientific community, our knowledge and understanding of Antarctic atmospheric processes is underdeveloped compared to that of other areas of the globe.

The number of manned stations making year-round surface meteorological observations in Antarctica peaked during the International Geophysical Year (IGY) of July 1957 to December 1958. The IGY consisted of a comprehensive, multi-national series of global activities that allowed scientists to make co-ordinated observations of various geophysical phenomena (www.nas.edu/history/igy/).

Since the early 1980's the number of manned, surface meteorological stations has declined markedly. Similarly, the number of stations making regular upper-air observations on the Antarctic continent has decline, down from seventeen during the IGY to thirteen today. Only one year-round, inland upper-air station remains, the US station Amundsen-Scott located at the South Pole (King and Turner 1997).

On a positive note, the last decade has seen a substantial increase in the number of drifting buoy deployments in the Southern Ocean. Most of these buoys provide atmospheric pressure reports and transmit their data in near real time via the Global Telecommunications System (GTS) to meteorological centres around the world. Also the past decade has seen a dramatic increase in the number of automatic weather stations (AWS) operating in Antarctica. Good networks now exist over parts of the continent distant from manned stations and also provide near real time data to the international community (Turner et al. 1996, Turner and Pendlebury 2000). Figure 1.2.1 shows the network of known AWS as at April 2000.

The number of drifting buoys reporting meteorological parameters in Antarctic waters is far less than in other oceans. With the creation of the International Programme for Antarctic Buoys has come an ongoing commitment from several nations to continue regular buoy deployments in the Antarctic sea ice zone (Australia, Brazil, Finland, Germany, Italy, Japan, South Africa, UK and USA) (King and Turner 1997). However, the waters adjacent to Australia's Antarctic Territory rarely contain more than three or four buoys south of 60°S. Typically the Australian Antarctic Division (AAD) and/or ABOM have deployed those. Figure 1.2.2 shows a recent map of buoy distribution in the Indian Ocean sector.

The importance of satellites to Antarctic and Southern Ocean Meteorology cannot be understated. For the purposes of manual analysis of synoptic weather systems

around the coastal fringe of the Antarctic continent, and further seaward, satellite imagery is a fundamental tool. Other remotely sensed data play an important role in Antarctic meteorological analysis, but tend to be used more in numerical systems than by personnel. The TIROS Operational Vertical Sounder (TOVS), flown on the NOAA series of polar orbiting satellites, provides an important source of vertical

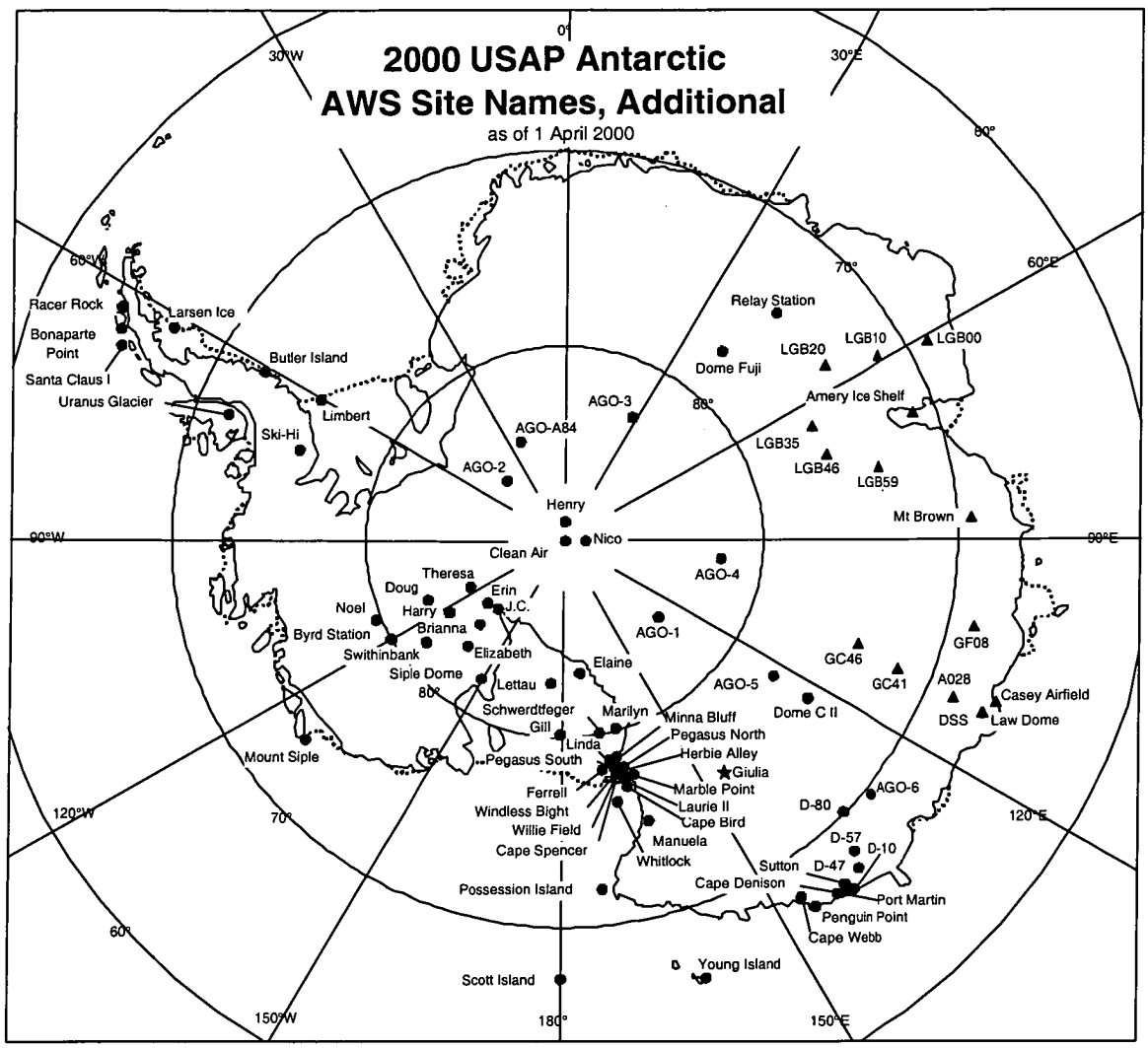

Figure 1.2.1 Map of Antarctica showing the location of automatic weather stations (Provided by M. Lazzara, March 2002). Figure includes USAP AWS and AGO sites (circles), ANARE sites (triangles) and one Italian Antartide site (star). Further sites (not shown) exist in the vicinity of Terra Nova Bay and on Inexpressible Island (Turner and Pendlebury 2000). See Turner and Pendlebury (2000) for a comprehensive listing of AWS. See Appendix 1 for a listing of staffed stations and some AWS.

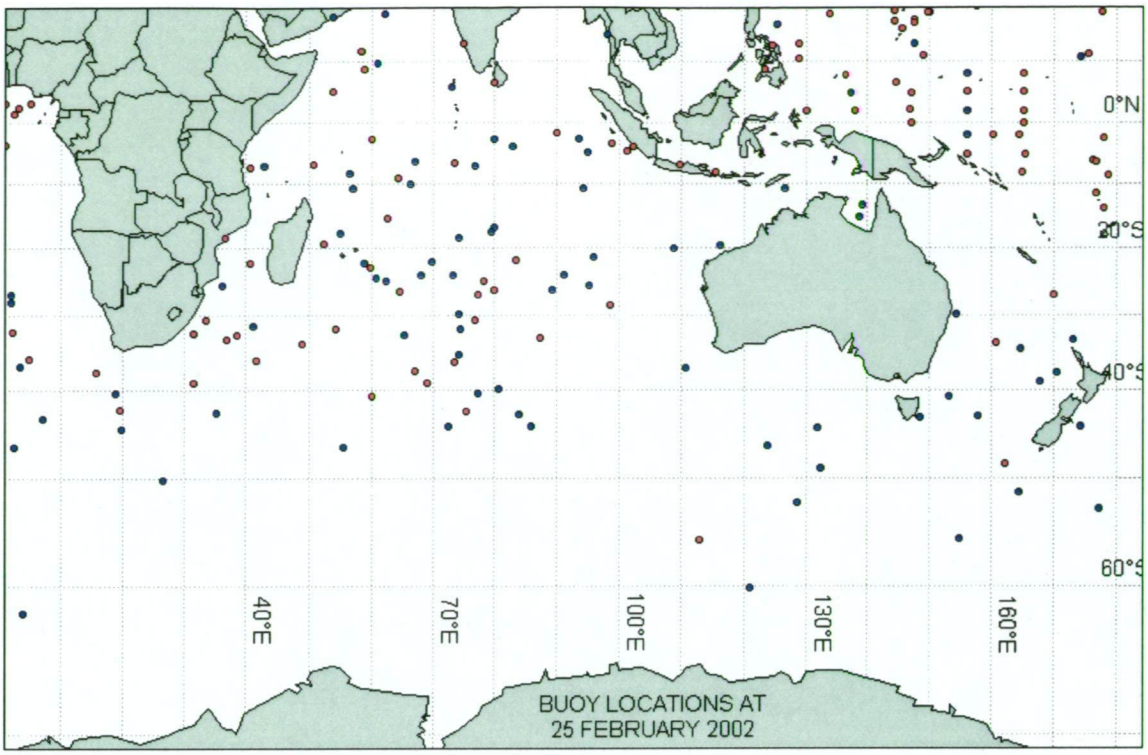

Figure 1.2.2 Map showing the distribution of drifting buoys as at 25 February 2002 (from MOU 2002). Blue dots indicate buoys that report air pressure; red dots indicate buoys that do not report air pressure.

sounding data over areas remote from radiosonde stations and its data are used heavily in a number of global numerical systems. Low-level TOVS data are known to be of lower quality over ice; hence usage in Antarctica is restricted.

Attempts to provide meteorological support for Antarctic logistic operations have become more sophisticated over the past decade. With the installation of good quality, high-speed telecommunication facilities to and from Antarctica, the trend to have meteorologists posted at Antarctic research stations has increased. The Australian Bureau of Meteorology (ABOM) maintained a summer meteorological forecasting centre at Casey for several years during the 1990s (Adams 2002). They plan to reopen the facility in 2003 to coincide with the Australian Government's proposal to operate intercontinental aircraft between Hobart and Casey (www.aad.gov.au). Similar meteorological centres have operated at McMurdo (USA), Rothera (United Kingdom) and Molodezhnaya (Russia) all attempting to

provide accurate weather forecasts for aircraft, ships and field personnel (Turner and Pendlebury 2000).

There have been significant improvements in the resolution of global numerical weather prediction (NWP) systems over the past decade. The advent of high-speed telecommunication links to and from Antarctica and the advent of the internet have made NWP data easier to access. Numerical analysis and forecast quality in the Antarctic region is still less than that of other continents. Until recently, NWP systems lacked the temporal and spatial resolution to capture mesoscale features (Pendlebury et al. 2003). While recent advances have been considerable, a continuing lack of predictive reliability makes forecasting for weather sensitive activities problematic. For aircraft operation around Antarctica's coastal fringe, unpredictable mesoscale phenomena represent the greatest hazard.

1.3 Manual and numerical meteorological analysis

Subjective, manual meteorological analysis continues to be performed routinely in weather centres around the world. Antarctic forecasting personnel use a combination of human-observed data, automatic weather station (AWS) data, subjective interpretation of satellite imagery and NWP output to produce routine analysis fields of sea-level pressure and standard-level geopotential height and wind (Turner and Pendlebury 2000). These analyses, together with NWP prognoses, form the basis of the forecasting (and nowcasting) process.

One of the earliest examples of mean sea level pressure analysis of the Antarctic and Southern Ocean region was the sequence constructed by Kidson (1947). These were based on observations from Mawson's expedition to Macquarie Island and Antarctica, Scott's expedition to the Ross Sea and observations from Australia and New Zealand (Streten 2001). Figure 1.3.1 is an example mean sea level pressure (MSLP) analysis chart from Kidson (1947).

The International Antarctic Analysis Centre (IAAC; later named the International Antarctic Meteorological Research Centre) operated in Melbourne, Australia, between 1959 and 1969. Established in the years prior to the availability of regular satellite imagery or NWP system data, IAAC concentrated on manual, subjective

meteorological analysis of the Antarctic and Southern Ocean surface and radiosonde network. Data gathered during the IGY formed an important part of the analysis (Phillpot 1997).

In 1964 ABOM began reception of TIROS satellite images. These led to considerably improved meteorological analyses over the Southern Ocean.

The development of NWP at ABOM began in the late 1960s with the first Australian region operational prognoses issued in 1970. Operational numerical analyses and prognoses of the full southern hemisphere began in 1972 (Zillman 2001). The Hemispheric Assimilation and Prognosis System (HASP) was implemented at ABOM in March 1985.

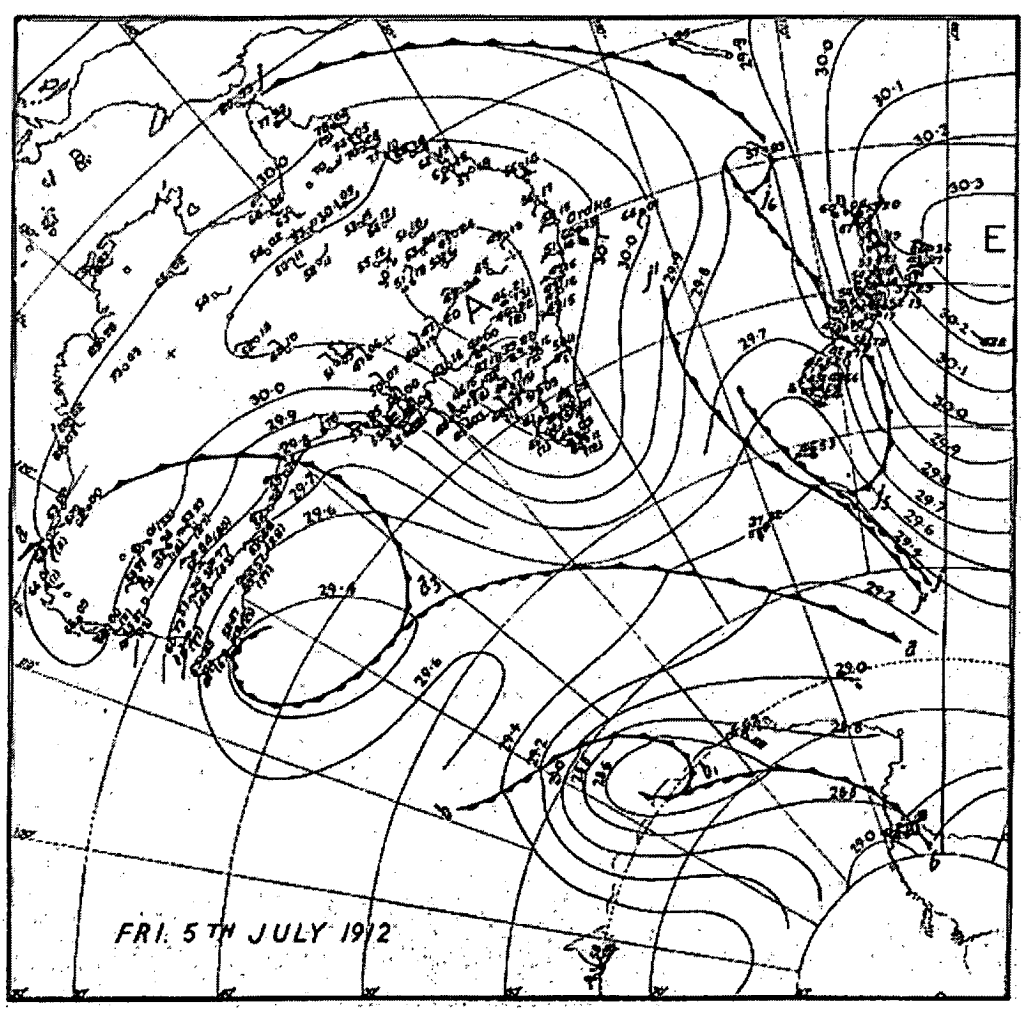

Figure 1.3.1 MSLP analysis (5 July 1912) of the Australian region plus parts of the Southern Ocean and Antarctica (from Streten 2001 after Kidson 1947). (Inches of mercury).

It was identified during the 1980s that NWP systems performed less reliably over the Antarctic region than over other continents (Trenberth and Olson 1988). That observation and renewed interest in Antarctic weather forecasting by the SCAR Working Group on Meteorology and Atmosphere Physics led to the establishment of the First Regional Observing Study of the Antarctic Troposphere (FROST) during the 1990s (Turner 1999, Turner et al. 1996). FROST was primarily a data gathering, analysis and evaluation project during which all available meteorological data, however observed or derived, were gathered and analysed. The study concentrated on the entire area south of 50°S during the three one-month "special observing periods" (SOPs): 1 – 31 July 1994 (SOP1), 16 October – 15 November 1994 (SOP2), and 1 – 31 January 1995 (SOP3).

Starting with the routine NWP products and other available data, manual meteorological re-analysis formed the backbone of the FROST experiment and the basis of most of its goals:

(i) to assess the quality and reliability of the Antarctic observing network and supporting data handling and transmission systems (Colwell and Turner 1999, Turner et al. 1996, Turner et al. 1999a);

(ii) to assess the strengths and weaknesses of numerical analyses and prognoses in the Antarctic region (Bromwich et al. 1999, Turner et al. 1999b);

(iii) to assess the value of remotely sensed data in Antarctic and Southern Ocean Meteorology (Adams et al. 1999, Jacka 1999); and

(iv) to further our understanding of Antarctic atmospheric processes (Lieder and Heinemann 1999, Marshall and Turner 1999, Pook and Cowled 1999, Pook and Gibson 1999, Simmonds and Murray 1999, Simmonds et al. 1999).

The assessment of NWP output is a non-trivial task, particularly in the Antarctic region where we have a limited network of stations against which we can ground-truth data. FROST produced a series of manually derived meteorological fields against which, it was proposed, NWP data could be assessed. However, it is widely recognised that modern NWP systems out-perform manual efforts in several areas:

- the temporal and spatial consistency of systematic numerical analysis is superior to that of manual analysis;
- numerical systems better maintain the four-dimensional structure of the atmosphere in balance; and

- numerical systems can be coupled to simulations of the dynamics, physics and chemistry of the oceans, sea ice and land.

These benefits make it more practical for NWP systems to process the suite of observational and remotely sensed data now available. The data can be assimilated to gain the most favourable compromise between adequate coverage and higher accuracy. Advanced NWP systems have the power to maintain simultaneous quality checks between observing systems. Where biases are detected the system can apply bias corrections. Where random errors are detected the system can limit the impact of errors by minimising the use of erroneous data. It is difficult to control such issues in a manual analysis project.

An operational NWP system needs a rapid processing time. This is the primary factor limiting model resolution. Limited model resolution causes several problems specific to the Antarctic region. The steepness of the Antarctic topography cannot be well represented in low resolution numerical models. Since topographical features largely drive the characteristics of the coastal surface wind regime, poor topographical representation leads to poor wind speed analysis and prediction.

Figure 1.3.2 shows the surface topography of the Antarctic continent. This diagram shows surface contours based on 5km resolution data from the BEDMAP project (Lythe et al. 2001). Figures 1.3.3 show the GASP representation of surface topography. Clear improvements in GASP topography have occurred with the advent of the T_L239 version (approximately 75km resolution) but some limitations still remain.

Figure 1.3.4 shows two significantly different GASP topography fields (T_L239 and R53) in cross-section through the Lambert Glacier Basin. This geographic feature is known to be of considerable importance for the forecasting of significant meteorological phenomena at Davis and Zhongshan (Turner and Pendlebury 2000).

The differences shown here are not likely to have had a great impact on model performance over the hemisphere or over the Australian region. But the impact on local analysis and prognosis skill would doubtless be great. Note that the horizontal grid spacing of the ECMWF global system is approximately half that of GASP.

Antarctic mesoscale storms are typically small and short-lived (Marshall and Turner 1997b). They are often not well captured by NWP systems yet they commonly produce significant precipitation and hazardous weather conditions for aircraft operations.

The boundary layer over the Antarctic continent is difficult to represent in a NWP system with a limited, coarse vertical resolution. The magnitude of the near-surface temperature inversion typically exceeds 25°C over a large part of the interior plateau. Data from stations high on the plateau indicate that inversion strengths of 35°C are not uncommon. Inversion depths can range from as low as 50m to more typical depths of 500m to 1500m depending on strength (Turner and Pendlebury 2000, Bromwich and Parish, 1998). The most prevalent and hazardous of the weather phenomena experienced around coastal Antarctica develop as a direct consequence of the features of the atmospheric boundary layer, the steep surface.

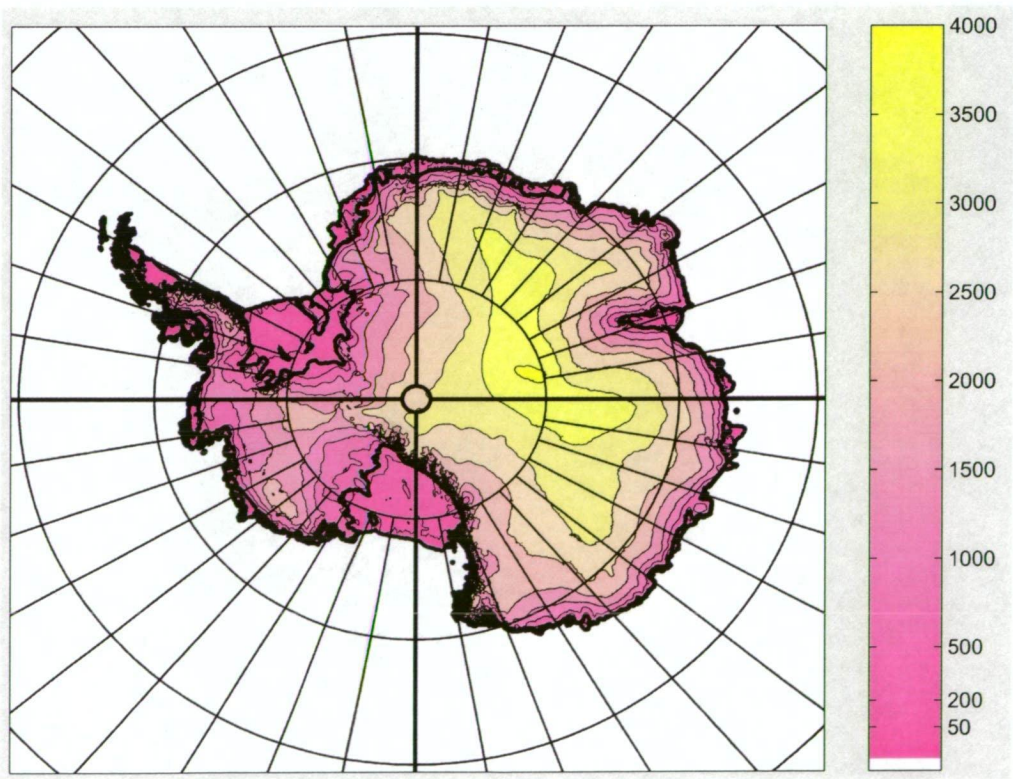

Figure 1.3.2 Map of Antarctica showing surface topography based on 5km resolution data from the BEDMAP project (Lythe et al. 2001).

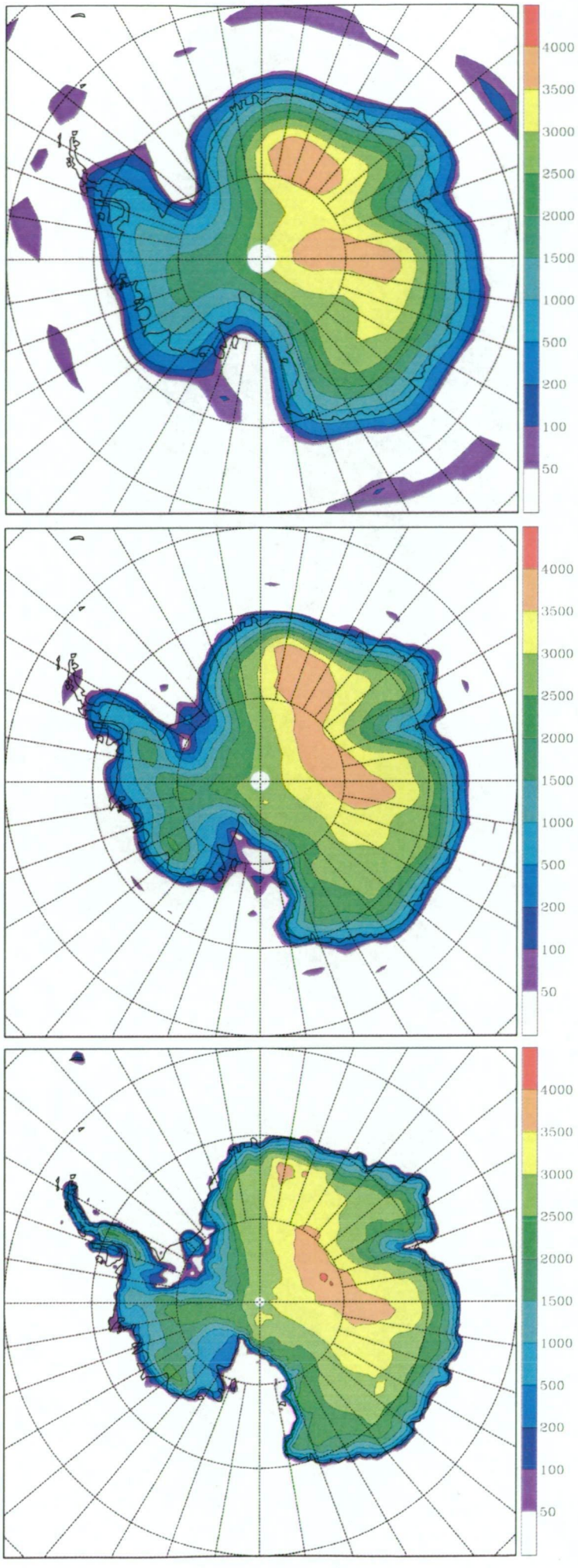

Figure 1.3.3
GASP representation of the surface topography over the Antarctic continent. Three GASP model resolutions are shown:

Top: R31.

Middle: T79 (≈ R53).

Bottom: T_L239.

slope and abrupt coastline. To satisfactorily represent these unique features in a NWP system requires high vertical, horizontal and temporal resolution.

The global NWP system used primarily for Australian research and weather forecasting in Antarctica is the Global Assimilation and Prediction System (GASP) developed by the ABOM Research Centre (Bourke et al. 1995, Seaman et al. 1995). A nested regional system is currently under development for use over the Antarctic region (Adams 2001).

The GASP configuration used in this study, including FROST related work between 1994 and 1997, had a resolution of rhomboidal wave number 53 on 19 σ levels (R53L19). GASP used a multivariate statistical interpolation assimilation scheme (Lorenc 1981).

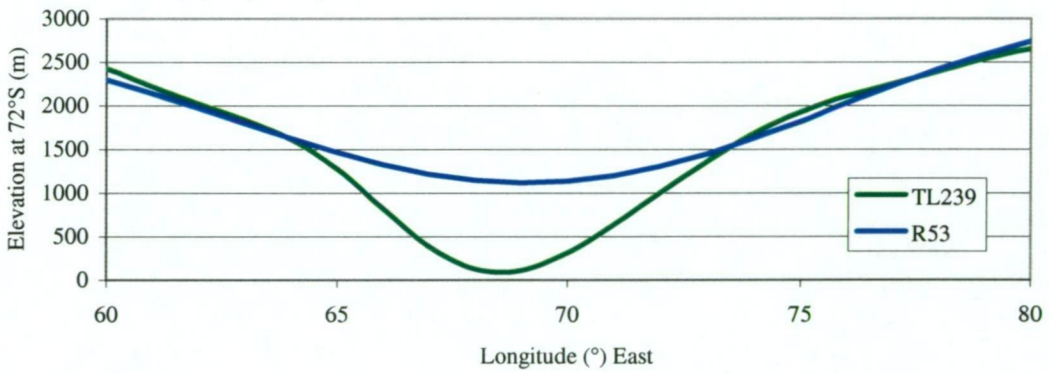

Figure 1.3.4 West-to-east cross-section of the GASP model topography (m) across the Lambert Glacier Basin, East Antarctica, at T_L239 and R53 resolution.

1.4 Remote sensing for Antarctic and Southern Ocean Meteorology

The most substantial development in the Science of Meteorology for a century was the launch of the first weather satellite, TIROS-1, in 1960 (Vaughan and Johnson 1994). Early polar orbiting satellites helped researchers and forecasters develop an

understanding of meteorological processes and interpretation for the purposes of analysis (Guymer 1978). Since then many other polar orbiting satellites for weather observation have been developed for continuing operational services.

Later geostationary weather satellites provided regular imagery at a constant look-angle and helped with the monitoring of development and movement of weather systems. Two valuable references for further general reading on remote sensing techniques in polar regions are Bader et al. (1995) and Massom (1991).

More recent remote sensing advances have delivered a new suite of data to the meteorologist. Arguably the most important of these is the wind scatterometer. The scatterometer is an active microwave instrument that records the backscatter from the Earth's surface of a microwave pulse.

The earliest record of a spacecraft mounted scatterometer instrument was that on the Skylab missions of 1973. The short Skylab voyages (four missions totalling 171 days) carried an active microwave radiometer, scatterometer and altimeter operating at 13.9GHz (λ = 2.16cm) (history.nasa.gov).

The SEASAT satellite operated between June and October 1978. The SEASAT-A Satellite Scatterometer (commonly called SASS) used two antennae on each side of the satellite to illuminate parallel swathes of ocean surface below. The use of only two antennae made surface wind direction difficult to resolve. The instrument used a 14.595GHz pulse (λ = 2.06cm). For further reading on SEASAT see Bernstein (1982) and Stewart (1988). The impact of SASS data on a NWP system was discussed by Ingleby and Bromley (1991) – see the discussion in Section 4.1.

A 5.3GHz (λ = 5.66cm) scatterometer, with three antennae, was flown on ERS-1 (1991 to 2000) and ERS-2 (1995 to present). Further details are given in Section 2.2 of this thesis.

The NASA scatterometer, NSCAT, was mounted on-board the NASDA ADEOS satellite (August 1996 to June 1997). NSCAT operated at a frequency of 13.995GHz (λ = 2.14cm) with six antennae, three on either side of the spacecraft. The instrument provided high quality wind data and operated during the life of the

ERS-2 system thus providing an interesting period of duel operation (Pouliquen et al. 1997). The satellite failed after only a short period (Triendl 1997). For further reading on NSCAT see the collection of papers in the *Journal of Geophysical Research (Oceans)* volume 104 (C5).

SeaWinds on-board the QuikSCAT satellite (June 1999 to present i.e. March 2002) is a scatterometer instrument in the configuration of a 1m diameter rotating dish with two beams. They illuminate a 1800km wide swathe with a 13.4GHz (λ = 2.24cm) pulse. A similar system is planned for the ADEOS-II satellite due to be launched late in 2002.

ASCAT is the scatterometer system planned for the MetOp-1 satellite due to be launched in 2005. ASCAT will use the same configuration as ERS-1 and ERS-2 but will provide simultaneous swathes of data on either side of the sub-satellite track. Pulse frequency will be 5.255GHz (λ = 5.71cm).

Also of some relevance to the current discussion is the planned WindSat instrument to be mounted on-board the Coriolis satellite (August 2002 launch). WindSat is a passive radiometric system as distinct from a scatterometer (active) instrument. Using a multi-frequency polarimetric radiometer WindSat will provide a 1025km wide swathe of wind speed and direction data with accuracy and resolution statistics similar to scatterometer instruments.

A summary of details on satellite missions including sensing for surface winds is shown below in Table 1.4.1.

1.5 Scatterometer wind impact study

This thesis describes an impact study involving the use of ERS-1 satellite scatterometer wind data in the GASP system. The study follows on from related work in the ABOM Research Centre including impact experiments evaluating the relative contributions obtained from drifting buoys, cloud drift winds, "bogus" pressure data (derived from manually prepared mean sea level pressure analyses) and conventional observations (Seaman et al. 1993, Seaman 1994, Le Marshall and Pescod 1994).

Wind finding system; Satellite	Satellite life span	Satellite orbit	Wind finding instrument configuration	Wind finding system operating frequency	Wind vector swathe width; Resolution	Objective speed accuracy; range; and Direction accuracy
SASS; SEASAT	June 1978 - Oct. 1978	Height: 805km Inclination: 108.0° Period: 100.63min	Four antennae at -135°, -45°, +45° and +135° to sub-satellite track	Active microwave: 14.595GHz	600km wide; 50km resolution	$\pm 2 ms^{-1}$; 7 to 50 ms^{-1}; ±20°
AMI; ERS-1	July 1991 - March 2000	Height: 780km Inclination: 98.52° Period: 100.50min	Three antennae at +45°, +90° and +135° to sub-satellite track	Active microwave: 5.3GHz	500km wide; 45km resolution	$\pm 2 ms^{-1}$ or 10%; 4 to 24ms^{-1}; ±20°
AMI; ERS-2	April 1995 – present *	Height: 780km Inclination: 98.52° Period: 100.50min	Three antennae at +45°, +90° and +135° to sub-satellite track	Active microwave: 5.3GHz	500km wide; 45km resolution	$\pm 2 ms^{-1}$ or 10%; 4 to 24ms^{-1}; ±20°
NSCAT; ADEOS	Aug. 1996 - June 1997	Height: 797km Inclination: 98.6° Period: 101min	Six antennae at -135°, -65°, -45°, +45°, +115° and +135° to sub-satellite track	Active microwave: 13.995GHz	2 x 600km wide separated by 330km; 50km resolution	±10%; 3 to 30 ms^{-1}; ±20°
SeaWinds; QuikSCAT	June 1999 - present	Height: 803km Inclination: 98.6° Period: 101min	1m diameter rotating dish with two beams	Active microwave: 13.4GHz	1800km wide; 25km resolution	$\pm 2 ms^{-1}$ or 10%; 3 to 30ms^{-1}; ±20°
SeaWinds; ADEOS-II	Late 2002 launch	Height: 803km Inclination: 98.6° Period: 101min	1m diameter rotating dish with two beams	Active microwave: 13.4GHz	1800km wide; 50km resolution	$\pm 2 ms^{-1}$; 3 to 20ms^{-1}; ±20°
WindSat; Coriolis	August 2002 launch	Height: 830km Inclination: 98.7° Period: 101min	Multi-frequency passive microwave polarimetric radiometer	Passive microwave: 6.8, 10.7, 18.7, 23.8 and 37.0GHz	1025km wide; 20km resolution	$\pm 2 ms^{-1}$ or 20%; 3 to 25ms^{-1}; ±20°
ASCAT; MetOp – 1	2005 launch	Height: 820km Inclination: 98.7° Period: 101min	Six antennae at -135°, -90°, -45°, +45°, +90° and +135° to sub-satellite track	Active microwave: 5.255GHz	2 x 550km wide separated by 660km; 25km resolution	$\pm 3 ms^{-1}$; 4 to 24ms^{-1}; ±20°

Table 1.4.1 Details of satellite missions carrying wind speed and direction finding instruments: scatterometer and radiometric (Massom 1991, Bernstein 1982, www.jpl.nasa.gov, www.esa.int, www.eumetsat.de). *ERS-2 scatterometer failed on 17 January 2001.

A related impact study conducted at the European Centre for Medium Range Weather Forecasts (ECMWF) (Stoffelen and Anderson 1995) formed the initial motivation for this work. Stoffelen and Anderson identified a small positive impact on medium range weather forecasts with the inclusion of ERS-1 scatterometer winds at assimilation. They also found that the magnitude of the impact of the scatterometer data was considerably more significant in trials absent of TOVS data, indicating some degree of data saturation with the inclusion of both data sources. Similar work followed at the National Centers for Environmental Prediction (NCEP) (Yu 1995, Yu and Derber 1995 and Yu et al. 1996). NCEP reprocessed winds from ERS-1 were used in a series of impact trials in 1995. A small positive impact was reported.

Both the NCEP and ECMWF studies linked the instances of largest analysis impact to the issue of quality control assessment of remote sea level pressure reports. The co-location of scatterometer winds would occasionally support (or refute) pressure reports from remote buoys and islands. The subsequent change in data usage caused substantial analysis impact and commonly constrained the magnitude of large error anomalies. While causing only small mean impact statistics, large case-by-case impact events were relatively common.

1.6 Further studies

The results of two companion studies are given in Chapter 5. The first deals with vertical atmospheric soundings from polar-orbiting satellites (TIROS Operational Vertical Sounder (TOVS)) over Antarctica and the Southern Ocean and their usage during the First Regional Observing Study of the Antarctic Troposphere (FROST).

The quality of TOVS was assessed against radiosonde data from several Antarctic and sub-Antarctic locations. The statistics presented in Chapter 5 indicate a sufficient degree of accuracy, particularly at high altitude, for the TOVS data to make a significant contribution towards the re-analysis programme of FROST.

Strong temperature inversions, known to be a problem in TOVS retrieval, are a particularly significant feature of the lower troposphere over the Antarctic ice sheet.

Errors in the derivation of TOVS over Antarctica are thought to be largely linked to the strength of the near-surface inversion.

The ABOM GASP system was used to assess the strength and distribution of the Antarctic inversion over the winter-spring period. The GASP depiction of the inversion (in strength and distribution) was found to be reliable compared to published observational and numerical modelling studies. The results of this work are included in Chapter 5.

CHAPTER 2

BACKGROUND

2.1 Introduction

Some background information is given here of the two primary tools discussed in this study.

(i) The scatterometer instrument provides a relatively new source of surface wind data derived from the ocean surface roughness. It is of particular value in the remote reaches of the Southern Ocean.

(ii) The ABOM GASP numerical assimilation and modelling system.

2.2 Scatterometer winds – origin, derivation and accuracy

ERS-1 has a sun-synchronous circular orbit with a period of 100.50 minutes. Each day fourteen full orbits are completed. The orbit is quasi-polar (98.52° inclination) with a mean altitude of 780km.

ERS-1 carries an Active Microwave Instrument (AMI). The AMI operates in three basic modes (Attema 1991):

(i) Imaging mode: The AMI is configured as a Synthetic Aperture Radar (SAR) with a nominal spatial resolution of 30m and swath width of 100km. The high output data rate of $105Mbs^{-1}$ precludes on-board storage so all data are immediately transmitted to Earth via an 8GHz data link. Data captured too distant from an operational ground station are lost.

(ii) Wave mode: The AMI is configured as a SAR but limited to provide images of 5km by 5km separated by 200km intervals along the sub-satellite track. The data rate is thus reduced to $345kbs^{-1}$ allowing for on-board storage. This configuration is designed primarily for the derivation of ocean wave patterns.

(iii) Wind mode: The AMI is configured as a wind scatterometer and provides three radar images of the ocean surface with a spatial resolution of 50km

and swathe width of 500km. The three images are acquired from different antennae aligned at 45°, 90° and 135° to the sub-satellite track.

This thesis concentrates on data from the AMI wind mode – the scatterometer.

Typically an aircraft or spacecraft mounted scatterometer records the backscattered radiation from a remote surface illuminated by a microwave pulse. The ERS-1 and ERS-2 satellites use successive 5.3GHz (λ = 5.66cm) pulses to illuminate a 500km wide sub-satellite swathe.

The technique of calculation of wind speed and direction from raw microwave backscatter data is complex. King and Turner (1997) provides further easy to read background information. Marshall and Turner (1997a), Marshall and Turner (1997b) and Turner and Thomas (1992) provide good examples of scatterometer data applications in the Antarctic region. Offiler (1994), Stoffelen and Anderson (1997b) and CERSAT (1996) give details of data derivation and expand on the explanation given here.

The AMI on the ERS-1 satellite includes a three antennae scatterometer instrument. The antennae are aligned at angles of 45°, 90° and 135° to the sub-satellite track respectively. The AMI uses the three antennae in turn to illuminate a 500km wide swathe of the ocean surface with successive 5.3GHz pulses. Pulse duration is 130μs with a repetition frequency of 98Hz (fore- and aft-beams); 70μs and 115Hz (mid-beam). The illuminated swathe lies between 200km to 700km aside of the sub-satellite track.

On return of the radar echo from the Earth surface signal strength from each of the three antennae is recorded, data are stored on-board and later transmitted to one of several ground stations for processing.

After a series of processing steps to calibrate and reduce data noise, a matrix of values, representing the normalised backscattering cross section (Long 1983) recorded by each of the three antennae, fore (45°), mid (90°) and aft (135°) respectively, is obtained. Hereafter the normalised backscattering cross section from the three antennae is termed σ°_{fore}, σ°_{mid} and σ°_{aft}.

The triplet of σ° values at each node across the 500km wide swathe is fitted to a complex model transfer function representing the empirical relationship between the three σ° values and the zonal and meridional components of the wind at 10m above the ocean surface, u_{10} and v_{10}. Figure 2.2.1 shows a schematic representation of this relationship.

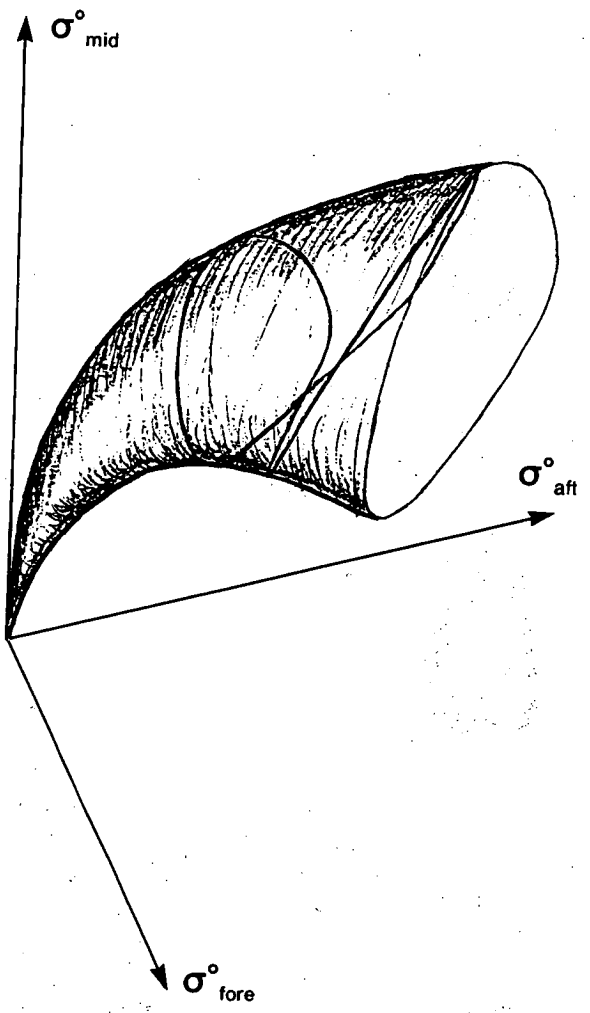

Figure 2.2.1 Simplified representation of the surface on which σ° triplets should lie for a given node. The surface actually consists of two skins that can intersect, but this is not shown in the schematic. A curve to represent constant wind speed, as though drawn on two intersecting skins, is shown. From Stoffelen and Anderson (1995), based on Cavanié and Lecomte (1987).

An exact solution for u_{10} and v_{10} is not generally obtainable. Rather, a set of up to four possible solutions, each representing a small departure from the model transfer function, is most commonly obtained. While all four solutions typically represent similar wind speeds (though not identical), wind directions are markedly different, with the better two usually representing solutions whose wind directions differ by approximately 180°. This is the basis behind the wind direction ambiguity problem frequently referred to in related literature. See Figure 2.2.2 for an example.

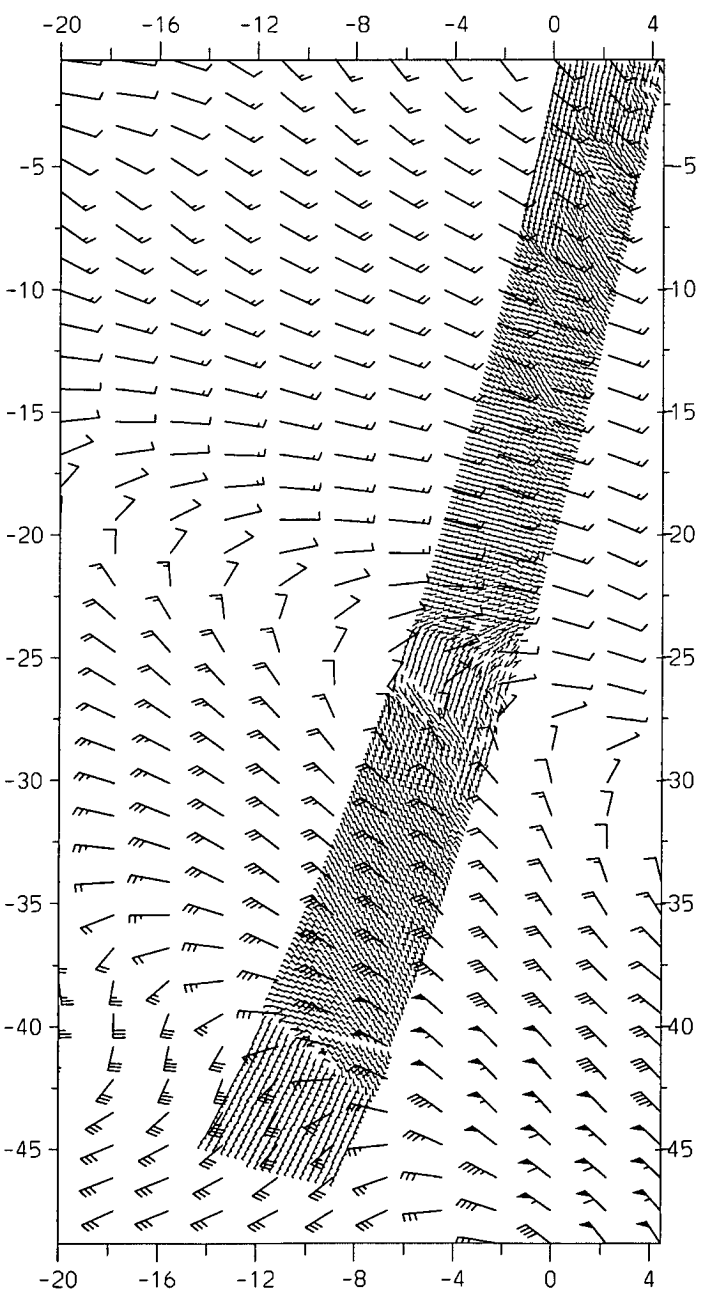

Figure 2.2.2
Example of scatterometer wind data (10m) plotted together with wind data from a co-incident GASP R53L19 analysis ($\sigma = 0.991$).
(Shown in knots where 1.0knot = 0.5148ms^{-1}).
Note the plots of inconsistent wind direction near 40°S.

The next step in the process is to choose one of the wind direction solutions. This requires consideration of the magnitude of the departure from the model transfer function, the continuity of wind directions over the swathe and, if necessary, the coincident wind direction from an independent NWP analysis system.

The numerous wind derivation systems in use around the world use different combinations of processes to deduce their final output.

In a final step sea ice contaminated areas are removed by elimination of all data whose backscatter properties exceed a pre-set threshold departure from the model transfer function.

Figure 2.2.3 shows a 24 hour sample of ERS-1 scatterometer coverage. Wind speed is shown over ocean areas.

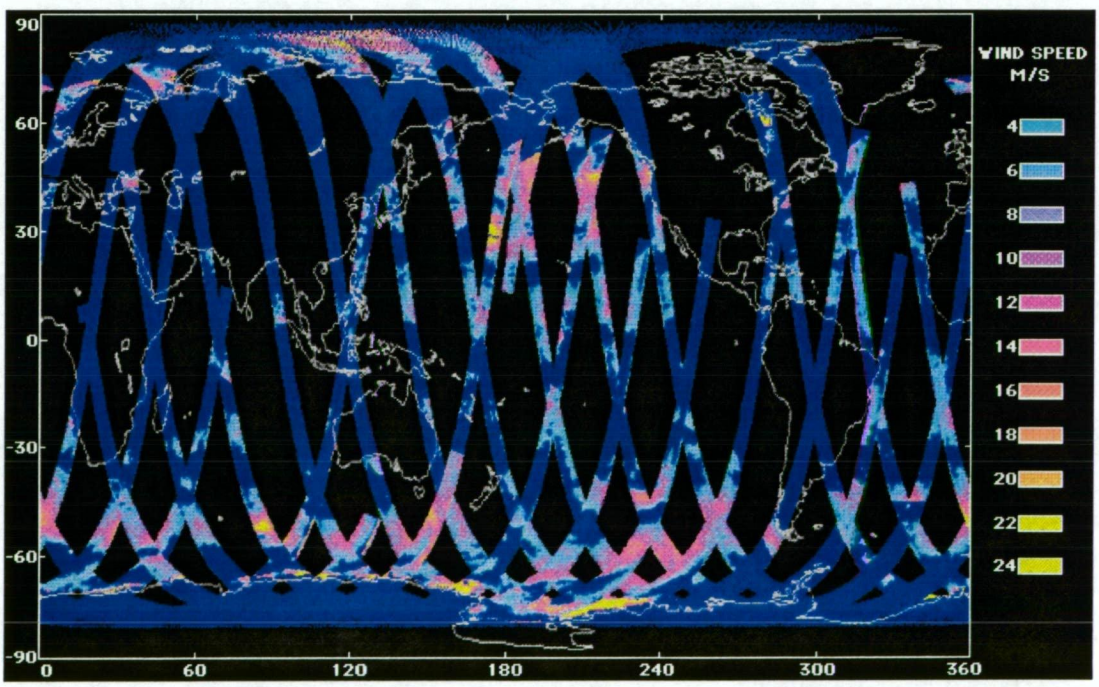

Figure 2.2.3 Sample of ERS-1 scatterometer wind speed data (ms^{-1}) showing the ground coverage of the instrument in 24 hours (reproduced from earth.esa.int). Winds cannot be calculated over land areas.

2.3 The GASP system

The Australian Bureau of Meteorology (ABOM) maintains a global spectral NWP system called GASP (Bourke et al. 1995, Seaman et al. 1995). The GASP system is an operational forecasting aid used for the one to seven-day outlook period.

The GASP system is a four-dimensional assimilation scheme consisting of analysis, initialisation and forecast cycles. The assimilation system merges atmospheric observational data into a dynamically consistent representation of the atmosphere. The forecast model then carries these data forward in space and time to produce an atmospheric forecast and provide a first guess for the next data assimilation process.

The input observational network for GASP includes surface pressure observations from meteorological stations, automatic weather stations, ships and drifting buoys; and upper-level observations from radiosondes and TOVS satellite soundings. An analysis first guess is provided by running the predictive model forward in time from the last completed analysis.

Observational data that differ from the first guess by more than a specified tolerance, and are not supported by neighbouring observations, are not used in the analysis.

The analysis technique is based on statistical interpolation that weighs both the forecasting model errors and observational errors to produce an analysis that statistically minimises the mean square deviation of the analysed value from the observed values. The method employs a six hourly forward assimilation.

After the assimilation and analysis process GASP employs a spectral prediction model to carry information forward in space and time.

The configuration of GASP has evolved substantially over the last decade including improvements to model physics, enhancements to assimilation methodology, and increases in horizontal and vertical resolution. Increases in available computing

power have allowed for large step-wise improvements over time without loss of processing speed.

The most important steps in the evolution of GASP are detailed in Appendix 2. A discussion of the forecast performance of GASP, and some historical comparisons between GASP and other global NWP systems, is given in Chapter 6.

The version of GASP used predominantly in this study and for the FROST period analyses was that introduced into operations in March 1994: The R53L19 system.

That system was run on a cyclic basis every six hours (at 0500UTC, 1100UTC, 1700UTC and 2300UTC daily) with a data cut-off of ±3 hours. The forecast model was run twice daily at 1100UTC and 2300UTC and produced output to 7 days.

ABOM also maintains several limited-area NWP systems nested in GASP output. Included in these is a recently developed regional grid point model, nested in GASP $T_L239L29$ output, providing high-resolution output over East Antarctica and neighbouring parts of the Southern Ocean. This model is currently undergoing tests in real-time (Adams 2001).

CHAPTER 3

SCATTEROMETER WIND DERIVATION AND ACCURACY

3.1 Introduction

The derivation of near-surface wind data over oceanic regions from a remote sensing satellite is highly complex. In the case of the ERS-1 and ERS-2 satellites the process involves microwave illumination of the ocean surface and interpretation of the reflected signal. To be useful in real-time meteorology the derivation system needs to be timely, accurate across the globe, reliable in both light and strong winds, and reliable in low or high ocean swell. Similarly, data contaminated by sea ice and other objects must be eliminated.

A major inventory of Antarctic and Southern Ocean meteorological data was conducted during the First Regional Observing Study of the Antarctic Troposphere (FROST). FROST was primarily a data gathering, analysis and evaluation project for which all available meteorological data, however observed or derived, were gathered and analysed. The study concentrated on the entire area south of 50°S during three one-month periods, namely 1 – 31 July 1994, 16 October – 15 November 1994, and 1 – 31 January 1995 (Turner et al. 1996).

During the re-analysis phase of FROST considerable use was made of wind information derived from ERS-1 scatterometer backscatter measurements. This source of satellite derived wind estimates was considered helpful for pin-pointing the location of cyclones and defining areas of strong winds during the re-analysis exercise (Hutchinson et al. 1999, Marshall and Turner 1999). It proved particularly valuable over the vast areas of the Southern Ocean devoid of conventional manual or automatic *in situ* meteorological measurements.

ERS-1 scatterometer winds were made available to analysts during the FROST manual reanalysis exercise. These were derived by the United Kingdom Meteorological Office (UKMO) via the CMOD4 model transfer function (Stoffelen

and Anderson 1997b) and a wind finding system developed by UKMO. Scatterometer winds were displayed in the form of plotted wind barbs on large analysis charts. While considered a valuable source of data for subjective analysis during FROST, it was noted that the winds were not always 100% reliable. There were recurrent problems in both wind direction and speed. Many instances of 180° wind reversal were identified. Scatterometer winds were generally relied upon as a last resort in areas devoid of any other data (Michael Pook and Lance Cowled, personal communication 1995).

Australian meteorologists, based in Australia and Antarctica, have used similar data for subjective real-time analysis for several years. Informal discussions have revealed similar problems with the ERS-1 wind data during the 1994 to 1996 period. The data in use at the time were derived via the CMOD4 algorithm and delivered direct from ESA.

3.2 Scatterometer wind accuracy – preliminary study

In the early stages of FROST the author conducted a survey of scatterometer wind accuracy in the area south of the Tasman Sea. Data were gathered from the area bounded by latitudes 45° and 60° South and longitudes 140° and 180° East (Figure 3.2.1) during the first FROST Special Observing Period (SOP1), July 1994. These were compared with coincident data from the ABOM GASP numerical analyses. GASP at that time was not making use of scatterometer winds.

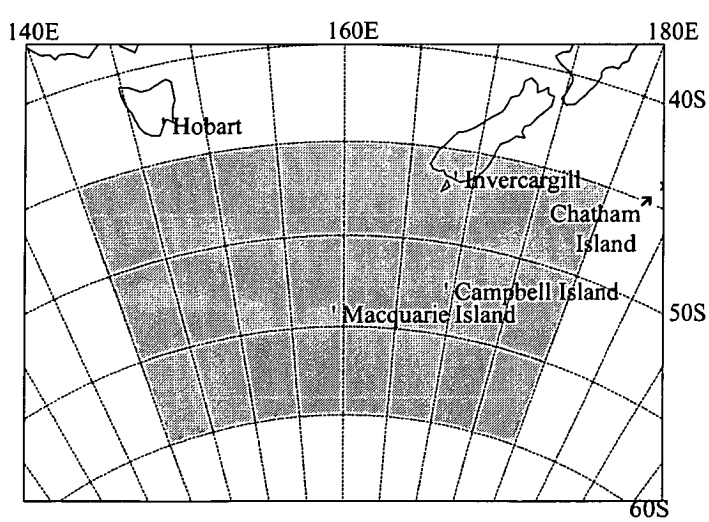

Figure 3.2.1
Study area bounded by latitudes 45° and 60° South and longitudes 140° and 180° East.

The area under study was entirely free of sea ice during the month. Several small islands lay within the area of interest, including Macquarie and Campbell Islands, where regular meteorological observations were recorded. The southern tip of New Zealand's South Island, including the meteorological station at Invercargill, also fell within the study area. MSLP reports from these stations were utilised by GASP, together with drifting buoy reports, TOVS, cloud drift winds and "bogus" MSLP reports. GASP analyses of this region were of high quality, relative to comparable global NWP systems, and provided a good source of data for comparison work.

ESA scatterometer wind data used in the study were the ESA "Fast Delivery Product" derived by ESA using the CMOD4 model transfer function. They represented wind speed and direction at 10m above the ocean surface.

The data from the GASP model used in the study were the meridional (u) and zonal (v) component winds at the $\sigma = 0.991$ level (approximately 75m above sea level) where $\sigma = P / P_{surf}$. Data from the daily 1100 and 2300UTC analyses were used for the comparison work.

GASP wind speed data were reduced to account for the speed difference between the $\sigma = 0.991$ level and 10m. A quick review of literature on the Ekman Spiral (for example Humphreys 1929) indicated that a simple static correction factor would suffice for the purposes of this preliminary study to relate the wind speed at 10m (V_{10}) to that at 75m (V_{75}) by:

$$V_{10} \approx \frac{V_{75}}{1.31}$$

This assumes a uniform surface roughness and uniform atmospheric boundary layer stability profile. There is, of course, the further assumption that $\sigma = 0.991$ at 75m. At this early stage in the project no Ekman Spiral-type correction was made for wind direction.

The choice of study area was controlled by the desire that the data from the two sources be approximately coincident in time. The chosen area was re-visited by the ERS-1 satellite at times close to the GASP model run times. An extension of the

study area to the West (or East) would have only added scatterometer data several hours older (or newer) than the comparison GASP analyses. The area was limited to the north by Australia and New Zealand and to the south by sea ice.

Scatterometer wind data outside an envelope of ±1½ hours from GASP input times were removed. Just over 40% of data remained for analysis. Scatterometer data recorded between 0930 and 1230UTC were compared with nearest-neighbour GASP data from the daily 1100UTC model run; scatterometer data recorded between 2130 and 0030UTC were compared with nearest-neighbour GASP daily 2300UTC data. GASP data were interpolated on to a 0.5° x 0.5° grid.

Figure 3.2.2 shows the distribution of the *u* component of GASP winds versus the corresponding *u* component of scatterometer data. Figure 3.2.3 is a similar

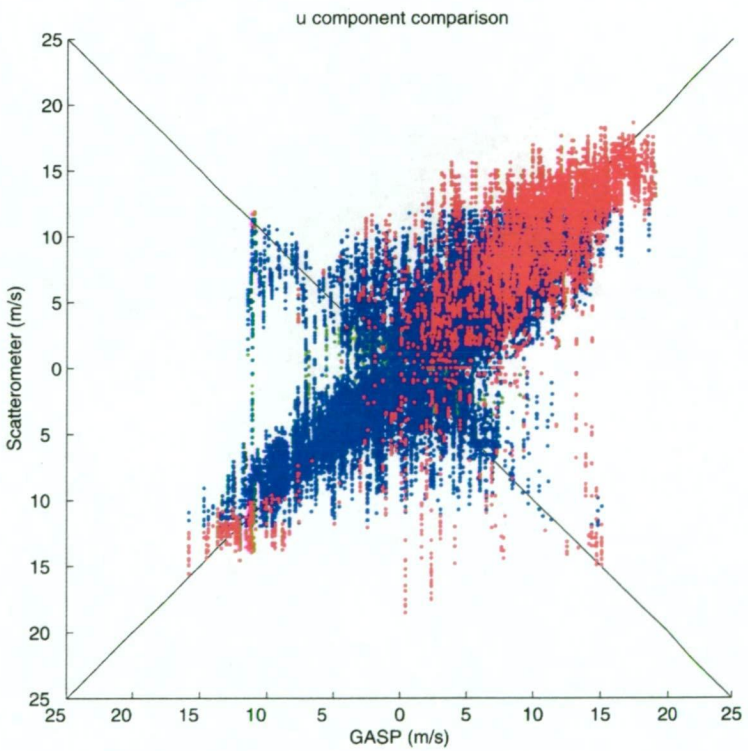

Figure 3.2.2 GASP *u*-component (scaled to 10m) verses scatterometer *u*-component (10m) from July 1994. (ms^{-1}).
Green: Scatterometer wind speed less than $4ms^{-1}$.
Blue: Scatterometer wind speed between 4 and $12ms^{-1}$.
Red: Scatterometer wind speed greater than $12ms^{-1}$.

presentation of *v* component data. In both cases the distribution of data shows close agreement between the two independent sets. In these plots colour is used to distinguish between light, moderate and strong scatterometer wind strength.

Plots of wind speed greater than $12ms^{-1}$ (shown in red) on Figures 3.2.2 and 3.2.3 tend to show good agreement between GASP and scatterometer. A far greater degree of scatter is shown amongst low speed plots.

This finding is highlighted on the three Figures 3.2.4. They indicate little or no relationship between the wind direction from the two sources when scatterometer wind speed is less than $4ms^{-1}$. The smaller population of scatterometer plots with wind speed greater than $12ms^{-1}$ indicate good wind direction agreement with coincident GASP data. The majority of plots (speed between 4 and $12ms^{-1}$) indicate an acceptable level of agreement and largely within the objective ±20° range.

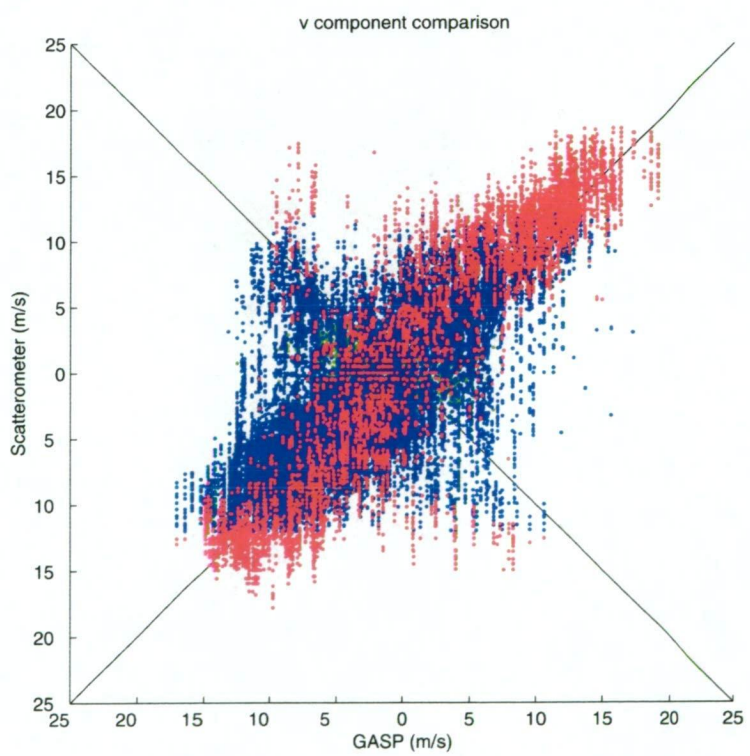

Figure 3.2.3 GASP *v*-component (scaled to 10m) verses scatterometer *v*-component (10m) from July 1994. (ms^{-1}).
Green: Scatterometer wind speed less than $4ms^{-1}$.
Blue: Scatterometer wind speed between 4 and $12ms^{-1}$.
Red: Scatterometer wind speed greater than $12ms^{-1}$.

In all three plots (Figures 3.2.4) a minor peak is seen along the 180° offset line. Those plots represent scatterometer wind direction exactly opposite to corresponding GASP wind direction. This well documented wind direction ambiguity problem was common in CMOD4 derived data (Gonzales and Long 1999, Stoffelen and Anderson 1997a). An example is given in Figure 2.2.2. Here it was found that approximately 3.4% of direction difference plots fell between 150° and 210°.

The 'arms' of data points aligned at right angles to the main distribution on Figures 3.2.2 and 3.2.3 were further evidence of the wind direction ambiguity problem.

A test was made involving the imposition of a 180° wind direction shift on data in the range 150° to 210°. This produced an improved correlation, but not a complete removal of outlying data.

Worthy of note is the prevalence of *u* component data (Figure 3.2.2) in the 0 to $+15ms^{-1}$ range and of *v* component data (Figure 3.2.3) in the 0 to $-15ms^{-1}$ range. This is due to the dominance of low-level northwest winds over the area of interest during the month. This is also shown in Figures 3.2.4. The greatest densities of data are in the regions corresponding to wind from the northeast, northwest and southwest with relatively few observations of wind from the southeast.

A comparison of GASP wind speed (corrected to 10m) verses ESA 10m wind speed data is shown in Figure 3.2.5. This figure shows collective data from the full study area and period – unfortunately insufficient to obtain any data above about $22ms^{-1}$. A detailed study of the wind speed relationship between the GASP 75m and ESA 10m data is hampered by the complexity of the structure of the lower atmosphere. While the data available in this preliminary study were insufficient to make a detailed quantitative assessment of the ESA wind derivation system, it was sufficient to conclude that broad agreement exists between the two data sets.

Wind speed data were also analysed separately for each model run. Close agreement was found between the GASP and ESA data at the higher wind speeds, but a trend indicating slightly poorer agreement at lower wind speeds was again identified. Daily variation in results tended to be small.

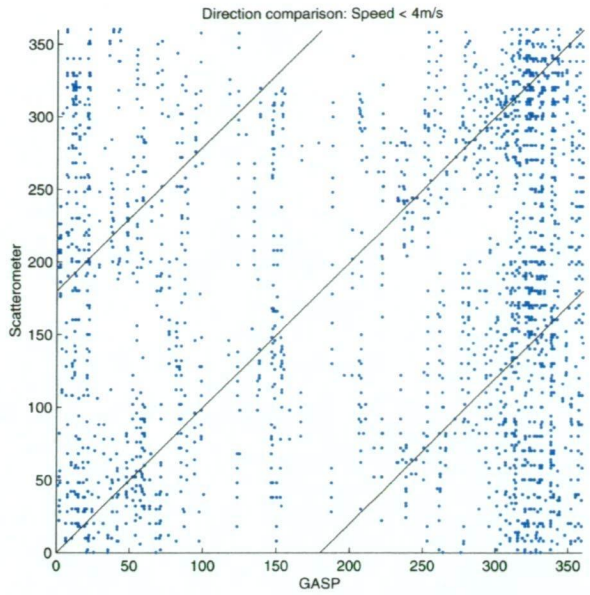

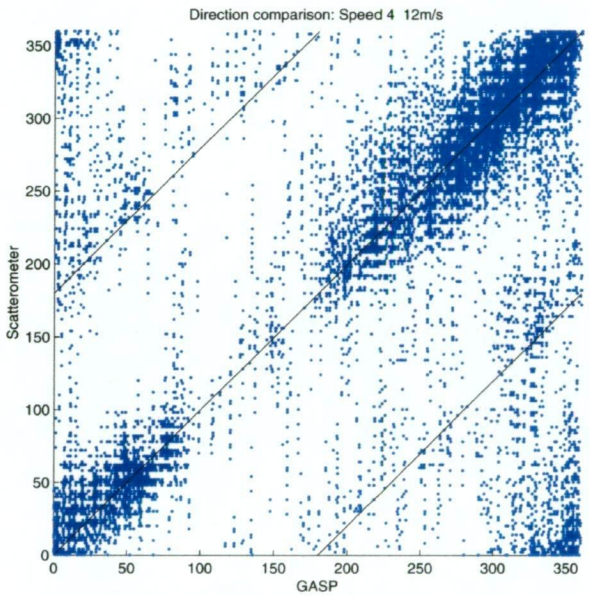

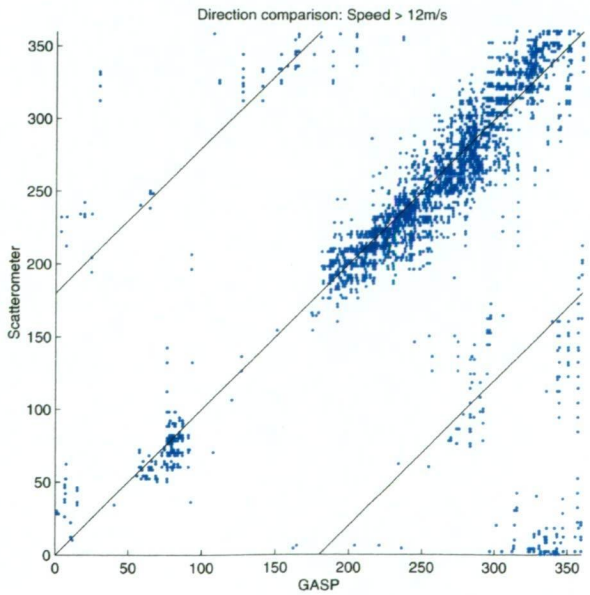

Figure 3.2.4

GASP 75m wind direction verses scatterometer 10m wind direction from July 1994. Ruled lines represent direction differences of −180°, 0° and +180°.

Top:

Scatterometer wind speed less than 4ms^{-1}.

Middle:

Scatterometer wind speed between 4ms^{-1} and 12ms^{-1}.

Bottom:

Scatterometer wind speed greater than 12ms^{-1}.

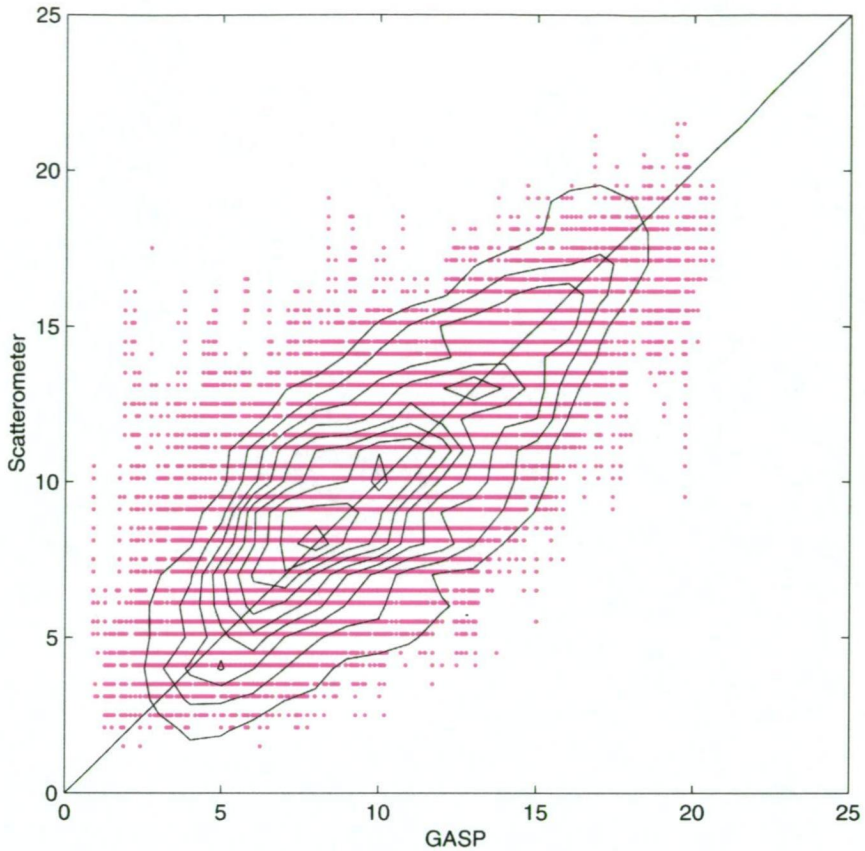

Figure 3.2.5 GASP wind speed (scaled to 10m) verses scatterometer wind speed (10m) from July 1994 (ms^{-1}). Contours represent deciles of population from 1 to 9.

3.3 Comparison between scatterometer derivation systems

During the FROST re-analysis exercise ERS-1 winds were primarily used to assist with subjective mean sea level pressure analysis of the ocean area south of 50°S. Analysts were provided with ERS-1 scatterometer wind data generated by the United Kingdom Meteorological Office (UKMO). They took the form of printed wind barbs on operational manual analysis charts (Turner et al. 1996).

The UKMO derived data were generated via use of the CMOD4 model transfer function and a UKMO developed wind direction ambiguity removal algorithm. UKMO perform wind retrieval in-house to ensure that the most up to date model background winds as an integral part of the ambiguity removal process (Bell 1994).

The years since the FROST data collection activities have seen further refinement of scatterometer wind generation algorithms. The Institut Français de Recherche pour l'Exploitation de la Mer (IFREMER), in partnership with the Centre ERS d'Archivage et de Traitement (CERSAT), the Centre National d'Etudes Spatiales (CNES), METEO FRANCE and ESA, has developed an algorithm to process ERS-1 and ERS-2 scatterometer winds off-line. These wind data (hereafter IFREMER) have been re-processed for several of the years of operation of the ERS-1 and ERS-2 scatterometers, including the periods of the FROST SOPs.

The stated accuracy of the IFREMER data is $\pm 2 ms^{-1}$ or 10%, whichever is greater, for wind speeds in the range 1 to $28 ms^{-1}$. No claims are made for higher values of wind speed. Wind direction accuracy is ±20° (CERSAT 1996). For this study data were obtained in compressed form on compact disk. A detailed description of the backscatter model transfer function, the wind direction ambiguity removal algorithm and other details are given in CERSAT (1996).

The published accuracy of wind speed data retrieved by the CMOD4 model transfer function is similar to that from CERSAT / IFREMER but only over a range of 4 to $24 ms^{-1}$ (King and Turner 1997). The CMOD4 data used in this study, including all possible solutions of wind direction, were also obtained from the CERSAT compact disk archive.

The work described in this chapter includes an analysis of CMOD4 and IFREMER data in comparison with analysed wind data from the ECMWF global model. The ECMWF analysis wind speeds used in this study were deduced without any wind scatterometer input (Didier Lemeur, personal communication 1997).

An analysis was completed for each of four one-month periods: 1 – 31 July 1994, 16 October – 15 November 1994, 1 – 31 January 1995, and 1 – 31 July 1995. The first three were the SOPs of FROST and the fourth was the period studied during the impact trial discussed in Chapter 4 of this thesis.

Scatterometer data have been analysed and compared over the area of the Southern Ocean between 40° and 65° South. This area was mostly free of sea ice throughout

all four of the one-month periods under study. It was also predominantly free of land. Where land or sea ice occurred the scatterometer data were omitted from the analyses.

This area is noted as having one of the strongest wind regimes of any ocean area on the globe. Swell patterns are known to be particularly complex here. The area thus provides a rigorous test bed for scatterometer wind finding systems. Figures 3.3.1 and 3.3.2 show the mean global distribution of wind speed and wave height. These fields were derived from three years of global GEOSAT data following a series of validation tests against *in situ* measurements (Young and Holland 1996).

Figure 3.3.3 shows the mean wind speed difference (ms^{-1}) between scatterometer wind data derived via the CMOD4 model transfer function and ECMWF analysis wind speed (July 1994). The data shown were analysed on a 1° by 1° grid between 40° and 65° South only. Regions of sea ice and land contamination have been removed. Positive values, shown in blue, represent regions where mean monthly scatterometer wind speed was greater than the mean monthly ECMWF wind speed. Negative values, red, show areas where the converse was true.

There are several factors to consider when attempting to interpret the results in Figure 3.3.3. Areas of greatest difference, positive or negative, may represent regions where the wind finding system has failed to accurately determine wind speed. Being such a complex wind determining process this could be for any of a number of physical or computational reasons. But the comparison is made against an imperfect control – the ECMWF analyses. A great deal of care needs to be taken in the manner in which we assess the scatterometer winds. The possibility exists that the ECMWF analysis wind data were not entirely accurate and the large differences shown represent the failing of the ECMWF system to represent the true wind field. It is more likely that the signal represented in the diagram shows a combination of both of the factors described. The reader is reminded that the ECMWF analysis wind speed data used in this study were deduced independently from any wind scatterometer input.

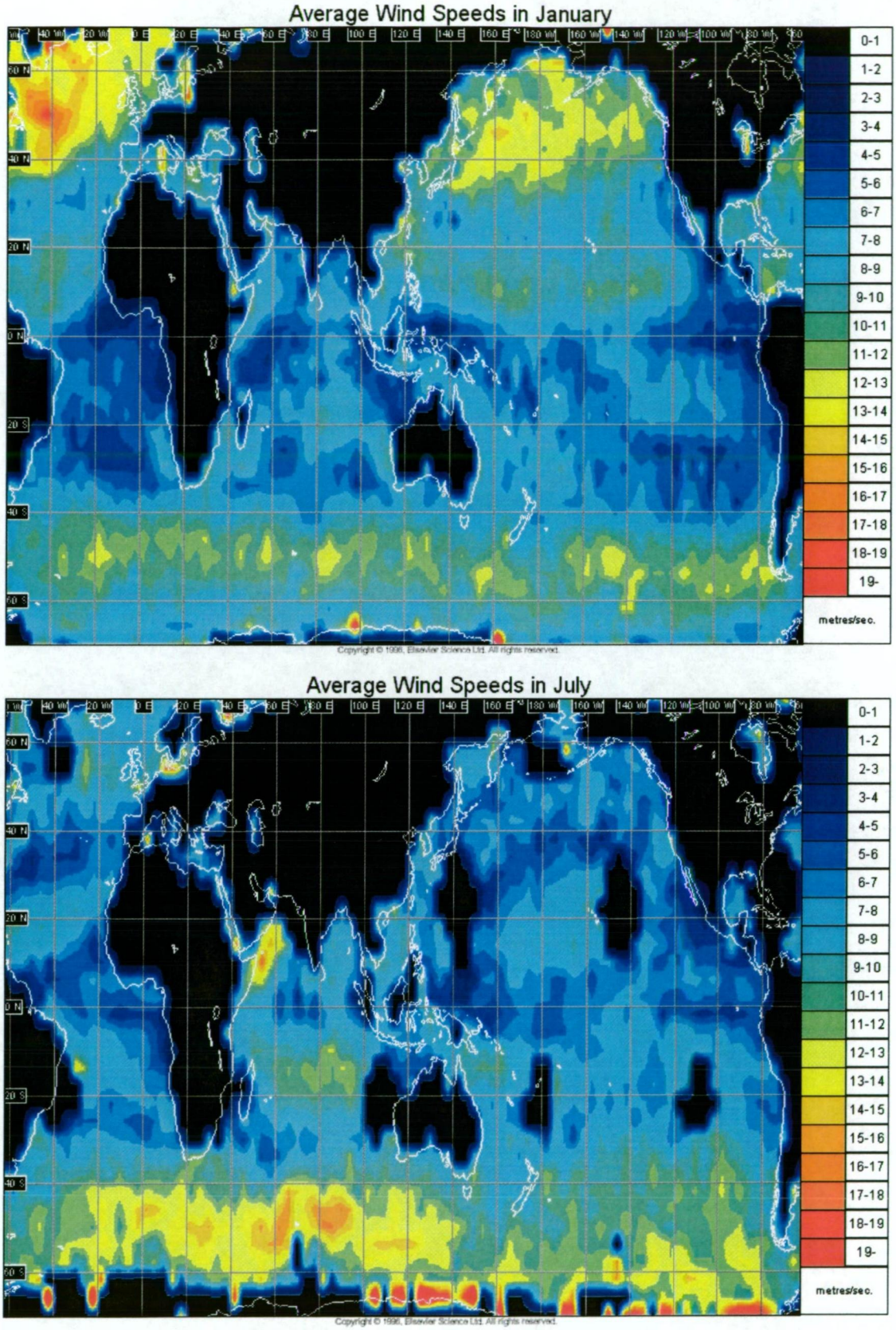

Figure 3.3.1 Global distribution of average **wind speed** for January (top) and July (bottom) derived from three years of GEOSAT altimeter data (from Young and Holland 1996). (ms^{-1}).

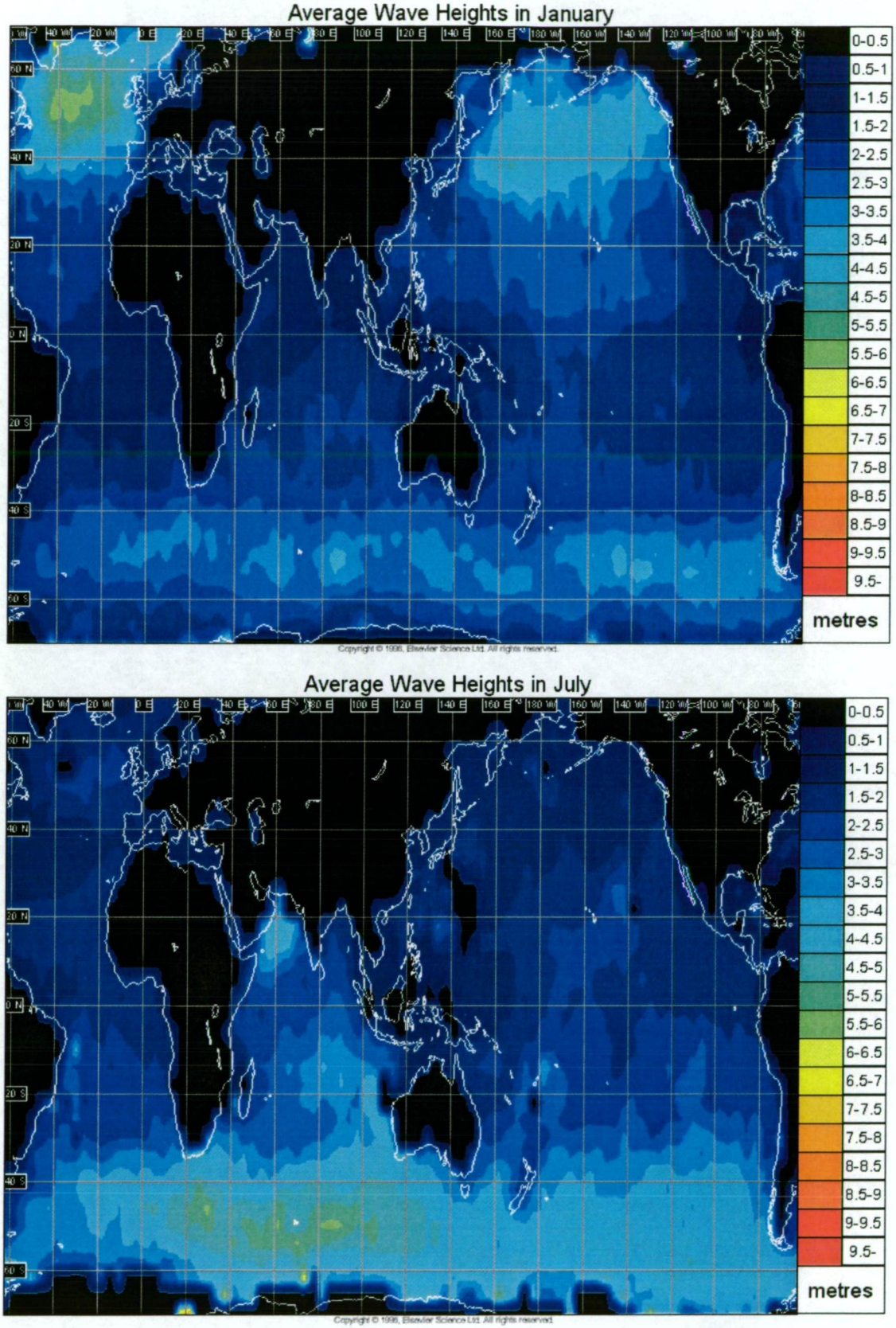

Figure 3.3.2 Global distribution of average **significant wave height** for January (top) and July (bottom) derived from three years of GEOSAT altimeter data (from Young and Holland 1996). (m).

Several island meteorological stations and drifting buoys in the Southern Ocean frequently report mean sea level pressure. During the period of FROST, radiosonde data were also available from these islands: Amsterdam, Campbell, Chatham, Macquarie, Marion, Kerguelen, Falkland and Gough. A more comprehensive listing of MSLP and upper-air reporting locations is shown in Appendix 1.

It is reasonable to expect that the ECMWF wind field would be more accurate near regularly reporting islands and buoys. The scatterometer wind field would only be affected by relatively large islands.

Relatively large differences are shown between the scatterometer wind speed and ECMWF analysis wind speed in the eastern Pacific zone of the Southern Ocean. There are no meteorological stations in that area, nor were there any drifting buoys during the period. Other areas of the hemisphere devoid of surface meteorological reports similarly coincided with relatively poor agreement between the scatterometer data and ECMWF. This hints at the possibility of a poor quality in the ECMWF data relative to the scatterometer in these regions. However not all areas from which meteorological reports were available coincided with good agreement between the scatterometer and ECMWF.

A recurring pattern of stronger sctterometer winds at relatively high latitudes, and weaker scatterometer winds at relatively low latitudes, (compared to ECMWF) appears across much of the Atlantic and Indian Ocean sectors. Also notable is the tendency for scatterometer winds to be stronger than ECMWF in the eastern half of the Pacific Ocean sector. Possible explanations include:

(i) ECMWF may be under-analysing the intensity of low-pressure systems in regions of poor data coverage, hence the poor match with scatterometer data in areas distant from *in situ* observations; and

(ii) The scatterometer algorithm may be providing wind speeds slightly too weak in high wind speed synoptic patterns, hence causing a less than perfect agreement in areas of good *in situ* observational coverage.

Some further evidence to support the latter emerges during data assimilation work detailed in Chapter 4.

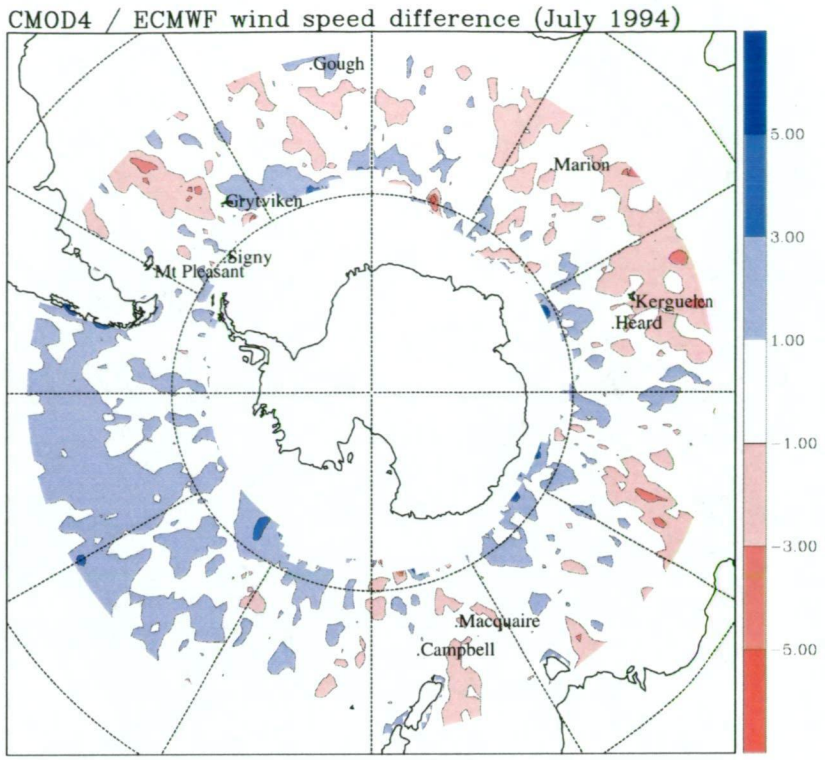

Figure 3.3.3 Mean (July 1994) CMOD4 derived scatterometer wind speed minus ECMWF co-located model wind speed. (ms^{-1}).

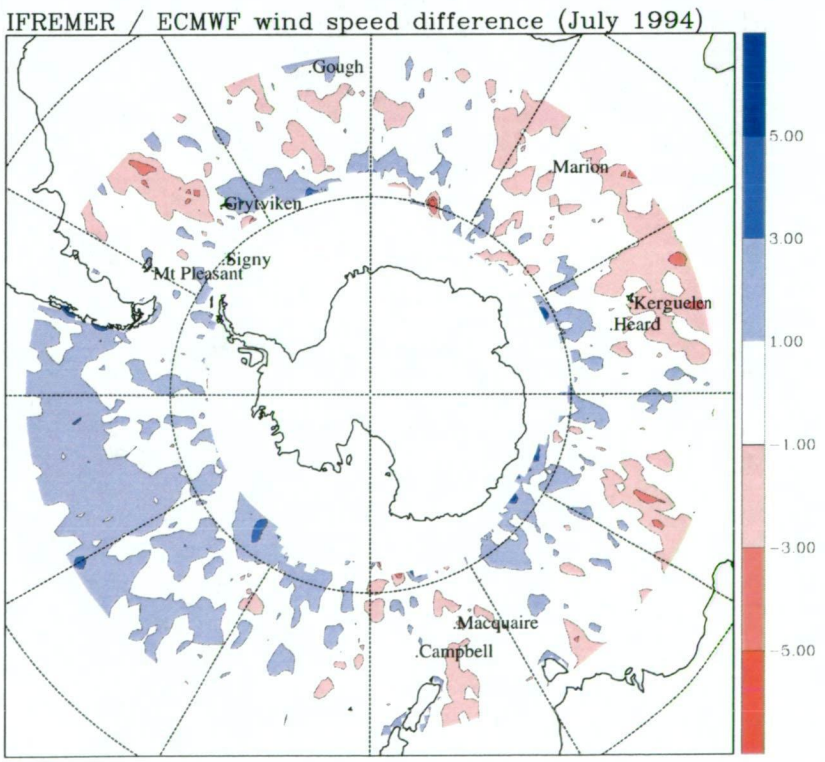

Figure 3.3.4 Mean (July 1994) IFREMER derived scatterometer wind speed minus ECMWF co-located model wind speed. (ms^{-1}).

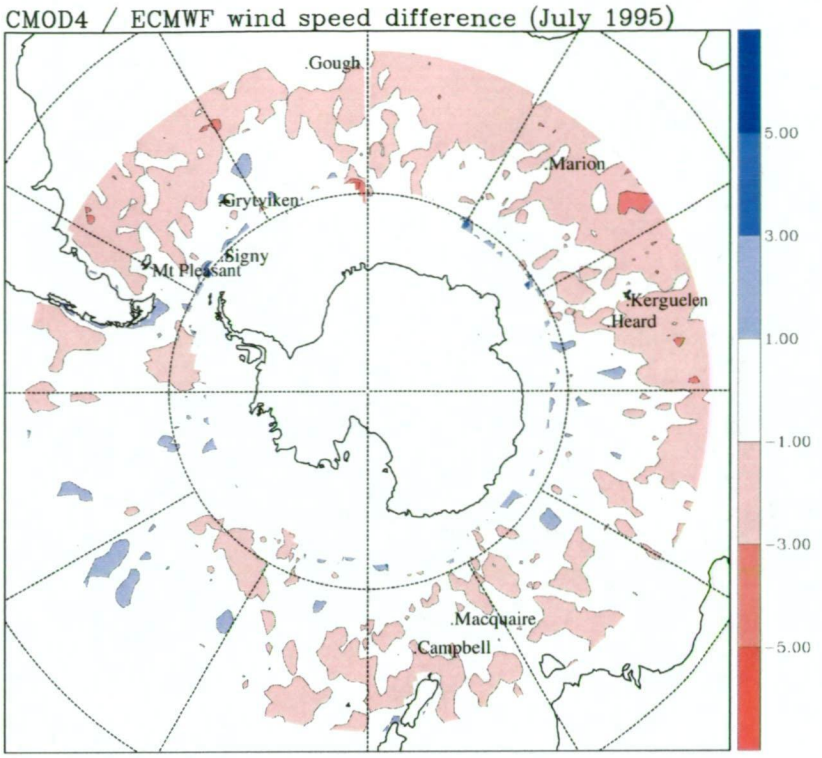

Figure 3.3.5 Mean (July 1995) CMOD4 derived scatterometer wind speed minus ECMWF co-located model wind speed. (ms^{-1}).

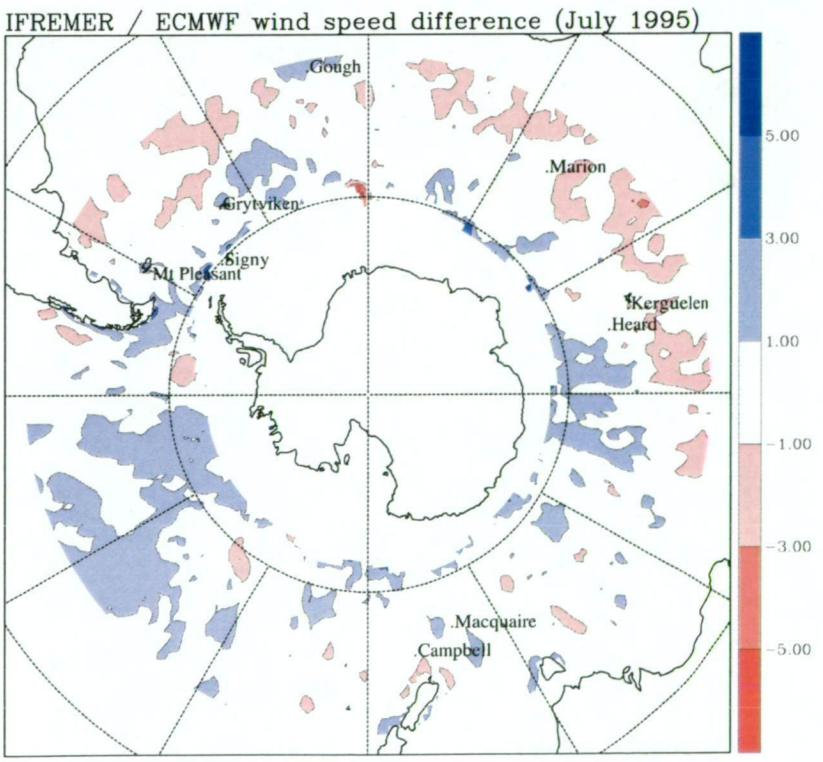

Figure 3.3.6 Mean (July 1995) IFREMER derived scatterometer wind speed minus ECMWF co-located model wind speed. (ms^{-1}).

The significance of Figure 3.3.3 is that it highlights areas where a breakdown in CMOD4 derived scatterometer wind data may have occurred. It is suggested that the accuracy of some of the FROST re-analysis charts may be affected by this result. The difference field, shown in Figure 3.3.3, should be used as a guide in determining areas of reduced confidence in the FROST analyses.

A similar presentation of scatterometer / ECMWF analysis wind speed differences to Figure 3.3.3 is shown in Figure 3.3.4, but IFREMER derived wind speed data are used in place of data derived via the CMOD4 model transfer function. The differences between Figure 3.3.3 and 3.3.4 are minor.

Comparisons for the other one-month periods under study show similar results and close similarity between the CMOD4 and IFREMER data (not shown). The exception is the July 1995 period. Figures 3.3.5 and 3.3.6, showing CMOD4 verses ECMWF and IFREMER verses ECMWF comparisons respectively, highlight some differences worthy of discussion. These are mostly within the range $\pm 2 ms^{-1}$ and tend to indicate CMOD4 winds as marginally low compared to both ECMWF and IFREMER.

It is important to note that a software processing upgrade occurred at IFREMER shortly prior to the July 1995 study period – a step from software versions 2.1 and 2.2 to the version 3.2. This upgrade was apparently designed to simplify and improve the wind direction ambiguity removal process (CERSAT 1996) but, from the results presented here, appears to also have generated some improvement in wind speed results. This is not altogether unexpected since the several alternative u_{10},v_{10} pairs, from which the ambiguity removal process selects one, do not all represent exactly the same wind speed. Thus an improved choice of u_{10},v_{10} pair would result in an improved representation of wind speed, not only wind direction.

Another point to raise is that there were significant meteorological differences between the months of July 1994 and July 1995. During July 1995 mean sea level pressure anomalies across the Southern Ocean were large with mean anomalies reaching -17hPa near New Zealand and +28hPa off the coast of Marie Byrd Land, Antarctica. The subsequent anomaly in the wind field was particularly significant in the South Pacific Ocean sector and waters adjacent to Antarctica (Figure 3.3.7).

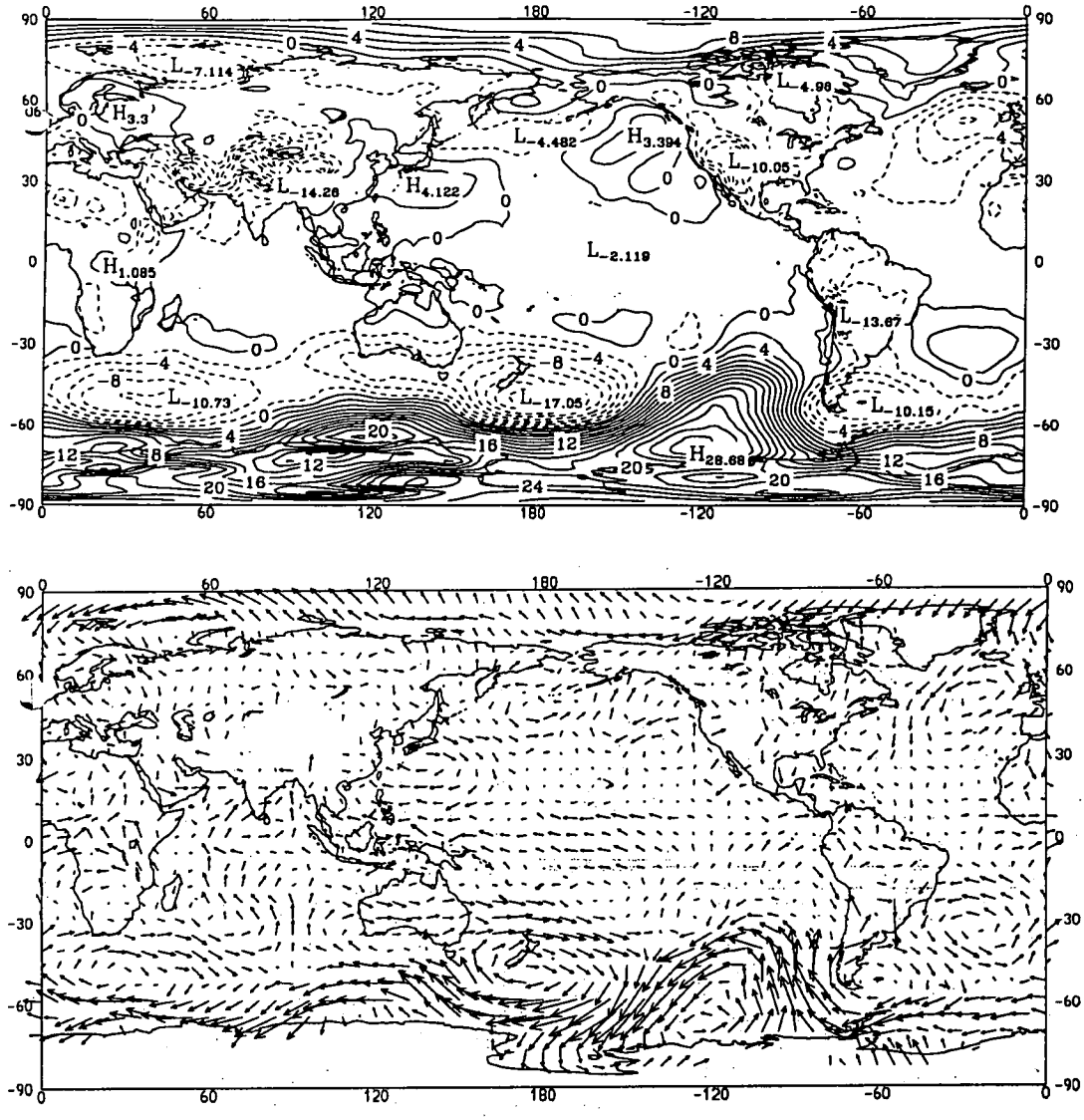

Figure 3.3.7 **Top:** Mean sea level pressure anomaly for July 1995. (hPa). **Bottom:** Schematic 850hPa wind anomaly for July 1995. (From NCC 1995).

The nature of the anomaly across the hemisphere suggests a weaker than average polar trough and a dampening of the common gales across much of the Southern Ocean. The month of July 1994 was closer to average (NCC 1994, NCC 1995). The difference between the months is not of direct concern to the study of scatterometer wind finding systems and their relative differences. But the reader should be aware of this difference while comparing the figures. It could explain some of the lessening of scatterometer verses ECMWF differences shown in both Figures 3.3.5 and 3.3.6. It could also explain much of the difference observed

between Figures 3.3.3 and 3.3.5: the two CMOD4 verses ECMWF difference fields. The possibility was flagged earlier, with reference to Figure 3.3.3, of ECMWF analyses tending to under estimate the high wind speed characteristics of July 1994.

Direct comparison is made between CMOD4 and IFREMER derived wind speed data in Figures 3.3.8. The July 1994 results indicate substantial speed differences between the wind finding systems in only 1 per 15000 data (±15% at high speeds and ±20% at low speeds). Agreement was lower in July 1995 following the installation of the updated processing algorithm at IFREMER.

Unfortunately no data were available during this study to simultaneously compare the differences between the IFREMER version 2.1/2.2 to version 3.2 products. However it is considered reasonable that the latter, derived via an updated algorithm, was thought to be of greater accuracy by the data suppliers.

For completeness a mention will be made of wind direction accuracy. An analysis of IFREMER (version 3.2) wind directions compared with ECMWF model wind directions was performed. Figure 3.3.9 shows the distribution of wind direction differences between the IFREMER scatterometer winds and ECMWF winds for July 1995. The major peak at ~0° represents useful agreement between IFREMER scatterometer winds and ECMWF. The secondary peak at ~180° represents erroneous scatterometer data contaminated by the up-wind / down-wind ambiguity problem. The remaining two peaks, at ~±90°, represent the small population of erroneous scatterometer data from the third and fourth solutions of the wind direction selection process. These erroneous data accounted for ~1.8% (~180° error) and ~0.3% (~±90° error) of the population respectively.

Interestingly, the three additional peaks on Figure 3.3.9 were not exactly centred at 180°, +90° and –90°. It is known, from Stoffelen and Anderson (1997b) and other references, that the four most likely wind direction solutions from raw backscatter measurements are not exactly perpendicular to one-another. Some discussion of this problem was given in Chapter 2.

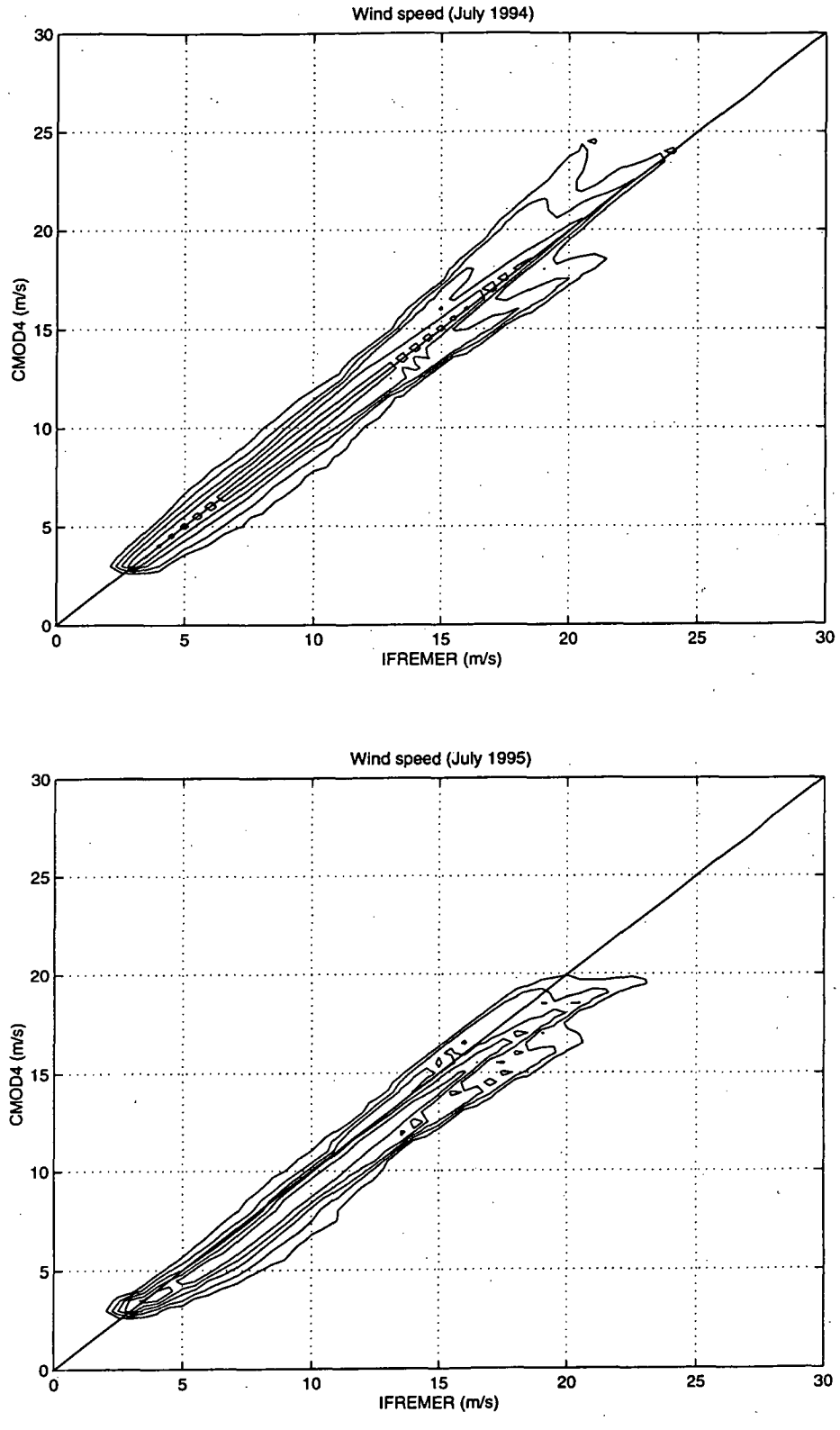

Figure 3.3.8 CMOD4 scatterometer wind speed verses IFREMER scatterometer wind speed from July 1994 (top) and July 1995 (bottom) (ms^{-1}). Contours represent percentiles of data population of 10^{-4}, 10^{-3}, 10^{-2}, 10^{-1} and 10^{0}.

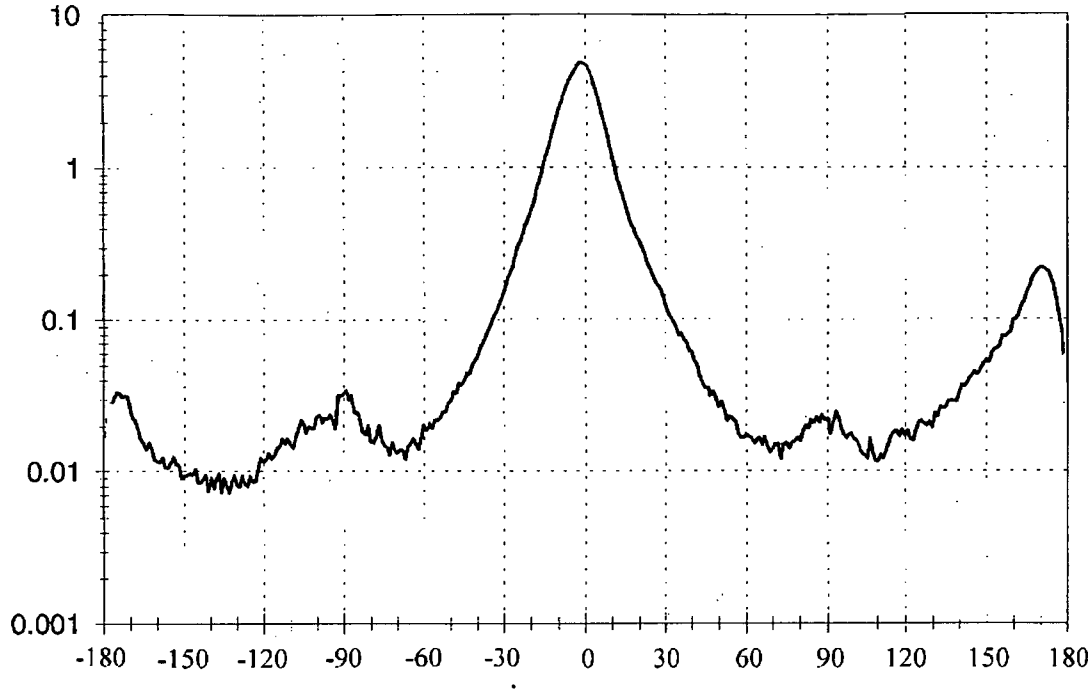

Figure 3.3.9 IFREMER scatterometer wind direction minus ECMWF wind direction represented in the form of a percentage frequency histogram (2° bins) with a logarithmic scale. Four peaks are evident, representing the four alternative wind direction solutions obtainable from the scatterometer model transfer function.

These wind direction errors were identified in spite of the use, at IFREMER, of a wind direction finding system reliant on input from background meteorological fields. During the periods under study those fields were the ECMWF analyses. The ESA wind field (CMOD4) was a fast delivery product whose development was independent of background meteorological fields.

In choosing a suitable source of data for use during the FROST re-analysis exercise many participants argued strongly that a source of data whose development relied on input from a numerical model was a less desirable source of data than one whose development was free of any model input. This philosophy followed the principle that if the development of the FROST manual re-analysis charts had some degree of input from any of the numerical modelling systems it would be of less value as a test-bed for comparison with numerical model output at a later date. It follows that CMOD4 data offered value to FROST that IFREMER data could not. Others

supported the multivariate approach where all available input would be considered in order to deduce the best product possible. The use of numerical techniques, it was argued, would add considerable value to the products and overcome many of the difficulties encountered by manual analysts.

As demonstrated in Chapter 4 of this thesis, numerical techniques also allow for the assessment of the relative value and impact of alternative data inputs by performing assimilation and analysis cycles with different combinations of observational data.

3.4 Summary of results

Here two independent experiments aimed at assessing the accuracy of ERS-1 scatterometer wind data were presented. The focus was specifically on the Southern Ocean region.

A slight low bias was identified in the scatterometer winds derived via the CMOD4 algorithm (Stoffelen and Anderson 1997b). The bias was more evident in strong wind events across the Southern Ocean. Scatterometer winds derived via the IFREMER algorithm (CERSAT 1996) showed signs of superior accuracy and negligible bias in comparison with ECMWF model winds.

From a population of CMOD4 data, approximately 3.4% appeared to be erroneous in wind direction by ~180°. This preliminary result was ascertained via comparison with GASP model winds across the Southern Ocean. Further comparative work, involving ECMWF winds, identified approximately 1.8% of a population of IFREMER derived scatterometer data were erroneous by ~180°. A further 0.3% (approximately) of data were erroneous by ~±90°.

The geographic distribution of disagreement between ECMWF and scatterometer winds (both CMOD4 and IFREMER) highlighted different levels of agreement across various parts of the Southern Ocean. A relationship was identified between the coverage of *in situ* observations and the extent of disagreement between ECMWF and scatterometer winds. It was inferred that the ECMWF system might have been under-analysing the intensity of some deep low-pressure systems.

For the most part, scatterometer winds were found to be sufficiently reliable in a broad range of conditions and geographic locations across the Southern Ocean for weather analysis and forecasting applications.

The fact that the derivation of scatterometer u,v from radar backscatter data is not dependent on location (apart from the necessity to remove land or sea ice contamination) leads to the conclusion that any systematic geographic bias, in comparisons between scatterometer winds and NWP winds, is more likely attributed to the latter. It is known that different ocean areas experience consistently stronger winds and higher swells that other ocean areas, and it is apparent that scatterometer data are less reliable in higher wind speed conditions. This can lead to an apparent systematic geographic bias in scatterometer data.

Based on the work presented here, their reliability was considered sufficient for the purposes of the FROST surface re-analysis work, and should be considered for inclusion in routine operational analysis and forecasting.

CHAPTER 4

SCATTEROMETER WIND IMPACT STUDIES

4.1 Introduction

Meteorological data from remote areas of the globe are of particular interest to the atmospheric modelling community. For Australian medium-range weather prediction, the sparseness of data over the Southern Ocean is a substantial problem that directly affects skill, but it is difficult to determine the magnitude of this effect without access to more comprehensive data.

The advent of Earth observing satellites has brought an improvement to the data coverage across the large oceans. The impact of these data is greatest over the southern hemisphere. But the assimilation of wind data into a numerical model is non-trivial. Furthermore, the complexity of the atmospheric boundary layer makes near-surface wind data all the more difficult to assimilate. Near-surface wind speed and direction are constrained by the roughness, orientation and steepness of the surface terrain. The wind speed profile is also affected by atmospheric stability and moisture distribution. Wind direction is also effected by Ekman spiral considerations. Consequently, near-surface wind reports from conventional meteorological stations, ships, buoys and AWS are not used in the GASP system. However, "cloud drift winds", estimates of wind velocity derived from cloud displacement between successive satellite images, have been used successfully for some time. That data assimilation methodology has been employed in this study for the treatment of scatterometer winds.

A number of studies have investigated the impact of scatterometer wind data in NWP systems. Notably the bulk of work to date has been concentrated in northern hemisphere research centres and largely focused on European and North American forecasting priorities. The work in this thesis represents the first trial of scatterometer data in the ABOM operational forecasting systems. It also represents

the first scatterometer wind impact experiment focused on the analysis and forecasting problems of Antarctica and the Southern Ocean.

In this study two experiments were undertaken to assess the impact of scatterometer wind data from the ERS-1 satellite on the ABOM GASP System.

This work was not intended to constitute an exhaustive study of the usefulness of scatterometer winds in the GASP system. Rather, it was a preliminary trial to assess the possible value of including the scatterometer winds in routine analyses and an attempt to estimate the likely degree of impact of their use.

The data used were wind speed and direction estimates at 10m above sea level across the entire globe. They were generated by ESA via the CMOD4 model transfer function (Stoffelen and Anderson 1997b). An ESA developed wind direction finding system was used to overcome wind direction ambiguity problems. The data were delivered to the ABOM via the Global Telecommunications System (GTS) in close to real time. The temporal extent of the trial was one month: July 1995.

Earlier work involving SASS and ERS-1 data formed the initial motivation for this study.

Ingleby and Bromley (1991) tested the impact of SASS data on a UKMO NWP system operating on 15 σ levels with the lowest at $\sigma = 0.997$ (approximately 25m). The data assimilation used a 3-D univariate statistical interpolation scheme. The forecast model was a global finite-difference model with a grid of 1.500° latitude by 1.875° longitude. The authors reported a low-level wind speed bias, SASS relative to the NWP control, of 3 to 5% in the levels up to 700hPa. Those biases were attributed to both the SASS wind derivation algorithm (winds too strong) and the control NWP system (winds too weak). The areas of greatest impact were found to be those parts of the observational network lacking data of other types – including the southern hemisphere south of 30°S – and on case by case analysis of individual storms. The study was probably too short (6½ days) for reliable statistics to be generated.

Following the launch of ERS-1, scatterometer data were trialed in several impact studies involving ECMWF numerical models. Hoffman (1993) tested the ECMWF 3D-var assimilation system, at T106L19, for the impact of ERS-1 winds. Using scatterometer data derived by a modified version of CMOD2 (Stoffelen and Anderson 1992), Hoffman (1993) identified only small analysis impact and neutral forecast impact from the inclusion of scatterometer winds.

By 1997, following further refinement of processing algorithms and use of a higher resolution version of the ECMWF model, Le Meur (1997) reported improvements in analysed and first guess surface winds through the use of scatterometer data. Clear improvements were also observed in the quality of short-range forecasts, especially over the southern hemisphere.

Le Meur (1997) also discussed on a short (one week) experiment involving data from the period of ERS-1 and ERS-2 tandem operations and their impact on the ECMWF 3D-var system. A small degree of increase in forecast skill was reported.

Isaksen (1997) trialed ERS-1 scatterometer data in the ECMWF 4D-var system. Relative to the 3D-var system, he reported little increase in impact over the southern hemisphere but notably increased impact in the northern hemisphere.

Andrews and Bell (1998) reported substantial reductions in root mean square error (RMSE) for all forecast ranges with the use of ERS-1 scatterometer data in the UKMO assimilation system. They reported up to 10% reduction in the forecast RMSE of MSLP and low-level geopotential height. The South Atlantic Ocean was identified as the region most affected. It was suggested that this result was partly due to the relative weakness of the UKMO products in comparison to those of ECMWF prior to scatterometer data inclusion.

Yu et al. (1996) assessed the impact of ERS-1 winds on the operational numerical weather analyses and prognoses of the US National Centers for Environmental Prediction (NCEP). They used a global spectral forecast model of triangular truncation of 62 waves and 28 σ levels (T62L28). Over the southern hemisphere summer period of 1995/1996, they found that ERS-1 scatterometer winds

contributed a small reduction in the RMSE of low-level wind speed in analyses and in forecasts up to five days.

Breivik and Schyberg (1997) reported a notable improvement in results from an experiment involving the use of an alternative dealiasing algorithm in a limited area weather prediction model at the Norwegian Meteorological Institute.

4.2 Preliminary assimilation trials

Several preliminary trials were necessary prior to the July 1995 analysis and forecast impact experiment. The purpose of these was to optimise data thinning and quality control systems and test programming code.

As discussed in Chapter 2, the source of scatterometer winds used contained a proportion of erroneous data. These were generally winds 180° off true wind direction due to an up-wind / down-wind ambiguity problem common to scatterometer wind finding algorithms.

A simple test was conducted involving four assimilation cycles over a 30-hour period of late May 1995. Parallel model runs were conducted involving

(i) All available data except scatterometer winds ("control");

(ii) All available data except scatterometer winds whose direction differed by >40° from the GASP model 6-hour first guess prediction ("test 1"); and

(iii) All available data including scatterometer winds, but scatterometer winds whose direction differed by >40° from the GASP model 6-hour first-guess prediction were transposed by 180° ("test 2").

The result of this relatively simple test was quite conclusive. "Test 1" and "test 2" both produced numerous events of substantial local analysis impact – generally these were coincident. The volume of data was so large, and the number of data eliminated via the "test 1" algorithm so small, that the impact of the removal of data likely to be erroneous was not considered to be a problem. Furthermore, the "test 2" algorithm produced a few instances where the corrected wind directions amongst some clusters of data contrasted unrealistically with neighbouring data. It was concluded that a transposition of winds by 180° was not warranted.

It was thus decided that scatterometer data differing by more than 40° from the GASP model 6-hour first-guess prediction (interpolated to 10m) be eliminated.

It was recognised that this system of elimination may have led to the removal of a non-trivial population of accurate scatterometer data. For example, in the hypothetical case of a misplaced low-pressure system in the GASP first-guess field, the inclusion of scatterometer winds may correctly reposition the low. But, due to their large difference in wind direction from the GASP first-guess, they would often be eliminated.

Nevertheless, the estimated population of ~3.4% of data of reversed wind direction was too great a number to allow them into the system untested. In addition to the internal consistency checks included in the ESA wind finding system, some possible additional methods of testing were considered:

(i) Winds could have been checked for internal consistency via an assessment of the continuity of vorticity along the swathe. Unrealistically high vorticity (particularly anticyclonic vorticity) could be a sign of erroneous data;

(ii) The location of centres of vorticity from the scatterometer winds could be tested against the location of centres of vorticity of the first-guess field; and

(iii) Both up-wind and down-wind alternative scatterometer winds could be used in the data assimilation process with a weighting system to distinguish the more likely alternative from its less likely counterpart.

For the purposes of this non-exhaustive study the relatively simple method of testing was chosen where winds differing by more than 40° from the GASP first-guess were eliminated. A more sophisticated test of internal consistency would be recommended for future work.

Consistent with other forms of wind data used in GASP, the scatterometer winds were uniformly assigned a relatively high observational error. As with aircraft wind observations, an error value of $4.0ms^{-1}$ was chosen.

The GASP assimilation scheme allows only a finite number of data to be considered in each of an array of pre-defined grid boxes across the globe. In an effort to speed

up processing time, a repeat test was conducted, again involving four assimilation cycles, to test the impact of thinning data volume. Parallel runs involved

(i) All available data except scatterometer winds ("control");

(ii) All available data including scatterometer winds whose direction satisfied the test described above; and

(iii) All available data including scatterometer winds whose direction satisfied the test described above, but thinned to one-third of the original density.

The test confirmed that thinning of data to one-third density had a negligible effect. The data resolution was so great compared to model resolution that the loss from thinning was almost undetectable. The resultant improvement in processing speed was significant enough to continue this process of thinning through the impact trial.

For clarification it should be mentioned that data were thinned uniformly across and along the scatterometer swathe. An equal population of data were used from all of the 19 nodes across the swathe, apart from whatever quality control preference may have resulted.

A multitude of further tests were conducted for periods of up to seven days using data from May, June and July 1995. Primarily those trials were used to fine-tune aspects of the programming code before the full experiment began. They were also used to investigate the behaviour of the assimilation and analysis system in response to the scatterometer data.

Several short trials were conducted involving the elimination of all data apart from scatterometer winds. Those trials were used to clarify several issues including: The effect of manipulating the number of model iterations; the treatment of scatterometer winds by the processes used to couple the mass and wind fields; and the treatment of the scatterometer assimilation by the model analysis, smoothing and initialisation processes.

Early experiments involved both the R31L19 and R53L19 systems. Little difference was identified in terms of analysis impact since the two systems shared the same vertical resolution in the boundary layer, and the horizontal resolution of

both systems was substantially less than the 25m resolution of the scatterometer winds.

The system operating routinely at the time was R53L19 and it was thus chosen for use in this study.

None of the above steps were designed to produce substantial results. Rather they were important early steps in fine-tuning. Their inclusion was aimed at maximising, as much as practicable, the value of the scatterometer winds to the GASP system. There is no doubt that additional steps could have been taken to improve the process further. Some potential examples are discussed later in this chapter.

4.3 Analysis impact experiment

An analysis impact experiment was conducted using data from the full month of July 1995. That month was chosen for the study because of the importance of the evaluation of data and analyses to compare with the FROST winter special observing period twelve months earlier. July 1995 was also the earliest lengthy period of availability of scatterometer winds at ABOM.

The model used in the experiment was the operational GASP system developed by the ABOM Research Centre. The model was at the time the primary, operational global system developed and maintained in ABOM for weather analysis and prediction. A multivariate statistical interpolation scheme was used as described by Bourke et al. (1995). Model resolution was rhomboidal 53 on 19 sigma levels (R53L19). The lowest level ($\sigma = 0.991$) represented a height of approximately 75m above the ocean surface. See Appendix 2 for further details of the technical aspects and development of the GASP system.

The experiment consisted of two parallel assimilation trials. In the first trial (hereafter *with-ESA*) all available data, including the scatterometer winds, were used at every assimilation step. As discussed in Section 4.2 data were thinned and checked for quality using a simple wind direction test. In the second trial (hereafter

without-ESA) all available data, apart from the scatterometer winds, were used at every assimilation step.

Impact was assessed by direct comparison between the various pairs of analyses.

The experiment was predominantly successful in that successive assimilation, analysis and prognosis cycles were run with only minimal computational difficulties. However a significant anti-baric flow problem arose on 18 July 1995. A strong anticyclonic circulation developed around a low at the 10hPa level above the Southwest Atlantic Ocean. The event caused the model code to fail in both the *with-ESA* and *without-ESA* trials. The same event was simultaneously observed in the ABOM operational model run and also caused that system to fail. The full details of the event, a computational problem, are somewhat beyond the scope of this thesis. The ABOM operational model was re-established on 19 July and on 20 July the scatterometer winds experiment was re-established using operational data as a new starting point. As a consequence, no results from the period between 0500UTC 18 July and 2300UTC 19 July 1995 are included in the data presented here.

Figures 4.3.1 show the mean analysed $\sigma = 0.991$ wind field (ms^{-1}) from the one-month trial *with* (top) and *without* (bottom) the scatterometer winds included in the assimilation. Figure 4.3.2 shows the vector difference between the two Figures 4.3.1. The greatest differences appear over those parts of the region most lacking in surface observations: Marie Byrd Land and the adjacent Southeast sector of the Pacific Ocean. The inclusion of the scatterometer data apparently led to the weakening of wind speeds over much of the Southern Ocean, though some localised areas of wind speed increase were also identified. The generally lower wind speeds in the *with-ESA* trial possibly suggest a systematic low bias in the scatterometer data, a hypothesis supported by the discussion in Chapter 3. The localised areas of significant change in the wind field (difference maxima on Figure 4.3.2) may be more significant to the NWP system than the broader areas of slight difference.

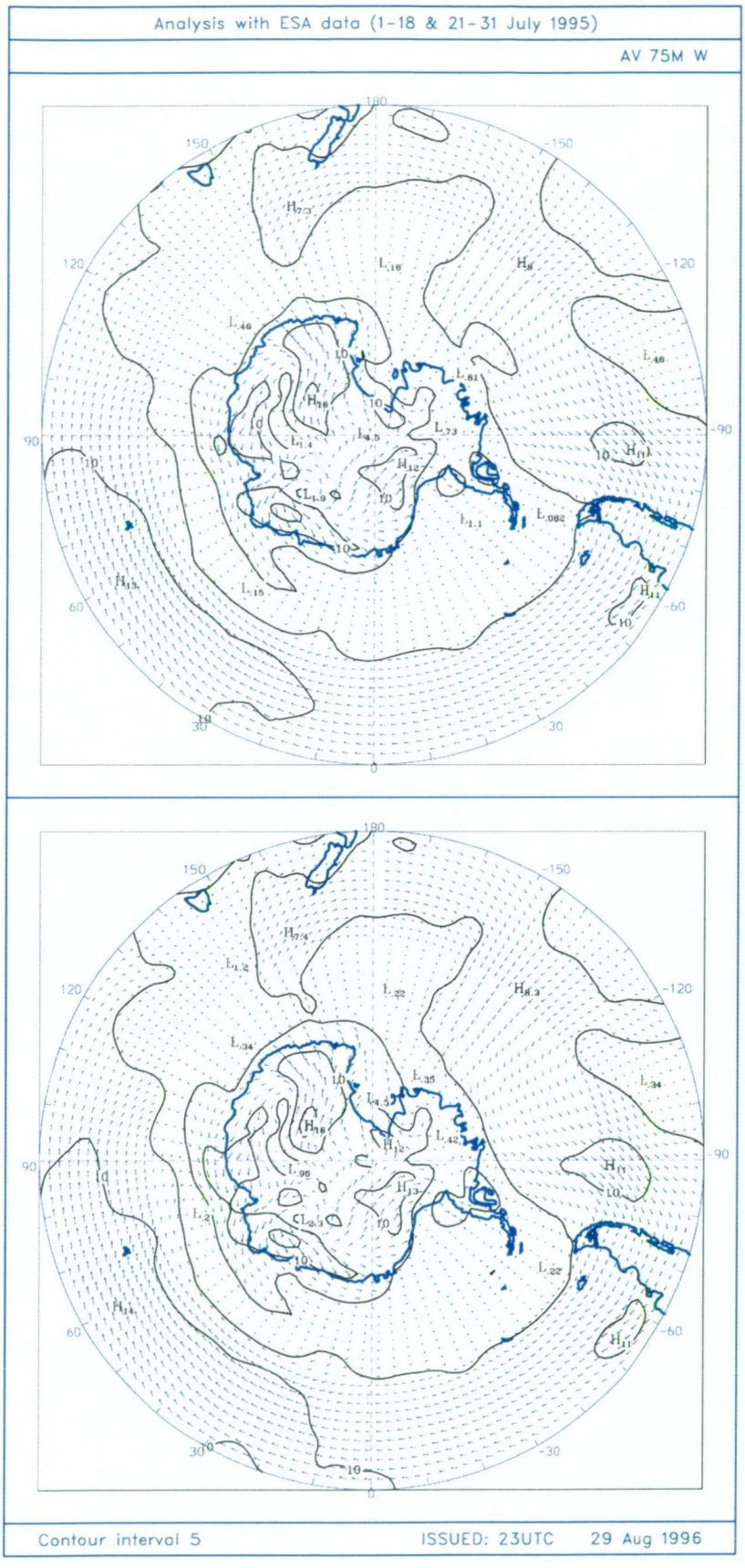

Figure 4.3.1 Mean wind at the $\sigma = 0.991$ level for July 1995. (ms^{-1}; contour interval $5.0ms^{-1}$).
Top: *With-ESA* trial. **Bottom:** *Without-ESA* trial.

Figure 4.3.2 Mean wind (*with-ESA* trial) minus mean wind (*without-ESA* trial) at the $\sigma = 0.991$ level for July 1995 (ms^{-1}; contour interval $1.0ms^{-1}$).

The difference between average mean sea level pressure analyses, derived *with* and *without* the scatterometer data (Figure 4.3.3), supports that theory. It shows a weakening of the circumpolar trough of the order of about 2hPa across a substantial area of the Southern Ocean from the inclusion of scatterometer winds. This finding could result from a systematic under-estimate of wind strength amongst the scatterometer data.

It is difficult to know if this result shows an improvement or degradation in analyses with scatterometer data included. The lack of manual wind reports from this part of the hemisphere makes any comparison with scatterometer winds difficult. Ship voyages through the area of interest are very infrequent and ship reports are notoriously difficult to use for this kind of comparison work.

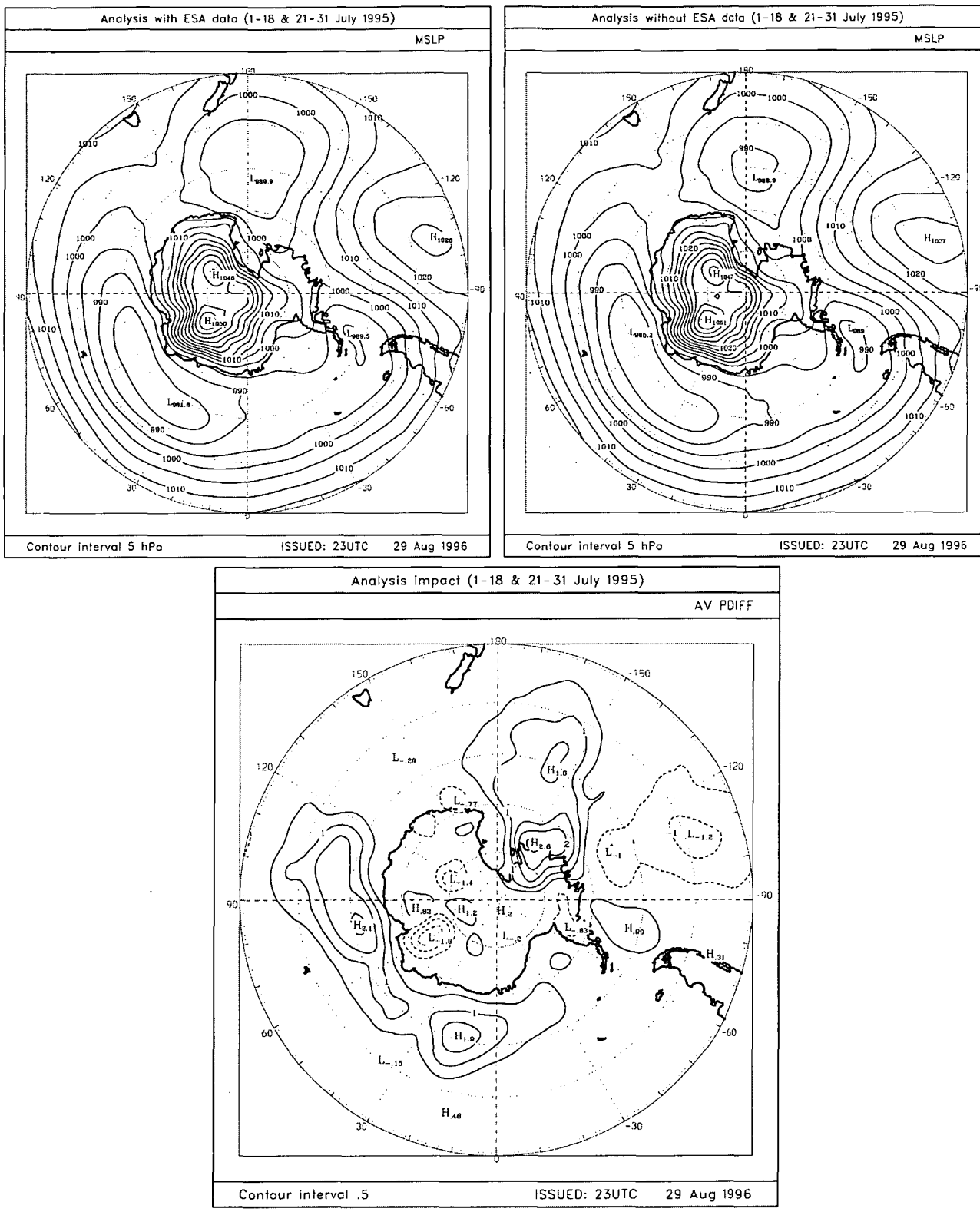

Figure 4.3.3 Mean MSLP for July 1995. (hPa; contour interval 5.0hPa).

Top left: *With-ESA* trial.

Top right: *Without-ESA* trial.

Bottom: Difference field: MSLP (*with-ESA*) minus MSLP (*without-ESA*). (hPa; contour interval 0.5hPa).

Figure 4.3.4, shows the same MSLP difference field as Figure 4.3.3 (bottom frame) but on a global projection. This highlights the remarkable concentration of significant mean impact to the Southern Ocean. That is in spite of the global distribution of the scatterometer winds utilised in the experiment. The low population of other observing systems in the Southern Ocean and Antarctic has led, in this example, to a relatively strong impact with the inclusion of scatterometer winds. The reliability and accuracy of NWP systems in different parts of the globe, and the relatively poor skill in the Antarctic region, are discussed in Chapter 6.

The areas of greatest mean (July 1995) analysis impact were mostly confined to the Antarctic sea ice zone and adjacent ocean areas. Generally MSLP (*with-ESA*) was greater than MSLP (*without-ESA*). A moderate opposite signal was identified in the Southeast Pacific Ocean sector. Some possible explanations are given here.

(i) The GASP system may have (*without-ESA*) been over strengthening low-pressure systems in the sea ice zone and the influence of the scatterometer winds was to cause a mean weakening.

(ii) The scatterometer winds may be biased too low and their inclusion in the GASP system caused a weakening of low-pressure systems in the polar trough. The areas of positive-sign on Figure 4.3.3 (bottom frame), MSLP (*with-ESA*) greater than MSLP (*without-ESA*), are coincident with the mean axis of the polar trough.

(iii) The influence of the scatterometer winds was to reduce the strength of the high-pressure system in the Southeast Pacific Ocean, a further sign in support of (i) and/or (ii) above.

Large signals were also identified over land and sea ice where scatterometer winds were not obtainable. This is most likely caused by the lack of conventional observational data available to anchor the analyses, and by the relatively high observational error attributed to the high altitude TOVS. It should also be noted that significant changes in the mass field are required over the Antarctic continent in order to impact on the wind field over the adjacent ocean area. The inclusion of scatterometer observations, which differ significantly from the first guess analyses, would necessitate such a mass field alteration over the continent.

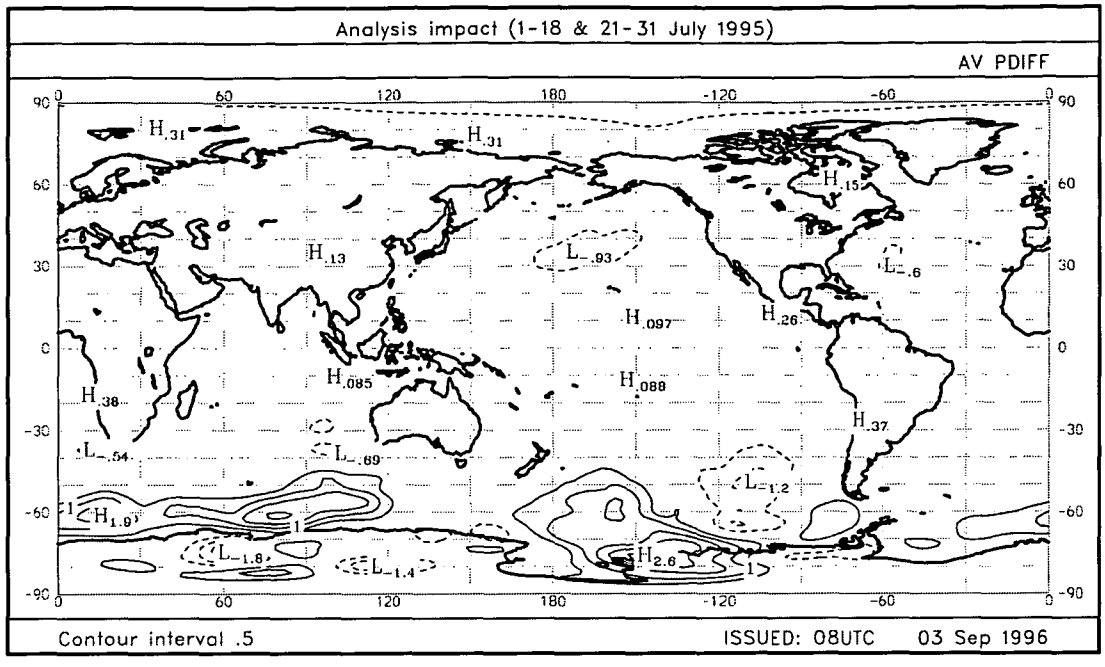

Figure 4.3.4 As for Figure 4.3.3 (bottom frame) but in global projection. (hPa; contour interval 0.5hPa).

The mean MSLP impact results shown above are in balanced agreement with the impact on mean 500hPa height (Figure 4.3.5). That figure demonstrates the spread of influence from the alteration of the surface wind field, via the inclusion of the scatterometer winds, to the mass-balance of the low and middle troposphere.

It is expected that the influence of scatterometer winds on July analyses would be somewhat stronger than that during other seasons of the year. Mean Southern Ocean wind speeds are greatest during July (see Figure 3.3.2) and the cycle of formation and decay of weather systems is fastest during the winter months.

The differences between the various numerical models' representation of wind in this area of the Southern Ocean are substantial. These differences are similar in magnitude to the differences recorded by the addition of scatterometer data.

There were multiple clear cases where the inclusion of the scatterometer data did impact heavily on analyses and subsequently led to improvement in forecast skill. But there were also cases where the scatterometer data had a negative influence,

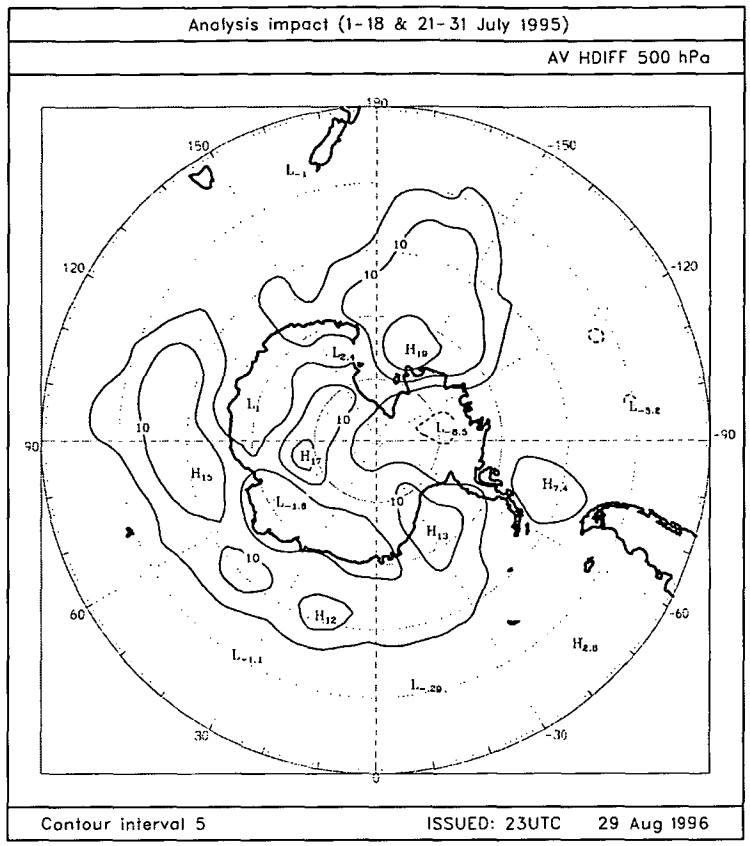

Figure 4.3.5 Mean **500hPa height** (*with-ESA* trial) minus mean **500hPa height** (*without-ESA* trial) for July 1995 (m; contour interval 5.0m).

judged by the comparison of the prognoses with the corresponding own analyses for each scheme.

Several significant potential problems were raised above. These involve both the quality and reliability of the original data, and perhaps methods used during assimilation. Real time operational requirements also demand that data be made available to processing centres in a timely manner.

Some improvements could potentially be made to the assimilation methods used in the experiment. The model used was a global model, run on 19 sigma levels, the lowest of which sits at approximately 75m above the ocean surface. The scatterometer data is a source of low level wind data derived purely from the reflection characteristics of a rough ocean surface to a microwave pulse directed from a remote sensing satellite. A model transfer function is then inversely utilised

to estimate the 10m wind speed and direction necessary to generate the surface roughness whose signature the microwave backscatter profile detected. A further step is then required to estimate a 75m wind speed and direction for use in the atmospheric model.

This series of steps may not be the ideal technique to use. Some very complex issues could be further investigated, including an estimate of the low level wind forcing of the ocean surface, the low-level atmospheric stability profile, and the possible impact of complex swell regimes involving super-imposed swell patterns.

Further work could address some of these issues in detail. They are important considerations especially for Southern Ocean application of the data.

4.4 Large impact case studies

Throughout the impact experiment many individual events involving large analysis impact were identified. Those events were almost exclusively confined to the remote ocean areas of the southern hemisphere and most common south of 40°S. Two examples of significance to the Australian region are discussed further here.

Amongst the Figures 4.4.1 is shown the difference between MSLP *with-ESA* and MSLP *without-ESA* analyses for 0500UTC 1 June 1995.

Throughout the assimilation process all observational data, regardless of origin, undergo a series of quality control tests. The assimilation process uses the GASP forecast model 6-hour first guess as a starting point. Observational data are assessed against near neighbours and against the 6-hour first guess. On the basis of those comparisons, observations are either used in a nudging process to alter the 6-hour first guess, or rejected on quality control grounds.

Buoy 74531, near 61.8°S 097.3°E, reported an air pressure of 956.6hPa just after 0600UTC 1 June 1995. Figure 4.4.1 (bottom right) shows the distribution of MSLP reports at that time (0500UTC ±3 hours) together with two swathes of scatterometer winds. Buoy 74531 is shown in Figure 4.4.1 (bottom right) as a small blue asterisk in the middle of one of those two swathes.

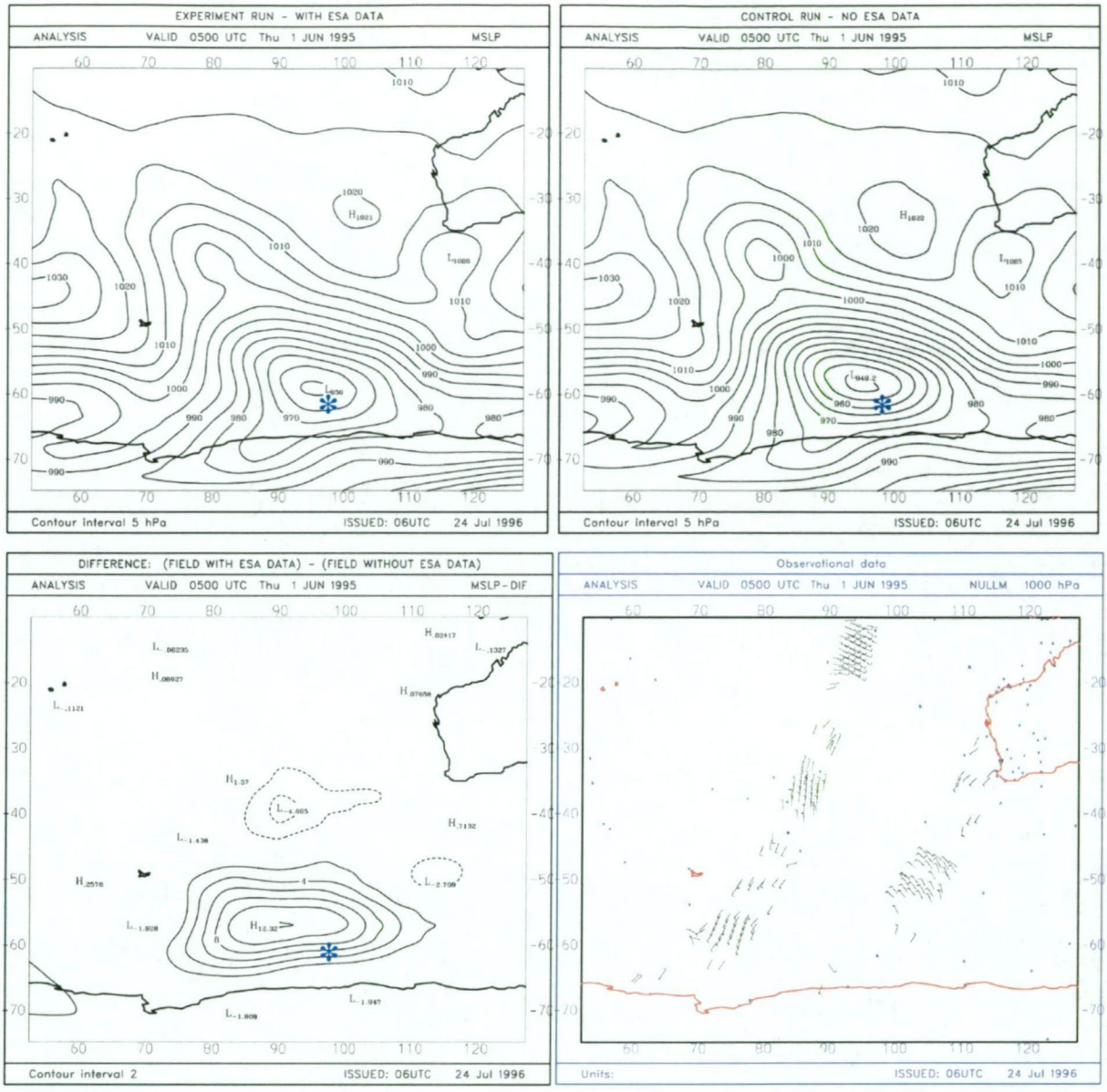

Figure 4.4.1

Top left: MSLP analysis (*with-ESA*) for 0500UTC 1 June 1995 (hPa; contour interval 5.0hPa). The location of buoy 74531 is also plotted.

Top right: MSLP analysis (*without-ESA*) for 0500UTC 1 June 1995 (hPa; contour interval 5.0hPa). The location of buoy 74531 is also plotted.

Bottom left: MSLP analysis (*with-ESA*) minus MSLP analysis (*without-ESA*) for 0500UTC 1 June 1995 (hPa; contour interval 2.0hPa). The location of buoy 74531 is also plotted.

Bottom right: Location of MSLP reporting stations and drifting buoys (including buoy 74531) together with scatterometer winds at 0500UTC (±3 hours) 1 June 1995. Scatterometer winds were thinned to one-third of their original density then further thinned by a quality control check against the GASP first guess wind field.

A continual supply of scatterometer data was obtained from before and after this time envelope (0500UTC ±3 hours) but is not shown here. For a view of global coverage obtainable in 24 hours refer back to Figure 2.2.3 in Chapter 2.

In this example, scatterometer wind data supported the buoy report (in the *with-ESA* trial) when the buoy had been rejected in the absence of scatterometer winds (*without-ESA* trial). Once again the impact of a single quality control decision generated a substantial analysis impact (shown in Figure 4.4.1 (bottom left)).

Stoffelen and Anderson (1995) identified similar events in ECMWF trials. They also reported instances of large impact of this nature elsewhere on the globe. In this study impact events of greater than 10hPa were only identified over the Southern Ocean.

Seaman (1994) quantified the importance of remote stations in terms of analysis and forecast impact. He identified remote buoys in the Southern Ocean as the single most influential source of MSLP data in the network.

A similar event, also off the East Antarctic coast, was identified in later scatterometer impact trials. It is probably not a coincidence that the same drifting buoy was involved. It was present in one of the most data sparse areas of the globe, and in an area identified by Seaman (1994) as highly influential in terms of MSLP impact.

On 4 July 1995 drifting buoy 74531 was located at 63.0°S 097.2°E moving slowly southwest. Just before 0600UTC the buoy reported an air pressure of 990.8hPa. During the *without-ESA* assimilation trial the buoy pressure report was rejected on quality control grounds because its report was ~14hPa higher than the 6-hour first guess. The inclusion of supporting data from a coincident swathe of scatterometer winds enabled the buoy report to be retained in the *with-ESA* trial.

The subsequent impact of this single event altered the analysis considerably (Figure 4.4.2) with correspondingly large consequences for the prognoses as shown below. The analysed central pressure of a low-pressure system west of the buoy was thus increased by more than 11hPa and its location shifted nearly 500km further west.

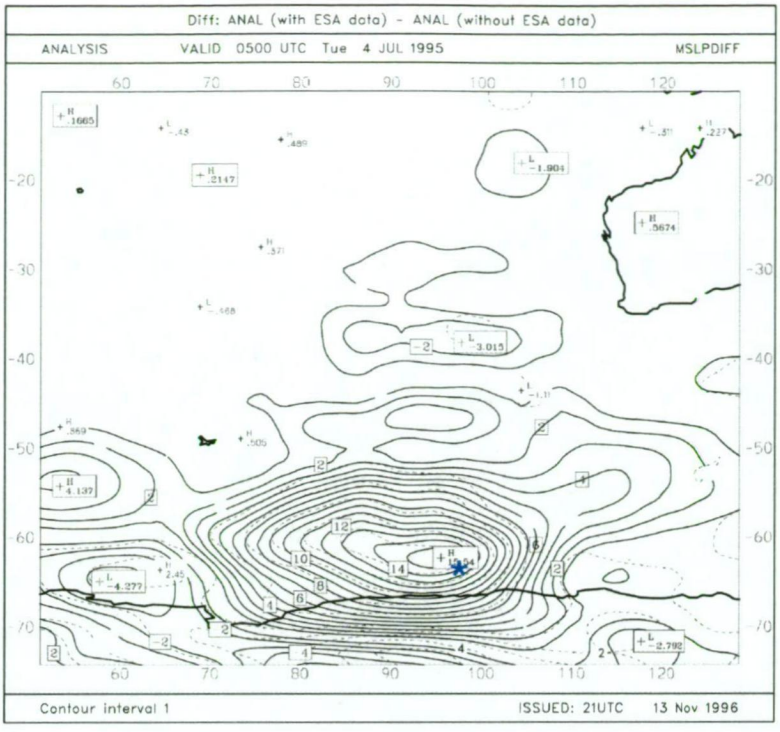

Figure 4.4.2 MSLP (*with-ESA* trial) minus MSLP (*without-ESA* trial) for 0500UTC 4 July 1995 (hPa; contour interval 2.0hPa). Dashed lines represent 1000-500hPa thickness difference (dam; contour interval 1.0dam). Buoy 74531 is plotted (★).

Figure 4.4.3 Air pressure data from drifting buoy number 74531 from July 1995 (hPa; ±0.3hPa). On 4 July the buoy was near 63.0°S 097.2°E and moving slowly southwest. Manufactured by TURO Technology Pty. Ltd., Australia, model T-701. Owned by the Antarctic CRC, Australia.

Air pressure data from buoy 74531 are shown in Figure 4.4.3. Independent tests indicate that the buoy data were reliable at the time.

The forecast model was run ahead 5 days from every 1100UTC daily analysis throughout the impact experiment. Forecasts were also generated at odd times for the purposes of case studies such as the particularly interesting case of 4 and 5 July 1995. The substantial difference in starting analysis, resulting from the scatterometer impact discussed above, generated two contrasting sets of forecasts: those generated from the *with-ESA* analysis and those generated from the *without-ESA* analysis.

The example results included here (Figures 4.4.4 and Figures 4.4.5) show the series of forecasts generated from a base analysis of 1700UTC 5 July 1995.

Figure 4.4.4 shows difference fields, MSLP (*with-ESA*) minus MSLP (*without-ESA*), of base analyses and of 24, 48 and 72-hour forecasts. It seems remarkable that such differences resulted from what was primarily a single quality control decision relating to a single drifting buoy report.

Forecast errors of this magnitude are substantial. Over the open ocean they can reach magnitudes of $20ms^{-1}$ in wind speed and several metres in wave height.

This example also clearly shows that the impact on prognosis accuracy from events in Antarctic waters can have a profound effect on forecast accuracy in Australia.

It will be shown in the next section (4.5) that the ~7 to 10 July period also exhibited an increased degree of forecast skill, in terms of S_1 skill-score and RMSE statistics, with the inclusion of scatterometer winds.

Figure 4.4.5 can be used to make direct comparison between 48-hour MSLP forecasts (*with ESA* and *without-ESA*) and coincident analyses (*with ESA* and *without-ESA*). Generally speaking the differences are minor but not trivial.

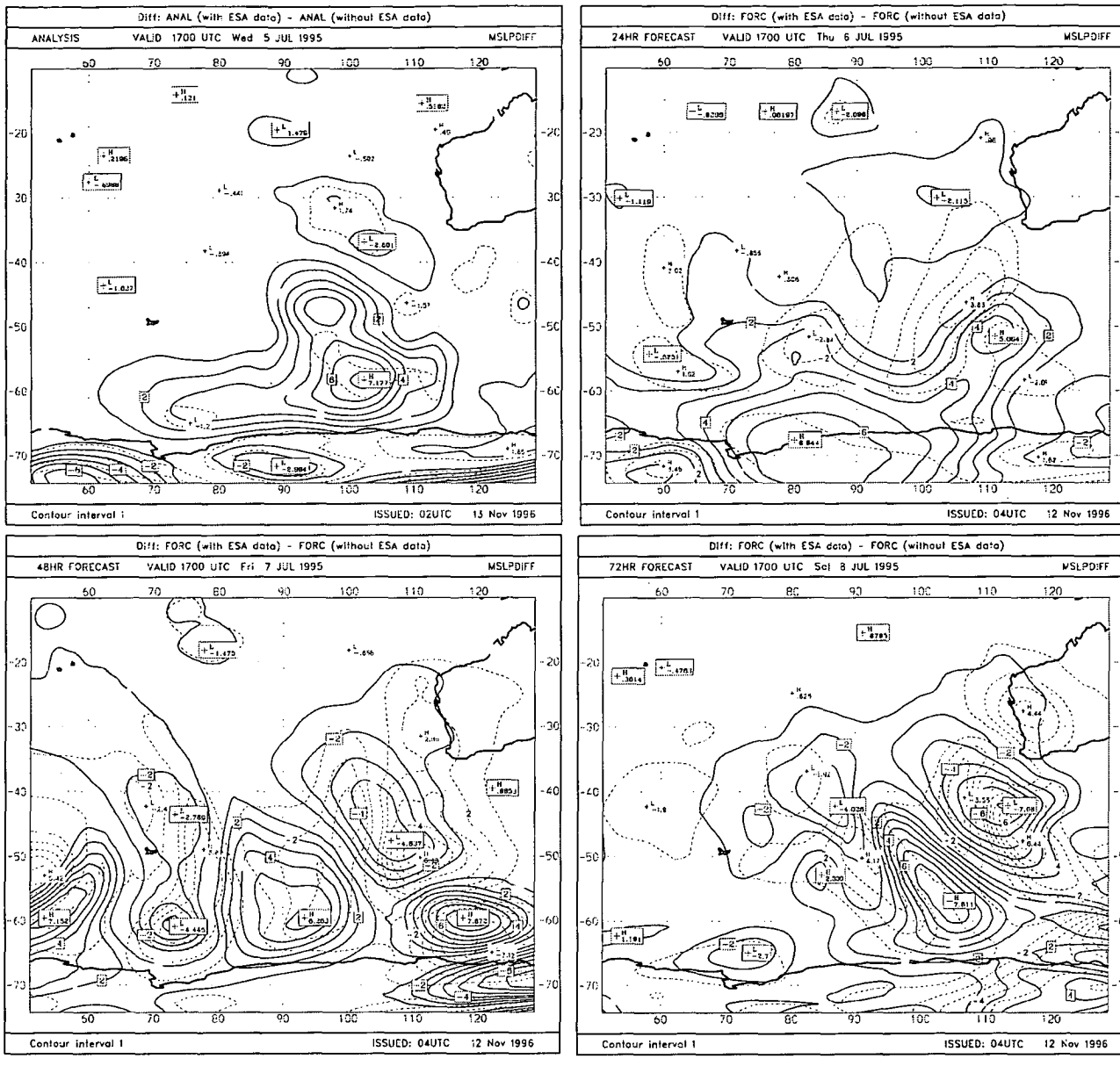

Figure 4.4.4 Difference fields, MSLP (*with-ESA*) minus MSLP (*without-ESA*), of:

Top left: Base analyses valid 1700UTC 5 July 1995.

Top right: 24-hour forecasts valid 1700UTC 6 July.

Bottom left: 48-hour forecasts valid 1700UTC 7 July.

Bottom right: 72-hour forecasts valid 1700UTC 8 July.

Solid contours are MSLP (hPa; contour interval 1.0hPa).

Dashed contours are 1000-500hPa thickness (dam; contour interval 1.0dam).

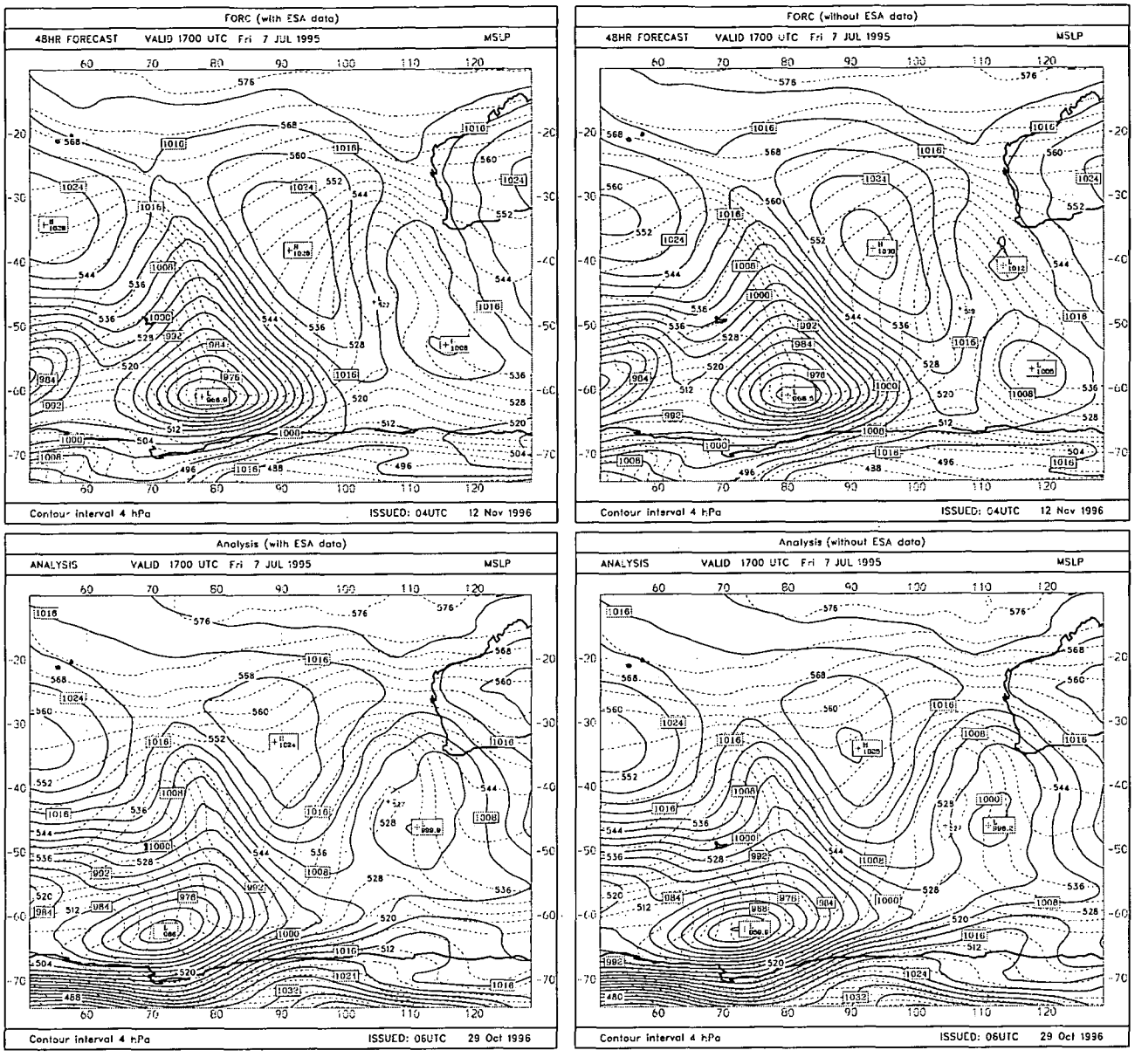

Figure 4.4.5 Pairs of 48-hour MSLP forecasts together with pairs of analyses for verification. All valid 1700UTC 7 July 1995.

Top left: 48-hour forecast generated from a *with-ESA* base analysis.

Top right: 48-hour forecast generated from a *without-ESA* base analysis.

Bottom left: Analysis (*with-ESA*).

Bottom right: Analysis (*without-ESA*).

Solid contours are MSLP (hPa; contour interval 4.0hPa).

Dashed contours are 1000-500hPa thickness (dam; contour interval 4.0dam).

4.5 Forecast impact experiment

The second phase of the experiment investigated forecast impact. Impact in the forecast quality context was determined by measurement of changes to forecast error. Forecasts of MSLP and 500hPa height were assessed against analyses of the same fields. In this experiment involving parallel trials, forecasts were assessed against analyses of the same trial. In other words, forecasts generated from the *with-ESA* trial were compared against analyses also from the *with-ESA* trial; and forecasts generated from the *without-ESA* trial were compared against analyses also from the *without-ESA* trial.

The forecast model was run forward to five days from each 1100UTC daily analysis. The result was a one-month long series of two parallel sets of forecasts.

Verification tools used in the study were bias, RMSE and the S_1 skill-score. Point by point, throughout each of several verification grids, they compared forecast parameters (F) against verifying analysis parameters (A) as follows (Teweles and Wobus 1954, Mullenmeister and Hart 1994):

$$\text{Bias} = \frac{\sum(F-A)}{n} \tag{1}$$

$$\text{RMSE} = \sqrt{\frac{\sum(F-A)^2}{n}} \tag{2}$$

$$S_1 = 100 * \frac{\sum_{i,j}|F(i,j)^i - A(i,j)^i| + \sum_{i,j}|F(i,j)^j - A(i,j)^j|}{\sum_{i,j}|G^i| + \sum_{i,j}|G^j|} \tag{3}$$

where predicted gradients were given by equations (4) and (5);

$$F(i,j)^i = F(i+1,j) - F(i-1,j) \tag{4}$$

$$F(i,j)^j = F(i,j+1) - F(i,j-1) \tag{5}$$

and verifying gradients were given by equations (6) and (7):

$$A(i,j)^i = A(i+1,j) - A(i-1,j) \tag{6}$$

$$A(i,j)^j = A(i,j+1) - A(i,j-1) \tag{7}$$

As such S_1 provided an assessment of pressure (or geopotential height) gradient forecast skill. The inclusion of the gradient terms, G^i and G^j, in equation (3) had the effect of scaling results in a manner proportional to gradient. Thus S_1 was able to provide comparable results across a range of pressure gradient regimes. G^i and G^j were given by equations (8) and (9):

$$G^i = \max [F(i,j)^i, A(i,j)^i] \quad (8)$$

$$G^j = \max [F(i,j)^j, A(i,j)^j] \quad (9)$$

Several predefined verification grids, of 2.5° latitude by 2.5° longitude, were used. The boundaries of those used in this study are given in Table 4.5.1.

Region	Southern boundary	Northern boundary	Western boundary	Eastern boundary
Antarctica / South Pole grid	90°S	55°S	–	–
Australian grid	45°S*	15°S	100°E	170°E
Southern Ocean grid	70°S	50°S	060°E	160°E
Southern Annulus grid	60°S	20°S	–	–
South American grid	57°S	12°S	118°W	042°W
Southern African grid	48°S	12°S	009°E	051°E
Global grid	90°S	90°N	–	–

Table 4.5.1 Details of the verification grids used in this study (from Mullenmeister and Hart 1994).

* The Australian grid also contains points to 55°S between 130° and 170°.

Tables 4.5.2 and 4.5.3 show comparisons between 24 and 48-hour MSLP and 500hPa height forecast results from the two parallel trials. Several different verification grids, in both the northern and southern hemispheres, were used in the analysis. The more interesting results were in the southern hemisphere with generally neutral forecast impact identified in the northern hemisphere.

Region	Trial	S_1 24 hrs	S_1 48 hrs	Bias 24 hrs	Bias 48 hrs	RMSE 24 hrs	RMSE 48 hrs
Antarctic / South Pole grid	*With-ESA*	**48.0**	59.9	0.43	0.09	6.49	**8.94**
	Without-ESA	46.9	59.7	0.15	-0.24	6.57	9.15
Australian grid	*With-ESA*	32.9	44.1	-0.01	0.57	1.66	3.00
	Without-ESA	32.8	43.4	0.07	0.65	1.68	3.01
Southern Ocean grid (60°E to 160°E sector)	*With-ESA*	45.9	58.7	1.05	1.27	5.31	7.55
	Without-ESA	45.7	59.3	0.98	1.38	5.34	7.70
Southern Annulus grid	*With-ESA*	**34.8**	**47.7**	0.27	0.47	2.89	4.63
	Without-ESA	33.6	46.7	0.28	0.54	2.86	4.64
South American grid	*With-ESA*	**34.4**	46.3	0.20	0.47	2.52	4.00
	Without-ESA	33.2	45.4	0.22	0.51	2.49	4.00
Southern African grid	*With-ESA*	**33.2**	44.6	0.04	-0.06	1.87	**3.09**
	Without-ESA	32.0	44.6	0.09	0.02	1.86	3.22
Global grid	*With-ESA*	41.1	51.7	0.02	0.03	2.75	3.99
	Without-ESA	40.1	51.0	0.02	0.03	2.77	4.02

Table 4.5.2 Mean S_1 skill-score, bias and RMSE data for 24 and 48-hour forecasts of **MSLP** (hPa). Cases of notable skill improvement *with-ESA* are shown in **blue**; cases of notable skill deterioration *with-ESA* are shown in **red** (notable defined as $\Delta S_1 \geq 1.0$, ΔBias $\geq$ 1.0hPa, ΔRMSE $\geq$ 2%).

At 24 hours, small mean S_1 skill-score increases (worsening of skill) were identified over almost all of the southern hemisphere verification grids. Mean 24-hour RMSE and bias results were close to neutral. This pattern suggests relatively small impact on absolute values of MSLP (no RMSE and bias change) but some negative impact on S_1 (worsening of gradient forecast skill). Scatterometer winds biased too low would be likely to produce such a result.

The exceptions were the Australian and Southern Ocean girds where 24-hour S_1 results were closer to neutral. Of the southern hemisphere verification grids used, the quantity of data from sources other than ERS-1 was greatest over the Australian and Southern Ocean regions. In comparison with Antarctica, Southern Africa and South America, Australia has a superior coverage of MSLP and upper-air reporting

Region	Trial	S_1 24 hrs	S_1 48 hrs	Bias 24 hrs	Bias 48 hrs	RMSE 24 hrs	RMSE 48 hrs
Antarctic / South Pole grid	*With-ESA*	41.5	53.9	-5.11	-8.44	47.6	73.5
	Without-ESA	41.0	53.4	-5.86	-8.12	47.4	73.6
Australian grid	*With-ESA*	22.5	31.5	-5.69	-5.23	17.6	30.6
	Without-ESA	22.4	31.1	-5.04	-4.45	17.4	30.0
Southern Ocean grid (60°E to 160°E sector)	*With-ESA*	36.3	47.7	-2.36	**-0.46**	44.3	**66.8**
	Without-ESA	36.5	48.1	-2.11	1.85	44.9	69.2
Southern Annulus grid	*With-ESA*	24.3	32.8	-5.54	**-6.97**	28.0	46.0
	Without-ESA	24.1	32.5	-5.07	-5.88	27.5	45.6
South American grid	*With-ESA*	24.9	33.2	-6.25	-7.34	24.9	40.1
	Without-ESA	24.6	32.8	-5.80	-6.53	24.4	39.8
Southern African grid	*With-ESA*	22.9	29.4	-9.15	**-16.78**	19.9	33.4
	Without-ESA	22.9	29.8	-8.66	-15.76	19.6	33.9
Global grid	*With-ESA*	30.8	40.2	-6.23	-9.32	22.9	36.3
	Without-ESA	30.4	39.9	-6.07	-9.03	22.6	36.1

Table 4.5.3 Mean S_1 skill-score, bias and RMSE data for 24 and 48-hour forecasts of **500hPa height** (m). Cases of notable skill improvement *with-ESA* are shown in **blue**; cases of notable skill deterioration *with-ESA* are shown in **red** (notable defined as $\Delta S_1 \geq 1.0$, ΔBias $\geq$ 1.0m, ΔRMSE $\geq$ 2%).

stations. Also, across Australia and the neighbouring sector of the Southern Ocean, GASP uses locally derived high-resolution cloud-drift winds and TOVS (Le Marshall et al. 1994, Le Marshall et al. 2001). The addition of ERS-1 scatterometer winds in the Australian region does little because of relative saturation of data from other good quality sources. In other parts of the southern hemisphere, where data coverage is significantly poorer, the forecast impact of the scatterometer winds is more notable.

Mean forecast MSLP S_1 skill-score impact at 48 hours was considerably greater than that at 24 hours in most regions. Two factors were likely to have contributed to this result:

No substantial analysis impact events were identified during the period flagged as having widespread RMSE increases: 13 to 18 July.

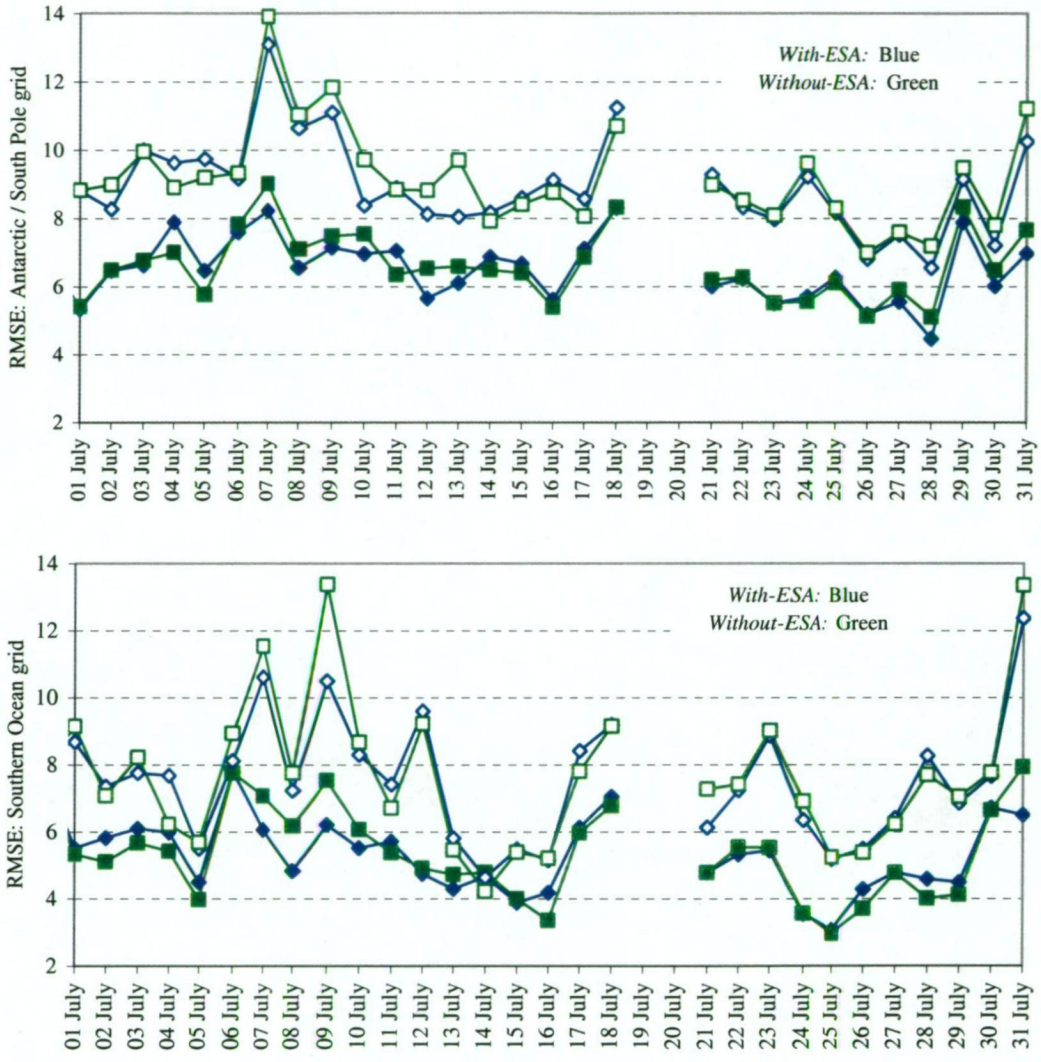

Figure 4.5.1 Daily variation of RMSE of 24 and 48-hour prognoses from the *with-ESA* (blue) and *without-ESA* (green) trials verified against their own series of analyses.

Top: Antarctic verification grid.

Bottom: Southern Ocean verification grid (60°E to 160°E).

The periods ~7 to 10 July and ~27 to 31 July show fairly consistent RMSE decrease with the inclusion of scatterometer winds. Reproduced from Appendix 3 where a full collection of S_1, RMSE and bias results from seven verification grids can be seen.

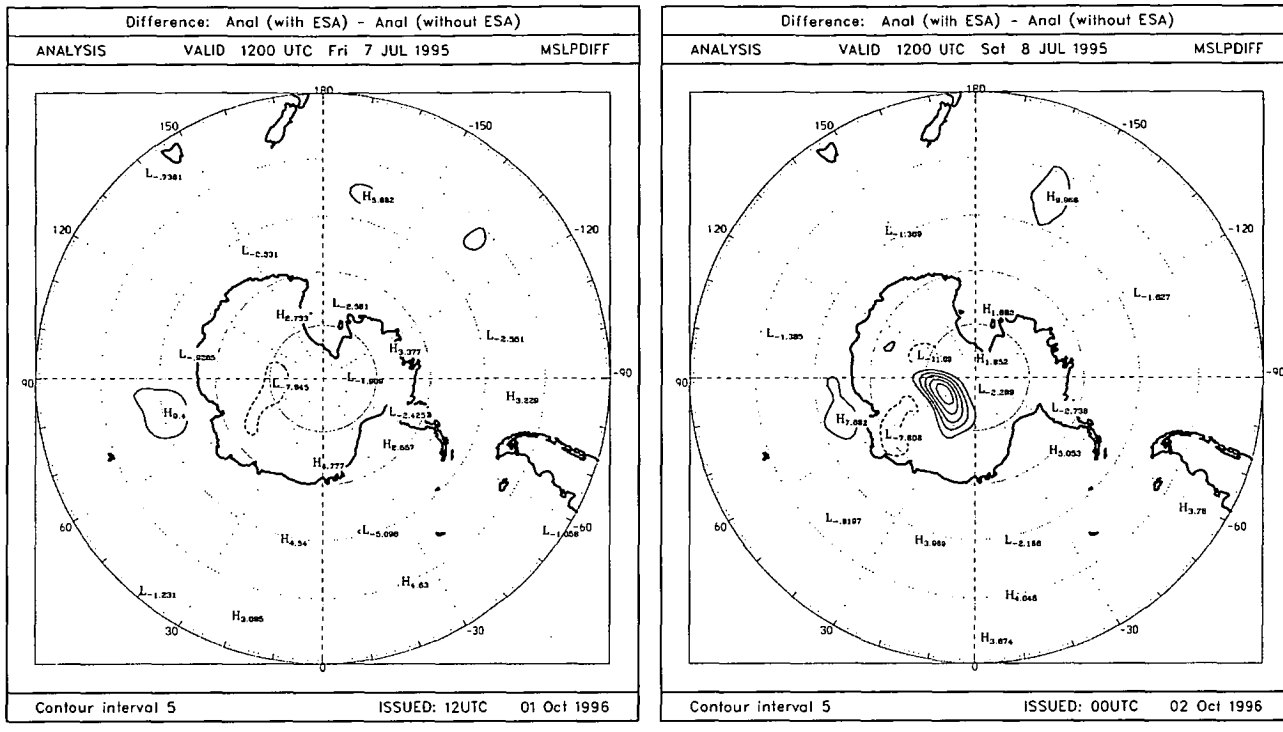

Figure 4.5.2 MSLP analysis (*with-ESA*) minus MSLP analysis (*without-ESA*) for 1200UTC 7 July 1995 (left) and 1200UTC 8 July 1995 (right). (hPa; contour interval 5.0hPa).

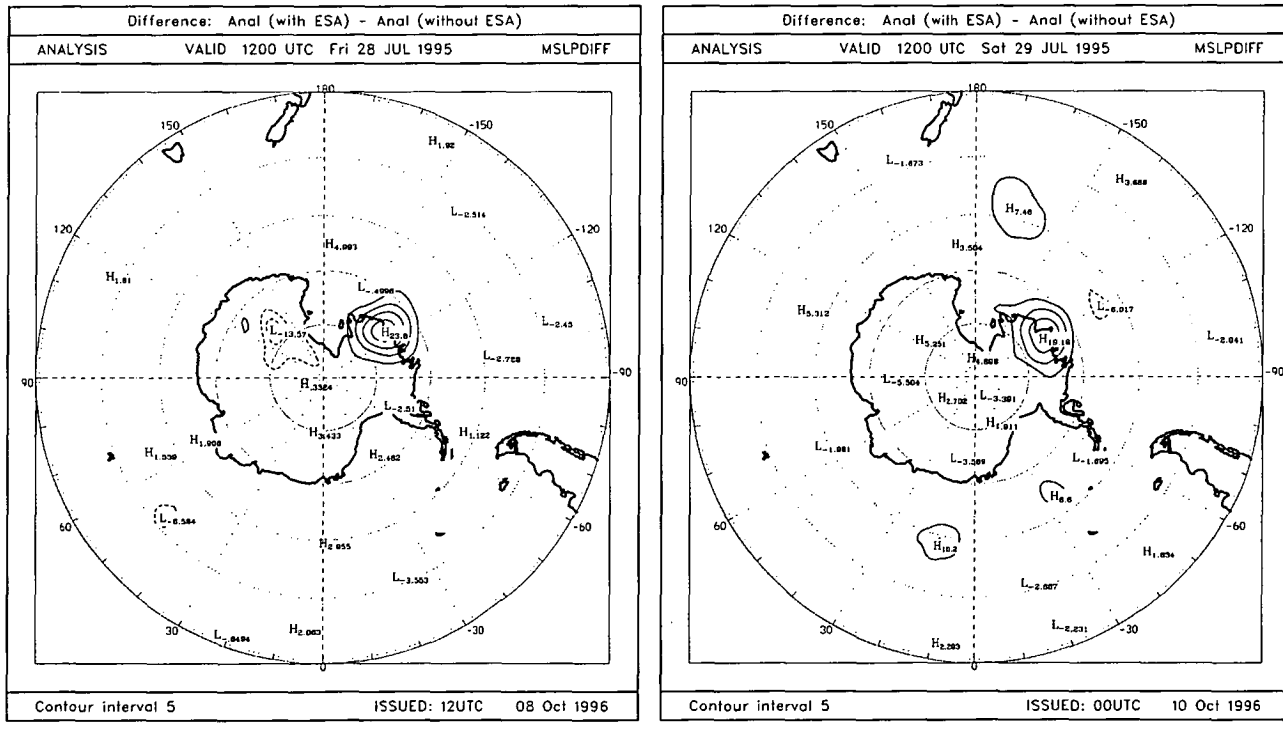

Figure 4.5.3 MSLP analysis (*with-ESA*) minus MSLP analysis (*without-ESA*) for 1200UTC 28 July 1995 (left) and 1200UTC 29 July 1995 (right). (hPa; contour interval 5.0hPa).

This pattern of behaviour, where

(i) substantial analysis impact events, with the inclusion of scatterometer winds, caused RMSE to decrease;

(ii) the absence of substantial analysis impact events caused RMSE to increase; and

(iii) S_1 was uniformly higher *with-ESA,* albeit only slightly;

suggests the impact of the scatterometer winds was to reduce prognostic skill most of the time, but increase skill on those occasions where their inclusion made an alteration to quality control decisions relating to remote MSLP reports. Skill, in this context, refers to that measured by S_1 and RMSE in comparison of prognoses with corresponding series of analyses.

Such a pattern could result from the apparent small systematic low bias in the scatterometer wind speeds raised in earlier discussion. Unfortunately IFREMER data, which showed less wind speed bias, were not available at the time of the impact study.

The verification grids showing the greatest degree of S_1 and RMSE variation were those over the Antarctic and Southern Ocean. In those regions data coverage from other sources is relatively limited and prognostic skill is typically poorer.

The verification grids showing the least daily variation were the larger grids: The Globe and the Southern Annulus. In the main, both have good data coverage from other sources, and the effects of the Southern Ocean dominate neither.

Figures 4.5.4 and Table 4.5.4 show frequency distributions of RMSE in daily 24 and 48-hour MSLP forecasts. They show the degree of RMSE rise or fall from the inclusion of scatterometer winds. They also indicate that the areas to benefit most from the inclusion of the scatterometer winds were the Antarctic region (at 24-hours) and the Antarctic and Southern Africa regions (at 48-hours) where the inclusion of the scatterometer winds caused RMSE to decrease on most days.

On the South American verification grid, RMSE of MSLP forecasts increased with the inclusion of scatterometer winds on most days. That result may have been induced by the steepness of the topography on the South American continent and,

24-hour RMSE	Australia	South America	Southern Africa	Southern Ocean	Antarctica
24% fall	0	0	2	0	0
21% fall	0	0	0	1	0
18% fall	0	0	0	2	0
15% fall	0	0	0	1	1
12% fall	0	0	0	0	1
9% fall	3	1	1	2	4
6% fall	4	1	3	0	5
3% fall	4	5	2	5	3
No rise or fall	10	9	8	5	6
3% rise	4	8	4	4	5
6% rise	3	3	3	2	2
9% rise	1	2	4	3	0
12% rise	1	0	0	1	3
15% rise	0	1	1	3	0
18% rise	0	0	1	0	0
21% rise	0	0	1	0	0
24% rise	0	0	0	1	0
Weighted mean	0.4% fall	1.5% rise	1.3% rise	0.9% rise	1.3% fall
48-hour RMSE	Australia	South America	Southern Africa	Southern Ocean	Antarctica
24% fall	0	0	2	0	0
21% fall	0	0	0	1	0
18% fall	1	0	2	0	1
15% fall	0	0	1	1	1
12% fall	1	1	3	0	0
9% fall	3	3	2	3	5
6% fall	2	2	3	4	2
3% fall	4	3	4	6	7
No rise or fall	7	5	4	3	5
3% rise	4	13	3	5	5
6% rise	3	0	2	2	3
9% rise	4	1	2	3	1
12% rise	0	1	0	1	0
15% rise	0	0	1	0	0
18% rise	1	1	0	0	0
21% rise	0	0	1	0	0
24% rise	0	0	0	1	0
Weighted mean	0.1% rise	0.6% rise	3.6% fall	0.5% fall	2.3% fall

Table 4.5.4 Frequency distribution of percentage changes in RMSE of daily forecast MSLP with the inclusion of scatterometer winds (3% bins). Results from thirty daily 24-hour (top) and 48-hour (bottom) forecasts over five verification grids are shown. The number of days (out of 30) is shown against percentage rise or fall in RMSE with the inclusion of scatterometer winds. Weighted means are also given, demonstrating significant 48-hour impact in the Southern Africa and Antarctic regions.

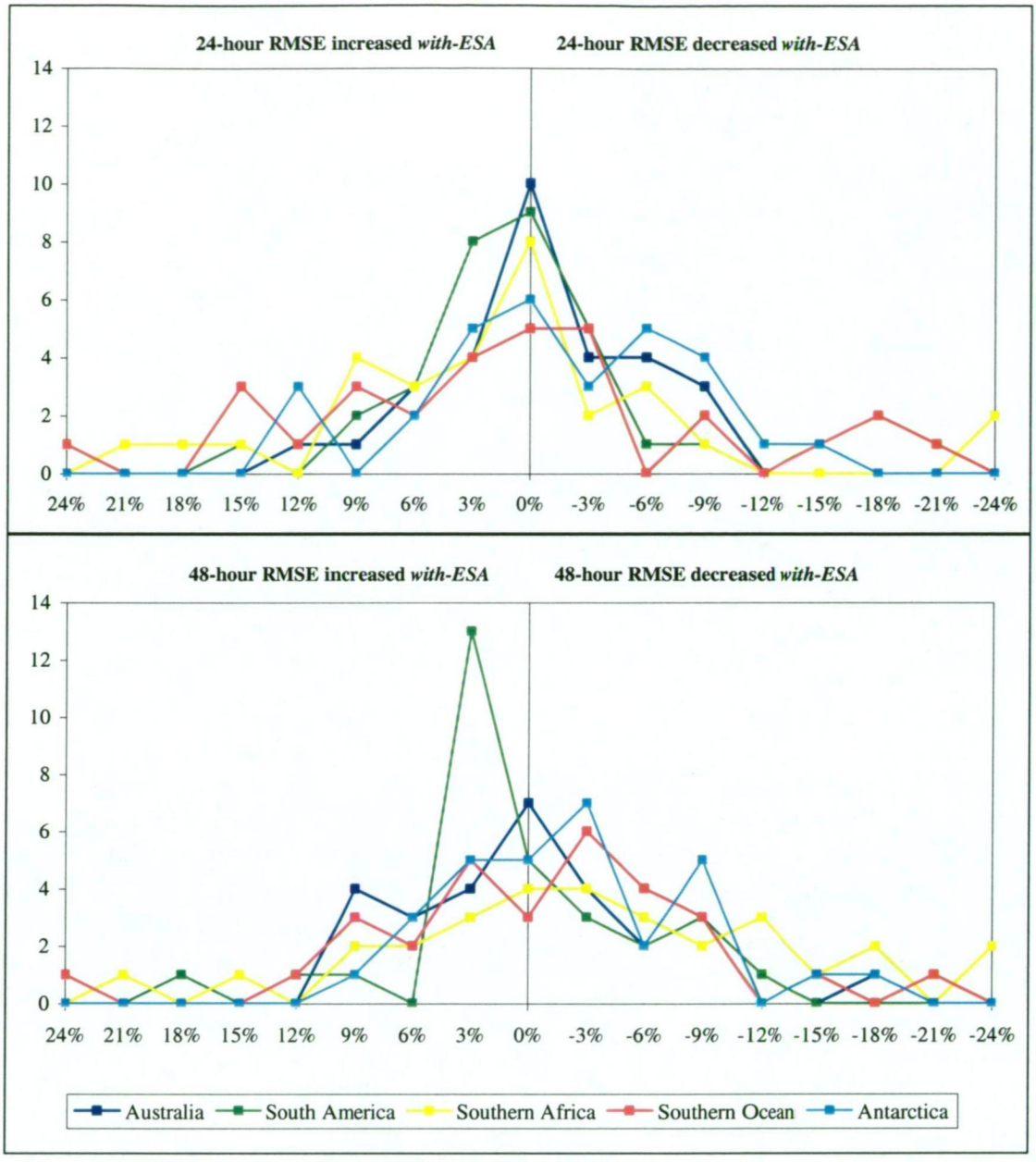

Figure 4.5.4 Histogram representation of the data in Table 4.5.4. The *y*-axis represents the number of days (out of 30); the *x*-axis represents percentage rise or fall in RMSE with the inclusion of scatterometer winds.

consequently, the artificially elevated model surface over neighbouring ocean areas. No definitive explanation has been identified.

The forecast impact at 500hPa was uniformly small. Indeed the impact that was observed was most likely entirely a result of changes to data rejection decisions

involving individual remote MSLP observations. The resultant mass field alteration was then substantial enough to be detectable at 500hPa. Nevertheless the scatterometer winds played an important role in those quality control decisions and are, therefore, closely linked to the forecast impact result observed.

To assist with the explanation of these results, a further comment is warranted on the difficult process of determination of accuracy of NWP systems over data sparse areas. The conventional methodology of verifying prognoses directly against analyses has inherent problems because, in data sparse areas, analyses are themselves quite imperfect with the prognoses providing the first-guess diagnosis for the analyses.

In a data sparse environment analysis errors can readily propagate through a time-series of analyses.

Figure 4.5.5 shows a schematic representation of the process of verifying prognoses against analyses. Considering a hypothetical situation where a poor quality analysis (at t = 0 hours) formed the basis of a series of prognoses. The next analysis in the analysis sequence (t = 6 hours) would be generated on the basis of a 6-hour first-guess prognosis stemmed from the base analysis (t = 0 hours) plus observations. Subsequent analyses are generated similarly.

In a data sparse environment the number of observations included at each 6-hourly assimilation cycle is limited. In some parts of the Southern Ocean and Antarctic region no observations are available. To complicate matters further, all observations are checked for quality against the 6-hour first-guess forecast before they are utilised. Lone observations, those unsupported by close neighbours, will be assumed erroneous if they differ sufficiently from the first-guess.

Consequently, errors in the base analysis (t = 0 hours) may not be corrected in subsequent analyses due to a lack of observational evidence.

The verification process which then occurs at t = 24 hours will verify a poor 24-hour forecast (stemmed from a poor base analysis) against an analysis also corrupted by errors from the same base (t = 0 hours) analysis.

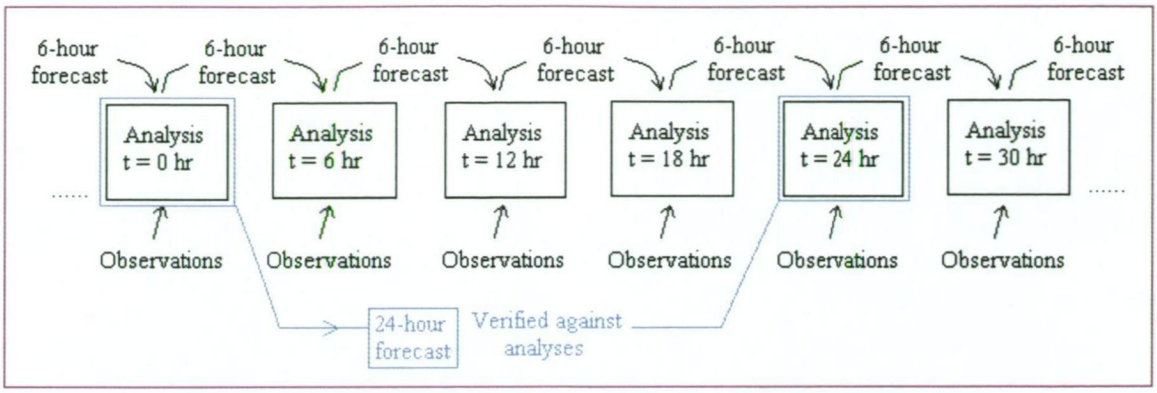

Figure 4.5.5 Schematic representation of the assimilation / analysis / prognosis sequence used by the GASP system. Successive analyses are formulated on the basis of a first-guess forecast, stemmed from a cycle 6-hours earlier, plus observational data tested for quality against one-another and against the first-guess. The process of verification against analyses involves comparison between a forecast derived from a base analysis (t = 0 hours) and successive analyses in the on-going sequence (t = 24 hours for example).

For these reasons, satellite-borne observing systems, which provide extensive, cumulative global coverage, offer a distinct benefit to analysis systems. Observing instruments on polar-orbiting satellites, such as the wind scatterometer and TOVS, provide particularly good coverage in the Antarctic and Southern Ocean region. Figure 2.2.3 (in Chapter 2) shows the ground coverage of the ERS-1 scatterometer instrument in a sample 24-hour period.

Alternative systems of verification exist. Two examples follow:

(i) Prognoses can be verified directly against reliable surface and radiosonde observations. This methodology has clear benefits but is not particularly feasible in the Antarctic and Southern Ocean region due to a lack of observational data against which to verify.

(ii) An independent NWP system can be used for verification. In data sparse environments large differences naturally exist between analyses and prognoses from different centres. Small differences, such as those that might arise from the inclusions of a new observing system, are not

detectable over the background of large differences between independent NWP systems.

In reality no perfect method exists and the most comprehensive of data impact trials may consider a combination of multiple methods.

4.6 Summary of results

A series of NWP data impact experiments was successfully completed involving the utilisation of scatterometer winds in the ABOM GASP system. Scatterometer winds derived via the CMOD4 algorithm (Stoffelen and Anderson 1997b) were successfully utilised in the GASP system during a one-month pseudo-operational trial. The global scatterometer data set was utilised to generate a full series of 6-hourly analyses and daily forecasts (to 24, 48, 72, 96 and 120-hours).

The inclusion of scatterometer winds generated many large local impacts on GASP analyses, particularly across the Southern Ocean. Multiple events were identified where the scatterometer winds effectively altered MSLP analyses by up to 15hPa over the Southern Ocean. The larger of these strong impact events resulted from scatterometer winds acting to reverse quality control decisions relating to the rejection of some individual drifting buoy reports.

Although the overall average improvement in skill was relatively small, it was found that:

- Large analysis impact events resulted in a large (positive) impact on forecast skill in all cases studied. Significant analysis impact events in or near the Antarctic sea ice zone resulted in significant (positive) medium-range forecast impact in Southern Australia.
- Mean analysis impact statistics were also significant. A mean increase in analysis MSLP (of approximately 2hPa) was detected across a substantial swathe of the Southern Ocean.

Prognoses were verified against analyses in a range of verification areas across the globe. The mean skill statistics indicated little MSLP or 500hPa height prognosis

impact from utilisation of the scatterometer winds, however those results do not adequately represent the large impacts found for some daily case studies.

A summary of daily prognosis skill (with verification against corresponding analyses) for the *with-* and *without-ESA* trials indicated a small degree of positive impact from the inclusion of scatterometer winds. When verified against analyses, RMSE and bias were reduced in most MSLP forecasts, particularly at 48-hours, for most of the continents of the southern hemisphere. The greatest impact, in terms of RMSE and bias, was over the Southern Ocean. S_1 skill-score impact was close to neutral.

In many cases of large forecast errors, the inclusion of scatterometer winds acted to reduce the magnitude forecast errors.

The results of this chapter indicate that the inclusion of scatterometer winds in the GASP R53L19 system improved the prognosis performance of the system most of the time. The regions of the globe where forecast skill was particularly lacking were the regions to benefit most from the utilisation of scatterometer winds.

It should be noted that the persistence of some errors from the analyses through the prognoses and subsequent analyses makes the evaluation of forecast skill difficult. The system of assessment of prognoses against the analysis is not as effective for evaluating the impact of the scatterometer data as consideration of the case studies involving large differences.

CHAPTER 5

ASSESSMENT OF SOME OTHER DATA SYSTEMS FOR THE ANTARCTIC AND SOUTHERN OCEAN REGION

5.1 Introduction

A substantial body of published work has addressed the quality assessment of remotely sensed data systems as well as buoys, AWS and ship data. Several have involved data impact experiments with the GASP NWP system, testing the inclusion of one or more of drifting buoys, cloud drift winds, manually derived "bogus" atmospheric pressure data and conventional observations. Examples include Seaman et al. (1993), Seaman (1994), Le Marshall and Pescod (1994) and Le Marshall et al. (2001). Other studies have investigated data quality over the Antarctic continent specifically (for example Adams et al. (1999) and Allison (1998)).

In this chapter an assessment is made of the value of satellite derived vertical sounding data (TIROS Operational Vertical Sounder (TOVS)) for atmospheric analyses over Antarctica and the Southern Ocean and of the problems in determining the surface temperature distribution over the Antarctic ice sheet.

5.2 TOVS quality study

Vertical atmospheric soundings from polar-orbiting satellites are a key component of the observing system over the Antarctic and Southern Ocean region. They contribute significantly to the analysis of the troposphere and stratosphere by operational NWP systems including those of ECMWF and ABOM.

Satellite soundings utilise the strong absorption bands of some atmospheric gases, where the absorption varies strongly with wavelength. At wavelengths near the centre of such bands, radiation from the atmosphere is absorbed and re-emitted over relatively short distances; radiation emerging from the top of the atmosphere will have originated from the upper atmosphere and will represent the temperature of

that region. In the wings of the bands the absorption is much less and the emerging radiation will, on average, have originated from lower in the atmosphere. The combination of instruments, collectively known as TOVS, comprises: (i) High Resolution Infrared Sounder (HIRS) which measures upwelling radiation at several wavelengths in the carbon dioxide 15μm infrared absorption band; (ii) Microwave Sounding Unit (MSU) which uses the oxygen absorption band (between 50.3GHz and 57.1GHz); and (iii) Stratospheric Sounding Instrument (SSU). Pre–processing steps are used to determine surface temperature and the presence of cloud or aerosol contamination in the column (Turner and Pendlebury 2000).

The derivation of vertical profiles of atmospheric temperature and water vapour from the TOVS measurements is not straightforward. A variety of techniques are used to detect problems in the observations and to give physically realistic profiles. These include statistical techniques based on regression between observed radiances and radiosonde measurements, or variational solutions starting from a physically realistic first-guess and adjusting the temperature and moisture (and perhaps cloud cover) through a radiative transfer scheme, until the best fit is obtained. The accuracy of the retrievals is typically regarded as about 2°C through most of the troposphere based on comparisons with collocated radiosondes. However, errors are considerably larger where there are sharp vertical discontinuities such as inversions (Turner and Pendlebury 2000).

During the first FROST special observing period (SOP1), July 1994, radiosonde data were obtained from a total of 19 stations within and just outside the FROST area of interest (the region South of 50°S). Of those 19 stations, 10 conducted twice-daily flights and the remaining 9 conducted flights daily, or less frequently (a map of Antarctica is shown in Figure 1.1.1; a listing of meteorological stations is included in Appendix 1). Over vast areas of the Southern Ocean data from satellite borne instruments was the only source of mid and upper-level atmospheric data available for the FROST SOP1 re-analysis study. NOAA/NESDIS TOVS thus became a fundamental component in the construction of the 500 and 250hPa level analyses under preparation during the FROST project. Figure 5.2.1 shows the elaborate method of construction of FROST analyses and the degree to which analyses of TOVS data were used. Figure 5.2.2 shows a segment of a manual analysis chart used during FROST.

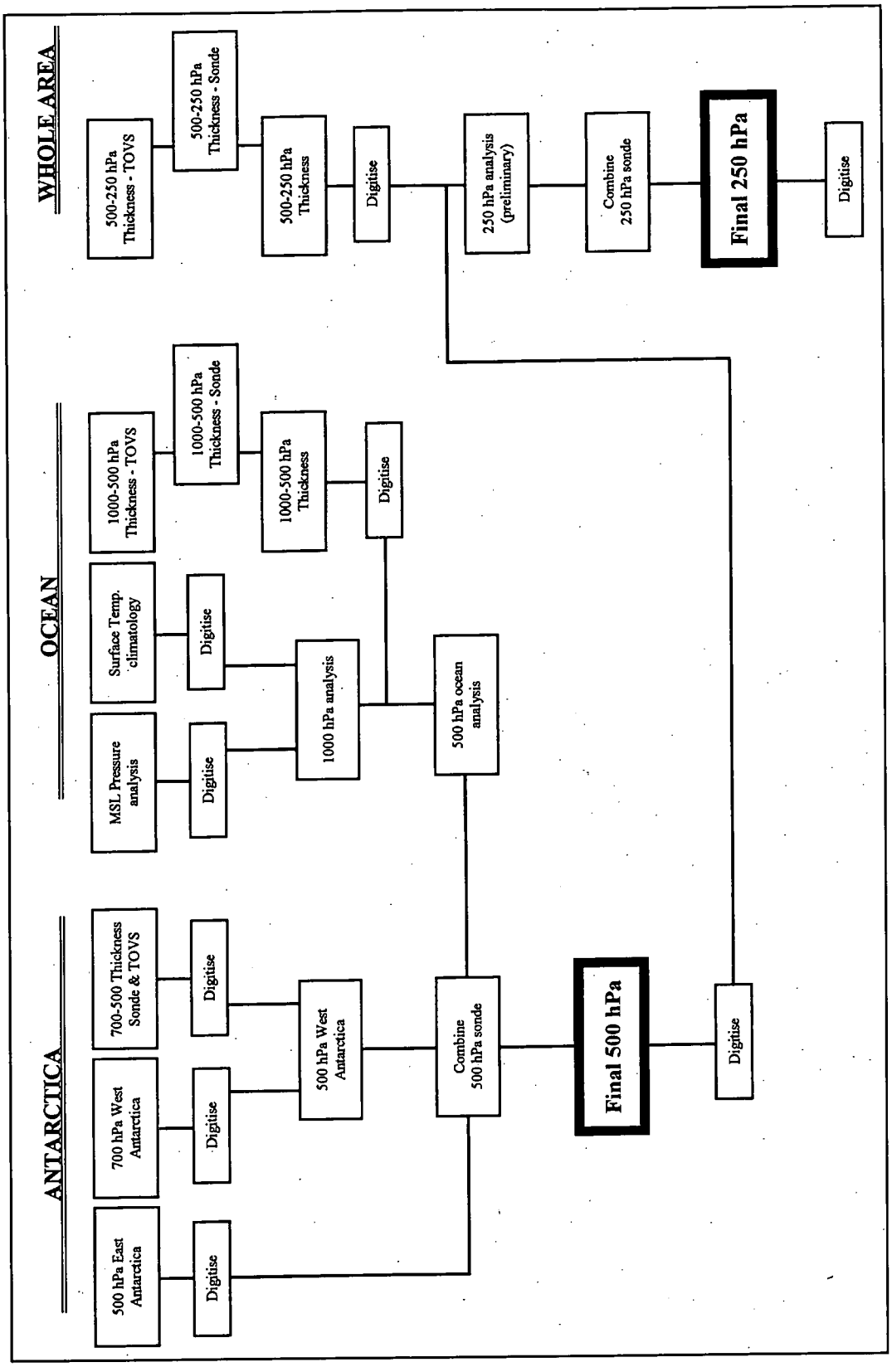

Figure 5.2.1 Schematic diagram of the FROST analysis routine (reproduced from Hutchinson 1996).

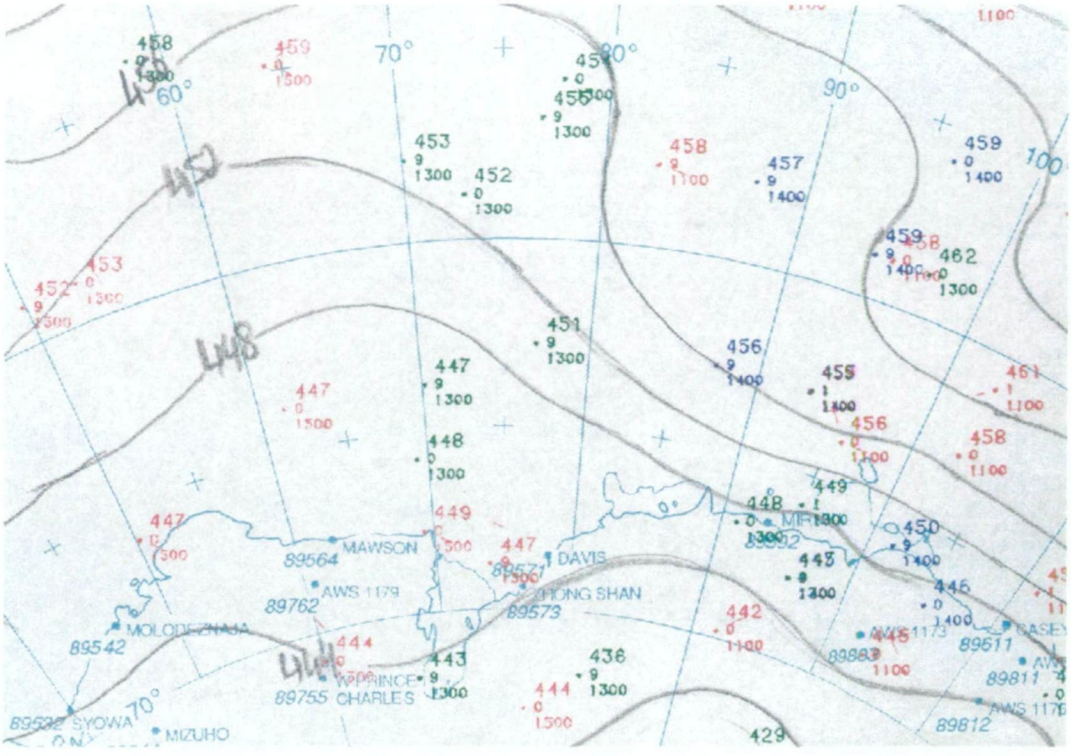

Figure 5.2.2 Example of a manual analysis chart used for the analysis of TOVS thickness data during FROST (0900 - 1500UTC 29 July 1994). 500 – 250hPa thickness TOVS (dam) are plotted together with a confidence flag (9 = *high-*, 1 = *low-*, 0 = *unspecified-*), a time stamp (UTC) and hand drawn contours at 4dam spacing.

This study constitutes a preliminary assessment of TOVS atmospheric thickness data quality over the FROST SOP1 area and period of interest.

Sonde data from 19 Antarctic and sub-Antarctic stations were directly compared with coincident NOAA/NESDIS TOVS thickness estimates (500km resolution) recorded over the area of interest.

The TOVS estimates under study consisted of NOAA/NESDIS derived values of 1000-500hPa, 700-500hPa and 500-250hPa thickness data. Each estimate was flagged as *high-confidence, low-confidence* or *unspecified-confidence* depending on the amount of cloud and the degree to which the High Resolution Infrared Radiation Sounder (HIRS) data could be used. HIRS measures scene radiances in multiple

spectral bands to permit the calculation of the vertical temperature profile in cloud-free conditions. The number of spectral bands measured in cloudy conditions is reduced. The *low-confidence* data constituted only a small proportion of the full population used for FROST.

Sonde data used for the study consisted of data from all known sonde flights during July 1994 South of 45°S apart from a number of flights from Amundsen-Scott and McMurdo stations where data transmission problems during the month hindered real-time reception. Those data that were received late were too late to be included in this part of the study.

Direct comparison was made between sonde measured atmospheric thickness data and TOVS derived thickness data within close distance and time proximity. In the first instance data within 500km of a radiosonde station were used in the comparison. TOVS recorded within an envelope of ±2 hours of a radiosonde flight were analysed. These criteria provided good data coverage over most stations. Data quantity from lower thickness levels was reduced over elevated land areas.

Figures 5.2.3 show comparisons between radiosonde and TOVS data for 1000 - 500hPa thickness, 700 - 500hPa thickness and 500 - 250hPa thickness. These each show data plots collectively from all three confidence groups and from all stations South of 45°S during July 1994. Colour is used to delineate different TOVS confidence ratings.

A histogram representation of the same data (Figure 5.2.4) shows a close to normal distribution but a somewhat greater degree of spread in the 1000 - 500hPa data results. In each case the mean of the distribution is located at a point slightly less than zero, indicating a small TOVS > radiosonde trend. All three TOVS confidence ratings considered together, the mean and standard deviation of the differences (errors) were estimated at:

	Mean	*SD*
1000 – 500hPa	15.3m	61.3m
700 – 500hPa	5.6m	30.0m
500 – 250hPa	7.1m	41.4m

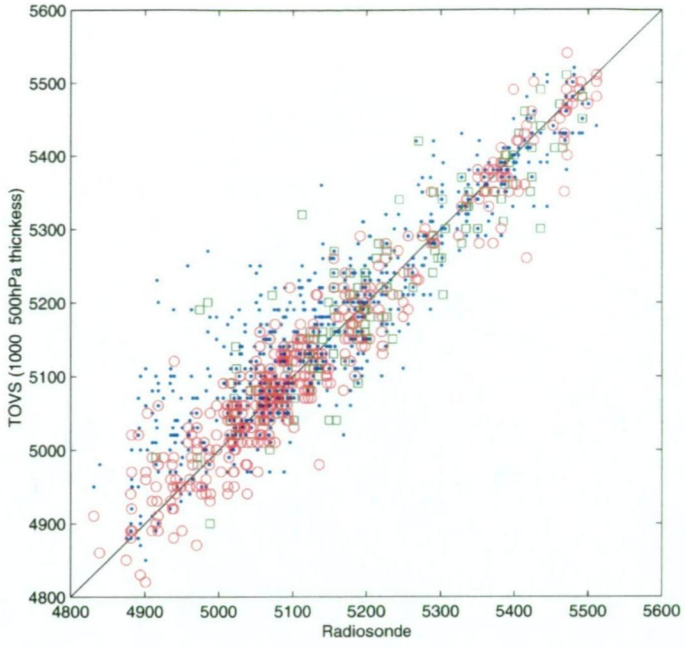

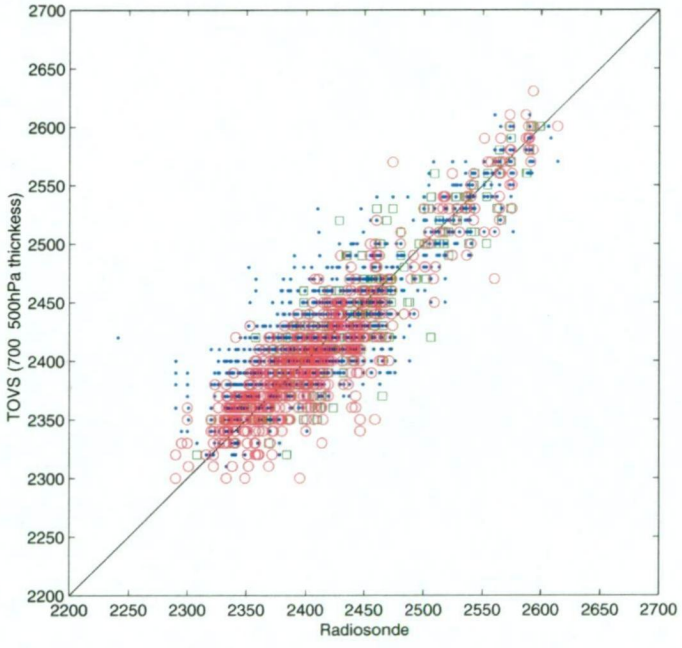

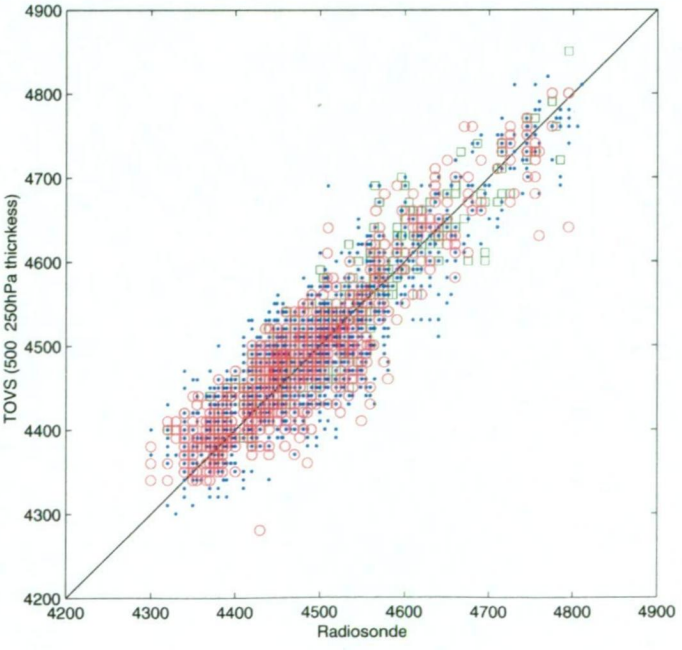

Figure 5.2.3

Radiosonde derived thickness verses TOVS derived thickness of layers:

Top: 1000 - 500hPa.

Middle: 700 - 500hPa.

Bottom: 500 - 250hPa.

TOVS data confidence ratings are plotted as follows:

Green squares: *Low.*

Red circles: *High.*

Blue dots: *Unspecified.*

Data are included from all radiosonde stations South of 45°S during July1994.

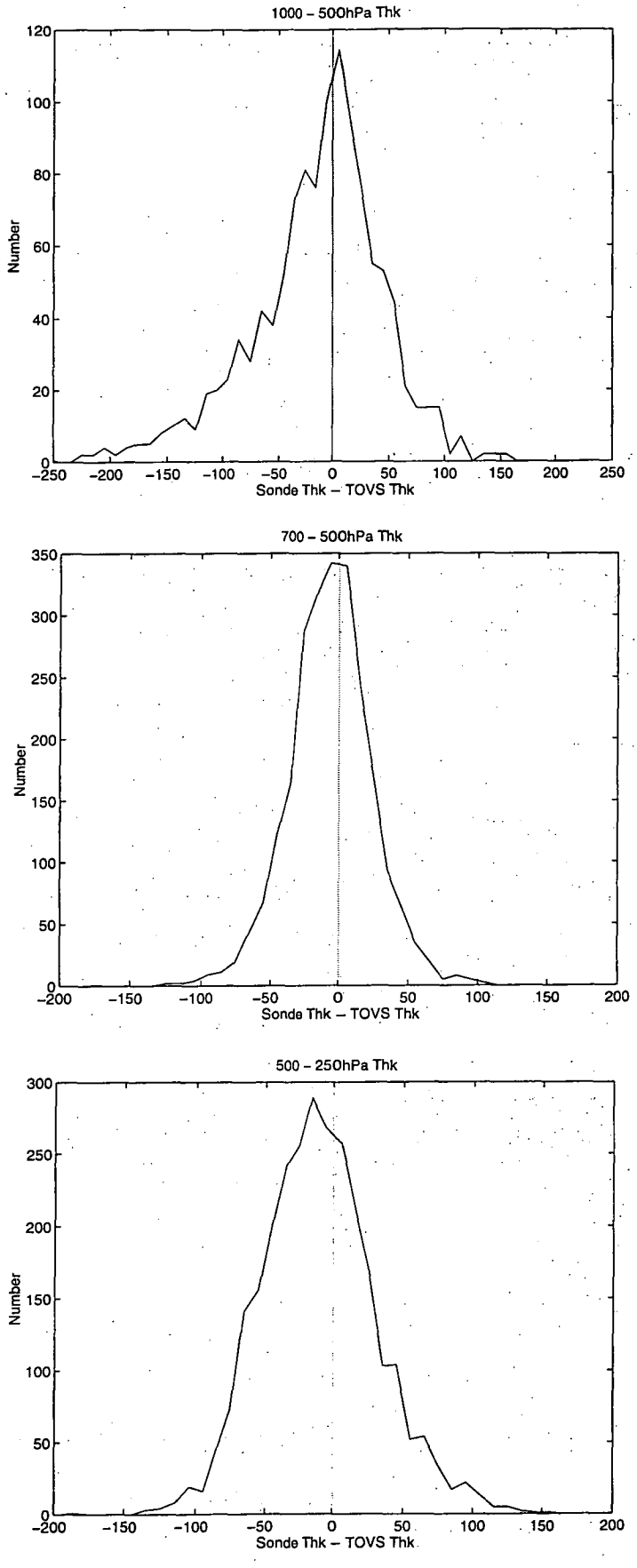

Figure 5.2.4
Histogram representation of radiosonde thickness minus TOVS thickness:
Top: 1000 - 500hPa.
Middle: 700 - 500hPa.
Bottom: 500 - 250hPa.

Includes all three confidence groups and data from all radiosonde stations South of 45°S during July 1994.

The degree of spread of *high-confidence* TOVS data was slightly less (superior agreement with radiosonde) than that of the other confidence groups. Error statistics, showing the mean and standard deviation of radiosonde minus TOVS thickness differences, are given in Table 5.2.1. The population of *high-confidence* data over the Antarctic continent was too small to warrant individual discussion.

Mean and Standard Deviation (m) of Radiosonde minus TOVS differences. Grouped by confidence rating. All regions combined.		*High-confidence*	*Low-confidence*	*Unspecified-confidence*
1000 – 500hPa thickness	Mean:	-0.8	-3.5	-25.8
	SD:	45.6	59.2	67.1
700 – 500hPa thickness	Mean:	0.7	1.2	-9.9
	SD:	26.5	28.6	31.2
500 – 250hPa thickness	Mean:	-7.0	-11.2	-6.7
	SD:	39.1	37.1	43.0

Table 5.2.1 Mean and standard deviation of radiosonde minus TOVS atmospheric thickness differences (m). Results of co-location with all available radiosonde flights are shown (South of 45°S; July 1994). Data are separated into the three TOVS confidence groups.

These 1000-500hPa results highlight the greater level of skill of the *high-confidence* data. The differences are less significant at the higher altitudes. That part of the atmosphere below 700hPa is more problematic, in terms of vertical temperature profiling, than at higher altitude. The near-surface temperature distribution is complex, particularly in the Antarctic region, and significant amounts of cloud lie below 700hPa. Both of these factors hinder the accuracy of TOVS.

Data were analysed in groupings of stations with similar latitude and geographic characteristics. The stations were grouped together as follows:

(i) Macquarie and Campbell Islands – Both islands distant from any continent, at latitudes of 54.5 and 52.6°S respectively;

(ii) Punta Arenas and Mt Pleasant Airport – the former at the Southern tip of South America (53.0°S) and the latter on the Falkland Islands (51.8°S); and

(iii) Mirny, Casey and Dumont D'urville – all coastal stations of East Antarctica at latitudes of 66.6, 66.3 and 66.7°S respectively.

Data from each of these groupings of stations were analysed separately for the three different prescribed data confidence ratings. The results showed an increased level of reliability in data with the *high-confidence* rating, but the differences were relatively small. The greater effect was that of geographic region with a substantial degradation in quality of data over the Antarctic continent.

Table 5.2.2 shows the mean and standard deviation of radiosonde minus TOVS thickness data. Due to the similarity of statistics from Macquarie and Campbell Islands with those from Punta Arenas and Mt Pleasant Airport, here all results are grouped into just two collections: Coastal Antarctica and sub-Antarctic / Oceanic.

Mean and Standard Deviation (m) of Radiosonde minus TOVS differences. **Grouped by region.** **All three confidence ratings combined.**		**Radiosonde group 1** Casey, Mirny, Dumont d'Urville.	**Radiosonde group 2** Macquarie Island, Campbell Island, Falkland Islands, Punta Arenas.
1000 – 500hPa thickness	Mean: SD:	-22.0 64.1	3.6 45.7
700 – 500hPa thickness	Mean: SD:	-0.4 33.3	-1.9 25.4
500 – 250hPa thickness	Mean: SD:	-0.8 42.3	-3.1 40.2

Table 5.2.2 Mean and standard deviation of radiosonde minus TOVS atmospheric thickness differences (m). Data with all confidence ratings are included. Results are separated into two groupings of radiosonde stations:

Group 1: Three coastal stations of East Antarctica with similar broad scale geographic characteristics.

Group 2: Three stations on sub-Antarctic islands plus Punta Arenas (near the southern tip of Chile).

Below 500hPa the radiosonde verses TOVS correlations were universally better over sub-Antarctic and oceanic areas than those over coastal Antarctica. The bias of the coastal Antarctic data was significant but essentially confined below 700hPa.

Figures 5.2.5 show 1000 – 500hPa thickness data from TOVS plotted against coincident data from radiosondes from two stations in the South American sector (top) and three stations on the East Antarctic coast (bottom). A substantially greater degree of scatter and bias is evident in the data from the East Antarctic region.

TOVS data over open ocean areas are shown to be of greatest confidence. But the lower frequency of repeat orbits of the satellites across these more northern sites meant a reduced population of data against which to verify.

The bias towards higher thickness in the TOVS data relative to radiosonde data, quantified above, is related to the vertical temperature distribution. Over the Antarctic ice sheet (and to a lesser extent over the adjacent sea ice zone) there exists a thin layer of particularly cold air close to the surface. This is capped by a strong temperature inversion. The limited vertical resolution of the TOVS system may cause the system to be unable to detect this important thin, cold, near-surface layer. One direct consequence would be an over-estimate of layer thickness.

The magnitude of such a bias could be accounted for if the strength and depth of the near-surface temperature inversion is closely linked to the TOVS bias. A NWP system could be used to quantify the likely TOVS bias from the characteristics of the modelled surface temperature distribution. This relatively simple process could be followed prior to data assimilation.

For the purposes of utilising TOVS data over the Antarctic region, it is clearly important to study the physics and dynamics of the Antarctic boundary layer and the characteristics of the surface inversion. Some of those issues are discussed further in Section 5.3. The strength of the near-surface temperature inversion is known to be far greater during the winter months than at other times of the year. It would be expected that the degree of bias in TOVS thickness would also have a seasonal connection. Unfortunately this validation study was limited to one winter.

Later work by Adams et al. (1999) identified a seasonal bias in a similar analysis of TOVS over Antarctica, with improved TOVS performance in the summer months.

Generally speaking, and from the perspective of FROST, TOVS data were found to be highly reliable. The findings of consistent bias in TOVS could be compensated for prior to analysis. The degree of random error could be tolerated in the absence of data from alternative sources. TOVS were regarded as particularly valuable, during FROST, over open ocean areas where data from other sources was badly lacking.

Data flagged *high-confidence* were found to be of highest quality, but *low-confidence* and *unspecified-confidence* data were also considered to be of considerable value during FROST.

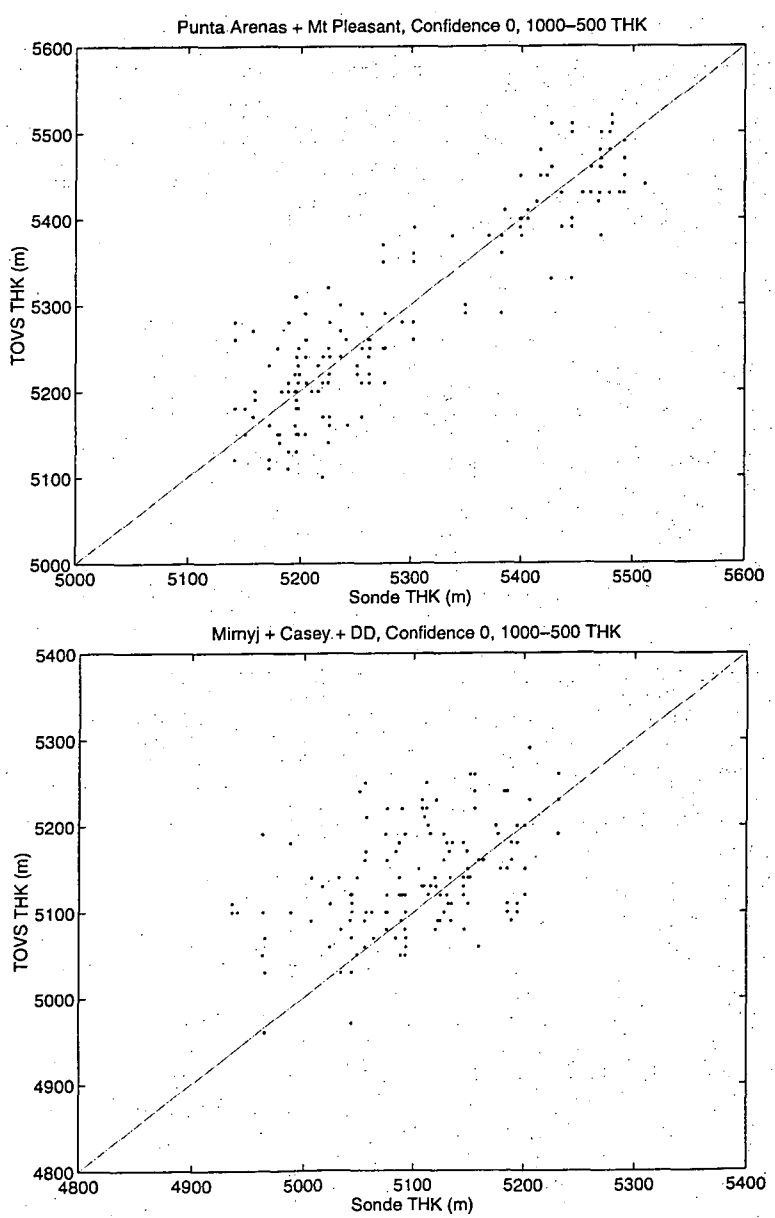

Figure 5.2.5
TOVS derived 1000 - 500hPa thickness (*unspecified-confidence*) plotted against radiosonde thickness from coincident radiosonde flights at:

Top: Punta Arenas and Falkland Islands.

Bottom: Mirny, Casey and Dumont d'Urville.

The analysis described here, and presented at an early FROST planning workshop, provided sufficient information on TOVS thickness data reliability for them to be utilised as the sole source of data, where necessary, over some remote areas during the FROST SOP-1 analysis programme. During FROST TOVS were used confidently over land and sea.

Some of the issues relating to the surface temperature distribution over Antarctica, important for the utilisation of TOVS, are discussed further in the next section.

5.3 Antarctic inversion study

Relatively few studies have closely investigated the strength of the low level Antarctic inversion. Refer to Murphy and Simmonds (1993), Phillpot and Zillman (1970), Allison (1998), Allison et al. (1993), Radok et al. (1996) and Connolley (1996) for examples of related work. King and Turner (1997) and Turner and Pendlebury (2000) also provide useful background reading in the context of weather forecasting and meteorology.

Most research has concentrated on the strength of the inversion as it relates to understanding the climatology of the region as distinct from the meteorology. The strength of the inversion, and its temporal and spatial distribution, profoundly affect the surface wind regime. Substantial changes in the inversion strength occur hour-by-hour. They occur as a result of forcing on the synoptic scale; in response to the development and movement of mesoscale systems; and in connection with the surface radiation and heat balances. They are also heavily influenced by the mixing effect of the surface wind. For the purposes of real-time weather forecasting for coastal Antarctic locations, the behaviour of the inland inversion is an important factor that must be considered.

An earlier study by Murphy and Simmonds (1993) concentrated on the use of a general circulation model in the Casey region of East Antarctica to determine the linkage between synoptic scale meteorological events and katabatic forcing on the generation of strong wind at the coast. They used a 21-wave model with nine σ levels (where $\sigma = P / P_{surf}$). The lowest was at $\sigma = 0.991$.

Murphy and Simmonds (1993) found that strong wind events at Casey were typically caused by the simultaneous superposition of strong gradient forcing and strong katabatic forcing. Inversion strength was a factor in influencing the evolution of katabatic flow, but it in turn was affected by the geostrophic wind (through the low-level mixing it induces) and the mixing performed by the katabatic wind itself. They indicated that the feedback mechanisms operating between the katabatic and gradient wind components caused a threefold increase in both.

Streten (1990) found that the influence of major depressions was almost always of critical importance when prolonged strong winds were observed at Casey.

This study investigates inversion strength and distribution as represented in the ABOM GASP T79L19 numerical analyses. The study concentrates on the winter and spring months of 1998.

The GASP data used in this study were represented on nineteen σ surfaces. The two σ surfaces closest to ground level were $\sigma = 0.991$ and $\sigma = 0.950$ representing heights of approximately 75m and 460m above ground level respectively. Over the high interior of the Antarctic continent (reaching 4,000m altitude) the surface air pressure is significantly lower than at mean sea level. There, roughly speaking, the $\sigma = 0.991$ and $\sigma = 0.950$ surfaces sit at around 50m and 400m respectively above the surface of the model topography.

The depth of the inversion is typically thought to reach over 500m in the winter months high on the Antarctic interior plateau, grading to about 300m at coastal locations (Turner and Pendlebury 2000, Schwerdtfeger 1984). Thus, in such typical cases, the separation of σ surfaces, and their height above ground level, together with σ surface temperature and wind fields provide a useful collection of data for the estimation of strength and distribution of the low-level inversion.

The average strength of the surface inversion in winter has been found to be approximately 5°C around most of the coastal fringe, grading to over 25°C in the interior (Phillpot and Zillman 1970). However the inversion strength is known,

from radiosonde data, to often exceed 30°C at Vostok (3488m elevation) (King and Turner 1997).

Figures 5.3.1 show the mean GASP temperature difference between the surface and the $\sigma = 0.991$ level (and between the surface and $\sigma = 0.950$ level) for the June to August period (hereafter JJA) of 1998. These figures show mean winter temperature differences in the thin near-surface layer in excess of 30°C over a large

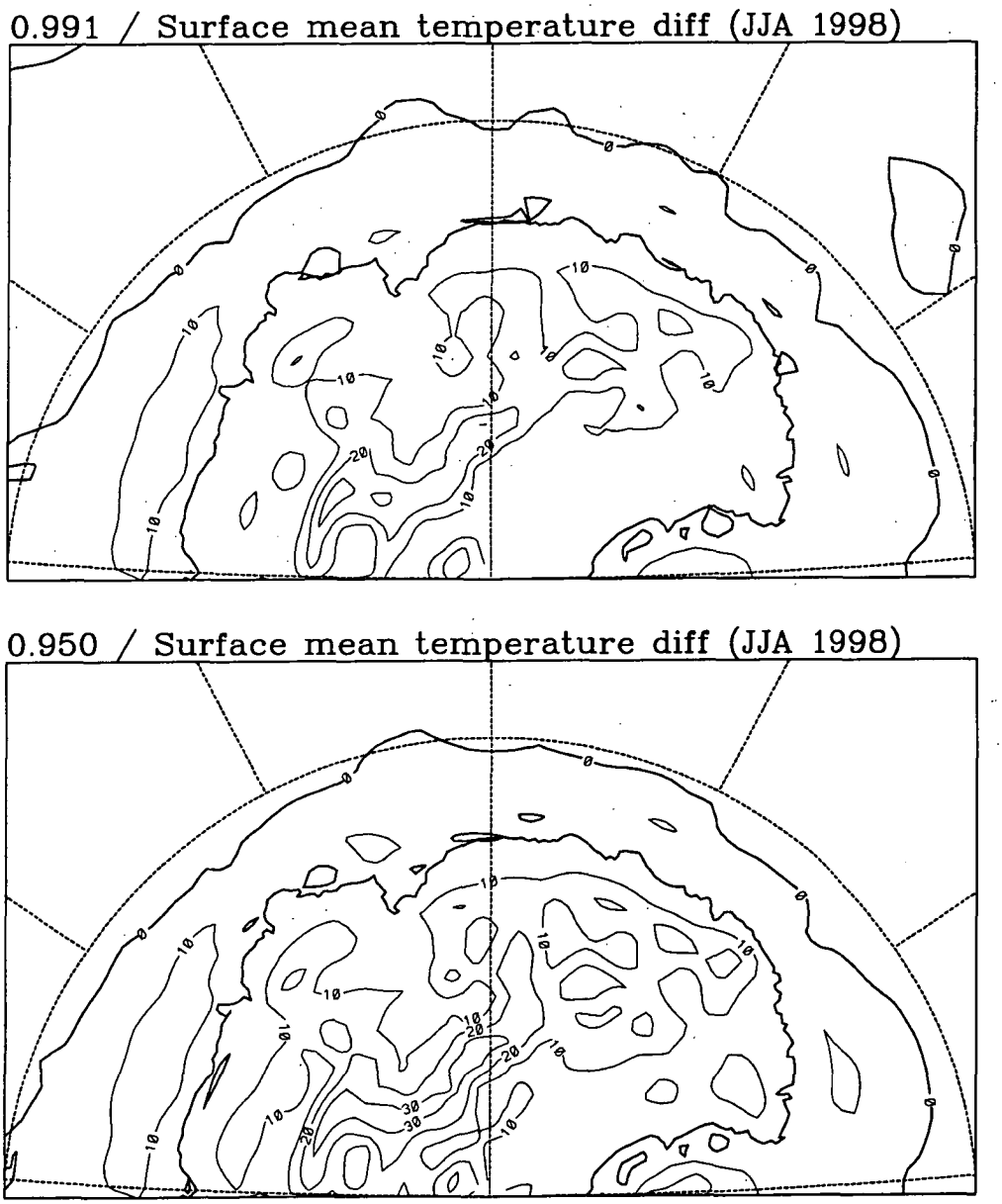

Figure 5.3.1 Mean GASP temperature differences for the **June to August** period of 1998 (°C; contour interval 10°C):
$T_{0.991}$ minus T_{surf} (top); and
$T_{0.950}$ minus T_{surf} (bottom).

area of the continental interior. The bulk of the inversion strength is captured in the surface to $\sigma = 0.991$ layer (approximately 50m thick).

A similar representation of layer temperature differences for September to November 1998 showed remarkably similar trends (Figures 5.3.2). Typically inversion strength was 5 to 10°C weaker than that of JJA but the distribution followed a similar pattern. The exception was the area around Dome Fuji which,

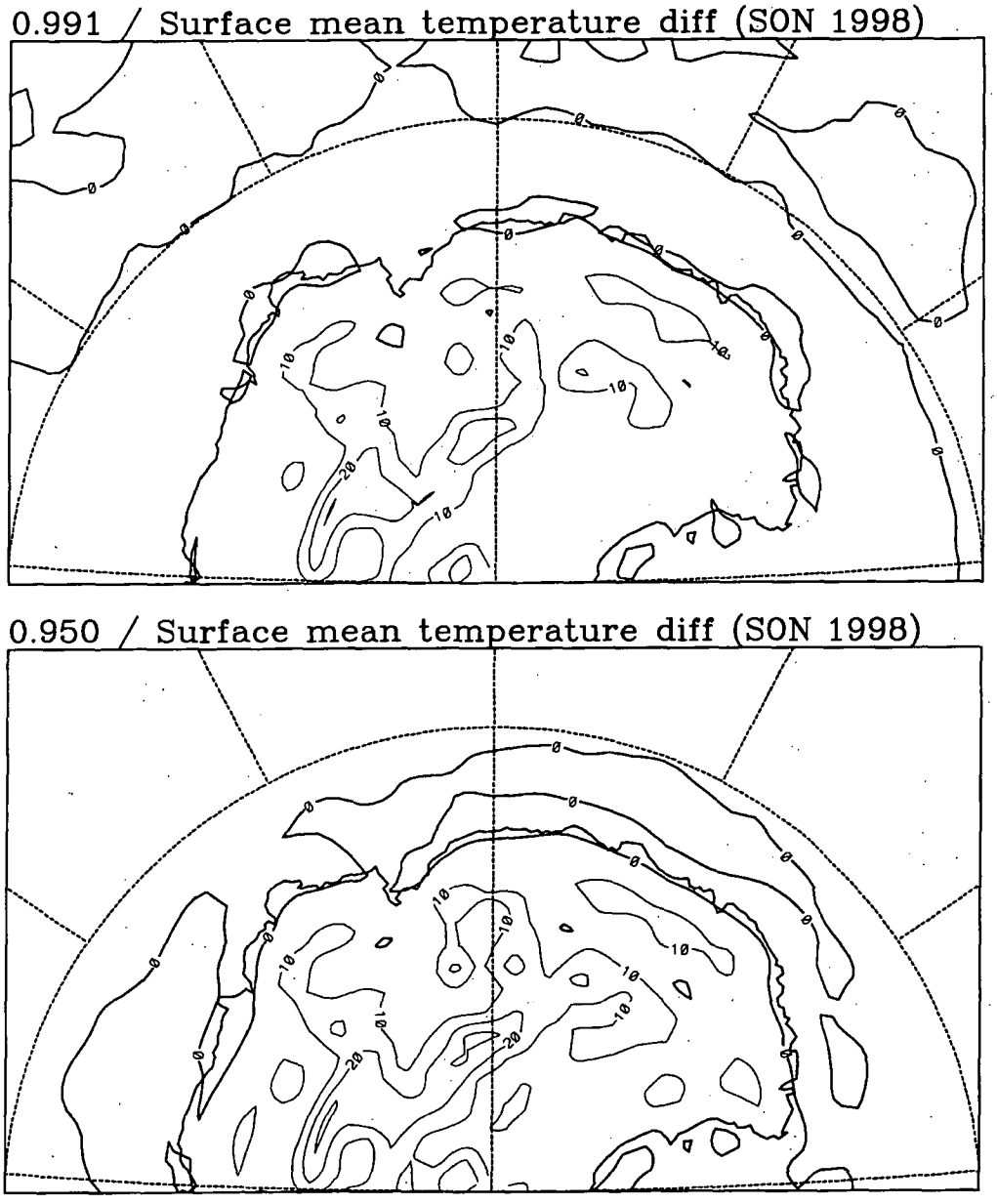

Figure 5.3.2 Mean GASP temperature differences for the **September to November** period of 1998 (°C; contour interval 10°C):
$T_{0.991}$ minus T_{surf} (top); and
$T_{0.950}$ minus T_{surf} (bottom).

throughout the June to November (1998) period, maintained a mean monthly surface to $\sigma = 0.991$ inversion of over 25°C.

Temperature differences between the second and third σ levels (0.950 and 0.900) and between the third and fourth σ levels (0.900 and 0.850) were found to be relatively minor in comparison to those closer to the surface. In other words, the inversion was most often confined within the layer below $\sigma = 0.950$ (about 400m). This result is supported by the several references (including Turner and Pendlebury 2000 and Schwerdtfeger 1984) which indicate that the typically depth of the winter-time inversion is about 500m on the Antarctic interior plateau.

These results show broad similarity to those of earlier observational studies referenced above. They also support the findings of Murphy and Simmonds (1993) in spite of the differences in model resolution and topography.

Many factors are implicit in the calculation of the surface inversion in a NWP system. The model representation of ice albedo, cloud thickness and distribution, and surface terrain all play an important role.

Also important is the availability of relevant observational data at the time of assimilation. The GASP model assimilation scheme here used no low or middle-atmosphere TOVS data over the Antarctic region, nor any wind, surface temperature or air temperature observations from surface stations. It did, however, assimilate surface pressure data from high altitude stations on the continent and radiosonde data from all Antarctic stations performing flights. The utilisation of surface air temperature (and potentially surface temperature) reports in the assimilation system, together with a boundary layer scheme that represents inversions well, may help to improve analysis skill.

Figures 1.3.3 in Chapter 1 show the topography as represented in the R31, T79 and T_L239 wave-number versions of GASP. Concentrating on the T79 topography, the bulk of the continent is fairly well represented by a smooth dome, reaching just under 4000m at its highest point, and an abrupt coastline. The major geographic features of the Ross Sea, Weddell Sea and Lambert Glacier Basin are also

represented with a reasonable degree of accuracy. Somewhat less well represented are the mountainous Antarctic Peninsula and the steep surface gradient on the western side of the Ross Sea. These problems are improved in the higher resolution T_L239 version.

From the results shown above it can be inferred that the T79 resolution GASP system performed satisfactorily in terms of its mean seasonal representation of the distribution and strength of the Antarctic inversion. Pendlebury et al. (2003) indicated that these good results are also evident in the higher resolution T_L239 version. A regional grid point model, currently under development at ABOM, shows promising early signs of improved boundary layer temperature distribution. Nested in GASP output, that system has a higher resolution horizontal grid and a greater concentration of vertical layers in the lower boundary layer (Adams 2001 and Neil Adams, personal communication, 2002).

For the purposes of weather forecasting it is of interest to investigate the model representation of the temporal and spatial distribution of inversion strength on short time scales. Rapid changes in the distribution and strength of areas of strong inversion bear a remarkable relationship with the wind strength at coastal stations. A NWP system with the capability of predicting inversion strength and the intricacies of its distribution would be a powerful tool for weather forecasting in Antarctica.

With a view to determining the usefulness of the GASP system at representing these short time scale changes, data from several strong wind events at Casey were considered together with:

(i) GASP wind strength and temperature data represented on σ surfaces;

(ii) fields of $T_{0.991} - T_{surf}$ (hereafter $\Delta T_{0.991}$) and $T_{0.950} - T_{surf}$ (hereafter $\Delta T_{0.950}$); and

(iii) fields of departure of $\Delta T_{0.991}$ and $\Delta T_{0.950}$ from the three-month climatology.

Five examples were identified over the JJA period in which departures of $\Delta T_{0.991}$ from climatology aided forecasting blizzard onset at Casey Station.

While no two cases were identical they all shared some similar features in development. A typical sequence of events preceding blizzard formation was:

- [t = -30 hours] $\Delta T_{0.991}$ close to climatology throughout Wilkes Land.
- [t = -24 to -12 hours] $\Delta T_{0.991}$ increases by as much as 15°C greater than climatology (inversion strengthened) centred along 70°S.
- [t = -6 hours] $\Delta T_{0.991}$ decreases and contracts as the surface wind rapidly increases at Casey.
- [t = 0 hours] Blizzard fully developed at Casey.

The following example showed some of these features (the next four figures relate):

- Between 1100UTC and 1700UTC 2 August 1998 a broad area of high $\Delta T_{0.991}$ (strong inversion) developed inland of Casey.
- By 2300UTC $\Delta T_{0.991}$ further increased to 14°C greater than climatology.
- Between 0500UTC and 1100UTC $\Delta T_{0.991}$ decreased (inversion weakened).
- Blizzard was fully formed at Casey by 1500UTC with winds in excess of 25ms^{-1} continuing for almost 48 hours.

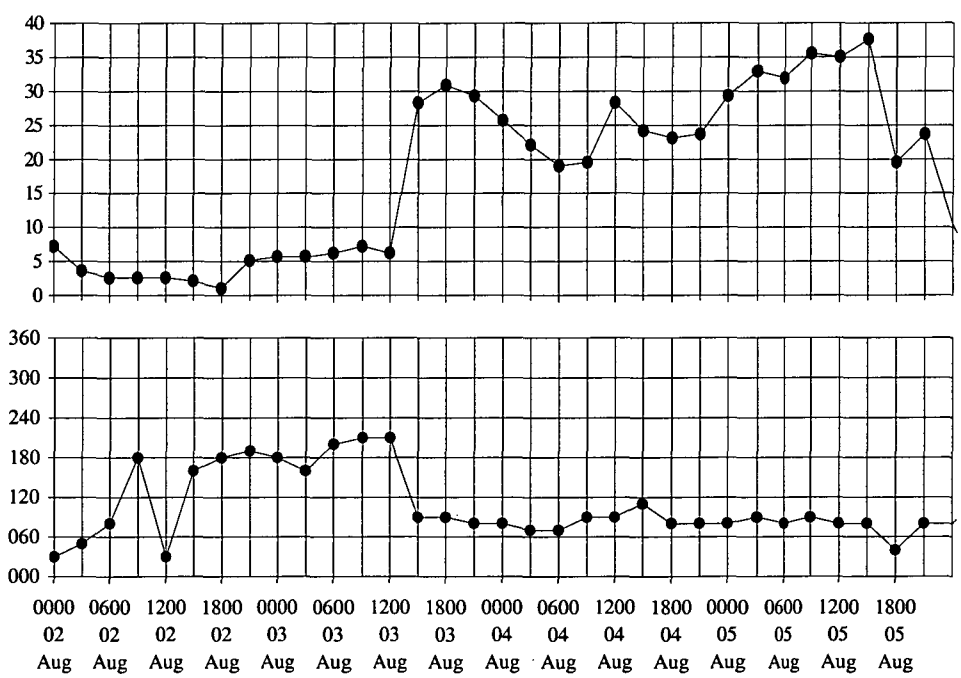

Figure 5.3.3 Three-hourly reports of **(top)** wind speed (ms^{-1}) and **(bottom)** wind direction (°True) from Casey between 0000UTC 2 August and 2400UTC 5 August 1998.

Clearly this is an imperfect categorisation, and by using it exclusively the majority of blizzards will not be forecast. Blizzard development and strength is dependent on multiple constraints operating on multiple spatial and temporal scales. This description only really considers one factor, albeit a particularly important factor. While the characteristics of the inland inversion play an important role in determining the onset, strength and longevity of blizzards, the interplay with synoptic- and meso-scale meteorological features is equally important. Therefore it is important to monitor the development of the inland inversion strength along with the onset of the synoptic conditions associated with strong wind conditions to assess the onset of blizzards.

The types of results presented here introduce what is likely to be a valuable forecasting aid. They help add value to NWP output and provide for better forecasting skill than consideration of model low-level wind fields alone. To that end it is proposed that this forecasting tool be trialed in an operational setting.

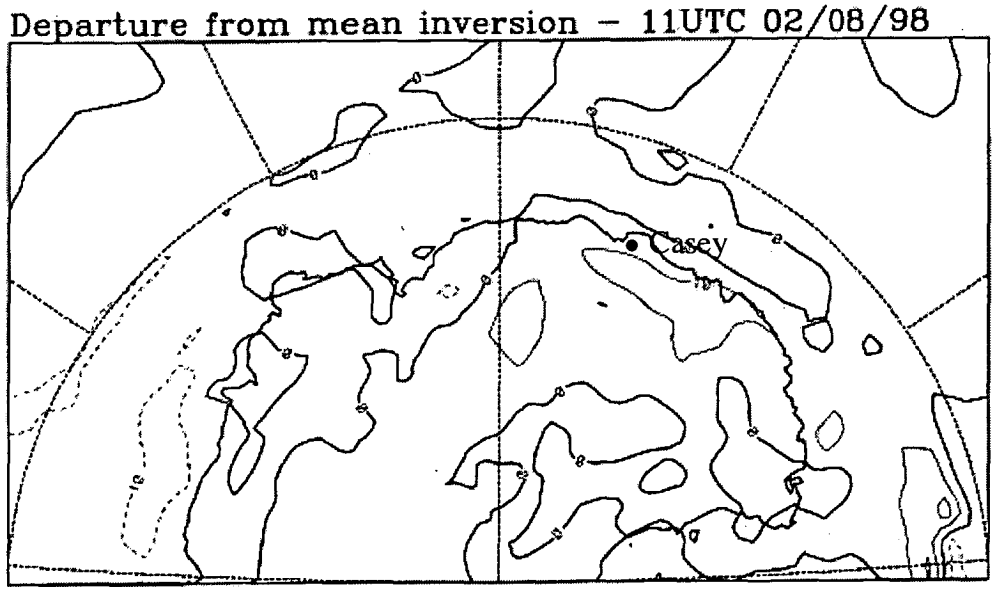

Figure 5.3.4 Departure from three-month mean inversion strength ($\Delta T_{0.99l}$) at **1100UTC 2 August 1998** (°C; contour interval 10°C). Positive values indicate areas of stronger than normal inversion; negative values (dashed contours) indicate areas of weaker than normal inversion. Approximate location of Casey Station is shown.

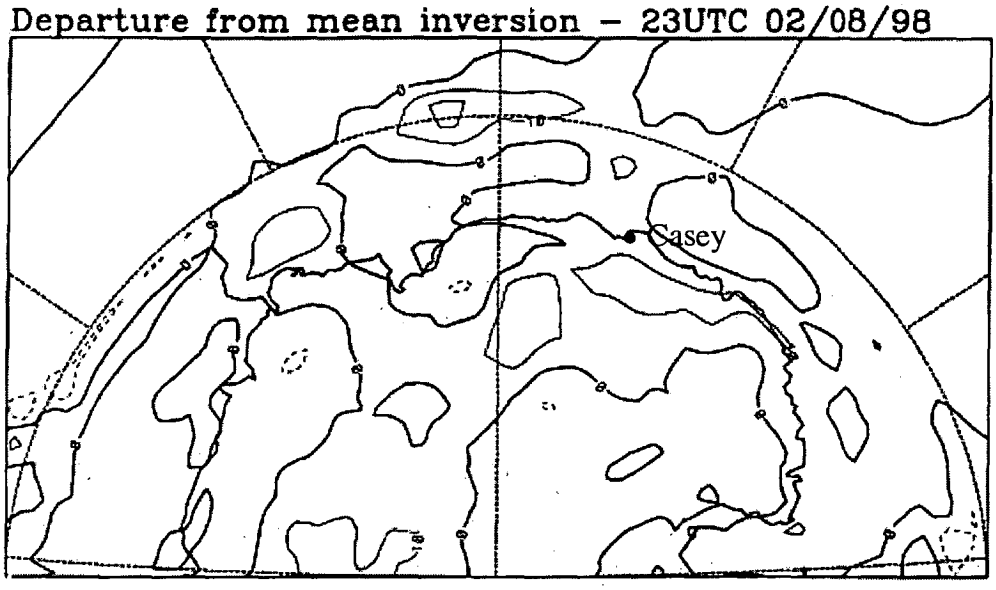

Figure 5.3.5 As for Figure 5.3.4 but at **2300UTC 2 August 1998.**

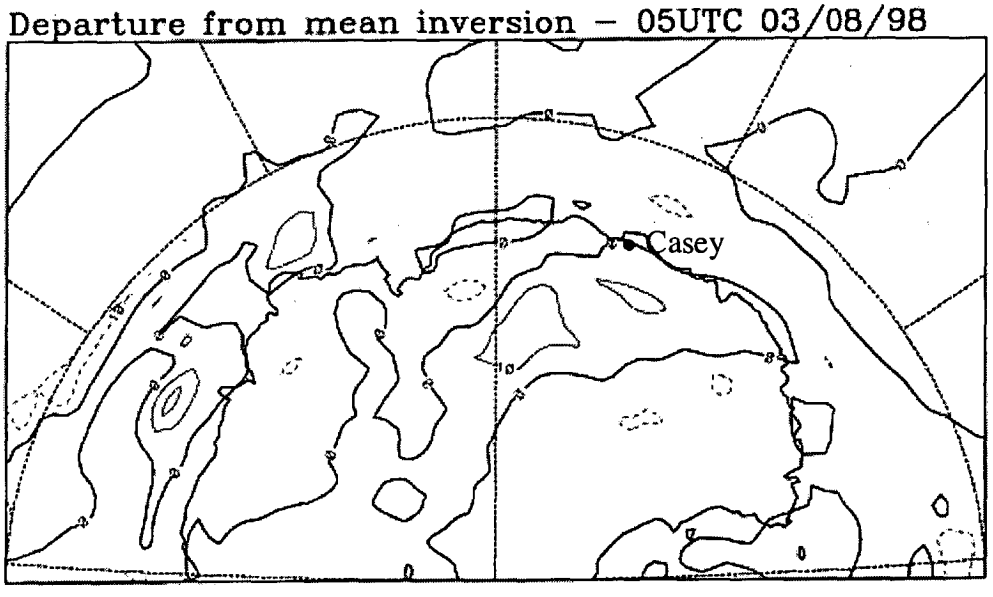

Figure 5.3.6 As for Figure 5.3.4 but at **0500UTC 3 August 1998.**

5.4 Summary of results

For the purposes of the FROST reanalysis TOVS atmospheric thickness data were tested for reliability against radiosonde data from multiple Antarctic and sub-Antarctic stations. TOVS were found to be sufficiently reliable for their use, in many areas, as the lone source of observational data. TOVS were relied upon particularly heavily over remote parts of the Southern Ocean and over some areas of the Antarctic interior.

The low-level TOVS thicknesses from over Antarctica were significantly less accurate than those from sub-Antarctic oceanic areas. The results of tests of higher level TOVS thicknesses were more positive and were found to be almost as reliable over Antarctica as over the Southern Ocean for the 700 – 500hPa and 500 – 250hpa layers.

The TOVS quality flags, set primarily on the basis of cloud coverage, were at least partially confirmed. TOVS *high-confidence* data were found to be of highest quality.

The strong, low-level temperature inversion over the Antarctic interior is a particularly important feature in terms of the meteorology and climatology of the region. The strength and depth of the inversion also affect the accurate derivation of TOVS data over Antarctica resulting in a mean positive bias in TOVS thickness for the 1000 – 500hPa layer near the coastal stations of ~20m.

The Antarctic inversion is a difficult feature to analyse numerically. In Section 5.3 a description is given of a test of the representation of the Antarctic surface inversion in the GASP system during the winter/spring period of 1998.

The GASP system captured the important features of the Antarctic inversion well in terms of geographic distribution, strength and depth.

The changes that occur on short time-scales to the depth, strength and distribution of the Antarctic inversion are also known to be connected to the time of onset of blizzards at some coastal locations.

From the results derived in this chapter, sufficient evidence exists for weather forecasting personnel to be confident of the GASP system's representation of the Antarctic inversion for the purposes of weather forecasting. The daily departure from climatology of the inversion strength and distribution was identified above as a valuable weather forecasting tool to aid the prediction of the onset of blizzards at the coast.

The difficulties of analysis of the lower boundary layer over Antarctica, and its impact on NWP skill and importance for the derivation of TOVS profiles, is an area in which improved data assimilation systems would play a role. The increasing network of AWS on the Antarctic ice sheet provides a unique collection of data for NWP. Modern AWS are accurate and reliable. In addition to surface pressure most provide surface and sub-surface temperature, air temperature and wind speed and direction. All are valuable data for NWP in Antarctica. Currently the GASP system utilises only station level pressure from Antarctic AWS.

CHAPTER 6

HISTORY OF IMPROVEMENTS IN NWP SYSTEMS

6.1 Introduction

The GASP system has undergone considerable on-going research and development since its inception. GASP is an ever-changing system whose development has been via step-wise improvements over many years. Those steps have included major improvements in numerical processing, increases in horizontal and vertical resolution and alterations to data assimilation procedures.

The development of the GASP system has generally focused on improving medium-range forecast skill in the Australian region. Similarly the primary focus at ECMWF is on medium-range prediction for Europe. Antarctic processes and forecast accuracy have been, in the main, regarded as secondary concerns to the developers of global NWP systems.

To date Australian meteorologists working in Antarctica have only had access to data from global NWP systems. For a multitude of reasons the readily available global systems lack the analysis and prognosis skill in Antarctica that they display over other continents (Trenberth and Olson 1988, Adams 1997, Leonard et al. 1997, Turner et al. 1999b, Pendlebury et al. 2003).

A regional scale NWP system, Antarctic-LAPS, is currently under development at the Antarctic CRC and ABOM for use in Antarctica (Adams 2001). This, so-far experimental, system is a regional grid point model nested in GASP output. Early trials have indicated good short-range prediction skill and improved representation of mesoscale phenomena (Adams 2001).

While Antarctic-LAPS is still in the experimental stages, Australian meteorologists in Antarctica rely on GASP and the global medium-range prognoses from ECMWF,

UKMO and NCEP. A summary of the operational systems available at ABOM (including its Antarctic Meteorological Centre) is given in Table 6.1.1.

While focused on forecasting problems in the Australian region, those involved in the development of GASP have been conscious of Antarctic meteorological processes and the impact of Antarctic processes on the Australian region. For those reasons some effort as been concentrated on improvements to the GASP treatment of Antarctica and Antarctic observational data. Improvements to skill over Antarctica have consequently been identified. The primary causes include:

- Increases in horizontal resolution (March 1994 and again December 1998);
- Increases in vertical resolution in the near-surface layers (December 1992 and again in December 1998);
- Improvements to allow for assimilation of surface pressure data from AWS high on the Antarctic plateau (March 1994); and
- Assimilation of TOVS raw radiances (August 2000).

At the same time data quality and quantity has generally improved, including:

- A gradual increase in the number of AWS in Antarctica;
- An increase in the number of drifting buoy deployments in the ocean waters off the East Antarctic coast;
- Improved quality, resolution and processing speed of TOVS data; and
- Improved quality and processing speed of cloud-drift winds, particularly locally derived data in the Australian region.

But with this increase in data from automated sources, the number of manned stations making year-round surface meteorological observations in Antarctica has declined. The decades since the International Geophysical Year (IGY) have also seen the number of stations making regular upper-air observations on the Antarctic continent decline, down from seventeen during the IGY to thirteen today (King and Turner 1997, Turner and Pendlebury 2000).

The importance of these data for mid-latitude weather prediction is well documented. Seaman (1994) identified the stations and buoys that generated the greatest MSLP impact on Australian prediction skill. Those around the Antarctic

Model	Domain	Type	Horizontal resolution	Number of levels	Forecast range (hrs)	Analysis scheme
LAPS*	16.75N - 65.00S 065.00E - 184.25E	Grid point	0.375° (~37.5km)	29	48	MVSI
Meso-LAPS*	4.875N - 55.00S 095.00E - 169.875E	Grid point	0.125° (~12.5km)	29	36	LAPS
Antarctic-LAPS†	35.00S - 80.00S 000.00E - 180.00E	Grid point	0.25° lat. 0.50° lon. (~25km)	29	48	MVSI
TLAPS	44.25N - 45.00S 070.00E - 189.25E	Grid point	0.375° (~37.5km)	29	48	Nudging
GASP	Global	Spectral	T_L239 (~83km)	29	192	MVSI
ECMWF	Global	Spectral	T_L511 (~40km)	60	168	4D-Var
NCEP* (Aviation run)	Global	Spectral	T_L170 (~116km)	42	72	SSI
UKMO*	Global	Grid point	60 km grid (approx.)	30	120	3D-Var
JMA*	Global	Spectral	T213 (~93km)	30	168	MVSI

Table 6.1.1 Operational broad-scale NWP models available at ABOM in early 2002 (from NMOC 2002). Note: For the spectral models the horizontal resolution given is the smallest half-wavelength resolved. A grid point model would need at least two grid points to resolve half a wave. T_L denotes triangular truncation but with the non-linear dynamics and physical parameterisations computed on a linear grid.

* These systems run with a short data cut-off time (2 - 3 hours) for operational reasons.

† Antarctic-LAPS is an experimental system currently undergoing operational tests.

coast, on Southern Ocean islands and Southern Ocean buoys clearly dominated the results.

Those results have been repeatedly confirmed in successive issues of the *Analysis and Prediction Quarterly Summary*, published by ABOM, over the eight years since the Seaman (1994) paper.

The changes to data availability, which have occurred over time, make it difficult to assess changes in prognostic skill in a controlled manner. There is no argument that the forecast skill of the GASP system has improved markedly over the Australian verification grid, but improvements in forecast skill in Antarctica and the Southern Ocean are more difficult to quantify.

This chapter contains a discussion of the historical improvements in NWP skill of several systems over global, hemispheric and regional scale domains. It is included here to help link the research results of Chapters 4 and 5 into the broad context of NWP developments at research centres world-wide.

6.2 Global and hemispheric forecast skill

Meteorological centres worldwide use a common system for numerical model verification endorsed by the World Meteorological Organisation Commission for Basic Systems. Published results tend to include data from the northern hemisphere as a whole, the southern hemisphere as a whole, and the Tropics. These data do not provide useful information for Antarctic or Southern Ocean Meteorology but they do help put the improvements noted in Antarctic NWP in context with developments on a global scale.

Figures 6.2.1 show comparative plots of northern hemisphere MSLP RMSE from eight global systems. These show a pronounced summer / winter oscillation with considerably lower RMSE in the summer months resulting from the relative stability of the northern hemisphere summer-time synoptic pattern. They also show a gradual lessening of RMSE over the period. As the only southern hemisphere based system of the eight shown, GASP is apparently the weakest of the systems in terms of northern hemisphere RMSE.

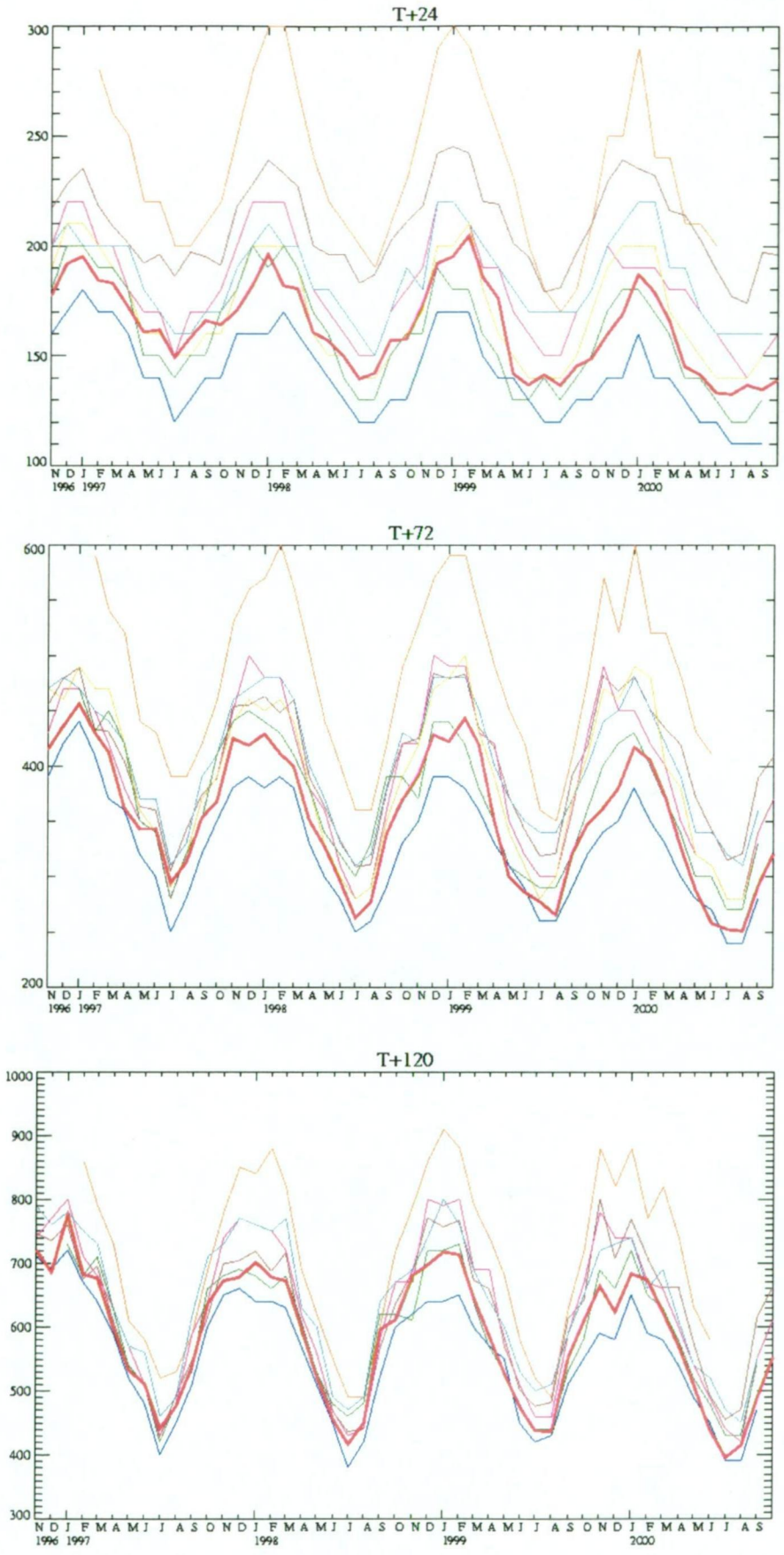

Figure 6.2.1

Northern hemisphere time-averaged RMSE of forecast MSLP minus analysis MSLP (Pa). Results from eight global NWP systems are shown between November 1996 and October 2000 (provided by ABOM Research Centre).

Top: 24 hour.

Middle: 72 hour.

Bottom: 120 hour.

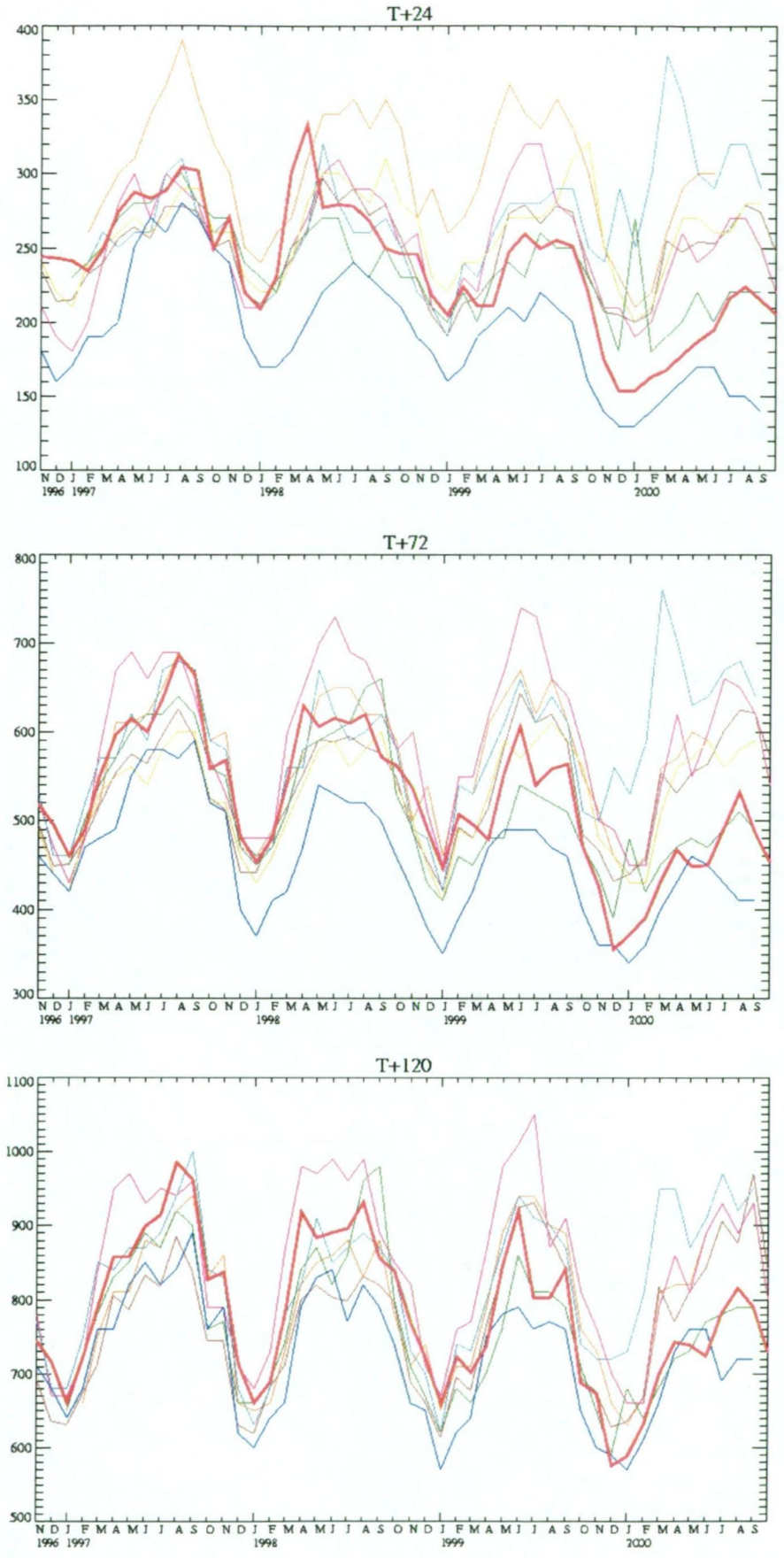

Figure 6.2.2
Southern hemisphere time-averaged RMSE of forecast MSLP minus analysis MSLP (Pa). Results from eight global NWP systems are shown between November 1996 and October 2000 (provided by ABOM Research Centre).

Top: 24 hour.

Middle: 72 hour.

Bottom: 120 hour.

Figures 6.2.2 show similar presentations of southern hemisphere RMSE results. RMSE in the southern hemisphere is universally higher than in the northern hemisphere. And skill improvement from year to year is generally less marked in the southern hemisphere.

GASP appears to perform as well as the other systems over the southern hemisphere. ECMWF outperforms all other systems, in both hemispheres, particularly in the 1 – 3 day timeframe.

ABOM Research Centre made similar comparisons of geopotential height, wind and temperature at 850hPa, 500hPa and 250hPa available for this study (but not shown here). To summarise, they show a fairly broad spread in results between the NWP systems; greater skill in the northern hemisphere than in the southern hemisphere; and generally improving skill over the period shown.

6.3 Australian and Antarctic forecast skill

NMOC (ABOM) monitor skill from multiple NWP systems, on various domains, on the Australian Irregular Verification Grid (defined earlier in Chapter 4 Section 4.5). A discussion of verification results is published quarterly in the NMOC *Analysis and Prediction Quarterly Summary.*

Figures 6.3.1 show a history of MSLP S_1 skill-scores of 24, 48, 72 and 120-hour forecasts from five global NWP systems including GASP. These results are time-filtered over a twelve-month period.

Consistent skill improvement over the years is clear in all of the systems shown. The most substantial upgrade events in the development of the GASP system, December 1992 and December 1998, both appear to have made an impact in terms of S_1 skill improvement in the Australian region (depicted as gradual increases in skill over the twelve-month period starting at the dates of the upgrade events). These important stages of development are also seen in Figures 6.3.2, a comparative representation of 500hPa height S_1 skill-scores of 72 and 120-hour forecasts.

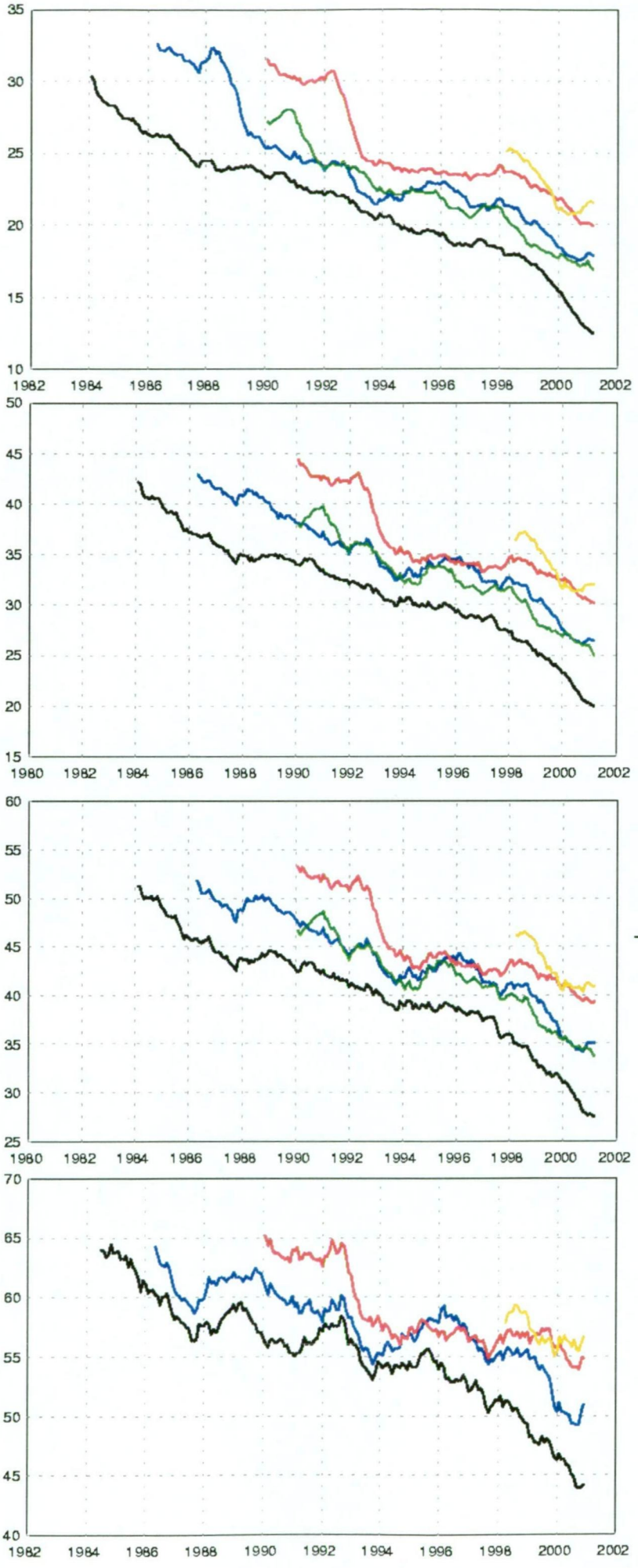

Figure 6.3.1
Time filtered averages of **MSLP** S_1 skill-score in the **Australian region.** From top to bottom these figures show 24, 48, 72 and 120 hour forecast skill. (From NMOC 2001).

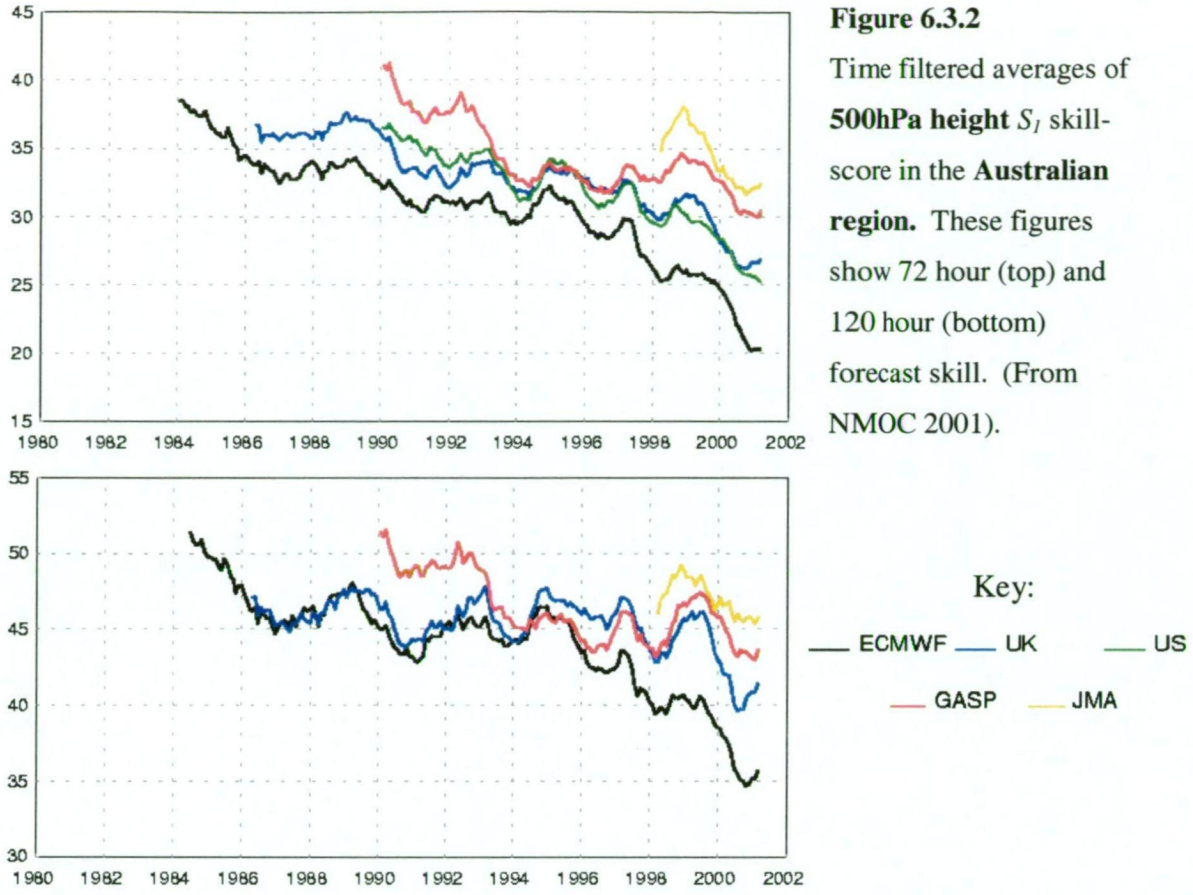

Figure 6.3.2
Time filtered averages of **500hPa height** S_1 skill-score in the **Australian region.** These figures show 72 hour (top) and 120 hour (bottom) forecast skill. (From NMOC 2001).

In the absence of time-filtering, the GASP resolution upgrade of December 1992 (December 1998) appears as an abrupt jump in skill of approximately six (four) S_1 skill points for short-range MSLP forecasts.

Forecast skill in the Australian region, while generally lower than that of northern hemisphere continents, is relatively high compared with other regions of the southern hemisphere. Australia's network of surface observations and radiosonde stations is superior to that of other southern hemisphere continents. And the low elevation surface terrain of Australia is more easily accounted for in NWP systems than that of the other southern hemisphere continents, particularly Antarctica.

NWP skill statistics for Antarctica are rarely published. Antarctica rates no mention in the World Meteorological Organisation's annual *World Weather Watch Technical Reports on the Global Data-Processing System* – the vehicle through which most meteorological agencies report NWP developments.

A small number of studies have emerged in recent years on the quality of NWP systems for Antarctic Meteorology.

Turner et al. (1999b) considered one week of data from FROST in comparison with operational analyses from four global NWP systems. That study identified a number of problems with NWP systems and their ability to analyse discrete synoptic systems and events. The depth and exact location of low-pressure systems was often inaccurately analysed in NWP systems. Such problems occurred most commonly in data sparse areas such as the Amundsen and Bellingshausen Seas. Some very large differences were noted between the analyses from GASP and NCEP in data sparse areas.

Nevertheless, the authors reported the generally encouraging finding that no large synoptic-scale systems were missing from analyses, and that few were grossly misplaced.

Adams (1997) reported some encouraging results on the improving ability of global NWP systems to forecast coastal meteorological phenomena. More importantly Adams (2001) reported on the development of Antarctic-LAPS, the experimental limited area grid point system nested in GASP.

A new study by Pendlebury et al. (2003) gives an account of the currently available global NWP systems and their forecast performance in Antarctica. They indicated a substantial degree of forecast skill in the modern global NWP systems and a clear history of increases in skill over the years studied. For example, in terms of the accuracy of 500hPa height forecasts over the Antarctic, it was reported that the 72-hour forecast RMSE had, by 2000, declined to a value similar to that of 48-hour forecasts only five years earlier.

The various NWP systems use inconsistent methods of derivation of MSLP. The lowest commonly used standard atmospheric level which does not intersect the ground over Antarctica is 500hPa. Hence, for comparison between NWP systems, 500hPa is the preferred level to study. Unfortunately the 500hPa level is of little use for coastal and oceanic comparisons.

Figure 6.3.3, based on data from Pendlebury et al. (2003), shows the steady improvement in S_1 skill-scores of 72-hour forecasts of 500hPa height. This figure also quite markedly highlights the rate of improvement in the ECMWF system relative to GASP over the 5½-year period shown.

The degree of scatter in the unsmoothed Figure 6.3.3 makes a search for distinct developmental features difficult. The December 1998 upgrade of the GASP system, from T79L19 to T_L239L29, is not obvious in this figure but may be becoming discernible towards the end of the period shown. Table 6.3.1 (also from Pendlebury et al. 2003) shows annual mean statistics of 500hPa height S_1 skill-score and RMSE of GASP, ECMWF and UKMO global systems. These data show quite clearly the jump in skill of the GASP system upon the December 1998 upgrade, at least out to 72-hours.

ECMWF data in Table 6.3.1 show that the March 1998 resolution upgrade of ECMWF, from T213 to T_L319, also appears to have heavily impacted on results over Antarctica.

Two important events in the development of the UKMO system, a resolution upgrade and a correction to the Antarctic orography (both in early 1998), also appear to have had a positive impact on Antarctic region forecasting skill.

A history of the major developments of the GASP system is given in Appendix 2. Some of the notable events in the development of the ECMWF and UKMO global systems between 1995 and 2000 are also listed in Appendix 2.

The extent to which skill statistics over the Antarctic region lag behind those over other parts of the globe is highlighted in Table 6.3.2. The RMSE of forecast 500hPa height is shown for year-2000 northern hemisphere, southern hemisphere and Antarctic region prognoses. These differences represent, for Antarctica, 30-45% greater RMSE than over the southern hemisphere, and 65-110% greater RMSE than over the northern hemisphere.

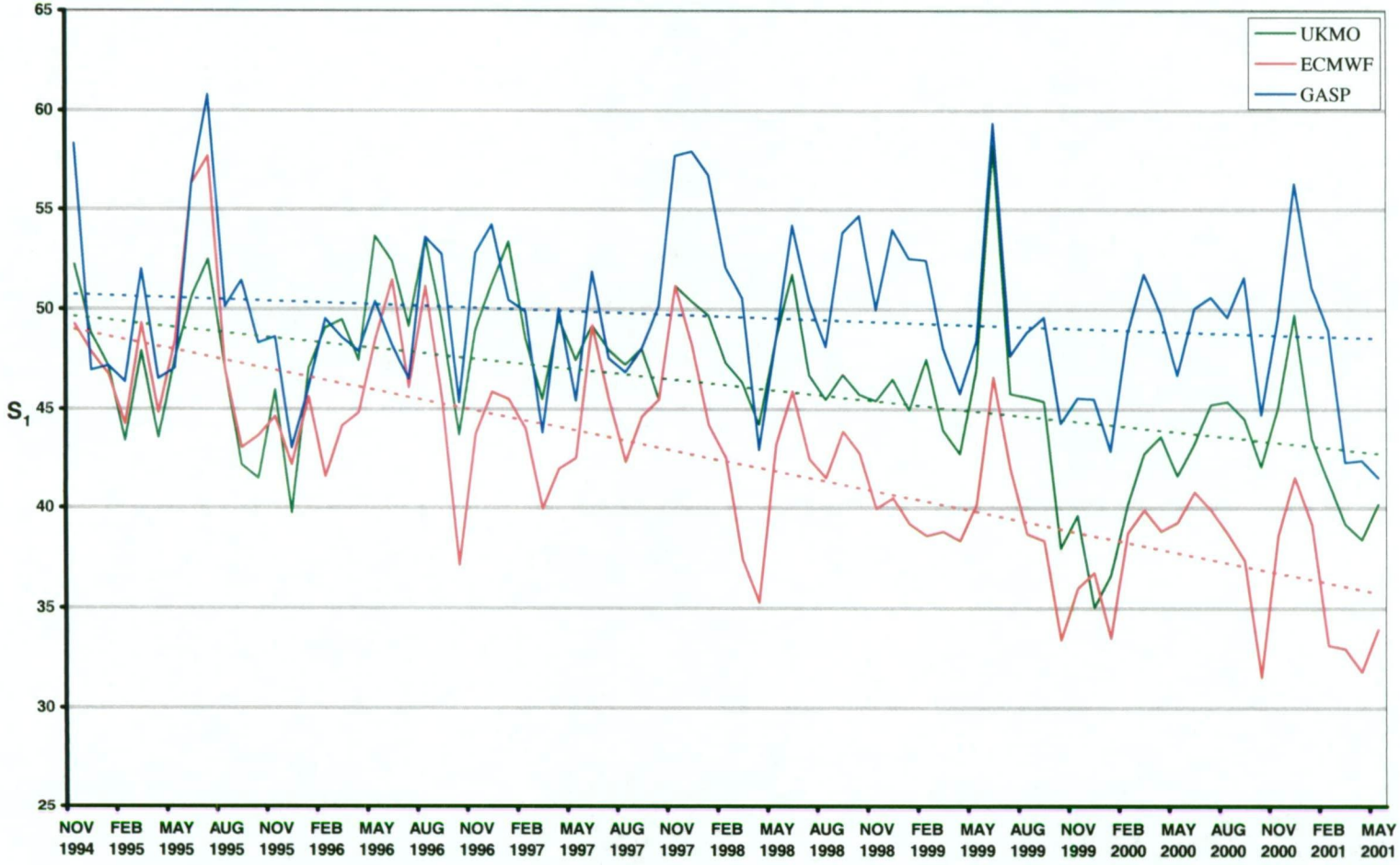

Figure 6.3.3 Unsmoothed monthly S_1 skill-scores of 72-hour forecasts of 500hPa height. Results from GASP, ECMWF and UKMO are shown for the region south of and including 55°S for the period November 1994 to May 2001. Dashed lines indicate linear regression. Data from Pendlebury et al. (2003).

500hPa height verification		GASP		UKMO		ECMWF	
		S_1	RMSE	S_1	RMSE	S_1	RMSE
+24 h	1995	31.2	40.6	20.7	26.5	23.2	28.7
	1996	30.6	38.3	21.8	28.6	21.1	26.0
	1997	31.5	40.1	21.2	28.5	21.8	28.0
	1998	32.8	40.4	21.1	28.8	19.7	23.9
	1999	27.1	35.1	21.5	28.4	17.6	21.4
	2000	25.6	30.6	20.5	23.4	15.2	16.9
+48 h	1995	42.4	62.2	34.8	46.9	37.0	48.8
	1996	41.8	59.3	37.4	52.9	34.8	46.3
	1997	42.7	60.3	36.9	52.4	34.9	49.4
	1998	44.1	59.8	36.0	52.0	32.0	42.4
	1999	40.3	56.8	34.9	50.1	29.7	38.9
	2000	39.6	51.7	33.1	41.4	27.4	33.3
+72 h	1995	49.8	81.2	45.8	69.3	47.3	72.2
	1996	49.7	77.5	49.6	75.9	45.5	68.9
	1997	50.0	77.5	48.7	74.3	45.0	69.4
	1998	51.3	75.2	47.0	74.3	41.6	62.3
	1999	45.2	75.3	41.6	70.0	35.9	56.9
	2000	49.4	72.6	43.3	60.3	38.2	51.4
+96 h	1995	55.2	111.0	54.3	102.3	54.7	104.3
	1996	55.9	96.4	58.5	98.5	53.6	89.7
	1997	55.4	92.9	56.3	94.7	52.5	89.2
	1998	56.8	90.2	54.7	94.5	49.7	81.8
	1999	54.9	92.2	51.2	87.9	47.3	76.8
	2000	57.5	90.9	51.4	79.6	47.4	70.2
+120 h	1995	59.7	111.3	60.5	106.8	60.2	109.1
	1996	60.8	109.2	65.0	116.6	59.6	107.9
	1997	60.7	107.3	62.6	111.4	58.3	106.2
	1998	60.7	102.4	59.6	110.7	56.1	99.6
	1999	59.7	107.4	56.6	105.2	53.9	94.7
	2000	62.0	106.3	58.6	97.9	54.6	89.3

Table 6.3.1 Mean annual 500hPa height S_1 skill-score and RMSE (m) of GASP, UKMO and ECMWF global systems from the area south of 55°S (from Pendlebury et al. 2003). Prognoses verified against analyses. GASP T79L19 results are shown in green; GASP T_L239L29 results are shown in blue.

	Northern Hemisphere[1]	Southern Hemisphere[1]	**Antarctica[2]**	Northern Hemisphere[1]	Southern Hemisphere[1]	**Antarctica[2]**	Northern Hemisphere[1]	Southern Hemisphere[1]	**Antarctica[2]**
	24-hour forecasts			72-hour forecasts			120-hour forecasts		
GASP	17.1	21.7	**30.6**	42.8	53.0	**72.6**	70.0	81.2	**106.3**
UKMO	12.4	17.2	**23.4**	32.1	43.9	**60.3**	57.6	73.9	**97.9**
ECMWF	10.2	12.8	**16.9**	29.0	38.3	**51.4**	53.9	68.0	**89.3**
JMA	14.6	22.6	**31.3**	35.5	55.9	**75.3**	61.5	84.6	**108.1**
NCEP[3]	11.8	16.4	**23.3**	33.9	44.1	**61.0**			

Table 6.3.2 Mean year-2000 RMSE of 24, 72 and 120-hour forecasts of 500hPa height from five global NWP systems (m; verified against analyses). Data from WMO (2001) and Pendlebury et al. (2003).

[1] Excluding the tropics 20°S-20°N.

[2] Antarctica plus the Southern Ocean south of 55°S.

[3] The NCEP Aviation model, shown here, does not run to 120-hours.

6.4 Summary of results

It has become clear that NWP skill over the Antarctic region has improved significantly over the past decade. The most substantial increases in skill were achieved in the period since the FROST study of 1994/1995. All readily available global systems considered, the improving trend in forecast skill continues to date. Nevertheless, forecast skill in the Antarctic lags significantly behind that over other regions of the globe.

Of the readily available global systems the ECMWF model out-perform all others in terms of medium-range 500hPa height prediction skill in the Antarctic region.

The impact of recent resolution upgrades in several NWP systems has led directly and quantifiably to skill improvements over the Antarctic region.

CHAPTER 7

CONCLUDING DISCUSSION AND RECOMMENDATIONS

7.1 Introduction

This chapter gives an overview and discussion of the important research findings in this thesis. It provides a summary of the main results found in earlier chapters; lists a number of proposals for future related work towards the incorporation of new observing systems and data into NWP systems; details the likely improvements from future developments; and lists several recommendations for future activities.

7.2 Summary of the important results found in the earlier chapters

The majority of the more important research findings from earlier chapters are reiterated here. This is not an all-encompassing list; rather it serves to remind the reader of the more significant research results.

In Chapter 3 the results of two independent experiments relating to the reliability and accuracy of ERS-1 scatterometer wind data were presented. In both experiments scatterometer data were tested against NWP analyses over the Southern Ocean. Scatterometer winds derived via two alternative derivation algorithms were studied. The more important results presented in Chapter 3 are listed here:

(i) When assessed in comparison with near-surface data from two independent global NWP systems, ERS-1 scatterometer winds were found to be reliable in a broad range of conditions and geographic locations across the Southern Ocean.

(ii) Scatterometer wind speeds derived via the CMOD4 algorithm (Stoffelen and Anderson 1997b) were found to have a slight low bias. The bias was most evident in strong wind events across the Southern Ocean.

(iii) Scatterometer winds derived via the IFREMER algorithm (CERSAT 1996) showed signs of superior accuracy and negligible bias in comparison with ECMWF model winds.

(iv) The determination of wind direction from scatterometer backscatter data appeared to be problematic in a small population of CMOD4 derived data. In a preliminary comparison with GASP model winds across the Southern Ocean, approximately 3.4% of a population of CMOD4 data appeared to be erroneous by ~180°. It is likely that further analysis could largely eliminate those.

(v) In comparison with ECMWF winds across the Southern Ocean, approximately 1.8% of a population of IFREMER derived scatterometer data were erroneous by ~180°. A further 0.3% (approximately) of data were erroneous by ~±90°.

(vi) A geographic distribution of disagreement between ECMWF and scatterometer winds (both CMOD4 and IFREMER) highlighted that different levels of agreement exist across various parts of the Southern Ocean.

(vii) The degree of disagreement identified between ECMWF and scatterometer winds in areas of the Southern Ocean devoid of *in situ* observations was larger than over other areas. A likely explanation is that the ECMWF system was under-analysing the intensity of some deep low-pressure systems.

Results were presented in Chapter 4 of a series of NWP data impact experiments involving the utilisation of scatterometer winds in the ABOM GASP system. The experiments tested the impact of scatterometer winds on analyses and prognoses across the globe. A series of conventional, mean data impact statistics was presented together with a detailed daily breakdown of impact results. Several case studies of significant analysis and prognosis impact were discussed. The more important results presented in Chapter 4 are listed here:

(viii) A large population of CMOD4 derived scatterometer winds, with global coverage, was successfully utilised in the GASP system during a one-month pseudo-operational trial. A full series of 6-hourly analyses and daily forecasts (24, 48, 72, 96 and 120-hours) were generated.

(ix) Although the overall average improvement in skill was relatively small, it was found that the inclusion of scatterometer winds generated large local impacts on GASP analyses, particularly across the Southern Ocean. **Several events were identified where the scatterometer winds effectively altered MSLP analyses by 10 to 15hPa over the Southern Ocean.** The larger of these strong impact events resulted from scatterometer winds acting to reverse quality control decisions relating to the rejection of some individual drifting buoy reports.

(x) In the several cases studied, **large analysis impact events inevitably resulted in a large (positive) impact on forecast skill.** It was found that significant analysis impact events in the Antarctic sea ice zone resulted in significant medium-range forecast impact in Southern Australia.

(xi) Mean analysis impact, over the one-month (July 1995) study period, was significant. The scatterometer winds appeared to weaken the GASP winds at the northern flank of the circumpolar trough. This effectively led to a weakening of the model representation of the circumpolar trough, by as much as 2hPa MSLP, across substantial longitudes of the Southern Ocean. This supports the results in (ii) above of a systematic under-estimate of wind strength amongst the CMOD4 scatterometer data.

(xii) A complete set of daily and mean 24 and 48-hour forecast skill statistics was generated over multiple verification grids covering the globe. These were S_1 skill-score, RMSE and bias of MSLP and 500hPa height.

(xiii) Mean forecast skill statistics showed little impact with the inclusion of scatterometer data in the GASP system. Results were neither strongly positive nor strongly negative over any of six southern hemisphere verification grids, nor over the globe as a whole. However the improvement with scatterometer data appeared to be strongest over the Southern Ocean and for the 48-hour forecast period.

(xiv) Daily variation of forecast skill highlighted a moderately strong positive signal of impact with the inclusion of scatterometer winds. The greatest impact was over the Southern Ocean. RMSE and bias were reduced in most 48-hour MSLP forecasts, and many 24-hour MSLP forecasts, across the southern hemisphere. S_1 skill-score impact was closer to neutral throughout.

(xv) **The inclusion of scatterometer winds appeared to reduce the magnitude of some of the largest forecast errors.** Several events were noted where

particularly high values of RMSE and S_1 skill-score were significantly reduced with the inclusion of scatterometer data.

A verification study was completed, under the framework of FROST, in which the accuracy of NOAA/NESDIS TOVS thickness data were assessed against radiosonde reports. The details were presented in Chapter 5. The study tested TOVS data against all available radiosonde flights throughout the Antarctic and sub-Antarctic during one winter month. The more important results of the TOVS verification study are listed here:

(xvi) Assessed against radiosonde data from multiple Antarctic and Southern Ocean stations, NOAA/NESDIS TOVS atmospheric thickness data were found to be reliable. From the perspective of the FROST re-analysis process, the value of TOVS was particularly great over open ocean areas where few data were available from other sources.

(xvii) TOVS data flagged *high-confidence* were found to be of highest quality, but *low-confidence* and *unspecified-confidence* data were also considered to be of value for the FROST re-analysis.

(xviii) TOVS data from sub-Antarctic open ocean areas were found to be of significantly greater quality than those over Antarctica. Over Antarctica the TOVS above 700hPa were found to be reliable but the near surface data were apparently biased by poor representation of the Antarctic surface inversion.

A series of experiments was undertaken during a six-month winter/spring period to assess the representation, in the GASP system, of the Antarctic near-surface temperature inversion. The results were presented in Chapter 5. The more important results are listed here:

(xix) A six-month climatology of the GASP (T79L19) representation of the near-surface temperature inversion over Antarctica was developed and found to be accurate in relation to other published results.

(xx) The daily departure from climatology of the inversion strength and distribution (inversion anomaly) was identified as a valuable weather forecasting tool to aid the prediction of onset of blizzard conditions at coastal locations.

In Chapter 6 a review was presented of the current status of global NWP accuracy over the Antarctic region. Some of the more important details from Chapter 6 are reiterated here:

(xxi) NWP skill over the Antarctic region has improved markedly over the past decade and particularly since the FROST period of 1994/1995. Of the readily available global systems the ECMWF model appears to out-perform all others in terms of medium-range 500hPa height prediction skill.

(xxii) The impact of recent resolution upgrades in several NWP systems has led directly and quantifiably to skill improvements over the Antarctic region.

These results represent a degree of advancement in Antarctic Meteorology and Antarctic and Southern Ocean region NWP. They also provide the reader with some pointers to where future research work should focus.

7.3 Future work on possible improvements to NWP analyses and prognoses

Further substantial improvements in NWP accuracy over Antarctica and the Southern Ocean region can be expected to occur as a result of:

(i) improvements to the quantity, quality and coverage (temporal and spatial) of meteorological observing systems;

(ii) advances in data assimilation; and

(iii) increases in model horizontal and vertical resolution.

Antarctic and Southern Ocean meteorological observing systems

A significant increase in the number of manual meteorological reporting stations in the Antarctic appears unlikely. The most comprehensive collection of manual observations available is that from the IGY more than forty years ago.

The steady increase in the number of *in situ* reports in recent years has come from AWS on the Antarctic continent and drifting buoys deployed in the Southern Ocean. Present indications are that these programmes of deployment will be, at least, maintained and are likely to be extended. Some examples of current and future Australian work follow.

- To coincide with the introduction of long-range aircraft operations over the next two years, AAD plan to deploy AWS with horizontal visibility and cloud height detection technology.
- In the years ahead ABOM propose to trial the use of a vertical wind profiler at a coastal Antarctic site.

Further advances in data communication will also add value to remote automatic stations.

- System ARGOS now includes the capability of two-way communication to field transmitters, thus allowing data (instructions) to be transmitted to remote stations.
- Some Italian AWS deployed in Victoria Land transmit voice messages via VHF radio on demand. Stations also have the capability to transmit regular data reports via HF radio.

The network of drifting buoys in the Southern Ocean will, most likely, be maintained in future years. Modern buoys are capable of survival in the high seas and sea ice zone, are easily deployed, provide reliable data and survive for many months (commonly 18 to 24 months). Meteorological agencies are conscious of the substantial prognostic impact they generate, indeed Southern Ocean buoys usually show the largest impact on GASP analyses of MSLP.

With some of the above advances in mind it is reasonable to expect that the most substantial increase in *in situ* data will flow from the increasing coverage of un-manned stations and drifting buoys. The inclusion of these additional stations, and the more complete utilisation of the data they provide, is expected to improve NWP analyses.

Earth-observing remote sensing technology is also advancing at a great rate. Proposed future satellite missions will offer much to Antarctic Atmospheric Science. Some examples of satellites missions and instruments of particular interest to Antarctic Meteorology follow.

ENVISAT (European Space Agency; launched March 2002; envisat.esa.int) carries a broad collection of instruments including:

- An advanced synthetic aperture radar developed from earlier systems carried on ERS-1 and ERS-2;
- A microwave radiometer designed to measure the integrated atmospheric water vapour column and cloud liquid water content;
- A high precision radar altimeter; and
- An advanced along-track scanning radiometer designed, predominantly, to provide accurate sea-surface temperature data.

ADEOS-II (NASDA Japan; launch planned for 2002; www.nasda.go.jp) will carry a collection of instruments including:

- An advanced microwave scanning radiometer. This is a passive microwave instrument to be used for the detection of water vapour, precipitation, sea-surface temperature, surface wind speed and sea ice distribution; and
- SeaWinds, a scatterometer instrument developed from a predecessor, NSCAT, flown on-board ADEOS-I.

Constellation Observing System for Meteorology, Ionosphere and Climate (COSMIC; USA/Taiwan; programme beginning 2005; www.cosmic.ucar.edu) will consist of six spacecraft, each with three instruments. The instrument of great interest to Meteorology is the GPS/MET receiver. Using the technique of GPS Meteorology, the proposed network is expected to be capable of accurate and continuous measurements of integrated perceptible water vapour.

MetOp-1 (European Space Agency; launch planned for 2005; www.eumetsat.de) will carry these instruments:

- An advanced very high-resolution radiometer capable of providing global imagery of clouds and the ocean and land surface;
- A high-resolution infrared radiation sounder designed to provide temperature and humidity of the global atmosphere in cloud-free conditions;
- An advanced microwave sounding unit designed to provide temperature of the global atmosphere in all-weather conditions;
- A microwave humidity sounder deigned to provide global atmospheric humidity;
- An infrared atmospheric sounding interferometer deigned to provide high quality atmospheric sounding data;

- A global navigation satellite system receiver for atmospheric sounding. This is designed to record temperature of the stratosphere and upper troposphere with high vertical resolution;
- An advanced scatterometer instrument including six antennae; and
- A global ozone monitoring system designed to provide profiles of ozone and other atmospheric constituents.

Coriolis (USA; launch planned for August 2002; www.pxi.com/windsat) will carry the WindSat instrument. WindSat is a multi-frequency polarimetric radiometer designed to determine ocean-surface wind speed and direction at high resolution.

Data assimilation

In an environment where data supply is particularly limited, the data that are available must be utilised as fully as possible.

Substantial advances in data assimilation systems have taken place at the various NWP centres in recent years.

Work is now underway at ABOM Research Centre to assess the impact of QuikSCAT winds on the GASP system (T_L239L29) with an additional σ level closer to the surface at ~10m.

With the ongoing deployment of remote un-manned observing systems and space-borne remote sensing systems the challenge will be on NWP centres to utilise data towards positive forecast impact in their numerical systems. This will be necessary before further substantial NWP skill improvements result in the Antarctic region.

Antarctic and Southern Ocean NWP

Recent years have seen a dramatic increase in NWP skill over Antarctica. This has derived from a variety of factors, most importantly increases in model horizontal resolution.

Nevertheless, forecast skill in Antarctica continues to lag well behind that of other continents. Table 6.3.2 shows the stark differences in 500hPa height forecast RMSE between the northern hemisphere, the southern hemisphere and the Antarctic region.

The meteorological processes occurring in the planetary boundary layer over Antarctica are of particular importance. The manner in which NWP systems depict the geography of the continent contributes largely to the accuracy of their output.

Changes in horizontal resolution of GASP over the past decade have included improvements to the system's topography field. Figures 1.3.3 demonstrated the improvements in GASP topography over the continent with each significant resolution upgrade from R31 to T79 to T_L239. Figure 1.3.4 highlighted those improvements on a local scale - in cross-section through the Lambert Glacier Basin.

Significant NWP analysis and prognosis skill improvements will require further significant increases in horizontal resolution.

Figure 7.3.2 highlights the substantial differences in vertical resolution between successive upgrades of the GASP system. For comparison it is interesting to note that, since October 1999, the ECMWF global system has operated on 60 vertical levels.

The vertical resolution in the planetary boundary layer is of particular importance in the Antarctic region where major atmospheric forcing events occur entirely within the lowest 500m of the atmosphere. To better capture the structure of these important physical features, further vertical resolution upgrades will be necessary.

Another important consideration concerns the methodologies used for NWP skill measurement and comparison. The traditional approach of directly comparing NWP prognoses against NWP analyses has inherent problems, particularly in data sparse environments, as discussed in the later parts of Chapter 4. The measurement of impact of additional observational data systems is similarly problematic.

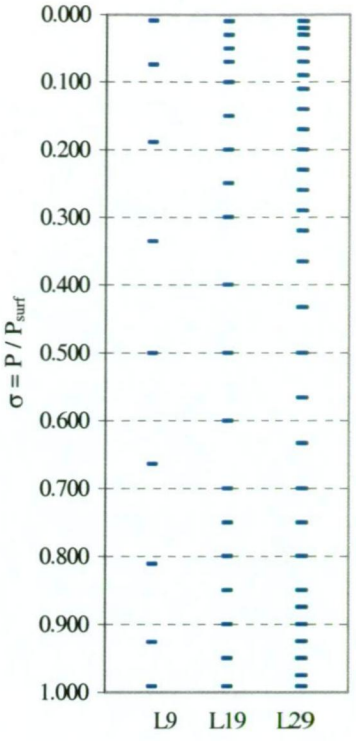

Figure 7.3.2

Schematic representation of the distribution of σ levels in the five GASP configurations: R31L9, R31L19 / R53L19 / T79L19 and T_L239L29.

7.4 This work in the context of global-scale processes

It was demonstrated by Seaman (1994) that reports from remote Southern Ocean and Antarctic locations impact strongly on NWP performance in the Australian region. It was further demonstrated in Chapter 4 of this thesis that the use of scatterometer winds from distant parts of the Southern Ocean made impacts on NWP performance over all four southern hemisphere continents.

The importance of atmospheric dynamics, physics and chemistry in the Antarctic region is significant in the determination of meteorology for the whole hemisphere. The quality of our analyses of the state of the atmosphere over the Antarctic and Southern Ocean hinges heavily on the data gained from a limited number of observing systems providing data of often limited quality.

It is a fact that the most influential region of the hemisphere, in terms of broad-scale atmospheric forcing and high variability, is also the most poorly observed and most poorly understood.

It is also recognised that the Antarctic and Southern Ocean region plays a particularly important role in the global climate system. Via NWP simulation the

scientific community is able to improve its understanding of the meteorological and climatological processes of the region and thus contribute to a better understanding of global-scale processes.

Figure 7.4.1 gives a schematic insight into some of more important boundary layer processes operating over the Antarctic continent. Together with the similarly important processes over the sea ice zone, they heavily influence the broad-scale meteorology and climatology of the entire region. A few of these issues have been discussed, from a meteorological perspective, in earlier chapters of this thesis. Figure 7.4.1 highlights important regional-scale systems, many of which impact on global-scale processes.

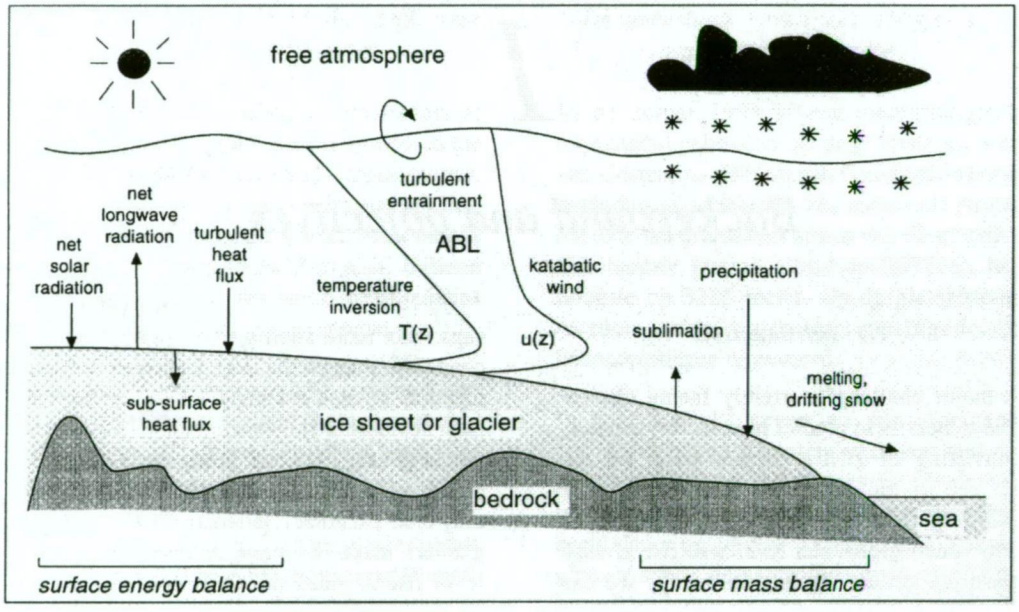

Figure 7.4.1 Schematic representation of the processes occurring in the atmospheric boundary layer over ice sheets and glaciers (from van den Broeke 1996).

7.5 Recommendations

A series of recommendations have evolved from the work presented in this thesis. These specifically concern the ongoing development of meteorological data networks and NWP in the Antarctic and Southern Ocean region.

The impact of meteorological observations in the Antarctic and Southern Ocean region on NWP performance over other continents of the southern hemisphere is profoundly clear.

The primary reason for reduced performance of global NWP systems in the southern hemisphere, compared to that of the northern hemisphere, is due to the comparative sparseness of the observing network compounded by the very high seasonal variability of the atmospheric conditions.

These gaps in data coverage can, at least partially, be filled by remote sensing systems. But such systems require ground checking and verification in a range of geographic environments and atmospheric conditions.

The requirement for a comprehensive and multi-modal observing network remains.

> **Recommendation 1.** *That Antarctic Treaty Nations make a concerted effort to, at least, maintain the existing manual surface and upper-air observing network in the Antarctic and sub-Antarctic. This should be regarded as a shared multi-national responsibility.*

> **Recommendation 2.** *That Australia's programme of deployment of drifting buoys in the East Antarctic sea ice zone should be increased. In addition, that AAD and ABOM co-operate to ensure the configuration and deployment location of all buoys meets the data requirements of both organisations and the International Meteorological Community.*

> **Recommendation 3.** *That the rate of installation of AWS in Antarctica be, at least, maintained. In addition, that AAD and ABOM co-operate to ensure that all future installations meet, as far as practical, the technical standards set by the WMO for the provision of surface meteorological reports and that the data be relayed in real time for operational meteorological analysis.*

It is recognised that valuable additional work on scatterometer data assimilation has been undertaken at ABOM Research Centre in recent years (Kepert et al. 2001).

Recommendation 4. *That ABOM continue research work on (i) the assimilation of scatterometer winds with NWP systems, (ii) the assimilation of raw scatterometer backscatter data with NWP systems, (iii) the use of scatterometer winds as a source of data for "first-guess prediction" error checking, and (iv) the use of scatterometer winds to quality control test other observing systems during the data assimilation process.*

During the 1990s three marine science research expeditions were undertaken in Southern Ocean waters, all on-board *RSV Aurora Australis,* during which regular radiosonde flights were conducted. The third of these, *The Mertz Glacier Polynya Experiment* of winter 1999, included twice-daily radiosonde flights and the deployment of multiple drifting buoys and automatic weather stations.

The data collected during the 1999 experiment would make a particularly worthwhile impact study on a global or regional scale NWP system.

Recommendation 5. *That a NWP data impact experiment be considered involving data from* The Mertz Glacier Polynya Experiment *of 1999. In addition, if substantial supporting evidence can be gathered, consideration be given to having* RSV Aurora Australis *equipped and suitably staffed to provide 3-hourly surface observations and 12-hourly upper-air observations throughout its annual periods of charter to AAD.*

AAD recently announced plans to fly fixed-wing aircraft between Australia and Antarctica and over long-range routes within Antarctica. During each six-month summer season they plan a total of 110 long flight legs: 25 return flights between Hobart and Casey; 20 return flights between Casey and Davis; 10 return flights between Davis and Mawson; and multiple short-range flights between stations and field camps (www.aad.gov.au).

Aircraft fitted with suitable automatic equipment, such as the common AMDAR (Automated Meteorological Data Relay) system, would provide valuable

meteorological data for real-time NWP. Both the high-altitude transects and the vertical profiles gained from every take-off and landing would provide useful data.

> **Recommendation 6.** *That all aircraft involved in the AAD Air Transport Program be fitted with AMDAR (Automated Meteorological Data Relay) systems or similar.*

The predictive performance of GASP in the Antarctic region has improved markedly with each resolution upgrade over the past decade. The relative performance of the higher resolution ECMWF system demonstrates that, with further resolution enhancements, GASP's Australian region (and Antarctic region) predictive skill would likely increase.

The representation of the Antarctic planetary boundary layer in GASP output may benefit from the addition of more near-surface σ levels. The dynamical meteorological processes occurring in the planetary boundary layer over Antarctica are of considerable importance in the formation of weather systems further north.

A second likely benefit from an increase in the near-surface vertical resolution would be an improved ability to assimilate surface and near-surface observational data. One case-in-point is the scatterometer data discussed in detail in this thesis.

> **Recommendation 7.** *That ABOM continue the development of GASP via further increases in model resolution and the addition of more σ levels in the planetary boundary layer.*

One of the more significant developments in Antarctic Meteorology in recent years is the development of a nested limited area NWP system over the continent (Antarctic-LAPS). This system, undergoing operational trials as during 2002, is expected to become the future backbone of ABOM's forecasting services in the Australian Antarctic Territory.

> **Recommendation 8.** *That the Antarctic CRC and ABOM continue work on the development of Antarctic-LAPS and investigate the applicability of appropriate parts of the Antarctic-LAPS system to*

improve GASP performance over Antarctica and the Southern Ocean sea ice zone.

The apparent useful quality of low and mid-level TOVS data over the Antarctic continent and adjacent sea ice was discussed in Chapter 5 of this thesis. Those results were confirmed by Adams et al. (1999). In recognition of those findings it is suggested that ABOM undertake a prognosis impact study, in the framework of either GASP or Antarctic-LAPS, to assess the value of low and mid-level TOVS over the Antarctic region on forecast quality.

Recommendation 9. *That ABOM test the impact of low and mid-level TOVS over Antarctica and the Southern Ocean sea ice zone on the prognostic skill of its NWP systems.*

In Chapter 5 of this thesis results were presented on the accuracy of the GASP representation of the Antarctic near-surface temperature inversion. It was found that the temperature differences between successive near-surface σ levels and the surface provided a good indication of inversion strength. Changes in inversion strength and distribution were linked to blizzard onset at coastal stations.

A lengthy climatology of inversion strength, as represented in the GASP system, together with 6-hourly fields of departure from inversion strength climatology would be a useful weather forecasting tool.

Recommendation 10. *That ABOM determine the monthly NWP inversion strength climatology over Antarctica and, based on that climatology, test the value of NWP prognoses of departure from inversion strength climatology for operational weather forecasting in Antarctica.*

As a means of promoting discussion and interest in NWP results for the Antarctic and Southern Ocean, meteorological agencies should be encouraged to publish NWP accuracy results for all continents and significant ocean areas. This may act to foster greater interest in NWP performance generally, and specifically in regions other than Europe, North America, East Asia and Australia.

Recommendation 11. *That meteorological agencies world-wide be encouraged to report global NWP prognosis verification data, in a common format, for all continents and significant ocean areas. This could be achieved via the World Meteorological Organisation's annual* World Weather Watch Technical Reports on the Global Data-Processing System.

7.6 Conclusions

A broad range of topics has been discussed in this thesis. They include the accuracy of remotely sensed oceanic winds and TOVS vertical profiles; the utilisation of oceanic winds in a global NWP system; the prognosis impact of oceanic winds on NWP products; and the representation of the planetary boundary layer over Antarctica in a global NWP system.

The research focus and the key research findings documented here all address one single purpose: to improve medium-range weather forecasts in the Antarctic and Southern Ocean region. To that end the research has been focused on some of the more practical and realistically attainable methods.

The first series of experiments using remotely sensed scatterometer winds on ABOM NWP systems was described in Chapter 4. The results were positive and indicated a reduction in forecast errors on most occasions. The supply of scatterometer data will continue to grow in the years ahead. Following some further refinement of data assimilation and quality control methods, the potential for future strong prognosis impact exists.

The supply of data from AWS on the Antarctic ice sheet will continue to grow in the future. Modern AWS are robust and provide high quality data. Substantial NWP skill benefits will arise from the use of AWS wind, air temperature and ice surface temperature – particularly in terms of the provision of forecasting products to personnel and aircraft in the region.

The next generation of remote sensing systems will also provide atmospheric data of value to Antarctic and Southern Ocean region NWP.

The accuracy of weather forecasting products for the Antarctic region is improving. Continued efforts to improve NWP systems, and their handling of observational data, together with ongoing advances in remote sensing technology will ensure continuing forecast skill improvements into the future.

REFERENCES

Adams, N. D. (1997) Model prediction performance over the Southern Ocean and coastal region around east Antarctica. *Aust. Meteor. Mag.* **46:** 287-296.

Adams N. D. (2001) Numerical weather prediction in east Antarctica. In: *Proc. 6th Conf. on Polar Meteor.,* San Diego, USA, Amer. Meteor. Soc., 331-334.

Adams, N. D. (2002) Advances in forecasting systems at the Antarctic Meteorological Centre, Casey. *Meteor. Appl.* **9:** 335-343.

Adams, N. D., Hutchinson, H. and Hart, T. (1999) An Analysis of TOVS data during the FROST special observing periods. *Aust. Meteor. Mag.* **Special Edition:** 15-24.

Allison, I. (1998) Surface climate of the interior of the Lambert Glacier Basin, Antarctica, from automatic weather station data. *Ann. Glaciol.* **27:** 515-520.

Allison, I., Wendler, G. and Radok, U. (1993) Climatology of the east Antarctic ice sheet (100°E to 140°E) derived from automatic weather stations. *J. Geophys. Res.* **98:** 8815-8823.

Andrews, P. L. and Bell, R. S. (1998) Optimizing the United Kingdom Meteorological Office data assimilation for *ERS-1* scatterometer winds. *Mon. Weather Rev.* **126:** 736–746.

Attema, E. P. W. (1991) The Active Microwave Instrument on-board the ERS-1 satellite. *Proc. IEEE* **79:** 791–799.

Bader, M. J., Forbes, G. S., Grant, J. R., Lilley, R. B. E. and Waters, A. J. (1995) *Images in Weather Forecasting: A Practical Guide for Interpreting Satellite and Radar Imagery,* Cambridge University Press, Cambridge, UK.

Bell (1994) *The Assimilation of ERS-1 Scatterometer Winds* [Forecasting Research Division Technical Report No. 89] United Kingdom Meteorological Office, 41pp.

Bernstein, R. L. (1982) SEASAT I. *J. Geophys. Res.* **87:** 3173-3438.

BMRC (1999) *Researching Sky and Sea*, Bureau of Meteorology Research Centre, Melbourne, Australia, 36pp.

Bourke, W. (1988) Spectral methods in climate models. In: *Physically-Based Modelling and Simulation of Climate and Climatic Change, Part 1.* Kluwer Academic Publishers, Dordrecht, 375-431.

Bourke, W., Hart, T., Steinle, P., Seaman, R., Embery, G., Naughton, M. and Rickus, L. (1995) Evolution of the Bureau of Meteorology's Global Assimilation and Prediction System. Part 2: Resolution enhancements and case studies. *Aust. Meteor. Mag.* **44:** 19-40.

Bourke, W., Embery, G., Harris, B. R., Le, T., Naughton, M. J., Paevere, J., Rikus, L. J., Seaman, R. S., Steinle, P. J., Sun, Z. and Xiao, Y. (1999) Global assimilation and prediction in the Bureau of Meteorology. In: *Proc. 11th BMRC Modelling Workshop* [BMRC Research Report 75], Melbourne, Australia, Bureau of Meteorology, 1-7.

Breivik, L-A. and Schyberg, H. (1997) Assimilation of scatterometer wind pairs and altimeter wind speeds in a limited area weather prediction model. In: *Proc. 3rd ERS Symp.,* Florence, Italy, European Space Agency, 1181-1185.

Bromwich, D. H. and Parish, T. R. (1998) Meteorology of the Antarctic. In: *Meteorology of the Southern Hemisphere* [Meteorological Monographs, Vol. 27, No. 49, Edited by D. J. Karoly and D. G. Vincent], Amer. Meteor. Soc., Boston, MA, USA, 175-200.

Bromwich, D. H., Cullather, R. I. and Grumbine, R. W. (1999) An assessment of the NCEP operational global spectral model forecasts and analyses for Antarctica during FROST. *Weather & Forecasting* **14:** 835–850.

Cavanié, A. and Lecomte, P. (1987) *Vol 1 - Study of a Method to Dealias Winds from ERS-1 Data, Vol 2 - Wind Retrieval and Dealiasing Subroutines* (ESA contract 6874/87/CP-I(sc)), ESTEC, Noordwijk, The Netherlands.

CERSAT (1996) *WNF Products - User Manual* [Ref. C2-MUT-W-01-IF, Ver. 2.0], Centre ERS d'Archivage et de Traitement, Plouzane, France.

Collonney, W. M. (1996) The Antarctic temperature inversion. *Int. J. Clim.* **16:** 1333-1342.

Colman, R. A. and McAvaney, B. J. (1991) *Experiments Using the BMRC General Circulation Model with a Heat Balance Ocean* [BMRC Research Report 24], Bureau of Meteorology, Melbourne, Australia, 31pp.

Colwell, S. and Turner, J. (1999) Antarctic meteorological observations on the GTS during the FROST project. *Weather & Forecasting* **14:** 811-816.

Gonzales, A. E. and Long, D. G. (1999) An assessment of NSCAT ambiguity removal. *J. Geophys. Res.* **104:** 11449-11457.

Guymer, L. B. (1978) *Operational Application of Satellite Imagery to Synoptic Analysis in the Southern Hemisphere* [Technical Report 29], Bureau of Meteorology, Melbourne, Australia.

Hart, T., Gay, M. and Bourke, W. (1988) Sensitivity studies with the physical parameterization in the BMRC global atmospheric spectral model. *Aust. Meteor. Mag.* **36:** 47-60.

Hart, T., Bourke, W., McAvaney, B. and Forgan, B. (1990) Atmospheric general circulation simulations with the BMRC global spectral model: The impact of revised physical parameterisations. *J. Climate* **3:** 436-459.

Hoffman, R. N. (1993) A preliminary study of the impact of the ERS 1 C band scatterometer wind data on the European Centre for Medium-Range Weather Forecasts global data assimilation system. *J. Geophys. Res.* **98:** 10233-10244.

Humphreys, W. J. (1929) *Physics of the Air,* McGraw-Hill Book Company Inc., New York, USA, 654pp.

Hutchinson, H. (1996) First Regional Observing Study of the Troposphere South of Latitude 50°S (FROST). In: *Proc. 6th Annual BMRC Modelling Workshop* [BMRC Research Report 52], Melbourne, Australia, Bureau of Meteorology, 83-96.

Hutchinson, H., Dixon, T., Adams, N., Jacka, K., Pendlebury, S., Marsh, L., Cowled, L., Phillpot, H., Pook, M. and Turner, J. (1999) On the reanalysis of southern hemisphere charts for the FROST project. *Weather & Forecasting* **14:** 909-919.

Ingleby, N. B. and Bromley, R. A. (1991) A diagnostic study of the impact of SEASAT scatterometer winds on numerical weather prediction. *Mon. Weather Rev.* **119:** 84-103.

Isaksen, L. (1997) Impact of ERS scatterometer data in the ECMWF 4D-Var assimilation system. Preliminary studies. In: *Proc. 3rd ERS Symp.,* Florence, Italy, European Space Agency, 1829-1851.

Jacka, K. J. (1999) An impact study involving ERS-1 scatterometer wind data – implications for the 'FROST' project. *Aust. Meteor. Mag.* **Special Edition:** 25-34.

Kepert, J., Steinle, P., Paevere, J., Seaman, R. S. and Bourke, W. (2001) *Scatterometer Assimilation.* Paper presented to the ABOM Research Centre Seminar Series, Melbourne, Australia, 8 August 2001.

Kidson E. (1947) *Australasian Antarctic Expedition 1911–1914 Reports* Series B Vol VII Meteorology. Government Printer Sydney 31 pp and charts.

King, J. C. and Turner, J. (1997) *Antarctic Meteorology and Climatology*, Cambridge Univ. Press, Cambridge, UK, 409pp.

King, P. (1993) Use of ERS-1 scatterometer winds in Canadian forecast centres. In: *Proc. 1st ERS-1 Symp.*, Cannes, France, European Space Agency, 721-724.

Kuo, H. L. (1974) Further studies of the parameterization of the influence of cumulus convection on large-scale flow. *J. Atmos. Sci.* **31:** 1232-1240.

Le Marshall, J. F. and Pescod, N. R. (1994) Generation and operational application of cloud drift winds in the Australian region – recent advances. In: *Tech. Proc. 2nd Pacific Ocean Remote Sensing Conf.*, Melbourne, Australia, Bureau of Meteorology Research Centre, 467-474.

Le Marshall, J. F., Riley, P. A., Rouse, B. J., Mills, G. A., Wu, Z. -J., Stewart, P. K. and Smith, W. L. (1994) Real-time assimilation and synoptic application of local TOVS raw radiance observations. *Aust. Meteor. Mag.* **43:** 153-166.

Le Marshall, J. F., Seecamp, R., Harris, B. and Tingwell, C. (2001) First results from the use of local ATOVS data in the Australian region. *Aust. Meteor. Mag.* **50:** 159-163.

Le Meur, D. (1997) Impact of ERS-1/ERS-2 scatterometer tandem operations on the ECMWF 3D-var assimilation system. In: *Abstracts 3rd ERS Symp.*, Florence, Italy, European Space Agency, (available at earth.esa.int/symposia/papers/lemeur/).

Leonard, S., Turner, J. and Milton, S. (1997) An assessment of UK Meteorological Office numerical weather prediction analyses and forecasts for the Antarctic. *Antarctic Sci.* **9:** 100-109.

Lieder, M. and Heinemann, G. (1999) A summertime Antarctic mesocyclone event over the southern Pacific during FROST SOP-3: A mesoscale analysis using AVHRR, SSM/I, ERS, and numerical model data. *Weather & Forecasting* **14:** 893–908.

Long, M. W. (1983) *Radar Reflectivity of Land and Sea*, second edition, Artech House, Dedham, MA, USA, 385pp.

Lorenc. A. C. (1981) A global three-dimensional multivariate statistical interpolation scheme. *Mon. Weather Rev.* **109:** 701-721.

Lythe, M. B., Vaughan, D. G. and BEDMAP Consortium (2001) BEDMAP: A new ice thickness and subglacial topographic model of Antarctica. *J. Geophys. Res.* **106:** 11335-11351.

Marshall, G. J. and Turner, J. (1997a) ERS scatterometer observations of katabatic winds over a polynya. In: *Proc. 3rd ERS Symp.*, Florence, Italy, European Space Agency, 1591-1596.

Marshall, G. J. and Turner, J. (1997b) Surface wind fields of Antarctic mesocyclones derived from ERS 1 scatterometer data. *J. Geophys. Res.* **102:** 13907-13921.

Marshall, G. J. and Turner, J. (1999) Synoptic-scale weather systems observed during the FROST project via scatterometer winds. *Weather & Forecasting* **14:** 867–877.

Massom, R. (1991) *Satellite Remote Sensing of Polar Regions: Applications, Limitations and Data Availability,* Belhaven Press, London, UK.

McAvaney, B. J., Fraser, T. L., Hart, T. L., Rikus, L. J., Naughton, M. J. and Mullenmeister, P. (1991) *Circulation Statistics from a Non-Diurnal Seasonal Simulation with the BMRC Atmospheric GCM: R21L9.* [BMRC Research Report 29], Bureau of Meteorology, Melbourne, Australia, 231pp.

McAvaney, B. J. and Colman, R. A. (1993) *The AMIP Experiment: The BMRC AGCM Configuration* [BMRC Research Report 38], Bureau of Meteorology, Melbourne, Australia, 43pp.

MOU (2002) *Buoy Status Report for February 2002,* Bureau of Meteorology Marine Observations Unit, Melbourne, Australia, 7pp.

Mullenmeister, P. and Hart, T. (1994) *The UNIX Verification Utility Programs.* [BMRC Research Report 40], Bureau of Meteorology, Melbourne, Australia, 38pp.

Murphy, B. F. and Simmonds, I. (1993) An analysis of strong wind events simulated in a GCM near Casey in the Antarctic. *Mon. Weather Rev.* **121:** 522-534.

NCC (1994) *Climate Monitoring Bulletin Australia* [Issue 102, July 1994], Bureau of Meteorology National Climate Centre, Melbourne, Australia.

NCC (1995) *Climate Monitoring Bulletin Australia* [Issue 114, July 1995], Bureau of Meteorology National Climate Centre, Melbourne, Australia.

NMOC (2001) *Analysis and Prediction Quarterly Summary: July to September 2001,* Bureau of Meteorology National Meteorological and Oceanographic Centre, Melbourne, Australia.

NMOC (2002) *Analysis and Prediction Quarterly Summary: October to December 2001,* Bureau of Meteorology National Meteorological and Oceanographic Centre, Melbourne, Australia.

Offiler, D. (1994) The calibration of *ERS-1* satellite scatterometer winds. *J. Atmos. & Oceanic Technol.* **11:** 1002-1017.

Parish, T. R. and Bromwich, D. H. (1987) The surface windfield over the Antarctic ice sheets. *Nature* **328:** 51-54.

Pendlebury, S. F., Adams, N. D., Hart, T. L. and Turner, J. (2003) Numerical weather prediction model performance over high southern latitudes. *Mon. Weather Rev.* **131:** 335-353.

Phillpot, H. R. (1997) *Some Observationally-Identified Meteorological Features of East Antarctica* [Meteorological Study 42], Bureau of Meteorology, Melbourne, Australia, 275pp.

Phillpot, H. R and Zillman, J. W. (1970) The surface temperature inversion over the Antarctic continent. *J. Geophys. Res.* **75:** 4161-4169.

Pook, M. J. and Cowled, L. (1999) On the detection of weather systems over the Antarctic interior in the FROST analyses. *Weather & Forecasting* **14:** 920-929.

Pook, M. J. and Gibson, T. (1999) Atmospheric blocking and storm tracks during SOP-1 of the FROST project. *Aust. Meteor. Mag.* **Special Edition:** 51-60.

Pouliquen, S., Bentamy, A., Harscoat, V. and Queffeulou, P. (1997) ERS-2/NSCAT co-located database. In: *Proc. 3rd ERS Symp.*, Florence, Italy, European Space Agency, 1217-1218.

Radok, U., Allison, I. and Wendler, G. (1996) Atmospheric surface pressure over the interior of Antarctica. *Antarctic Sci.* **2:** 209-217.

Rikus, L. (1991) *The Role of Clouds in Global Climate Modelling* [BMRC Research Report 25], Bureau of Meteorology, Melbourne, Australia, 43pp.

Schwerdtfeger, W. (1984) *Weather and Climate of the Antarctic*, Elsevier, New York, USA, 261pp.

Seaman, R. S., Steinle, P., Bourke, W. and Hart, T. (1993) The impact of manually derived southern hemisphere sea level pressure data upon forecasts from a global model. *Weather & Forecasting* **8:** 363-368.

Seaman, R. S. (1994) Monitoring a data assimilation system for the impact of observations. *Aust. Meteor. Mag.* **43:** 41-48.

Seaman, R. S., Bourke, W., Steinle, P., Hart, T., Embery, G., Naughton, M. and Rickus, L. (1995) Evolution of the Bureau of Meteorology's global assimilation and prediction system. Part 1: Analysis and initialisation. *Aust. Meteor. Mag.* **44:** 1-18.

Simmonds, I. and Murray, R. J. (1999) Southern extratropical cyclone behavior in ECMWF analyses during the FROST special observing periods. *Weather & Forecasting* **14:** 878-891.

Simmonds, I., Murray, R. J. and Leighton, R. M. (1999) A refinement of cyclone tracking methods with data from FROST. *Aust. Meteor. Mag.* **Special Edition:** 35-49.

Stewart, R. H. (1988) SEASAT: Results of the mission. *Bull. Amer. Meteor. Soc.* **69:** 1441-1447.

Stoffelen, A. and Anderson, D. L. T. (1992) ERS-1 scatterometer calibration and validation activities at ECMWF, A: The quality and characteristics of radar backscatter measurements. In: *ERS-1 Geophysical Validation,* European Space Agency, Paris, 83-88.

Stoffelen, A. and Anderson, D. L. T. (1995) *The ECMWF Contribution to the Characterisation, Interpretation, Calibration and Validation of ERS-1 Scatterometer Backscatter Measurements and Winds, and their use in Numerical Weather Prediction Models* [European Space Agency Contract Report], European Centre for Medium-Range Weather Forecasts, Reading, Berkshire, UK, 92pp.

Stoffelen, A and Anderson, D. L. T. (1997a) Ambiguity removal and assimilation of scatterometer data. *Quart. J. Roy. Meteor. Soc.* **123:** 491-518.

Stoffelen, A and Anderson, D. L. T. (1997b) Scatterometer data interpretation: estimation and validation of the transfer function CMOD4. *J. Geophys. Res.* **102:** 5767–5780.

Streten, N. A. (2001) Antarctic Operational Meteorology. In: *Federation and Meteorology*, Australian Science and Technology Heritage Centre, Melbourne, Australia, 1582-1594.

Streten, N. A. (1990) A review of the climate of Mawson – A representative strong wind site in east Antarctica. *Antarctic Sci.* **2:** 79-89.

Teweles, S. and Wobus, H. B. (1954) Verification of prognostic charts. *Bull. Amer. Meteor. Soc.* **35:** 455-463.

Tiedtke, M. (1983) The sensitivity of the time-mean large-scale flow to cumulus convection the ECMWF model. In: *Proc. ECMWF Workshop on Convection in Large-Scale Models,* ECMWF Reading, UK, 297-316.

Tiedtke, M. (1988) Parameterization of cumulus convection large-scale models. In: *Physically Based Modelling and Simulation of Climate and Climate Change, Part 1,* Kluwer Academic Publishers, Dordrecht, 375-431.

Tiedtke, M. (1989) A comprehensive mass flux scheme for cumulus parameterisation in large-scale models, *Mon. Weather Rev.* **117:** 1779-1800.

Trenberth, K. E. and Olson, J. G. (1988) An evaluation and intercomparison of global analyses from the National Meteorological Center and the European Centre for Medium Range Weather Forecasts. *Bull. Amer. Meteor. Soc.* **69:** 1047-1057.

Triendl, R. (1997) Loss of Japanese satellite deals blow to remote sensing efforts. *Nature* **388:** 105.

Turner, J. and Thomas, J. P. (1992) A first assessment of the value of ERS-1 scatterometer winds for meteorological studies in the polar regions. In: *Proc. 1st ERS-1 Symp.*, Cannes, France, European Space Agency, 701-704.

Turner, J., Bromwich, D., Colwell, S., Dixon, S., Gibson, T., Hart, T., Heinemann, G., Hutchinson, H., Jacka, K., Leonard, S., Lieder, M., Marsh, L., Pendlebury, S., Phillpot, H., Pook, M. and Simmonds, I. (1996) The Antarctic First Regional

Observing Study of the Troposphere (FROST) project. *Bull. Amer. Meteor. Soc.* **77:** 2007-2032.

Turner, J. (1999) An overview of the Antarctic FROST project. *Aust. Meteor. Mag.* **Special Edition:** 3-7.

Turner, J., Colwell, S. and Leonard, S. (1999a) Data collected during the FROST project. *Aust. Meteor. Mag.* **Special Edition:** 9-14.

Turner, J., Leonard, S., Marshall, G., Pook, M., Cowled, L., Jardine, R., Pendlebury, S. and Adams, N. (1999b) An assessment of operational Antarctic analyses based on data from the FROST project. *Weather & Forecasting* **14:** 817-834.

Turner, J. and Pendlebury, S. (editors) (2000) *The International Antarctic Weather Forecasting Handbook* (Version 1.1). Available on Compact disk and Internet (www.comnap.aq). British Antarctic Survey / Australian Bureau of Meteorology, 691pp.

van den Broeke, M. R. (1996) *The Atmospheric Boundary Layer over Ice Sheets and Glaciers,* Universiteit Utrecht, Utrecht, The Netherlands, 178pp.

Vaughan, W. W. and Johnson, D. L. (1994) Meteorological satellites – the very early years prior to the launch of *TIROS-1. Bull. Amer. Meteor. Soc.,* **75:** 2295-2302.

Wilson, L. J., Dunlap, E. and Olsen, R. (1997) Impact of the assimilation of ERS-1 and ERS-2 data into a north Atlantic regional version of WAM. In: *Proc. 3rd ERS Symp.,* Florence, Italy, European Space Agency, 1137-1142.

WMO (1996) *World Weather Watch Technical Report on the Global Data-Processing System: 1995* [WMO Tech. Doc. 744], World Meteor. Org., 244pp.

WMO (1997) *World Weather Watch Technical Report on the Global Data-Processing System: 1996* [WMO Tech. Doc. 807], World Meteor. Org., 217pp.

WMO (1998) *World Weather Watch Technical Report on the Global Data-Processing System: 1997* [WMO Tech. Doc. 896], World Meteor. Org., 254pp.

WMO (1999) *World Weather Watch Technical Report on the Global Data-Processing System: 1998* [WMO Tech. Doc. 945], World Meteor. Org., 262pp.

WMO (2000) *World Weather Watch Technical Report on the Global Data-Processing System: 1999* [WMO Tech. Doc. 996], World Meteor. Org., 297pp.

WMO (2001) *World Weather Watch Technical Report on the Global Data-Processing System: 2000* [WMO Tech. Doc. 1061], World Meteor. Org., 271pp.

Young, I. R. and Holland, G. J. (1996) *Atlas of the Oceans: Wind and Wave Climate*. Pergamon, New York, USA, 241pp plus compact disk.

Yu, T. -W. (1995) *Assimilation Experiments with ERS-1 Winds: Part (II) Use of Vector Winds in the NCEP Spectral Statistical Analysis System* [NCEP / OPC Technical Note 117], Nat. Centers for Environmental Prediction, Washington, DC, USA.

Yu, T. -W. and Derber, J. C. (1995) *Assimilation Experiments with ERS-1 Winds: Part (I) Use of Backscatter Measurements in the NCEP Spectral Statistical Analysis System* [NCEP / OPC Technical Note 116], Nat. Centers for Environmental Prediction, Washington, DC, USA.

Yu, T. -W., Iredell, M. D. and Zhu, Y. (1996) The impact of ERS-1 winds on NCEP operational numerical weather analyses and forecasts. In: *Proc. 11th Conf. on Numerical Weather Prediction,* Norfolk, VA, USA, Amer. Meteor. Soc., 276-277.

Zillman, J. (2001) A Hundred Years of Science and Service: Australian Meteorology through the 20th Century. In: *Federation and Meteorology*, Australian Science and Technology Heritage Centre, Melbourne, Australia, 1595-1616.

APPENDIX 1

LOCATIONS REFERRED TO IN THE TEXT

The following list includes some of the locations in the mid to high-latitudes of the southern hemisphere from which meteorological reports were available during the study periods. Manned stations ( ), radiosonde stations (↑) and automatic weather stations (AWS) are indicated by symbols. Latitude, longitude, altitude and operating nations are also shown.

Amsterdam Island	↑	37.8°S	077.5°E	27m	France
Amundsen-Scott	↑	90.0°S		2835m	USA
Balaena Island	AWS	66.0°S	111.1°E	8m	Australia
Bellingshausen	↑	62.2°S	058.9°W	16m	Russia
Campbell Island	AWS*	52.6°S	169.2°E	15m	New Zealand
Casey	↑	66.3°S	110.5°E	41m	Australia
Casey (airstrip)	AWS	66.3°S	110.8°E	390m	Australia
Chatham Island	↑	44.0°S	176.6°W	44m	New Zealand
Davis	↑	68.6°S	078.0°E	13m	Australia
Dome Fuji	AWS	77.3°S	039.7°E	3810m	Japan
Dumont d'Urville	↑	66.7°S	140.0°E	43m	France
Falkland Is. (Mt. Pleasant airport)	↑	51.8°S	058.5°W	74m	United Kingdom
Georg von Neumayer	↑	70.6°S	008.4°W	50m	Germany
Gough Island	↑	40.4°S	009.9°W	54m	South Africa
Halley	↑	75.5°S	026.7°W	39m	United Kingdom
Haupt Nunatak	AWS	66.6°S	110.7°E	81m	Australia
Heard Island (Atlas Cove)	AWS	53.0°S	073.4°E	3m	Australia
Hobart		42.9°S	147.3°E	51m	Australia
Hobart (airport)	↑	42.8°S	147.5°E	4m	Australia
Invercargill	↑	46.7°S	168.6°E	4m	New Zealand

Kerguelen Is. (Port aux Français)	↑	49.4°S	070.3°E	29m	France
Law Dome Summit	AWS	66.7°S	112.7°E	1366m	Australia
Law Dome Summit South	AWS	66.7°S	112.9°E	1375m	Australia
Maatsuyker Island		43.7°S	146.3°E	147m	Australia
Macquarie Island	↑	54.5°S	158.9°E	30m	Australia
Marambio	↑	64.2°S	056.7°W	198m	Argentina
Marion Island	↑	46.9°S	037.9°E	22m	South Africa
Mawson	↑	67.6°S	062.9°E	16m	Australia
McMurdo	↑	77.9°S	166.7°E	24m	USA
Mirny	↑	66.6°S	093.0°E	30m	Russia
Molodezhnaya		67.7°S	045.9°E	40m	Russia
Novolazarevskaja	↑	70.8°S	011.8°E	99m	Russia
Orcadas		60.8°S	044.7°W	6m	Argentina
Penguin Point	AWS	67.6°S	146.2°E	30m	USA
Perth (airport)	↑	31.9°S	116.0°E	20m	Australia
Punta Arenas	↑	53.0°S	070.9°W	37m	Chile
Rothera		67.5°S	068.1°W	16m	United Kingdom
Signy Island		60.7°S	045.6°W	6m	United Kingdom
South Georgia Is. (Grytviken)		54.3°S	036.5°W	3m	United Kingdom
Snyder Rocks	AWS	66.6°S	107.8°E	40m	Australia
Syowa	↑	69.0°S	039.6°E	21m	Japan
Vostok	↑	78.5°S	106.9°E	3488m	Russia
Zhongshan		69.4°S	076.4°E	15m	China

* Campbell Island was a manned radiosonde station during the period of the FROST project (1994/1995).

APPENDIX 2

HISTORY OF DEVELOPMENT OF GLOBAL NWP SYSTEMS: GAPS, ECMWF AND UKMO.

GASP

The GASP system has been developed in a step-wise fashion over the past two decades. Since it's operational inception in 1990 the system has undergone a series of important resolution and performance upgrades. A summary of the most important details of the evolution of GASP, between 1990 and 2001, is given here with a focus on developments of greatest interest to the Antarctic and Southern Ocean region. (Compiled from multiple issues of *Analysis and Prediction Operations Bulletin* (1990 to 2000), ABOM; multiple issues of *NMC* (later *NMOC*) *Melbourne Quarterly Summary* (1990 to 2001), ABOM; and the references quoted below).

For further reading see Bourke et al. 1995, Seaman et al. 1995, Bourke et al. 1999, Hart et al. 1990, Bourke 1988, Hart et al. 1988, Colman and McAvaney 1991, Rikus 1991, McAvaney and Colman 1993 and McAvaney et al. 1991.

October 1990: Operational implementation of the R31L9 system.

This operational version of the GASP system (R31L9) replaced the earlier Hemispheric Assimilation and Prognosis System (HASP) implemented in March 1985 (resolution R21L9 with horizontal grid spacing of approximately 350km and nine vertical levels).

This original GASP system was a global stand-alone spectral assimilation and prognosis system. It had a resolution of rhomboidal 31 (approximately 240km horizontal grid spacing) and operated on nine σ levels at: 0.9911, 0.9259, 0.8114, 0.6639, 0.5000, 0.3360, 0.1886, 0.0741 and 0.0089 of the surface pressure.

The analysis scheme was univariate with six hourly assimilation and prognosis cycling. The assimilation process used up to 16 observations at each grid point. Observational data received within seven hours of the analysis time were utilised in the assimilation.

The R31L9 GASP was run operationally twice daily (base times of 1100 and 2300UTC). It provided forecast periods to 5 days (from the 1100UTC base run) and 2 days (from the 2300UTC base run).

Primitive-equation dynamics were primarily expressed in terms of vorticity, divergence, temperature, surface pressure and specific humidity.

Deep convection was simulated by a variation of the method of Kuo (1974). Shallow convection is as per the method of Tiedtke (1983) and Tiedtke (1988).

Monthly mean sea ice extents were used, and updated every five days by interpolation. Southern Ocean sea ice was held at 1m thick; Arctic sea ice was held at 2m thick.

December 1992: Operational implementation of the R31L19 system.

This upgrade included an increase from nine σ levels to nineteen σ levels at: 0.991, 0.950, 0.900, 0.850, 0.800, 0.750, 0.700, 0.600, 0.500, 0.400, 0.300, 0.250, 0.200, 0.150, 0.100, 0.070, 0.050, 0.030 and 0.010 of the surface pressure.

The analysis system was completely re-written (as per Lorenc 1981), including the introduction of multivariate statistical interpolation.

The assimilation system was altered to select up to 150 observations over large areas (~1500km diameter) to analyse multiple grid points. The observation selection and quality control procedures were overhauled, and the system used to reject erroneous data was improved.

The system was altered to analyse geopotential rather than surface pressure and temperature. This eliminated the need to assimilate TOVS temperatures rather than

the more reliable layer thicknesses. Both 250 and 500km resolution TOVS data were used.

March 1994: Operational implementation of the R53L19 system.

This version saw an increase in grid point horizontal resolution to about 200km.

The upgrade included refinements to the multivariate analysis scheme. These allowed for the incorporation of station level pressures from higher altitude stations including AWS high on the Antarctic plateau.

The radiation scheme of the model was upgraded to give more accurate results. This included diurnal cycling, diagnostic clouds and interactive optical properties.

Figure A2.1 Schematic diagram of the GASP R53L19 grid point horizontal resolution of ~200km (from BMRC 1999).

The upgrade also included improved techniques to monitor data quality and flag systematic observational errors.

The full prognosis model was run twice daily to 7 days from base times of 1100 and 2300UTC.

December 1995: Operational implementation of the T79L19 system.

This upgrade included the replacement of the Kuo (1974) moist convection scheme with the more detailed and physically realistic mass flux scheme developed by Tiedtke (1989). The parameterisation considered three types of convection: penetrative convection in large-scale convergent flow, shallow convection in suppressed conditions and mid-level convection associated with extratopical large-scale ascent.

The analysis of moisture was improved with the introduction of relative humidity analysis using a statistical interpolation technique. This replaces the earlier systems' analysis of mixing ratios

The triangular truncation of spectral coefficients at wave number 79 was introduced to replace rhomboidal 53. This provided several performance improvements but did not represent a significant change in resolution.

The code was also re-written to allow for different grids for the analysis and prediction components. This provided the facility to use fewer longitude points at higher latitudes.

December 1998: Operational implementation of the T_L239L29 system.

This upgrade included a substantial (three-fold) increase in horizontal resolution from ~200km to ~75km. The T_L annotation denotes triangular truncation but with the non-linear dynamics and physical parameterisations computed on a linear grid (which has about half the number of points in the quadratic grid traditionally used in spectral models).

Figure A2.2 Schematic diagram of the GASP $T_L239L29$ grid point horizontal resolution of ~75km (from BMRC 1999).

The vertical resolution increased from nineteen σ levels to twenty-nine σ levels, but the vertical bounds of the system remained at σ = 0.991 and 0.010. The twenty-nine σ levels were at: 0.991, 0.975, 0.950, 0.925, 0.900, 0.875, 0.850, 0.800, 0.750, 0.700, 0.633, 0.566, 0.500, 0.433, 0.366, 0.320, 0.290, 0.260, 0.230, 0.200, 0.170, 0.140, 0.110, 0.090, 0.070, 0.050, 0.030, 0.020 and 0.010.

The upgrade included the implementation of a semi-implicit semi-Lagrangian time stepping algorithm allowing a time step of 600 seconds at T_L239 resolution, up from 540 seconds at T79 resolution.

The system used a multivariate statistical interpolation scheme that, in this version, would permit direct assimilation of radiances from TOVS instruments. Operational use of TOVS radiances came with the next major upgrade in August 2000.

Assimilation of TOVS data from the 1000-850hPa layer (over open ocean) began with this upgrade. Over sea ice TOVS were used above 300hPa only. Previously TOVS above 850hPa were used over open ocean and sea ice indiscriminately. Over land areas TOVS above 100hPa were used (unchanged from earlier versions).

Several alterations to the handling of observations were included in this upgrade. One substantial change allowed for the inclusion of all observations within a six-hour window to be considered. Subsequently, in the case of multiple observations from a single station, the report closest to analysis time was used. Earlier versions always used the latest report.

The full prognosis model was run twice daily to 8 days from base times of 0000 and 1200UTC.

August 2000: Operational implementation of 1DVAR.

The analysis component of GASP was upgraded to use a one-dimensional variational radiance assimilation scheme (1DVAR). Radiances estimated from the first guess profile of moisture and temperature were compared with the observed values and the profile adjusted using a variational scheme to give a best fit to all the observed radiances. The scheme also included a comprehensive bias correction system. NOAA NESDIS TOVS continued to be used above 100hPa.

June 2001: Operational trial of GASP ensemble prediction.

The trial ensemble consisted of a suite of 33 versions of GASP at resolution $T_L119L19$. Prognoses were provided to 10 days. Results were presented in the form of on-screen "spaghetti diagrams" (time evolution of particular contours from all member forecasts), "tubes" (forecasts identified as most divergent from the mean) and "postage stamps" (thumbnails and plots of individual member forecasts).

July 2001: Correction to sea ice error.

An error, which had apparently been present since August 2000, was identified in the GASP system. The error had the effect of removing all sea ice from the model surface scheme. A parallel trial was conducted over 28 runs with and without sea ice to assess the impact of the error. Surprisingly little impact was identified.

ECMWF

The notable events in the development of the ECMWF global NWP system, between 1995 and 2000, are briefly listed here. (Compiled from WMO 1996, WMO 1997, WMO 1998, WMO 1999, WMO 2000, WMO 2001 and www.ecmwf.int).

Jan. 1995 Resolution T213L31.

Apr. 1995 Several model changes were implemented including the introduction of a smoothed mean orography to replace the previous envelope orography, and a new subgrid orography parameterisation.

Jan. 1996 A 3D-Var analysis scheme was introduced, replacing the previous optimum interpolation system.

Apr. 1996 A new definition of the sea surface temperature and sea ice was introduced. The input to the scheme became the 1-degree sea surface temperature analysis from NCEP and the gridded ice fields derived from SSM/I data from NESDIS.

Dec. 1996 The forecast model was modified to use a two-time-level semi-Langrangian scheme.

Nov. 1997 A 4D variational data assimilation scheme was put into operations.

Dec. 1997 A revised physics package was implemented. Its main features were a refined the radiation scheme, a new convective closure assumption and a new treatment of cloud ice fall-out.

Mar. 1998 The two-time-level semi-Langrangian temporal scheme was re-formulated and the model spectral resolution was increased from T213 to T_L319. This was made possible the use of a linear Gaussian grid reflected by the T_L notation.

June 1998	The oceanic wave model was fully coupled to the atmospheric model; Some DMSP-13 SSMI channels were actively assimilated under the form of total column water vapour content;
June 1998	Temperature was used instead of height as the mass information retrieved from radiosonde flights, plus use of 'significant' levels in addition to 'standard' levels; Maximum frequency of assimilation of data from fixed stations was increased to hourly instead of 6-hourly; and Increase in the number of TOVS channels used over land.
Mar. 1999	Vertical resolution increased from 31 levels to 50 levels with the extra resolution was mainly in the stratosphere and mesosphere.
May 1999	Raw MSU (NOAA 14) and AMSU (NOAA 15) radiances were introduced in the data assimilation.
July 1999	Winds from NOAA/FSL demonstration network of profilers were activated in the assimilation; A screen-level humidity and temperature analysis was introduced for the optimum interpolation of soil temperature and water content; and A new bias correction scheme for radiosonde temperatures was activated, as well as a new numerical scheme for physical tendencies.
Oct. 1999	Vertical resolution increased from 50 levels to 60 levels with the extra resolution mainly in the planetary boundary layer; A new parameterisation of precipitation accounting for cloud and precipitation partial overlap was introduced; The prescribed model background error statistics used in the data assimilation were revised using an ensemble of perturbed analyses; and A 1D-Var assimilation of SSMI winds was activated.
Apr. 2000	Revised use of SSM/I radiance including new bias correction and prevention of assimilation where precipitation occurs; Quality control procedure changes for dropsonde data; Modifications of the assimilation of humidity in the stratosphere; and Bug fix in the gravity wave drag formulation in the stratosphere.

June 2000 New parameterisation schemes for the land surface, lying snow and sea ice;
Revised snow analysis;
New long-wave radiation scheme;
Improved ozone model;
Improved treatment of precipitation processes in the first time-step;
Use of more TOVS/ATOVS data;
Use of actual buoy heights; and
Revised observation and background error variances in 4D-Var.

Sep. 2000 Change of cycling period of the assimilation from 6 to 12 hours; Use of more accurate background trajectory in 4D-Var;
New quality control step that prevents the use of observations which the incremental formulation of 4D-Var cannot handle; and
Resetting of the stratospheric ozone and switching off the multivariate coupling between ozone and vorticity.

Nov. 2000 The deterministic model and the outer loops of 4D-Var were run at T_L511 (increase from T_L319); the 12h inner loops (increments) of 4D-Var were run at T_L159 (increase from T63).

UKMO

The notable events in the development of the UKMO global NWP system, between 1995 and 2000, are briefly listed here. (Compiled from WMO 1996, WMO 1997, WMO 1998, WMO 1999, WMO 2000 and WMO 2001).

Jan. 1995 Resolution 0.83° latitude by 1.25° longitude and 19 vertical levels.

Jan. 1995 Gravity wave drag was revised to allow for wave breaking at low level;
The specification of orographic roughness was improved; and
Adjustments were made in the modelling of surface fluxes of heat and moisture.

Apr. 1995 Winds computed from visible imagery on GMS-5 were included in the data assimilation.

June 1995 Horizontal diffusion was switched off near steep orography.

Oct. 1995	Winds computed from visible imagery on METEOSAT were included in the data assimilation;
Jan. 1996	Several physical routines were revised including: A change in the formulation of mixed cloud; A correction to saturation vapour pressure; A revised parameterisation for the radius of water drops; and Small modifications to the precipitation scheme.
Apr. 1996	Temperature information from TOVS radiances assimilated using 1D-Var.
Nov. 1996	Advection scheme changed from second order to fourth order; The convection scheme was enhanced to include convective momentum transports; Revisions were made to the gravity wave drag parameterisation scheme; and Humidity information from TOVS radiances assimilated.
June 1997	The model was changed to use a climatological ice-edge, as transmission of routine bulletins from the USA ceased.
Jan. 1998	The model resolution was increased to 0.56° latitude by 0.83° longitude (60km at mid-latitudes) and 30 vertical levels.
May 1998	A new global orography was introduces with significant corrections over Antarctica.
Feb. 1999	Meteosat-5 satellite winds over the Indian Ocean were introduced.
Mar. 1999	Started to use high level (above 400hPa) GMS satellite water-vapour winds; Introduction of a 3D-Var system as a replacement for the analysis correction scheme; and Assimilation of 1D-Var retrievals from ATOVS were thinned to one report per 2 degrees.
July 1999	Sea ice analysis using SSM/I was introduced; Upgrade to the global data assimilation system: revised the covariance model to use ATOVS over Siberia and thinned scatterometer winds to one per analysis grid box.
Oct. 1999	Upgrade to the assimilation system: Started to use SSM/I wind speeds thinned to one report per 125km;

	Introduction of direct assimilation of TOVS/ATOVS radiances in 3D-Var; Increased use of station level pressure in place of MSLP; Upgraded the statistics for the covariance model; and Aircraft observational errors were reduced and modest thinning was introduced.
Dec. 1999	ERS-2 scatterometer winds were disabled.
June 2000	Introduction of a new land surface exchange system including a thermal vegetative canopy.
May 2000	Introduced interpolation of model background to observation time; Began using observed rather than retrieved ATOVS radiances; and Introduced an alternative covariance model allowing longer scales in the stratosphere.
Nov. 2000	Converted the stratospheric data assimilation system to 3D-Var.

APPENDIX 3

SCATTEROMETER IMPACT STUDY: DAILY VARIATION OF S_1, RMSE AND BIAS

Analysis of S_1 skill-score, RMSE and bias was used to assess the impact of ERS-1 scatterometer wind data on forecasts from the GASP R53L19 system. These data were collated daily from a network of seven verification grids, the details of which are shown in Table 4.5.1. *With-ESA* and *without-ESA* results were derived for 24 and 48-hour prognoses of MSLP and 500hPa height.

The full collection of results is plotted on the following pages (Figures A3.1 to A3.14).

Key to Figures A3.1 to A3.14

With-ESA 24-hour prognoses: Blue closed markers ♦

With-ESA 48-hour prognoses: Blue open markers ◇

Without-ESA 24-hour prognoses: Green closed markers ■

Without-ESA 48-hour prognoses: Green open markers □

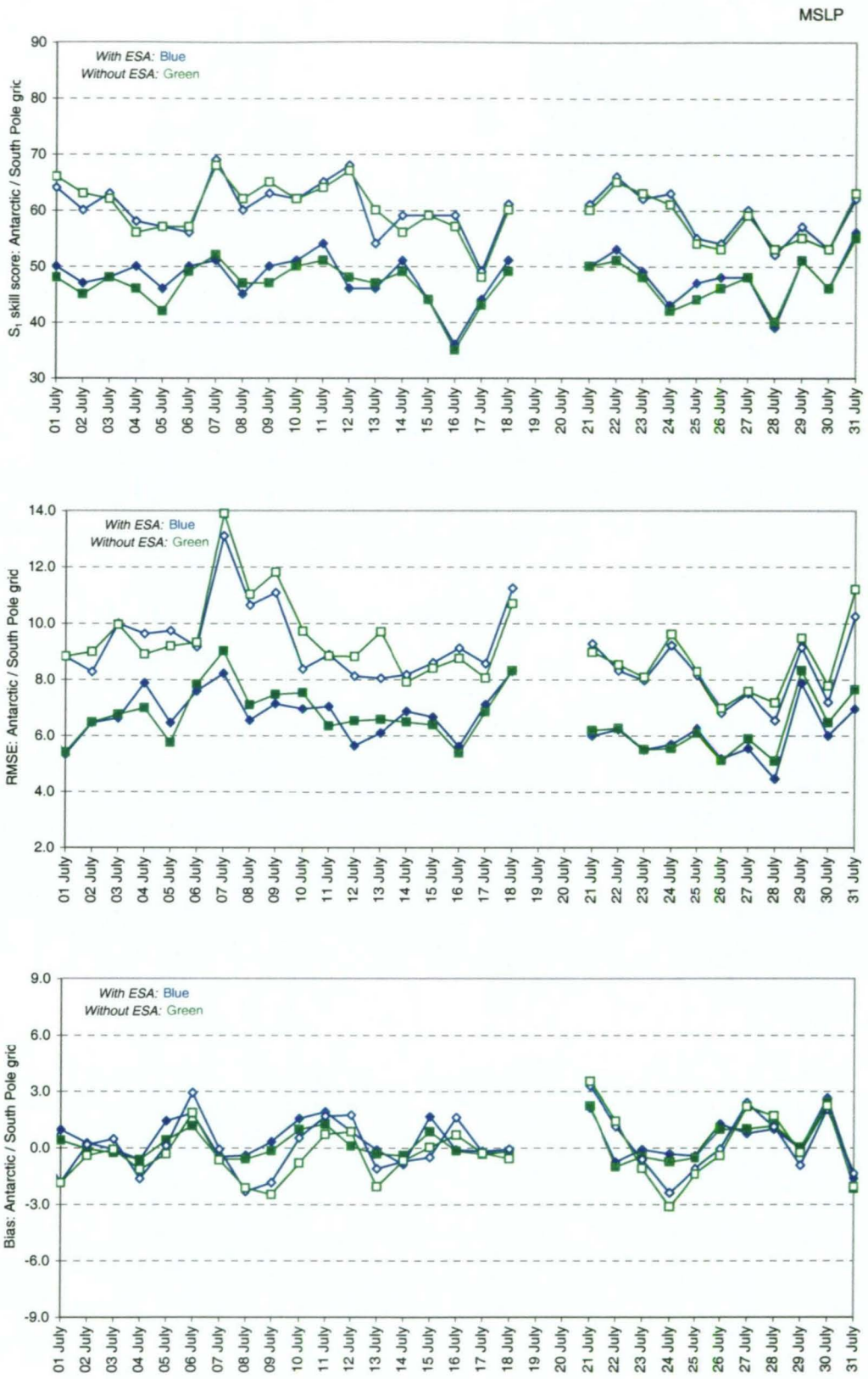

Figure A3.1 Daily variation of S_1 skill-score (top), RMSE (middle) and bias (bottom) comparing 24 and 48-hour prognoses of **MSLP** from both the *with-ESA* and *without-ESA* trials (July 1995; hPa). **Antarctic / South Pole verification grid.**

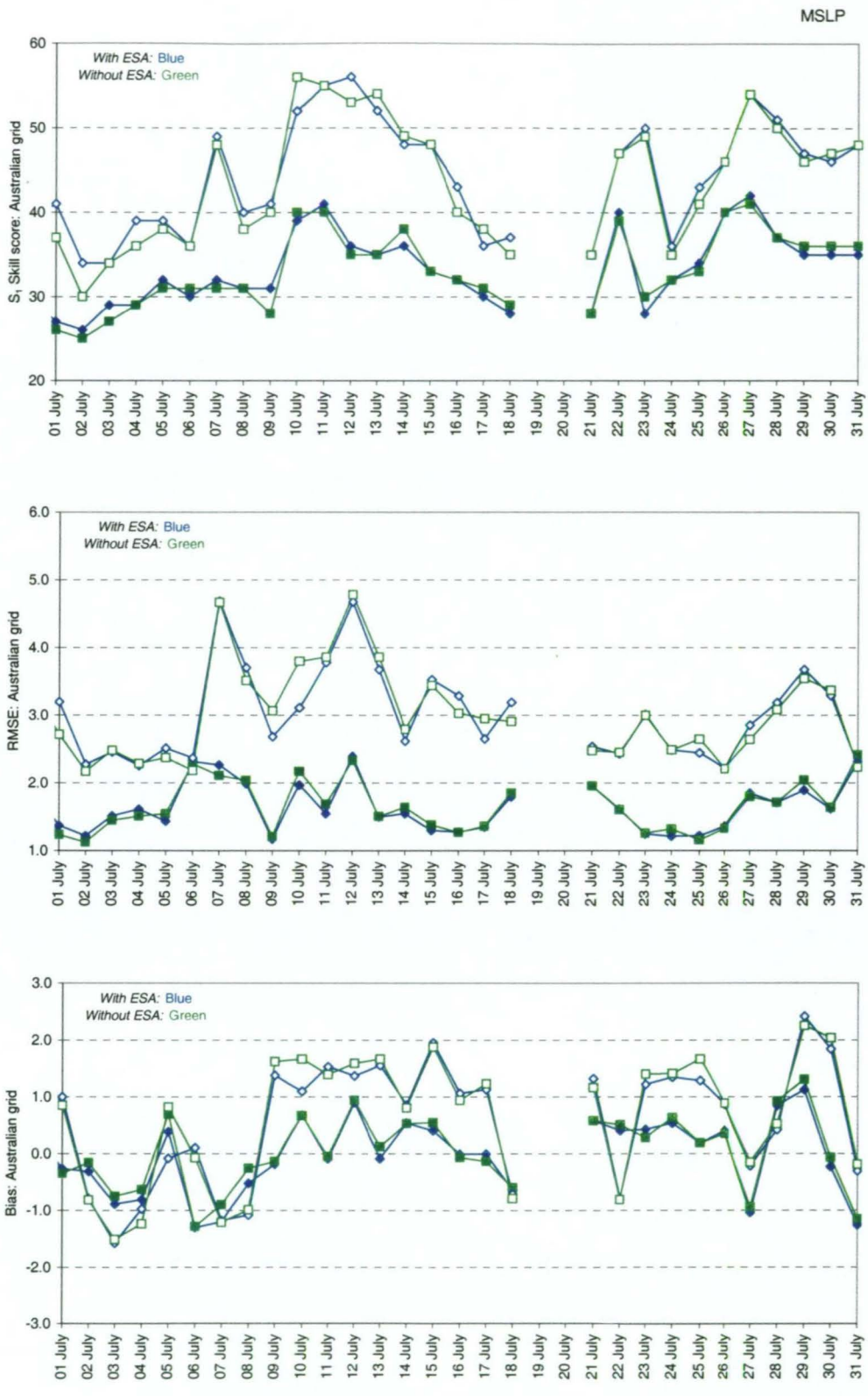

Figure A3.2 Daily variation of S_1 skill-score (top), RMSE (middle) and bias (bottom) comparing 24 and 48-hour prognoses of **MSLP** from both the *with-ESA* and *without-ESA* trials (July 1995; hPa). **Australian verification grid.**

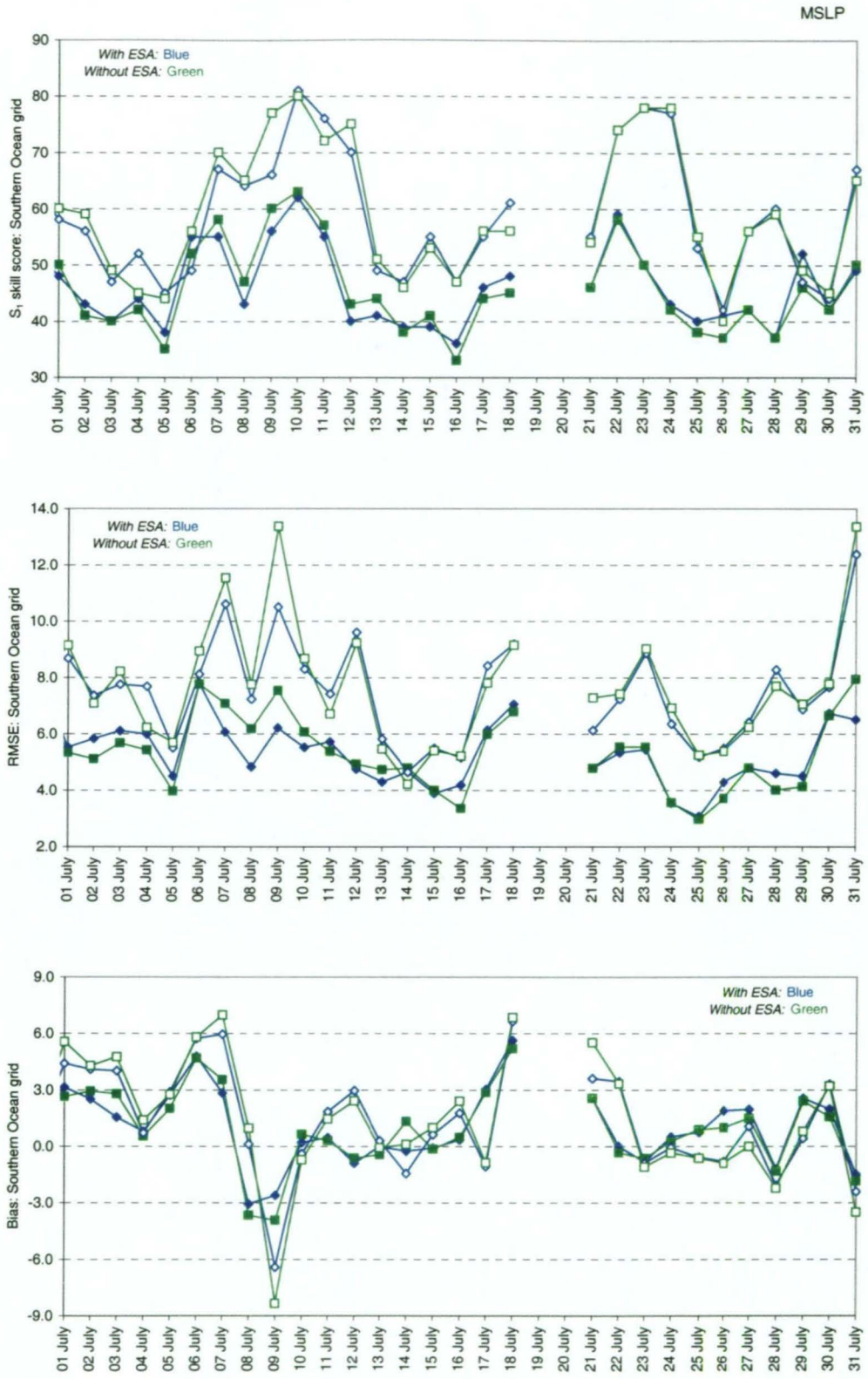

Figure A3.3 Daily variation of S_1 skill-score (top), RMSE (middle) and bias (bottom) comparing 24 and 48-hour prognoses of **MSLP** from both the *with-ESA* and *without-ESA* trials (July 1995; hPa). **Southern Ocean verification grid (60°E to 160°E sector).**

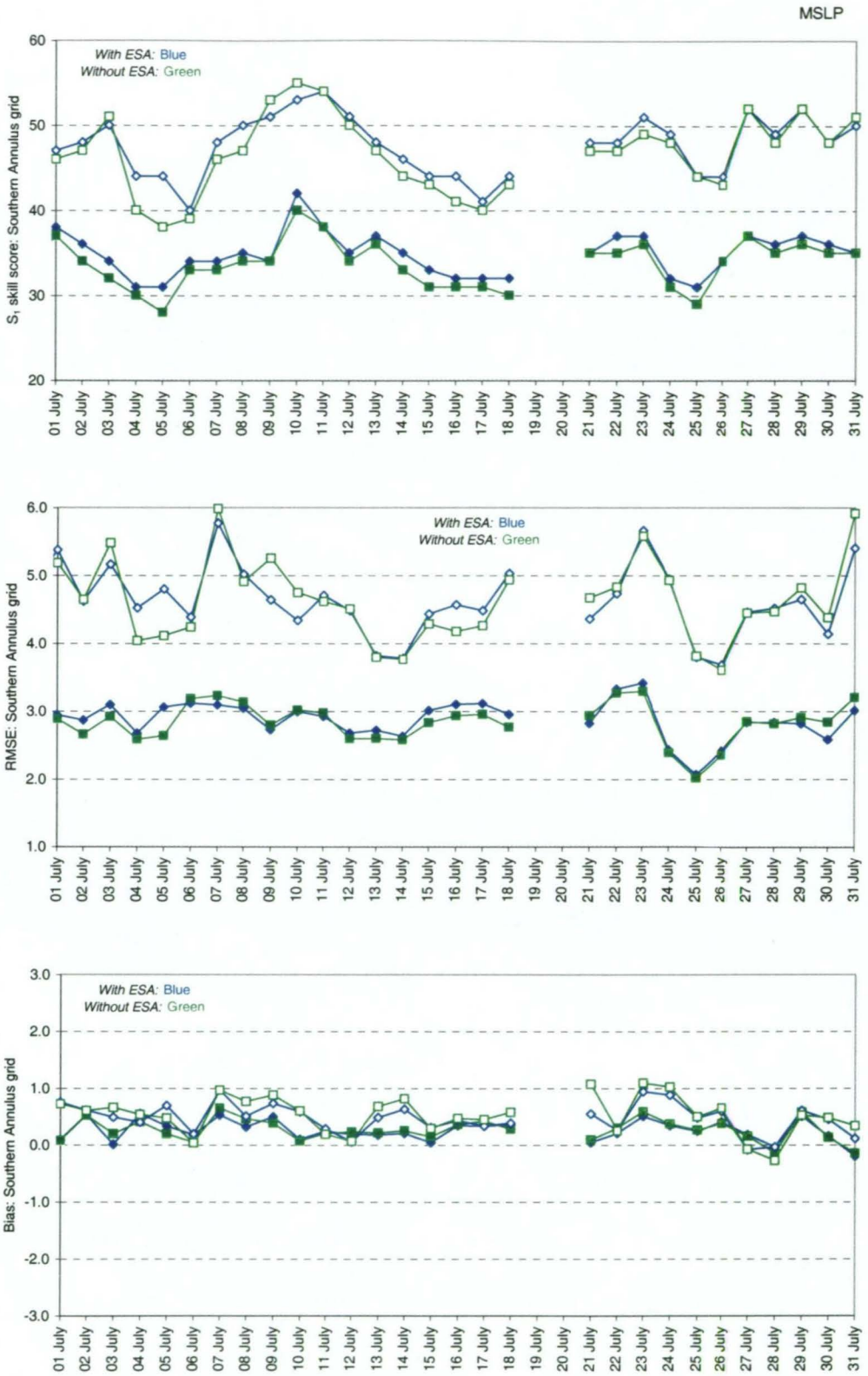

Figure A3.4 Daily variation of S_1 skill-score (top), RMSE (middle) and bias (bottom) comparing 24 and 48-hour prognoses of **MSLP** from both the *with-ESA* and *without-ESA* trials (July 1995; hPa). **Southern Annulus verification grid.**

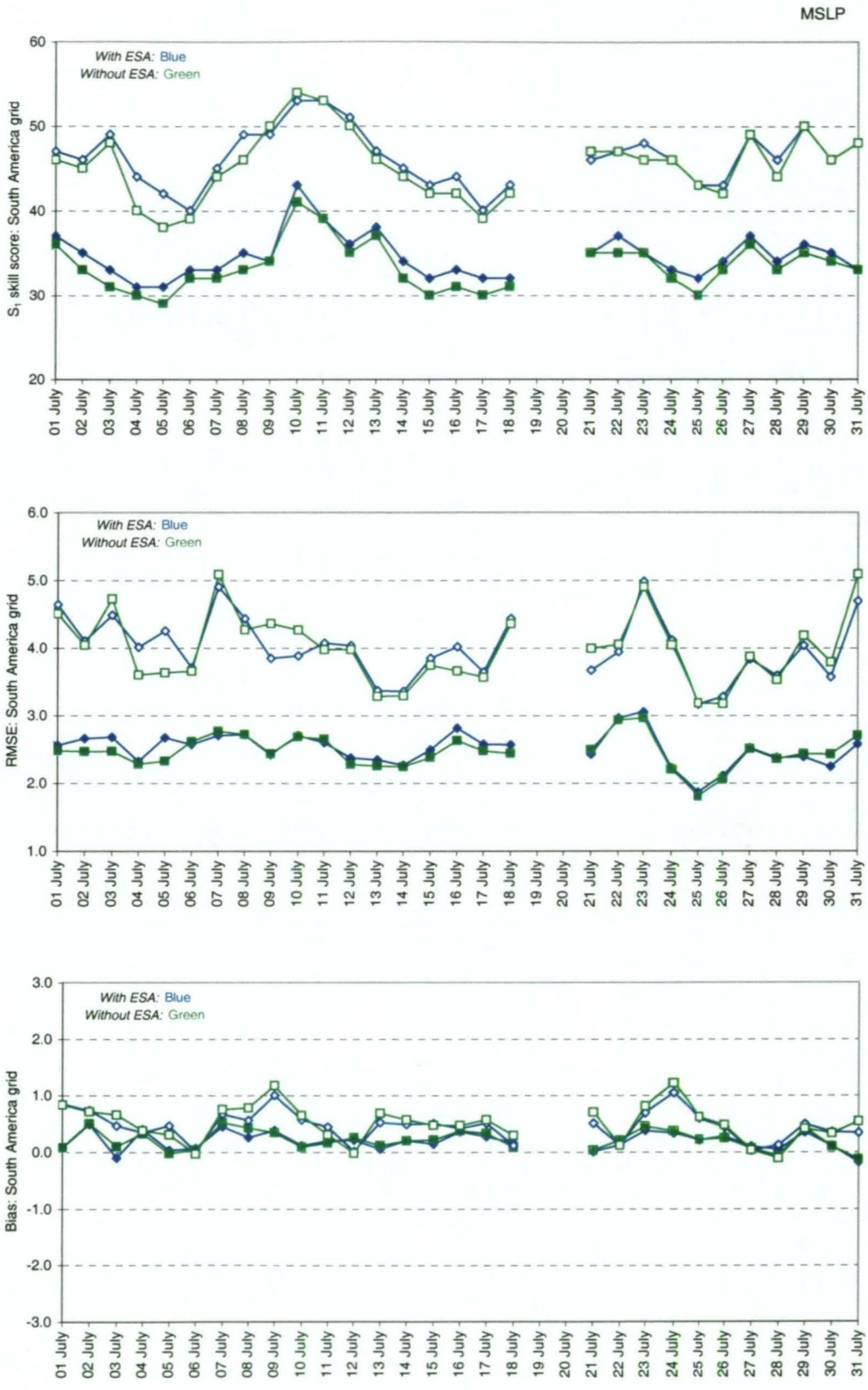

Figure A3.5 Daily variation of S_1 skill-score (top), RMSE (middle) and bias (bottom) comparing 24 and 48-hour prognoses of **MSLP** from both the *with-ESA* and *without-ESA* trials (July 1995; hPa). **South American verification grid.**

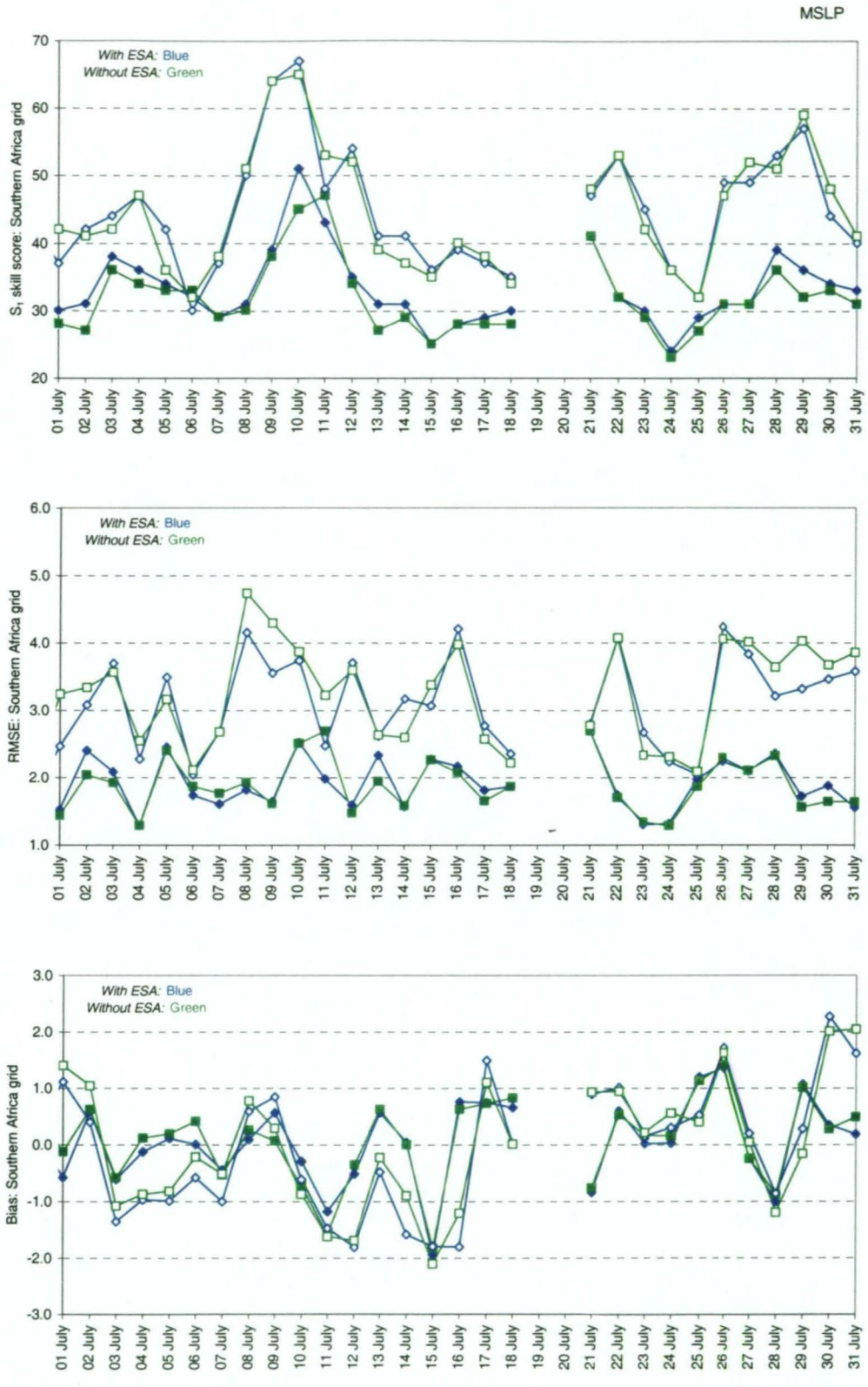

Figure A3.6 Daily variation of S_1 skill-score (top), RMSE (middle) and bias (bottom) comparing 24 and 48-hour prognoses of **MSLP** from both the *with-ESA* and *without-ESA* trials (July 1995; hPa). **Southern Africa verification grid.**

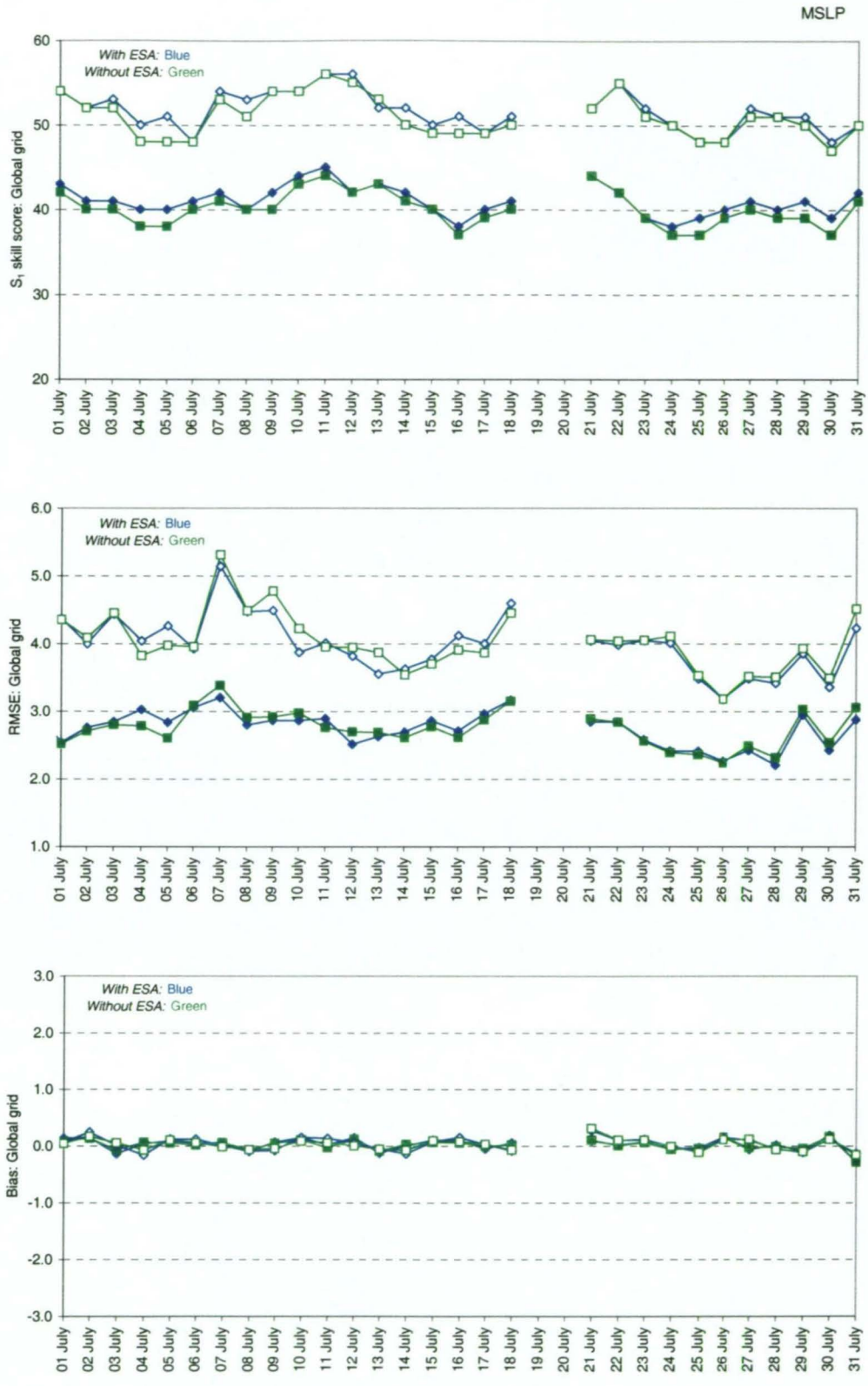

Figure A3.7 Daily variation of S_1 skill-score (top), RMSE (middle) and bias (bottom) comparing 24 and 48-hour prognoses of **MSLP** from both the *with-ESA* and *without-ESA* trials (July 1995; hPa). **Global verification grid.**

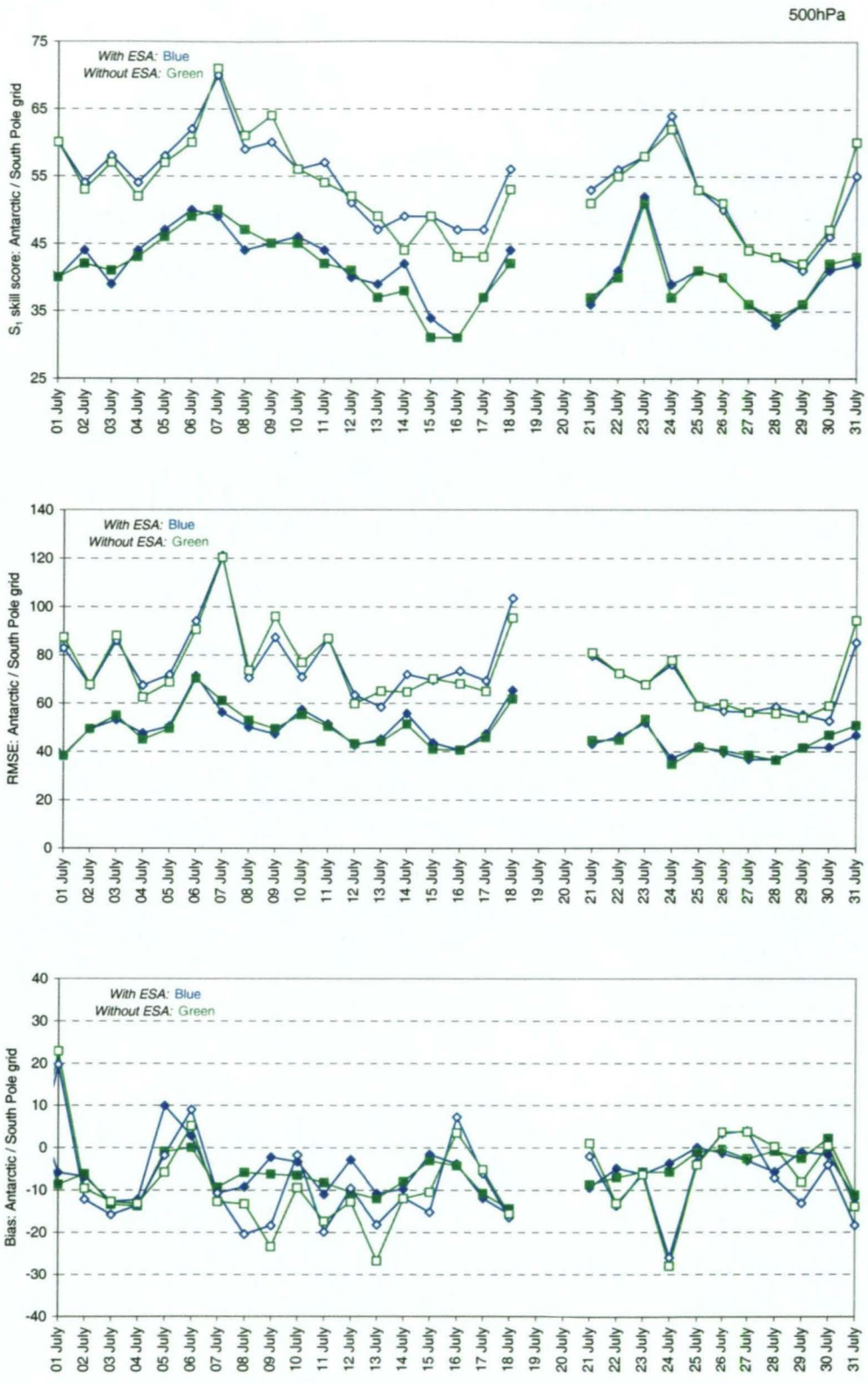

Figure A3.8 Daily variation of S_1 skill-score (top), RMSE (middle) and bias (bottom) comparing 24 and 48-hour prognoses of **500hPa height** from both the *with-ESA* and *without-ESA* trials (July 1995; m). **Antarctic / South Pole verification grid.**

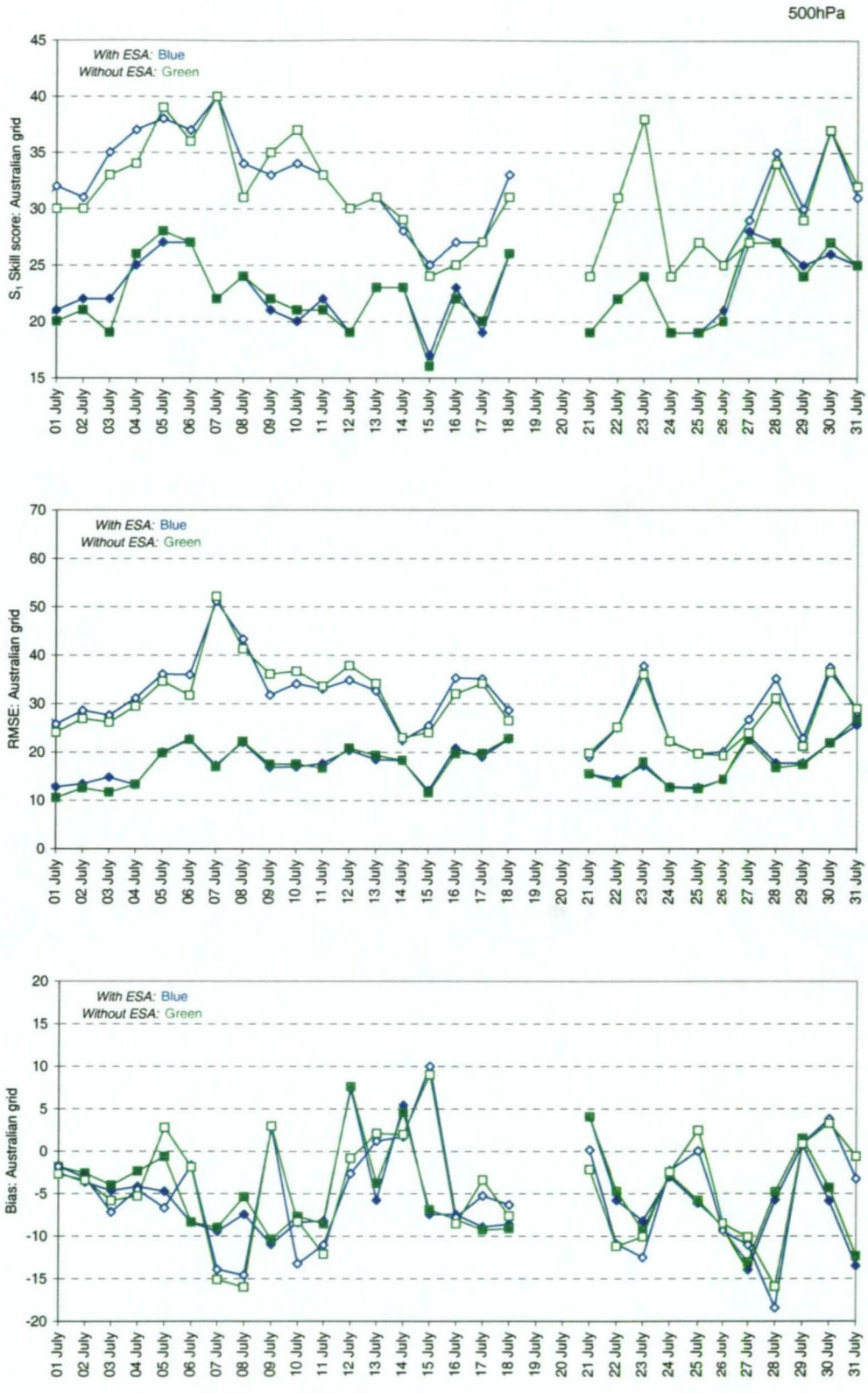

Figure A3.9 Daily variation of S_1 skill-score (top), RMSE (middle) and bias (bottom) comparing 24 and 48-hour prognoses of **500hPa height** from both the *with-ESA* and *without-ESA* trials (July 1995; m). **Australian verification grid.**

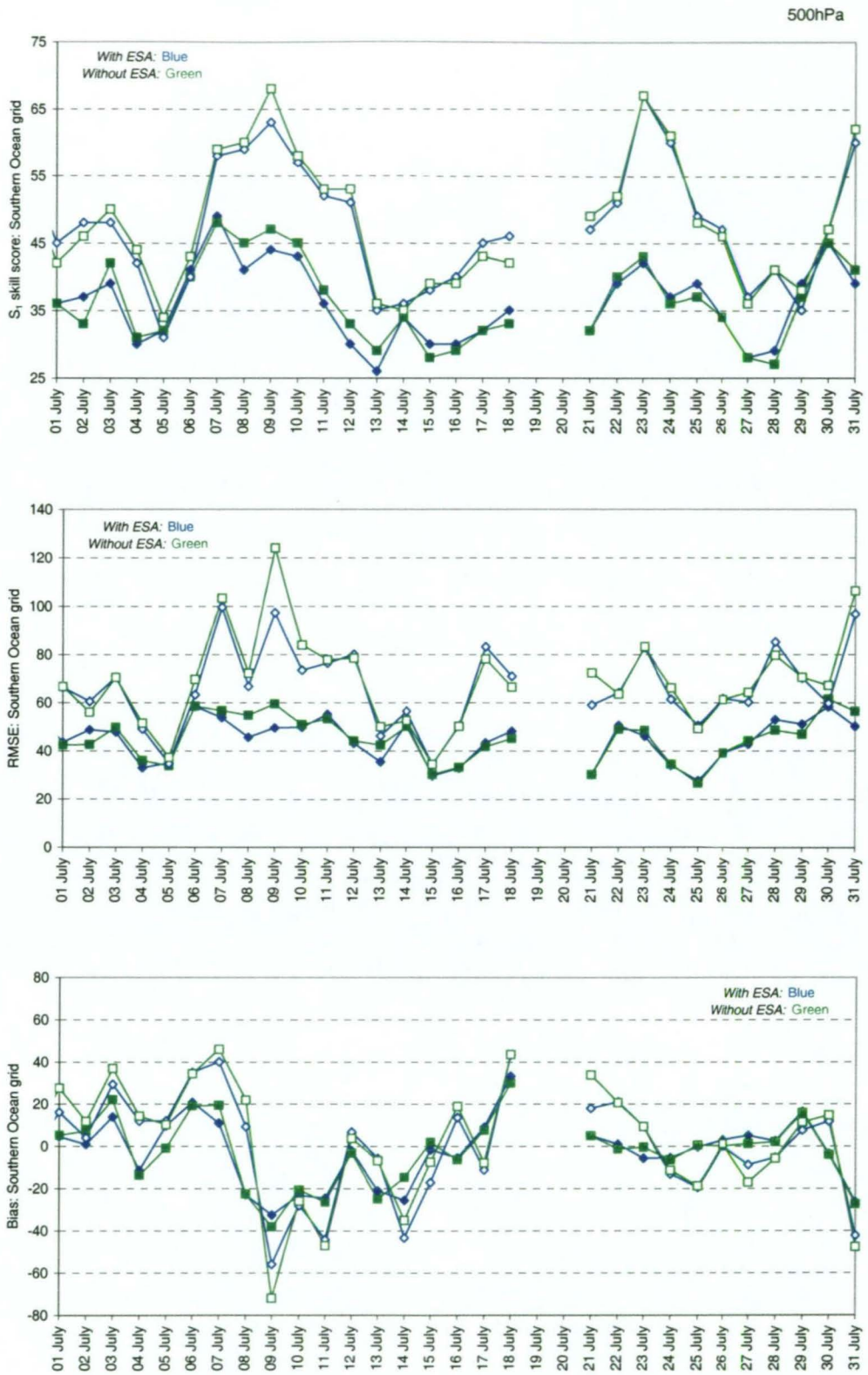

Figure A3.10 Daily variation of S_1 skill-score (top), RMSE (middle) and bias (bottom) comparing 24 and 48-hour prognoses of **500hPa height** from both the *with-ESA* and *without-ESA* trials (July 1995; m). **Southern Ocean verification grid (60°E to 160°E sector).**

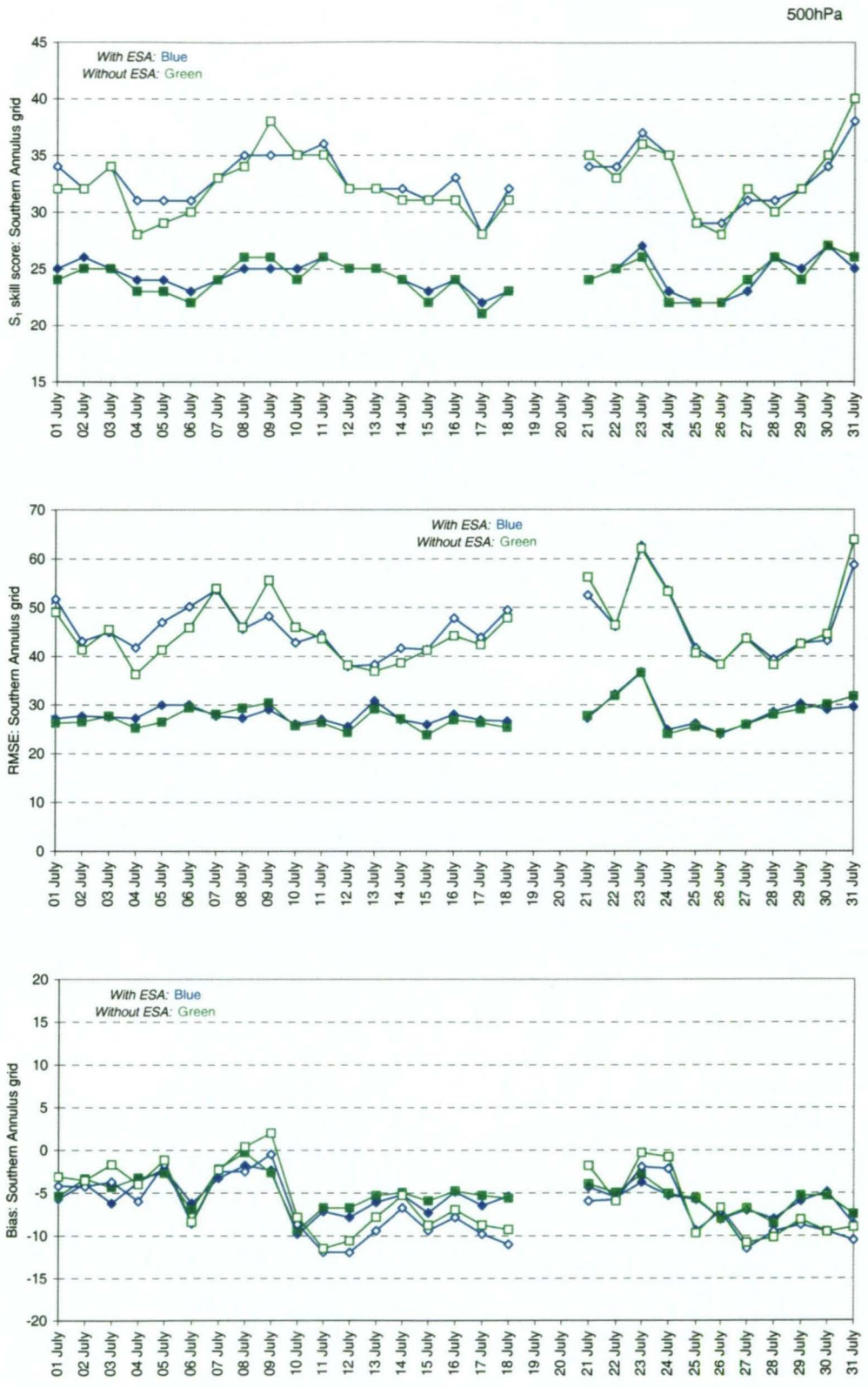

Figure A3.11 Daily variation of S_1 skill-score (top), RMSE (middle) and bias (bottom) comparing 24 and 48-hour prognoses of **500hPa height** from both the *with-ESA* and *without-ESA* trials (July 1995; m). **Southern Annulus verification grid.**

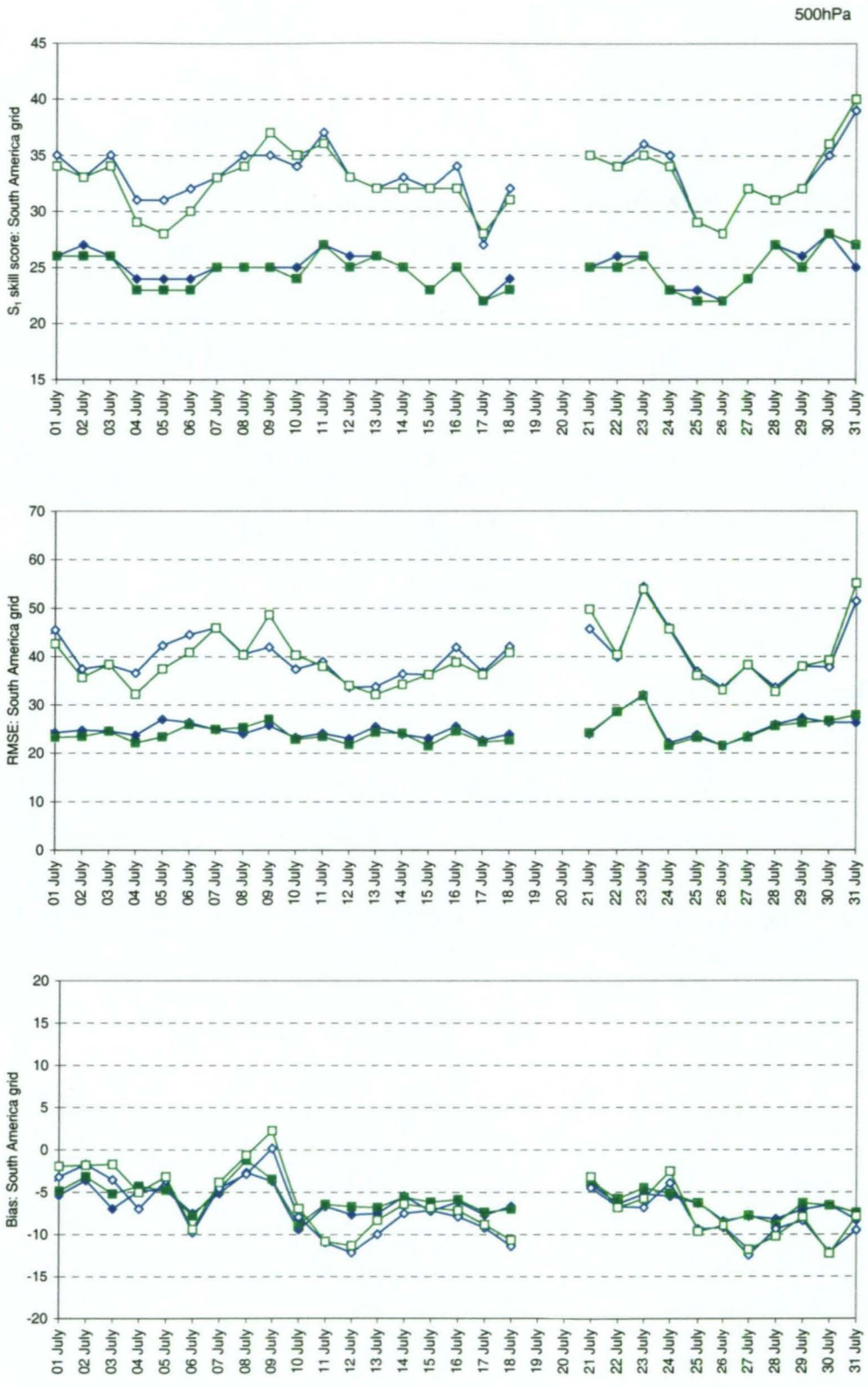

Figure A3.12 Daily variation of S_1 skill-score (top), RMSE (middle) and bias (bottom) comparing 24 and 48-hour prognoses of **500hPa height** from both the *with-ESA* and *without-ESA* trials (July 1995; m). **South American verification grid.**

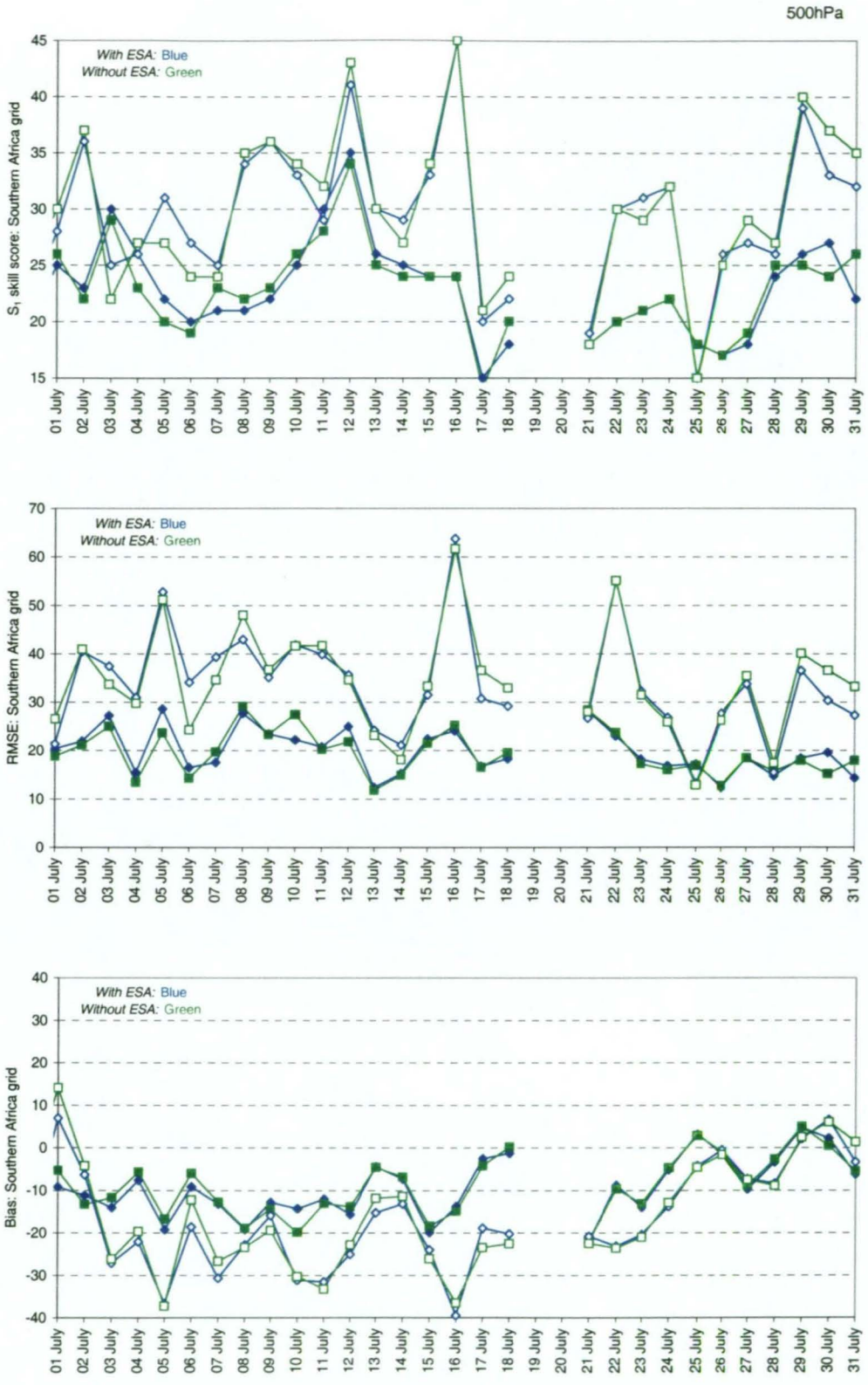

Figure A3.13 Daily variation of S_1 skill-score (top), RMSE (middle) and bias (bottom) comparing 24 and 48-hour prognoses of **500hPa height** from both the *with-ESA* and *without-ESA* trials (July 1995; m). **Southern Africa verification grid.**

Figure A3.14 Daily variation of S_1 skill-score (top), RMSE (middle) and bias (bottom) comparing 24 and 48-hour prognoses of **500hPa height** from both the *with-ESA* and *without-ESA* trials (July 1995; m). **Global verification grid.**

APPENDIX 4

RELATED PUBLICATION:

Jacka, K. (1999) An impact study involving ERS-1 scatterometer wind data - implications for the 'FROST' project. *Aust. Meteor. Mag.* Special Ed: 25-34.

The attached paper was published in a special edition of the *Australian Meteorological Magazine* focused to the 'FROST' project.

Author:	Kieran Jo Jacka
Title:	An impact study involving ERS-1 scatterometer wind data – implications for the 'FROST' project
Source:	*Australian Meteorological Magazine*, July 1999 Special Edition, pages 25-34
Publisher:	Australian Government Publishing Service